Total proton flux and balancing in genome-scale models: The case for the updated model of *Clostridium acetobutylicum* ATCC 824

Michael J. McAnulty

Thesis submitted to the faculty of the

Virginia Polytechnic Institute and State University

in partial fulfillment for the requirements for the degree of

Master of Science

in

Biological Systems Engineering

Ryan S. Senger, Chair

Eva Collakova

Chenming Zhang

Jactone Arogo Ogejo

August 5, 2011

Blacksburg, Virginia

Keywords: genome-scale modeling, proton balancing, *Clostridium acetobutylicum*, biofuels, acidogenesis, solventogenesis, P/O ratio

Total proton flux and balancing in genome-scale models: The case for the updated model of *Clostridium acetobutylicum* ATCC 824

Michael J. McAnulty

ABSTRACT

Genome-scale modeling and new strategies for constraining these models were applied in this research to find new insights into cellular metabolism and identify potential metabolic engineering strategies. A newly updated genome-scale model for *Clostridium acetobutylicum*, *iMM864*, was constructed, largely based on the previously published *iRS552* model. The new model was built using a newly developed genome-scale model database, and updates were derived from new insights into clostridial metabolism. Novel methods of proton-balancing and setting flux (defined as reaction rate (mmol/g biomass/hr)) ratio constraints were applied to create simulations made with the *iMM864* model approximate observed experimental results. It was determined that the following constraints must be applied to properly model *C. acetobutylicum* metabolism: (1) proton-balancing, (2) constraining the specific proton flux (SPF), and (3) installing proper flux ratio constraints. Simulations indicate that the metabolic shift into solventogenesis is not due to optimizing growth at different pH conditions. However, they provide evidence that *C. acetobutylicum* has developed strictly genetically regulated solventogenic metabolic pathways for the purpose of increasing its surrounding pH to decrease the toxic effects of high proton concentrations.

Applying a ratio constraint for the P/O ratio (a measure of aerobic respiratory efficiency) to the *iAF1260* genome-scale model of *E. coli* K12 MG1655 was explored. Relationships were found

between: (1) the P/O ratio, (2) the SPF, (3) the growth rate, and (4) the production of acetate. As was expected, higher acetate production correlates with lower P/O ratios, while higher growth correlates with higher P/O ratios. For the first time, a genome-scale model was able to quantify this relationship and targeting both the P/O ratio and the SFP is required to produce an *E. coli* K12 strain with either (i) maximized growth rate (and minimized acetate production) or (ii) maximized acetate production (at the expense of cell growth). A gene knockout mutant, *Δndh*, was created with *E. coli* BL-21 to study the effects of forcibly higher P/O ratios on growth. The results suggest that a metabolic bottleneck lies with the NADH-1 complex, the NADH dehydrogenase that contributes to the generation of a proton motive force.

Acknowledgements

I would like to take this opportunity to thank my advisor and committee chair, Dr. Ryan Senger, for all his advice and support that helped this research progress forward, even when complicated issues with the modeling had been encountered. I am also grateful for having Dr. Mike Zhang, Dr. Eva Collakova, and Dr. Jactone Arogo Ogejo serve on my committee, and for all their advice as well.

I value the help and advice from everyone in the Dr. Senger lab that I had been given. Their help allowed me to get past programming issues quickly, and to understand practices done in the lab easily. I am always thankful for my family; my parents, brother, and sisters for their never-ending support. I am thankful for my friends for great times and unforgettable memories at Virginia Tech. And I thank God for granting me the wisdom and perseverance to accomplish this work.

TABLE OF CONTENTS

LIST OF FIGURES

LIST OF TABLES

1. Introduction

1.1. The role of butanol as a biofuel

Humanity is facing an increasing dependence on non-renewable energy sources and the apparent consequences of their use are coming to fruition. Scientific findings indicate that fossil fuel use has indeed contributed to global warming (*1, 2*). Since petroleum-derived fuels are non-renewable, their supplies will constantly decrease while demand for them continues, causing a continuous price increase and an eventual shortage. Thus, their use is unsustainable, and researchers are seeking alternatives. Butanol has been identified as one potential liquid alternative fuel. Unlike most other renewable liquid biofuels, pure butanol may be used directly in unmodified ignition spark engines and transported safely in pipelines (*3*). Therefore, butanol may be incorporated easily into the existing transportation infrastructure.

Throughout the first half of the 20th century, butanol production was heavily dependent on the acetone-butanol-ethanol (ABE) fermentation process, and with the advance of genomic technologies and metabolic engineering, interest is returning. This process has traditionally used the anaerobic spore-former, *Clostridium acetobutylicum*, to ferment glucose and starch into ABE products. The metabolism of this organism is commonly characterized by two different phases: (i) acidogenesis and (ii) solventogenesis. During the acidogenic phase, cells uptake a carbon source (e.g., glucose) and secrete the weak acids (i) butyrate, (ii) acetate, and (iii) lactate along with hydrogen gas and carbon dioxide. Once the pH of the extracellular medium decreases, the cells undergo a genetic shift that up-regulates solvent production genes (*4, 5*). In this solventogenic phase, the cells re-uptake the secreted acetate and butyrate and convert these to acetone and butanol, respectively. The goal of the research presented in this thesis is to fully

understand the capabilities of *C. acetobutylicum* for butanol production. In particular, *in silico* metabolic engineering is used to identify if/how the organism can be manipulated to maximize butanol production while minimizing its growth rate. Highly productive strains that grow slowly are of considerable interest to biotechnology, as higher growth rates usually lead to the diversion of metabolic fluxes away from the production of desired products.

1.2. Modeling metabolism with genome-scale flux models

Metabolism can be modeled effectively using a genome-scale flux model (*6-8*). A genome-scale model is a mathematical model that contains stoichiometric information for all known reactions involved in metabolism of a particular organism. Such models have been constructed for a wide variety of organisms with sequenced genomes (*9*). Their primary uses are three-fold (*10*): (i) discovering gaps in information regarding metabolism, (ii) planning metabolic engineering strategies to enhance the production of a desired product, and (iii) performing gene essentiality studies in pathogens to provide targets for drug development. One of the main purposes of building a model for *C. acetobutylicum* is to simulate metabolism in order to find metabolic engineering strategies that enhance butanol production. Two genome-scale models already exist for this organism (*11, 12*).

Since *C. acetobutylicum* undergoes shifts in metabolism corresponding to changes in pH, it is of interest to design an algorithm that properly proton balances reactions of a genome-scale model given specified pH conditions. Compounds are protonated (and deprotonated) to different extents according to their pK_a values and the pH of their surroundings. An algorithm that keeps track of this protonation (and deprotonation) will yield more accurate representations of metabolic reactions in terms of the (i) consumption, (ii) production, and (iii) transport of protons.

Previous results have demonstrated the extremely sensitive nature of genome-scale models to the influx/efflux of protons through the cell membrane (*13, 14*), making proper proton balancing absolutely essential. In essence, a proton balancing algorithm may be used to examine changes in cellular metabolism in response to different extracellular, as well as intracellular, pH conditions.

New insights from biochemical data in the literature have illuminated new aspects of *C. acetobutylicum* metabolism (e.g., its incomplete TCA cycle). In this thesis, an updated genome-scale model for *C. acetobutylicum* is presented. In addition to new reactions, the new genome-scale model also is fully proton balanced, based on pK_a values for all metabolites in the cell, and input pH values. This method is novel and demonstrates the relationships between the intracellular and extracellular pH on metabolism. The new model is also presented with a novel method for identifying or setting "flux ratios" that is critical to determining how metabolic flux is distributed through the metabolic network.

Genome-scale models, in general, are constructed using various online databases that have metabolic reaction information available for different organisms. These include the Kyoto Encyclopedia for Genes and Genomes (KEGG) (*15*), the SEED database (*16*), BioCyc (*17*), and the Biochemical Genetic and Genomic knowledgebase (BiGG) (*18*). Unfortunately, these databases and even some individual models have their own ways of identifying or formatting compounds and reactions. This makes it very difficult to join information from these databases, as well as readily contrast and compare different models. Therefore, the Senger research group has created a new unified database containing compound and reaction information starting with several genome-scale models. Work on building a database for compound information (e.g., compound name(s), identifiers, formula, molecular weight, pK_a values, etc.) is presented in this thesis. Examples are given showing how genome-scale models prepared by different

laboratories using different databases and identifiers can be mapped into the database created by the Senger research group. These models are then extracted from the database using the unique identifiers created in this research and can be run simultaneously on the same MATLAB platform. For the first time, this allows for direct comparison of different genome-scale models prepared by different laboratories in terms of metabolic reactions and compounds accounted for.

1.3. Deriving flux ratios to solve singularities

Fermentative metabolism in *C. acetobutylicum* has been found to contain several singularities. For example, the cell may balance NAD/NADH through acid production pathways or this may be done "artificially" in reaction "loops" that are present in the network but do not occur in reality. These "loops" are also called futile cycles. In clostridial metabolism, these futile cycles related to NAD/NADH balancing have been identified in reactions catalyzed by the hydrogenase enzymes. In many instances, optimization algorithms that are used to find fluxes through different pathways indicate the use of strictly one pathway over another. This is not very representative of metabolism in reality. Flux ratios were thus derived to present a solution to these singularities and force flux to go through pathways that are not used *in silico*. These ratios may represent metabolism more realistically, as enzyme kinetics and regulatory effects may indicate that the flux through one reaction (or pathway) may occur as a ratio in relation to the flux in another reaction (or pathway).

While *Escherichia coli* K12 has a radically different metabolism than *C. acetobutylicum*, it secretes some of the same products, including acetate and ethanol. *E. coli*, grown under aerobic conditions, may be analyzed in terms of metabolic efficiency by calculating its P/O ratio (*19*). The P/O ratio is the amount of ATP produced (through phosphorylation of ADP) to the amount

of oxygen consumed. It is possible to manipulate the P/O ratio of *E. coli* K12 by re-directing metabolic flux within (i) central carbon metabolism, (ii) the energy production pathways, and (iii) the electron transport chain (ETC). It has been hypothesized that *E. coli* K12 produces greater amounts of acetate at lower P/O ratios at the expense of having a lower cellular growth rate. Engineering high production and lower growth rates is ideal for biotechnology. However, acetate is inhibitory to the production of certain valuable products. So, depending on the application, acetate production must be minimized or maximized, and it is of interest to better characterize the relationship between acetate production and the P/O ratio. In this thesis, a genome-scale model of *E. coli* K12 MG1655 (*20*) was used along with the novel ratio constraint technique to define the P/O ratio. Modeling results have located capabilities of *E. coli* K12 metabolism to accommodate high acetate production along with a low growth rate. Knowledge of these capabilities is critical to further metabolic engineering.

1.4. Research objectives

The focus of this research was to create/modify and work with genome-scale models to characterize metabolic phenotypes and provide possible metabolic engineering strategies. Novel algorithms of pH balancing and defining flux ratios were developed and have been used to generate simulations of metabolism. This allowed for the identification of highly productive and slow growing phenotypes. Overall, the specific objectives of this research were to:

1) Create an updated genome-scale model of *C. acetobutylicum*. The goal for this objective was to add information based on new insights of *C. acetobutylicum* metabolism that have been found since previous models were published.

2) Develop a proton balancing algorithm for genome-scale models that is responsive to pH conditions. An algorithm that modifies reactions of a genome-scale model based on varying pH conditions has not been published previously.
3) Develop a method for specifying flux ratios in a genome-scale model and constrain critical branch points in *C. acetobutylicum* metabolism using this method. Simulations of the new *C. acetobutylicum* model were performed, given proton balancing and flux ratio constraints. Modeling the onset of acidogenesis and solventogenesis was of particular importance. Contrasts between the new and old models were prepared.
4) Prepare a compound database as a contribution to the new genome-scale model database. The construction of the genome-scale model database was a team effort, but the work presented in this thesis was based on retrieving information for the compound database.
5) Perform simulations relating the P/O ratio to acetate production and growth in *E. coli* K12 MG1655. Also, a gene knockout in the electron transport chain of *E. coli* K12 was performed in the laboratory.

1.5. References

1. Litynski, J. T., Klara, S. M., McIlvried, H. G., and Srivastava, R. D. (2006) The United States Department of Energy's Regional Carbon Sequestration Partnerships program: a collaborative approach to carbon management, *Environ Int 32*, 128-144.
2. Southward, A. J., Langmead, O., Hardman-Mountford, N. J., Aiken, J., Boalch, G. T., Dando, P. R., Genner, M. J., Joint, I., Kendall, M. A., Halliday, N. C., Harris, R. P., Leaper, R., Mieszkowska, N., Pingree, R. D., Richardson, A. J., Sims, D. W., Smith, T.,

Walne, A. W., and Hawkins, S. J. (2005) Long-term oceanographic and ecological research in the Western English Channel, *Adv Mar Biol 47*, 1-105.

3. Szwaja, S., and Naber, J. D. (2010) Combustion of n-butanol in a spark-ignition IC engine, *Fuel 89*, 1573-1582.
4. Husemann, M. H., and Papoutsakis, E. T. (1988) Solventogenesis in Clostridium acetobutylicum fermentations related to carboxylic acid and proton concentrations, *Biotechnol Bioeng 32*, 843-852.
5. Papoutsakis, E. T. (2008) Engineering solventogenic clostridia, *Curr Opin Biotechnol 19*, 420-429.
6. Kauffman, K. J., Prakash, P., and Edwards, J. S. (2003) Advances in flux balance analysis, *Curr Opin Biotechnol 14*, 491-496.
7. Murabito, E., Simeonidis, E., Smallbone, K., and Swinton, J. (2009) Capturing the essence of a metabolic network: a flux balance analysis approach, *J Theor Biol 260*, 445-452.
8. Schilling, C. H., Edwards, J. S., Letscher, D., and Palsson, B. O. (2000) Combining pathway analysis with flux balance analysis for the comprehensive study of metabolic systems, *Biotechnol Bioeng 71*, 286-306.
9. Milne, C. B., Kim, P. J., Eddy, J. A., and Price, N. D. (2009) Accomplishments in genome-scale in silico modeling for industrial and medical biotechnology, *Biotechnol J 4*, 1653-1670.
10. Feist, A. M., and Palsson, B. O. (2008) The growing scope of applications of genome-scale metabolic reconstructions using Escherichia coli, *Nat Biotechnol 26*, 659-667.

11. Senger, R. S., and Papoutsakis, E. T. (2008) Genome-scale model for Clostridium acetobutylicum: Part I. Metabolic network resolution and analysis, *Biotechnol Bioeng 101*, 1036-1052.

12. Lee, J., Yun, H., Feist, A. M., Palsson, B. O., and Lee, S. Y. (2008) Genome-scale reconstruction and in silico analysis of the *Clostridium acetobutylicum* ATCC 824 metabolic network, *Appl Microbiol Biotechnol 80*, 849-862.

13. Senger, R. S., and Papoutsakis, E. T. (2008) Genome-scale model for Clostridium acetobutylicum: Part II. Development of specific proton flux states and numerically determined sub-systems, *Biotechnol Bioeng 101*, 1053-1071.

14. Senger, R. S. (2010) Biofuel production improvement with genome-scale models: The role of cell composition, *Biotechnol J 5*, 671-685.

15. Ogata, H., Goto, S., Sato, K., Fujibuchi, W., Bono, H., and Kanehisa, M. (1999) KEGG: Kyoto Encyclopedia of Genes and Genomes, *Nucleic Acids Res 27*, 29-34.

16. Overbeek, R., Begley, T., Butler, R. M., Choudhuri, J. V., Chuang, H. Y., Cohoon, M., de Crecy-Lagard, V., Diaz, N., Disz, T., Edwards, R., Fonstein, M., Frank, E. D., Gerdes, S., Glass, E. M., Goesmann, A., Hanson, A., Iwata-Reuyl, D., Jensen, R., Jamshidi, N., Krause, L., Kubal, M., Larsen, N., Linke, B., McHardy, A. C., Meyer, F., Neuweger, H., Olsen, G., Olson, R., Osterman, A., Portnoy, V., Pusch, G. D., Rodionov, D. A., Ruckert, C., Steiner, J., Stevens, R., Thiele, I., Vassieva, O., Ye, Y., Zagnitko, O., and Vonstein, V. (2005) The subsystems approach to genome annotation and its use in the project to annotate 1000 genomes, *Nucleic Acids Res 33*, 5691-5702.

17. Karp, P. D., Ouzounis, C. A., Moore-Kochlacs, C., Goldovsky, L., Kaipa, P., Ahren, D., Tsoka, S., Darzentas, N., Kunin, V., and Lopez-Bigas, N. (2005) Expansion of the

BioCyc collection of pathway/genome databases to 160 genomes, *Nucleic Acids Res 33*, 6083-6089.

18. Schellenberger, J., Park, J. O., Conrad, T. M., and Palsson, B. O. (2010) BiGG: a Biochemical Genetic and Genomic knowledgebase of large scale metabolic reconstructions, *Bmc Bioinformatics 11*, 213.

19. Calhoun, M. W., Oden, K. L., Gennis, R. B., de Mattos, M. J., and Neijssel, O. M. (1993) Energetic efficiency of Escherichia coli: effects of mutations in components of the aerobic respiratory chain, *J Bacteriol 175*, 3020-3025.

20. Feist, A. M., Henry, C. S., Reed, J. L., Krummenacker, M., Joyce, A. R., Karp, P. D., Broadbelt, L. J., Hatzimanikatis, V., and Palsson, B. O. (2007) A genome-scale metabolic reconstruction for Escherichia coli K-12 MG1655 that accounts for 1260 ORFs and thermodynamic information, *Mol Syst Biol 3*, 121.

2. Literature Review

2.1. Biofuels and butanol

2.1.1. The need for fuels from renewable resources

The world faces a dilemma of what to do with increasing dependence on non-renewable energy sources and the apparent consequences of their use. Perhaps the worst consequence of the use of fossil fuels is global warming. The combustion of fossil fuels releases carbon dioxide, a greenhouse gas, from solid and liquid reserves of oil and coal that reside beneath the Earth's surface. Studies have shown that the amount of carbon dioxide in the atmosphere has increased by about 30% since the dawn of the industrial age (*1*). While in the atmosphere, these greenhouse gases absorb more energy from the Sun, eventually leading to global warming. In fact, the global scientific community in general accepts the possibility that global warming is occurring and that it is due, to a certain extent, to anthropogenic activities such as fossil fuel use (*2, 3*).

Aside from the consequences of their use, fossil fuels are non-renewable resources. This is because it takes over 10,000 years for the conversion of biological material into oil and coal (*1*), and its rate of consumption greatly exceeds its rate of accumulation. So it is only a matter of time until the global supply of oil will be exhausted. Thus, investments in researching alternative sources of energy have increased dramatically in the past decade. Oil reserves are also geographically distributed irregularly. The Middle East holds more than half (roughly 65%) of the world's oil supply, Europe holds 11.7%, Africa 9.5%, Central and South America 8.6%, North America 5%, and Asia and the Pacific 3.4% (*4*). Because of this irregular distribution, many countries have to rely on oil imports to satisfy their energy demands. The United States

consumes roughly 20 million barrels of crude oil a day, 60% of which has to be imported (*5*). It would be very advantageous for these countries with more limited oil supplies to invest in alternative sources of energy, as this would decrease their reliance on oil imports.

2.1.2. Current production of biofuels

Various methods of producing alternative fuels have been found as more attention is being placed on decreasing our dependence on fossil fuels. Governments around the world are also supporting the production of alternative fuels through the use of subsidies and funds for research programs (*6*). But these alternative fuels have to meet certain requirements in order to be deemed appropriate for production and consumption. Biofuels in general are being brought up to replace oil-derived fuels in particular, since they may be used in modified or unmodified combustion engines in transportation. The two main biofuels currently being produced are ethanol and biodiesel (*6*). Other biofuels, such as butanol, are also being produced, but on a much smaller scale.

Currently, ethanol is the renewable fuel being produced on the largest scale. It is used as an additive to increase the octane number of gasoline and slightly offset gasoline use, but it may be used by itself as a fuel as well (*4*). The U.S., Canada, and India use it as an additive, while only Brazil produces E100 (a biofuel derived solely from ethanol, with no added gasoline) (*4*). However, engine modifications are needed to use ethanol even if it is only used as an additive (*7*). This fact reduces the value of ethanol, since it cannot be used in conventional internal combustion engines. Nevertheless, the U.S. has the most extensive bioethanol production, with over 4 billion gallons of ethanol being made per year (*5*). That is roughly half of the global ethanol production.

Bioethanol is derived from starch-based sources, or from lignocellulosic materials. Currently, almost all bioethanol production involves the fermentation of a sucrose or starch-based substrate into ethanol. Production in the U.S. is mainly derived from corn grain, and production in Brazil (the second greatest producer of bioethanol) is mainly based on sugarcane (*5*). Although ethanol production from starch is a very mature process with high efficiency, it is criticized heavily for using a food-based resource. Over 14 million hectares, or 1% of today's global farmlands, are used for biofuels (*4*). As more and more potential food supplies go to biofuel production instead, food prices will increase while the global supply decreases. At the same time, the U.S. is responsible for 70% of the world's corn exports (*4*). It is also suspected that biofuel programs may concentrate land ownership, increasing poverty and promoting the use of monocultures and intensified agriculture (*4*). In addition, even if all of the U.S. corn production were converted to biofuels, this would only constitute 12% of transportation fuel demand (*8*). Bioethanol has been criticized recently for yielding less energy than all the energy input into its production. However, at least one energy balance study has disproven this, indicating that ethanol yields 25% more energy than that invested in its production (*8*).

Although most bioethanol production is based off of a "food" substrate, it may be also be produced from other "non-food" substances such as lignocellulosic or biomass material (which is composed of 40-50% cellulose, 25-25% hemicellulose, and 15-20% lignin) (*5*). Lignocellulosic material is inedible, so its use as a biofuel substrate would not have terrible consequences on food prices and availability. And like starch, cellulose (the greatest component of biomass) is a polymer of glucose units. The main difference between cellulose and starch is the link between these glucose molecules, making cellulose more crystalline and difficult to hydrolyze. Current methods of production of lignocellulosic ethanol are still not economically viable compared to

starch-based bioethanol and especially against gasoline. But it still has great potential. For instance, the Department of Energy stated recently that the U.S. has the ability to produce 1 billion tons of biomass a year, which could end up replacing 30% of the gasoline usage (*7*). It is for this reason that the U.S. government provides more research funding towards lignocellulosic ethanol than any other country (*9*).

In contrast to bioethanol, biodiesel has received considerably more attention in Europe than in the U.S. This is primarily because their transportation infrastructure depends a lot more on diesel engines, and this dependence is constantly growing (*9*). In fact, the OECD member countries in Europe account for 56% of the world's biodiesel production (*9*). Biodiesel itself is a collection of monoalkyl esters of fatty acids made by the esterification of plant oils and animal fats (triacylglycerides) (*9, 10*). Biodiesel production in the U.S. is mainly derived from soybean oil (*8*). The esterification of triacylglycerides is performed in the presence of an acid or alkali catalyst. However, recent researched has focused attention to using lipases or fermentation (*10*). Like bioethanol, biodiesel production has been heavily criticized for using food-based resources. For instance, the production of biodiesel in Europe from vegetable oil raised vegetable oil prices upward, forcing margarine producers to request help from the European Union parliament (*4*).

2.1.3. Biobutanol

Butanol had not been regarded as a potential biofuel until very recently. Nonetheless, butanol has been produced on an industrial scale throughout the 20th century, mainly as a co-product in the acetone-butanol-ethanol (ABE) fermentation process. This process started at the beginning of the 20th century, when scientists in the United Kingdom launched this ABE process to produce precursors needed for synthetic rubber, such as acetone, butanol, and acetyl alcohol

(*11*). One of these scientists, Weizmann, succeeded in isolating an organism (later known as *Clostridium acetobutylicum* ATCC 4529) that produced larger amounts of acetone and butanol, and this strain became the organism of choice for the process (*11*). The UK then used this fermentation process during World War I to produce a constant supply of acetone needed for cordite (for ammunition) (*11*). Butanol production in this process was considered as a byproduct and was just stored, but that changed during the Prohibition in the U.S. There was a shortage of industrial solvents such as amyl alcohol (obtained via alcoholic fermentation), so butanol was then used to make butyl acetate as a quick drying lacquer for automobiles (*11*). Butanol was also used as a building block for a large variety of other end-products.

The use of the ABE process was widespread (it accounted for 66% of global butanol production) until 1950, when lower crude oil prices along with higher molasses (a major substrate used in the process) prices favored petrochemical butanol production (*11, 12*). However, the ABE process was still in use by a few countries, including South Africa, China, and the USSR (*13*). South Africa was able to continue using the process until the 1980's because it had an abundant supply of inexpensive molasses and did not have a readily available source of cheap petroleum (*13*). China, on the other hand, prompted heavy investing into starting up its own ABE industry at that time because of its internalized economy (*12*). In the 1980's China then relocated many of its ABE plants closer to agricultural districts, leading to a peak production of around 170,000 tons of solvents a year (*12*). A rapid increase in petrochemical butanol competition and increased grain prices led to the eventual complete shutdown of its ABE industry in the late 20th century (*12*). Due to the extensive ABE program in China, researchers made several improvements to the process, such as: (i) developing continuous fermentation, (ii) maintaining maximum growth and acidogenic phase, (iii) making multiple stages in the solvent-producing

growth phase (allowing gradual adaptation to increased solvent concentrations), (iv) experimenting with cell immobilization, (v) and incorporating stillage to offer enough nutrients to delay cell degeneration and sporulation (*12*).

Although low petrochemical prices eventually led to the discontinuation of the ABE process in many countries, greater interest in finding renewable sources of energy has completely renewed interest in the ABE process and biobutanol (i.e., butanol produced from biomass, which has the same physical properties as 'petrobutanol') production. In order to showcase the potential of biobutanol as a liquid transportation biofuel, David Ramey drove a 13 year-old Buick with an unmodified engine across the U.S. using pure biobutanol as fuel in 2005 (*11*). His company, Environmental Energy Inc., plans to produce biobutanol, and two larger companies, namely Dupont and BP, announced the start of their biobutanol production in 2007 (*11*). The future of biobutanol production looks bright.

Perhaps the largest advantage of biobutanol that has caused renewed interest is that pure butanol can be used in an unmodified ignition spark engine. On the other hand, ethanol cannot be run in a conventional engine, even at low mixes with gasoline. This property of butanol can be attributed to the fact that its thermo-physical properties are similar to gasoline with a PON (octane) rating of 87 (*14*). With respect to ethanol, butanol is (i) less corrosive and (ii) has a lower vapor pressure, (iii) does not absorb water (so there is no phase separation when mixed with gasoline), and (iv) it can be added to gasoline at the refinery and delivered through existing infrastructure (*11, 14*). When actually run through a conventional engine, some combustion knocking does occur, so the spark timing may need to be retarded in order to achieve maximum efficiency (*14*). Another study indicated that using biodiesel as an extractant for the ABE process not only increased butanol and total solvent production, but enhanced some properties of the

biodiesel (*15*). The cetane number increased (from 54 to 58) and the cold-filter plugging point decreased (from 5.8 to 0.2°C), making it less viscous and easier to transport at cold temperatures (*15*). So, butanol and ABE fermentation may have some use in the biodiesel industry as well.

Although the ABE process has been used extensively, improvements can always be made. An economic analysis on butanol fermentation indicated that the cost of the substrate used is the most influential factor in the final butanol price (*16*). The ABE process has typically used molasses or grains as a substrate, so its substrate situation is similar to that of bioethanol. Once more effective cellulose-degrading enzymes can be found, they may be used in the ABE process so that biomass can be used as a substrate instead. Another important factor that influences the price of butanol is its product yield, which is 20 g/L of solvents using current fermentation processes with *C. acetobutylicum* (or 0.30 to 0.33 g butanol / g substrate) (*16*). Butanol is inhibitory or toxic to *C. acetobutylicum*, explaining the low product yields. Designing more productive and solvent tolerant strains is a major research objective for metabolic engineering of *C. acetobutylicum.*

2.2. Solventogenic clostridia

2.2.1. The genus *Clostridium*

Clostridium acetobutylicum belongs to the genus *Clostridium*, which includes by definition: rod-shaped, gram-positive, obligate anaerobe bacteria capable of producing endospores. One major advantage for the use of clostridia in bioprocesses is their ability to use a wide variety of carbon substrates, such as: monosaccharides, oligosaccharides, polysaccharides (including refined and unrefined starches), and many pentoses and hexoses simultaneously (*17*).

Many clostridia also naturally produce complete or partial cellulosomes (complexes of proteins that can degrade cellulose), so they may directly use cellulose as a substrate (*17*).

The use of the definition of the *Clostridium* genus has led to the placement of many species into this genus that are distantly related to the type species of the genus, *C. butyricum* (*18*). Several 16S rRNA studies have suggested important changes to this genus, including the transfer of many previously defined *Clostridium* species to new genera within the *Clostridiaceae* family and to new families within the Firmicutes (*18*). Collins and coworkers (*19*) have also proposed that only species within a subset of the genus that have distinctly related 16S rRNA sequences (cluster I) should belong to the *Clostridium* genus. Cluster I, however, contains some species from other genera, and less than half of the current *Clostridium* species with validly published names (over 150 species) are part of this cluster (*18*). It is therefore very likely that major revisions will be done to this genus in the coming years.

2.2.2. Genetics and metabolism of *C. acetobutylicum*

C. acetobutylicum ATCC 824 is the most extensively studied strain of *C. acetobutylicum*, and is also considered to be the model solvent-producing strain in terms of research on strict anaerobes *(20, 21)*. Its complete genome was sequenced and published in 2001 (*22*). A comparison between the complete genome of *C. acetobutylicum* and that of *B. subtilis* (a related, more well-studied spore former) was made in the same study (*22*). The results from the study revealed that there is considerable local conservation of gene order between the two species. However, *C. acetobutylicum* also has many genes that are shared with distantly related bacteria and not with *B. subtilis*. The biggest difference comes from the strictly anaerobic metabolism of

C. acetobutylicum compared to the facultative aerobic metabolism of *B. subtilis*. Surprisingly, their genes responsible for sporulating are different as well.

The genome of *C. acetobutylicum* consists of a 3,940,880 bp chromosome (containing 3,740 identified ORFs) and a 192,000 bp megaplasmid pSOL1 (containing 178 ORFs) (*22, 23*). Various studies have been conducted on the M5 degenerate mutant lacking the pSol1 megaplasmid (*20, 21*). These studies indicate that pSol1 contains the genes responsible for solvent formulation, as well as sporulation (*21*). It has been shown that *C. acetobutylicum* tends to lose the megaplasmid upon serial subculturing or while in a continuous culture, but this can be prevented under phosphate-limited conditions (*21, 23*). One of these studies indicated that the original Weizmann strain (*C. acetobutylicum* ATCC 4529) contains a megaplasmid as well (pWEIZ), and degenerates in a similar manner without the plasmid (*21*).

C. acetobutylicum is a heterofermentative strict anaerobe capable of forming spores (*24*). Like other clostridia, it may grow on a wide variety of carbon substrates. It also naturally produces a complete cellulosome, but it cannot grow on cellulose effectively. The reason for this is not clearly known, and much research is being conducted on this topic (*18*). Because of its use in the bioprocessing industry (the ABE process in particular), solvent formation in *C. acetobutylicum* has been studied in detail. All studies on solvent formulation in this organism have described the process as follows (*21, 23-25*). Metabolic activity in this organism can be split into two distinct phases: (i) the acid production (i.e., acidogenic) phase and (ii) the solvent production (i.e., solventogenic) phase. During the acidogenic phase, the culture grows quickly and forms carboxylic acids (mainly acetate and butyrate), as well as hydrogen gas. As the secretion of these acids lead to the eventual lowering of extracellular pH, the cells undergo a major sigma factor governed regulatory shift into the solventogenic phase. They uptake the

previously secreted acids, metabolize them into butanol and acetone, and secrete these solvents back into the media. These solvent concentrations eventually accumulate to growth inhibitory levels and halt metabolism, leading to the onset of sporulation. It is hypothesized that the cells make the solventogenic shift in response to decreasing intracellular pH conditions. However, several hypotheses regarding solventogenesis onset still exist because the exact mechanisms of activation of the sigma factor governed process are still unknown.

The mechanisms behind butanol toxicity for *C. acetobutylicum* have been the subject of great interest, since finding ways to decrease its toxicity could help generate higher butanol yields. It is widely accepted that butanol disrupts both membrane fluidity and membrane function (*26, 27*). Results from one study (*26*) showed that higher butanol concentrations had numerous harmful effects on *C. acetobutylicum*: (i) cells lost the ability to maintain internal pH, (ii) membrane ATPase was partially inhibited, (iii) intracellular ATP levels collapsed, and (iv) glucose uptake rate decreased. All these effects can be accounted for by a disruption of membrane fluidity and a consequential loss of membrane-linked functions (*26*).

2.3. Genome-scale models

2.3.1. History of genome-scale models

Another method to potentially improve butanol production using *C. acetobutylicum* would be to identify metabolic engineering strategies using a genome-scale model. The concept of genome-scale modeling itself is relatively new. Although flux balance analysis has been used on small models since the 1980's (*28*), the development of "genome-scale" models based on genome annotations did not start until the late 1990's. In fact, the first genome-scale model was developed in 1999 for *Haemophilus influenzae*, and it was mainly based on its genome

annotation and available literature data (*29*). Metabolite and reaction databases (e.g., KEGG (*30*), Biocyc (*31*)) that these models depend on became more and more sophisticated as well. By the early 2000's, the databases started incorporating molecular charge and formula data, as well as containing reactions balanced based on stoichiometry and charge. Thermodynamics started coming into play as added constraints (*32, 33*), and cheminformatic algorithms have been used to generate physiochemical information on metabolites (*34*). Recently, more complex models have incorporated high-throughput and physiological data such as gene and proteome expression (*35*). From using these models to study metabolic flux, more recent advances have included transcriptional and translational regulatory circuits (*36*).

2.3.2. Mathematical concepts

Genome-scale models use flux balancing to calculate cellular metabolism (*37*). This approach is beneficial because enzyme kinetics are not required. Instead, flux balancing starts with the assumption that cellular metabolism attains a quasi-steady state (*37*). This assumption is accepted widely because metabolic reactions are much faster than the growth rate of the cell (*37*). The change in a metabolite's intracellular concentration is represented by Eq. 2.1.

$$\frac{dX_i}{dt} = \sum_j S_{ij} \cdot v_j \qquad Eq.\,2.1$$

Here, X_i is the concentration of the metabolite i, S_{ij} is a coefficient matrix containing the number of moles of metabolite i formed in reaction j, and v_j is the flux through reaction j (*38*). The stoichiometric matrix, S, is constructed from genome annotation and contains the stoichiometric parameters of all the metabolic reactions that occur in a certain strain (including transport reactions) (*37, 38*). Because of the steady-state assumption, Eq. 2.1 simplifies as follows.

$$\frac{dX_i}{dt} = 0 \qquad Eq. 2.2$$

This leads to the following simplified linear equation describing the steady-state representation of metabolic flux on the genome-scale (*38, 39*).

$$S \cdot v = 0 \qquad Eq. 2.3$$

Even though the model in Eq. 2.3 seems simplistic for modeling all chemical reactions within a cell, there are typically more reactions (represented as columns in S) than compounds (represented as rows in S). This makes Eq. 2.3 underdetermined (*37, 40*), creating a solution space that allows for multiple possible flux solutions (also referred to as the metabolic genotype or "phenotypic solution space") that the cell can use (*37*). An example model containing 3 fluxes may have a feasible solution domain as shown in Fig. 2.1. The optimized metabolic phenotype most likely lies on the edge of the solution space

The solution space can be further constrained by using linear inequality ($\alpha_i < v_i < \beta_i$) metabolic flux constraints (*38-41*). For instance, if it is determined that a reaction is irreversible in the forward direction, then its flux will have a lower constraint of 0 and an upper constraint of (possibly) infinity. Maximum flux constraints can be based on enzymatic capacity limitations or measured maximal uptake rates (*39*). Other constraints may also be added to analyze the *in silico* organism under certain media conditions by restricting the uptake of various metabolites (*40*). Experimental measurements of metabolic fluxes should be used to refine these constraints (*41*).

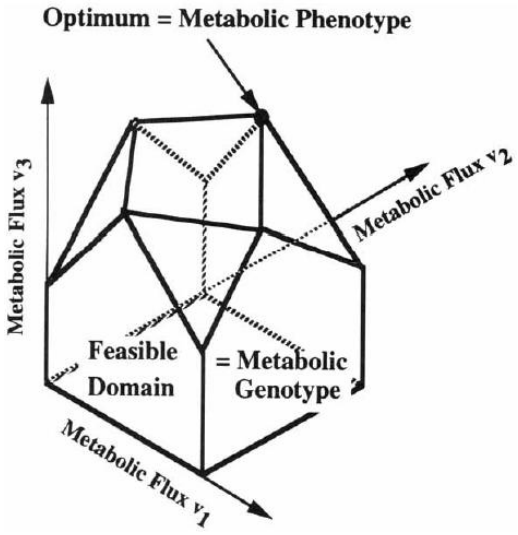

Fig. 2.1 Visualization of a phenotypic solution space for a model containing three reactions(originally published (37)).

Various techniques have been developed to predict the metabolic phenotype (i.e., a unique metabolic flux distribution lying within the constrained solution space that a strain will most likely undergo under certain environmental conditions) for a strain from its genotype. Most-commonly used methods include: (i) FBA (flux balance analysis) (*37*), (ii) MOMA (minimization of metabolic adjustment) (*42*), and (iii) ROOM (regulatory on/off minimization) (*43*). MOMA and ROOM depend on wild-type flux distribution data, but this data may be approximated using FBA. FBA typically uses linear programming to determine an optimal unique solution based on the maximizing or minimizing of an objective function (*38*). This objective function can be defined for any kind of objective or flux, including a metabolic engineering design objective (maximizing the production of a product) or maximum growth flux (in terms of biomass production) (*38*). In nature, a microorganism will typically use a flux distribution that would maximize its growth rate when given proper nutrients. Thus, maximizing the growth rate of a cell is the most widely used objective function in genome-scale modeling.

MOMA and ROOM have been designed particularly to study the effects of genetic or environmental perturbations. FBA can still be used for this application, just by having the constraints changed for the reactions becoming knocked out, and optimized growth is still assumed. MOMA uses linear or quadratic programming to optimize for a minimization of the total change of flux from the wild-type flux (which may use FBA) (*42*). So, this method is based on the assumption that the cell's objective function is to minimize the amount of perturbation rather than still maximize its growth rate (*42*). It therefore decreases the Euclidean distance between the flux solution of the mutant and that of the wild-type. ROOM is another algorithm similar to MOMA, but it is different in that the total number of fluxes being changed is minimized, rather than the total amount of flux or Euclidean distance (*43*). The main presumption of ROOM is that the microorganism will use short alternative pathways in response to a gene knockout. Studies have shown that MOMA is more accurate for determining flux solutions for an initial mutant, while FBA and ROOM are more accurate for determining the final flux solution of an adapted mutant (*43*).

While FBA is a commonly used method used to interrogate genome-scale models, caution should be taken when using it. There may be more than one equivalent solution that satisfies the optimization criteria, and many available software packages terminate after the first unique solution is found (*44*). This first solution may not be representative of the actual metabolic phenotype (i.e., it may be a 'silent' phenotype). More advanced FBA algorithms exist that can determine all these possible solutions and find which one utilizes the least amount of total flux. It is hypothesized that organisms likely minimize the total flux through their metabolic pathways (*45*).

FBA can also be combined with various types of high-throughput data to place tighter constraints on a model and provide for more robust and accurate simulations. Thermodynamic metabolic flux analysis (TMFA) utilizes thermodynamic principles and metabolite concentration data (when available) to determine which reaction directions are thermodynamically feasible (*33*). This method constrains flux solutions to disallow the use of thermodynamically infeasible pathways. It relies on the standard Gibbs free energy of formation $\left(\Delta G^{o}_{formation}\right)$ values for all the metabolites in a model. For each compound, $\Delta G^{o}_{formation}$ is calculated based on the substructures of the molecule using a group contribution method (GCM) model (*32*). Another method, called IOMA (integrative metabolic omics analysis) relies on the use of "-omics" data to place further constraints at the level of genetic regulation (*35*). .

2.3.3. Applications of genome-scale models

Genome-scale models are used to provide insights into metabolism. In doing so, they can be applied to improve bioprocesses through a variety of ways. The scientific community has employed these models to help analyze experimental data as well. Perhaps the most well-known application of genome scale models is providing gene-knockout simulations for the purpose of strain optimization. Algorithms such as OptKnock, OptFlux, and OptORF have been created that use genome-scale models for this purpose (*46-48*). In general, these algorithms pick out reaction deletions or gene deletions that ensure that the flux towards growth conditions lead to the production of a desired product (*46*). Metabolic engineers can use such algorithms to optimize strains resulting in increased production of a desired product. These algorithms have been used in industry to design non-intuitive, novel microbial strains for enhanced metabolite production (*49*). Examples include enhancing lactate yield in *E. coli*, ethanol yield in *S. cerevisiae*, and

succinate yields in *M. succiniproducens* (*34*). New genome-scale models have also become available for organisms used in bioremediation efforts (*49*). Gene knockout simulations in pathogens can also identify metabolic reactions (and the proteins that catalyze them) that are essential for growth. This method is used to identify potential targets for new antibiotics (*49*). Studies using this strategy have already identified many possible new drug targets for several pathogens, including *P. falciparum* (which causes malaria) and multi-drug resistant *A. baumannii AYE* (*50-52*).

In contrast to strain optimization, genome-scale models can also be used for substrate optimization. The objective function of the FBA algorithm may be analyzed under varying environmental conditions (by changing uptake rates of various nutrients). This method then determines which substrate conditions satisfies given criteria in order to improve a bioprocess. Criteria for this optimization may include (i) minimizing waste products, (ii) maximizing product formation, and/or (iii) maximizing growth rate (*37*).

2.3.4 Proton balancing

Any organism must keep its internal pH stable in order to function properly for a variety reasons. One is that intracellular enzymes keep their structure and are able to catalyze reactions only within certain ranges of pH. The proton motive force plays a vital role in the generation of cellular reducing power. This concept has even been ratified by genome-scale models (*39, 53*). Therefore, protonation-deprotonation reactions play vital roles in cellular metabolism, since cells may use them to keep their intracellular pH in a biological range (*54*). While it may be important for a genome-scale model to incorporate proton balancing to improve the accuracy of the model, reaction databases such as KEGG typically do not portray proton balancing accurately. Higher

organisms contain highly regulated mechanisms to strictly control their intracellular pH within biological limits (*54*), but this is not the case for the early prokaryotes, such as the clostridia. In these organisms, intracellular pH can drift as low as 5 (*55*). Because of this and the fact that total flux of protons across the cell membrane has been found to dramatically impact FBA solutions (*53*), a comprehensive rigorous balancing of protons is needed in genome-scale models. It will be useful to predict the pK_a values of all compounds involved in a genome-scale model. Given this, their average charges may be calculated for various pH ranges, allowing for proper protonation (or deprotonation) states of compounds to be represented in the model. This is especially important in an environment with a dynamic pH (e.g., a fermentation environment).

Various cheminformatic programs exist that can predict the pK_a values (for both protonation and deprotonation) of a molecule given its formula and structure. One such program, Marvin by ChemAxon, uses the algorithm shown in Fig. 2.2 (*56*). The following Eq. 2.4 is used to calculate the micro pK_a constant specific for an ionization site.

$$pK_a = a * Q + b * P + c * S + d \qquad Eq. 2.4$$

Here, Q is the partial charge increment, P is the polarizability increment, S is the sum of structure specific increments, and a,b,c, and d are coefficients specific to the ionization site (*57*). The macro or "true" ionization pK_a constants also take into account interactions between ionization sites (including effects of proton bonding and electron withdrawing effects through protonation/deprotonation), and are calculated from the micro pK_a constants (*57*). This program was tested for calculations of pK_a values from 1670 molecules against experimental data from the PhysProp database, and relatively strong accuracy was given by the model (r^2=0.95, s=0.72), but several erroneous results were omitted (*56*).

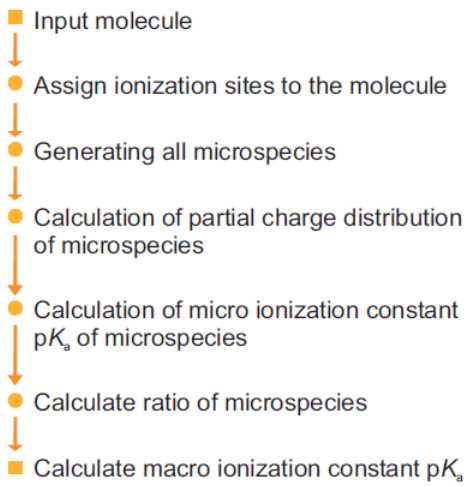

Fig. 2.2. Algorithm used by Marvin to predict pK_a constants (originally published (*56*)). Used under fair use guidelines, 2011.

Once the pK_a values for a molecule have been calculated, its average charge at a given pH is calculated according to the following procedure. The proportion of a protonated (or deprotonated) species relative to all its other protonated (or deprotonated) forms is determined by the following Eq. 2.5 (*58*).

$$\alpha_{Hn-j} = \frac{\left(\left(\prod_{j=1}^{j} k_i\right)[H^+]^{n-j}\right)}{D} \qquad Eq.\,2.5$$

In Eq. 2.5, $\alpha_{Hn\text{-}j}$ is the fraction of species in the form $H_{n\text{-}j}A$, k_i is the acid dissociation constant K_a (10^{-pKa}) of the i^{th} species, $[H^+]$ is the concentration of protons in solution, and D is defined in Eq. 2.6. (*58*).

$$D = [H^+]^n + k_1[H^+]^{n-1} + k_1k_2[H^+]^{n-2} + \cdots + k_1k_2 \ldots k_n \qquad Eq.\,2.6$$

Eq. 2.5 can also be manipulated to incorporate dissociation constants associated with protonation as well. So, once α is calculated for all species, the average charge of the molecule at the certain pH can be calculated using Eq. 2.7, where C is the average charge of the molecule and c_i is the formal charge of the i^{th} species.

$$C = \sum_{i=1}^{n} \alpha_i c_i \qquad Eq. 2.7$$

The actual charge balancing is simple with non-transport reactions. However, proton-balancing in transport reactions is complicated by the fact that the proton stoichiometries for more than compartment may have to be modified. Transportation reactions are further complicated by the possibility that some transport reactions are selective towards the degree of protonation of the substrate. Studies have indicated that transport reactions involving diffusion across a membrane (i.e. with acetate, butyrate, butanol) only occur with the neutral species (*59*). Not much literature data is available for selectivity of transport proteins towards the charge of its substrate. However, evidence has been provided that some transport proteins are selective towards the charge of the transported molecule (*60*).

2.4. Modeling clostridial metabolism

2.4.1. Previous models of *C. acetobutylicum*

Senger and Papoutsakis constructed the first genome-scale model for *C. acetobutylicum* in 2008 (*53, 61*). Their model was constructed using a semi-automated reverse engineering algorithm. Initial drafts of the model contained data from the biochemical pathway database KEGG. Incomplete metabolic pathways and missing metabolite membrane transport reactions were identified and fixed by finding "dead-ends" of relevant metabolic pathways using a novel analysis of the stoichiometric matrix. The resulting model consisted of 422 intracellular metabolites involved in 552 non-redundant reactions, 80 of these were membrane transport reactions. The model successfully characterized the phenotype of the butyrate-kinase knockout (the *buk* gene is knocked out to eliminate the production of butyrate) and the M5 degenerate

strain (genes on the pSOL1 megaplasmid are knocked, eliminating production of acetone and butanol and decreasing ethanol production) Senger and Papoutsakis also introduced the concept of constraining the specific proton flux in order to further limit the number of optimized flux solutions and predict extracellular pH (*53*). A numerically determined sub-system was also used to explore the use of constraints around identified network singularities. A singularity of a metabolic network consists of a group of reactions involved in "cycling" to where a unique solution cannot be found without further information. The secretion and re-uptake of acetate and butyrate by *C. acetobutylicum* is the most well-studied singularity of metabolic networks to date (*62*).

The need for improvements to the Senger and Papoutsakis model (*53, 61*) has been identified. Charge balances for the reactions were carried out in their model using fully protonated metabolites. So, the effect of intracellular pH on metabolism could not be measured and charge balancing of the reactions may not have been accurate. Also, literature data from other species, such as the closely-related *B. subtilis* and *Staphylococcus aureus*, were used to approximate the lipid and cell-wall composition of *C. acetobutylicum* due to lack of information specific in the literature. A second genome-scale model for *C. acetobutylicum* was constructed in 2008 by Lee et al. (*63*). Even though this model was prepared at the same time as the Senger and Papoutsakis model, with either group having knowledge of the other, these models are strikingly similar in size. The Lee et al. model accounts for 479 metabolites involved in 502 reactions. However, there are differences between the two. This reconstruction was curated manually and used biochemical reaction data mainly from KEGG and from other databases such as MetaCyc, BioSilico, and TIGR. One major difference in its reaction pathways is that the Senger and Papoutsakis model suggested that the urea cycle and amino acid biosynthesis

pathways contribute to formation of α-ketoglutarate in an incomplete tricarboxylic acid (TCA) cycle. The Lee et al. model followed the suggestion of Nolling et al. (*22*) that the reductive pathway between pyruvate and α-ketoglutarate are connected and the TCA cycle is complete. The Senger and Papoutsakis model used the novel method of proton efflux constraints to help their model distinguish between acidogenesis and solventogenesis. The Lee et al. model, on the other hand, used separate models for acidogenesis and solventogenesis and used a nonlinear programming approach to characterize the solventogenic phase. It is noted here that non-linear programming on the scale of a genome-scale model is extremely time-consuming from a processing standpoint. This distinction has provided a significant advantage to the approach taken by Senger and Papoutsakis.

2.4.2. Metabolic pathway characterization

A general overview of the primary fermentation pathways involved with acids and solvents production in *C. acetobutylicum* is shown in Fig. 2.3. This metabolic network is used primarily to regenerate ATP via phosphorylation, as well as balance NAD(P)H by providing an electron sink for these two cofactors. Studies have shown that the uptake of acids plays a pivotal role in solvent production by providing electron sinks, and that faster sugar uptake also leads to solvent formation (*64*). Studies have also shown that since an acid can only diffuse through the membrane in its fully protonated form (*59*), lower external pH conditions lead to greater uptake of acids, as more acids are available in their protonated forms (*64*).

The repression of the hydrogenase in this organism has been well-studied, since it directs the flow of electrons away from solvent production (*65-67*). It is known to be repressed by carbon monoxide (*65-67*). However, hydrogen may be considered to be another valuable end-

product or alternative fuel, so whether or not its production should be repressed depends on the application of the fermentation process. A maximum theoretical conversion efficiency of less than 4 mole H_2/mole hexose can be achieved through this fermentation process, with a maximum recorded H_2 yield of 68% of this value in *C. acetobutylicum* (*66*). Acetate and butyrate are the most produced side-products alongside hydrogen production (*66*). When the hydrogenase is repressed, acetate and butyrate are taken up by the cells at faster rates and a coincidental increase in solvent production and decrease in growth rate occurs (*65, 67*).

C. acetobutylicum has been identified as a species capable of performing nitrogen fixation (converting N_2 to biologically available ammonia) (*68*). This process is very energy intensive, as it requires large amounts of ATP to be dephosphorylated and ferredoxin to donate electrons to make ammonia from N_2 (*69*). Because solventogenesis and nitrogen fixation compete for the same reducing agent, it is hypothesized that cells undergoing nitrogen fixation produce less solvents. In fact, studies have revealed that solvent production can still occur during nitrogen fixation, but the greatest amount of nitrogen-fixing activity occurs during acidogenesis (*68*).

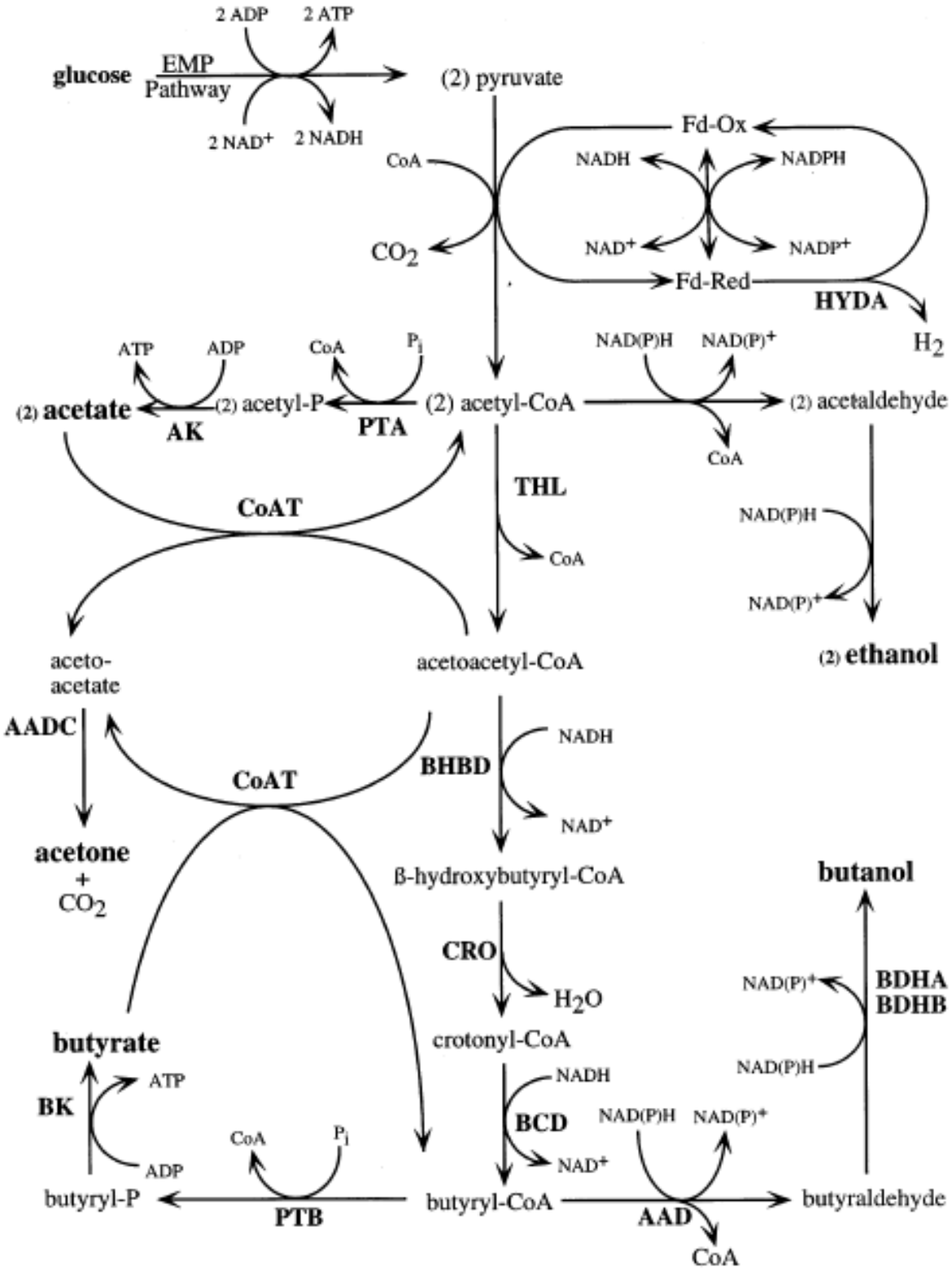

Fig. 2.3. General overview of fermentation in solventogenic clostridia (originally published (*70*)).

Used under fair use guidelines, 2011.

Although *C. acetobutylicum* has been used extensively in ABE industrial fermentation processes, many of its key metabolic pathways are still being characterized fully. One example is the TCA cycle, which remains ill-defined for several clostridia (*22, 61, 63, 71*). In anaerobes, this pathway is used to provide precursors for amino acid biosynthetic pathways. The initial genome sequencing revealed that genes encoding for the (i) citrate synthase, (ii) aconitase, (iii) isocitrate dehydrogenase, and (iv) succinate dehydrogenase were missing according to homolog comparisons (*22*). It is possible that *C. acetobutylicum* has genes encoding for some of these enzymes, but they could not be identified easily through traditional bioinformatics methods.

Recently, separate ^{13}C analyses were conducted to better characterize the TCA cycle in *C. acetobutylicum*. Results from one of the studies (*71*) indicated that *C. acetobutylicum* produces the appropriate enzymes to run a bifurcated TCA cycle in which both reducing and non-reducing paths lead to succinate production as shown in Fig. 2.4 (*71*). Results from the other study (*72*) coincided well with these results. The latter study indicated that the TCA cycle in *C. acetobutylicum* is run in the oxidative direction (clockwise) to produce α-ketoglutarate from citrate, and that there is no carbon flow between α-ketoglutarate and fumarate in either direction. These results provide further support of this organism having a split TCA cycle that ends up with succinate production at the reductive and oxidative ends. The intracellular metabolite concentrations that make this bifurcated TCA cycle of *C. acetobutylicum* thermodynamically feasible, however, have not yet been measured. Both studies also revealed the presence of a re-citrate synthase (as opposed to si-citrate synthase), and provided more evidence that the oxidative pentose phosphate pathway is not used in *C. acetobutylicum*.

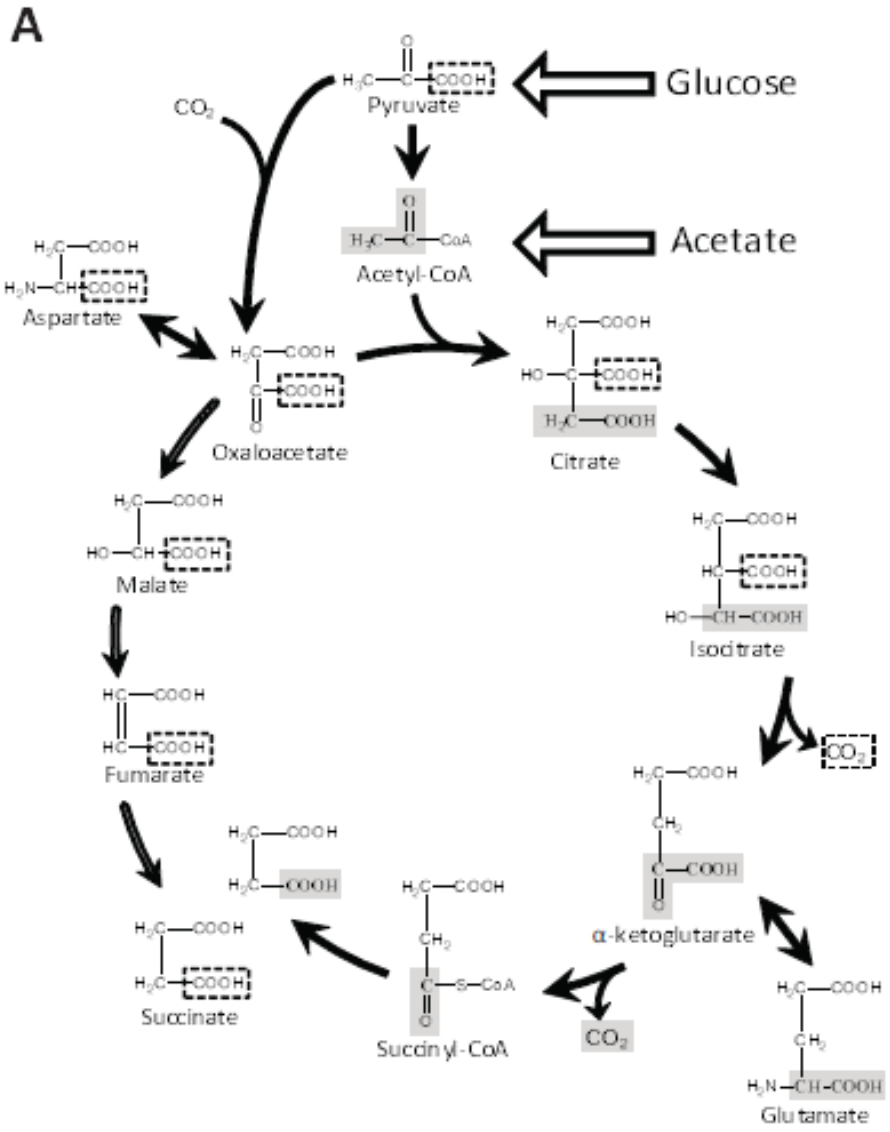

Fig. 2.4. Bifurcated TCA cycle in *C. acetobutylicum* proposed by Amador-Noguez et al. (originally published (*71*)). Used under fair use guidelines, 2011.

2.5. The P/O ratio in *E. coli*

2.5.1. Definition of the P/O ratio

In both anaerobic and aerobic bacteria, it is imperative to accurately portray the oxidoreductive and phosphorylating reactions involving different cofactors and reducing agents

since they directly relate to cell growth and maintenance. For this reason, the assessment of the energetic efficiency of the respiratory electron transport chain in aerobic bacterial metabolism is very important in both practical and fundamental viewpoints (*73*). The most widely used method to estimate the respiratory efficiency in aerobic bacteria is with the P/O ratio. This is defined as the number of ATP molecules synthesized (i.e., ADP phosphorylated) for every atom of oxygen consumed. Growth of aerobic organisms (e.g., *E. coli* K12) depends on energy supplies for biomass synthesis and the production of ATP (*74*). So, the P/O ratio may be used as a valid estimation of the overall efficiency of oxygen. As an example, *E. coli* has an *in vivo* P/O ratio of 1.4 to 1.5 for growth on glucose (*74*), and a theoretical maximum P/O ratio of 2 (*75*) or 2.3 (*74*). This would indicate that under normal conditions with glucose consumption, *E. coli* does not maximize its P/O ratio. In a similar fashion, *S. cerevisiae* has a maximum theoretical P/O ratio of 1.5, while *in vivo* studies have indicated that its apparent P/O ratio is 0.98 (*76*).

Several different metabolic pathways are important in the production of ATP. These pathways include the Embden-Meyerhoff-Parnas pathway, the Entner-Douderoff pathway, the TCA cycle, and the electron transport chain. Of these pathways, oxygen is consumed primarily by the electron transport chain. So, the P/O ratio can be calculated for overall aerobic cellular metabolism, or for just the electron transport chain in particular.

2.5.2. The electron transport chain in *E. coli*

The metabolic function of the electron transport chain is to pump protons across the cellular membrane to create a proton gradient between the cytoplasm and the extracellular space. The proton gradient may be used for many vital cellular functions, including (i) energy generation, (ii) the regeneration of cofactors, and (iii) cellular motility. In fact, because of its

imperative role in creating a proton motive force, all proteins associated with the electron transport chain are membrane-bound. Another major function is the use of an ATP synthase, which couples the transport of protons back into the cytoplasm with the phosphorylation of ADP to create ATP. ATPases notoriously vary in the number of protons needed to cross the membrane in order to generate one ATP molecule. In *E. coli*, it is common to assume this ratio is 4 protons per ATP produced (*75, 77*), even though more experimental evidence indicates that it is 3 protons per ATP produced (*74*).

The aerobic electron transport chain of *E. coli* consists of: (i) two NADH dehydrogenases that allow for electrons to transfer from NADH to quinol, and (ii) two quinol oxidases that couple the oxidation of quinol to the reduction of oxygen to water (*73*). *E. coli* contains two separate NADH dehydrogenases and two separate quinol oxidases. The two NADH dehydrogenases have been named as NADH-1 and NADH-2, and the two cytochrome oxidases are of the *bd* and *bo* type (*73*). Each of the NADH dehydrogenases and cytochrome oxidases differs in the proton motive force that it generates coupled to its associated electron transfer reaction. The NADH-1 transports 4 protons across the membrane per NADH oxidized (2 electron transfer) (*78*), while NADH-2 does not contribute to the proton motive force (*73*). The *bd*-type cytochrome oxidase transports 2 protons for every 2 electrons transferred, while the *bo*-type generates 4 protons for every 2 electrons transferred (*73*). *E. coli* may vary the ratios of the fluxes between these enzymes to adjust the P/O ratio to respond to different environmental conditions.

NADH-1 and NADH-2 vary greatly in terms of structure. NADH-1 is an enzyme complex that is made up of 14 subunits, all encoded by genes labeled as *nuoA-N* (*79-81*). It contains a membrane arm, a peripheral arm, and a connecting group that links the two complexes

together (*80*, *81*). Because it is made up of subunits, one subunit should be identified as crucial for catalytic function in order to plan a proper gene knockout strategy. The *nuoG* subunit has been labeled as crucial for proper assembly and function, as the knockout of the subunit (either through insertion or deletion) leads to a loss of functional NADH-1 (*79*). *nuoK* has also been identified as a crucial subunit for the proper function of the complex and plays a role in proton translocation (*81*). Unlike NADH-1, NADH-2 is a single enzymatic unit encoded by one gene, *ndh* (*73*).

2.5.3. Simulating and measuring the P/O ratio

A variety of methods have been developed to simulate and predict P/O ratios, some of which include the use of genome-scale models. In the case of eukaryotic organisms, where ATP production is specific for the mitochondria, the P/O ratio is calculated as the moles of ATP exported per mole of oxygen consumed by mitochondria (*76*). This method cannot be used for prokaryotic cells, as ATP production cannot be tracked through exchange or transport reactions. Other methods have estimated the P/O ratio using proton efflux through the electron transport chain (*75*). Another technique previously developed for other purposes may be used to constrain the P/O ratio to be a certain value within a genome-scale model. Constraints may be placed not only on singular reactions, but also on ratios between different reactions, while still preserving the linearity of the model itself (*53*). This technique would allow for the constraining of the P/O ratio by forcing the ratio between the sum of fluxes of reactions that produce ATP and the oxygen uptake to be a certain value.

Performing experimental measurements of the P/O ratio is difficult. Oxygen uptake rates are easily measured. However, since ATP and phosphate are mainly cycled internally, phosphate

assimilation to ATP cannot be calculated just by measuring phosphate uptake into the cell. A ^{31}P nuclear magnetic resonance (NMR) protocol presents a solution to this problem. It has been used to measure *in vivo* phosphate and ATP turnover rates for the purpose of calculating the P/O ratio in many microorganisms, including *E. coli* (*74, 82, 83*).

2.6. References

1. Lincoln, S. F. (2005) Fossil fuels in the 21st century, *Ambio 34*, 621-627.
2. Litynski, J. T., Klara, S. M., McIlvried, H. G., and Srivastava, R. D. (2006) The United States Department of Energy's Regional Carbon Sequestration Partnerships program: a collaborative approach to carbon management, *Environ Int 32,* 128-144.
3. Southward, A. J., Langmead, O., Hardman-Mountford, N. J., Aiken, J., Boalch, G. T., Dando, P. R., Genner, M. J., Joint, I., Kendall, M. A., Halliday, N. C., Harris, R. P., Leaper, R., Mieszkowska, N., Pingree, R. D., Richardson, A. J., Sims, D. W., Smith, T., Walne, A. W., and Hawkins, S. J. (2005) Long-term oceanographic and ecological research in the Western English Channel, *Adv Mar Biol 47*, 1-105.
4. Escobar, J. C., Lora, E. S., Venturini, O. J., Yanez, E. E., Castillo, E. F., and Almazan, O. (2009) Biofuels: Environment, technology and food security, *Renew Sust Energ Rev 13*, 1275-1287.
5. Gray, K. A., Zhao, L., and Emptage, M. (2006) Bioethanol, *Curr Opin Chem Biol 10*, 141-146.
6. Solomon, B. D. (2010) Biofuels and sustainability, *Ann N Y Acad Sci 1185*, 119-134.
7. Durre, P. (2007) Biobutanol: an attractive biofuel, *Biotechnol J 2*, 1525-1534.

8. Hill, J., Nelson, E., Tilman, D., Polasky, S., and Tiffany, D. (2006) Environmental, economic, and energetic costs and benefits of biodiesel and ethanol biofuels, *Proc Natl Acad Sci U S A 103*, 11206-11210.

9. Gnansounou, E. (2010) Production and use of lignocellulosic bioethanol in Europe: Current situation and perspectives, *Bioresour Technol 101*, 4842-4850.

10. Feofilova, E. P., Sergeeva, Y. E., and Ivashechkin, A. A. (2010) Biodiesel-fuel: Content, production, producers, contemporary biotechnology (Review), *Appl Biochem Micro+ 46*, 369-378.

11. Durre, P. (2008) Fermentative butanol production - Bulk chemical and biofuel, *Incredible Anaerobes: From Physiology to Genomics to Fuels 1125*, 353-362.

12. Chiao, J. S., and Sun, Z. H. (2007) History of the acetone-butanol-ethanol fermentation industry in China: development of continuous production technology, *J Mol Microbiol Biotechnol 13*, 12-14.

13. Jones, D. T., and Woods, D. R. (1986) Acetone-butanol fermentation revisited, *Microbiol Rev 50*, 484-524.

14. Szwaja, S., and Naber, J. D. (2010) Combustion of n-butanol in a spark-ignition IC engine, *Fuel 89*, 1573-1582.

15. Li, Q., Cai, H., Hao, B., Zhang, C., Yu, Z., Zhou, S., and Chenjuan, L. (2010) Enhancing Clostridial Acetone-Butanol-Ethanol (ABE) Production and Improving Fuel Properties of ABE-enriched Biodiesel by Extractive Fermentation with Biodiesel, *Appl Biochem Biotechnol*.

16. Qureshi, N., and Blaschek, H. P. (2000) Economics of butanol fermentation using hyper-butanol producing Clostridium beijerinckii BA101, *Food Bioprod Process 78*, 139-144.

17. Papoutsakis, E. T. (2008) Engineering solventogenic clostridia, *Curr Opin Biotechnol 19*, 420-429.

18. Gupta, R. S., and Gao, B. (2009) Phylogenomic analyses of clostridia and identification of novel protein signatures that are specific to the genus Clostridium sensu stricto (cluster I), *Int J Syst Evol Microbiol 59*, 285-294.

19. Collins, M. D., Lawson, P. A., Willems, A., Cordoba, J. J., Fernandez-Garayzabal, J., Garcia, P., Cai, J., Hippe, H., and Farrow, J. A. (1994) The phylogeny of the genus Clostridium: proposal of five new genera and eleven new species combinations, *Int J Syst Bacteriol 44*, 812-826.

20. Paredes, C. J., Alsaker, K. V., and Papoutsakis, E. T. (2005) A comparative genomic view of clostridial sporulation and physiology, *Nat Rev Microbiol 3*, 969-978.

21. Cornillot, E., Nair, R. V., Papoutsakis, E. T., and Soucaille, P. (1997) The genes for butanol and acetone formation in Clostridium acetobutylicum ATCC 824 reside on a large plasmid whose loss leads to degeneration of the strain, *J Bacteriol 179*, 5442-5447.

22. Nolling, J., Breton, G., Omelchenko, M. V., Makarova, K. S., Zeng, Q., Gibson, R., Lee, H. M., Dubois, J., Qiu, D., Hitti, J., Wolf, Y. I., Tatusov, R. L., Sabathe, F., Doucette-Stamm, L., Soucaille, P., Daly, M. J., Bennett, G. N., Koonin, E. V., and Smith, D. R. (2001) Genome sequence and comparative analysis of the solvent-producing bacterium Clostridium acetobutylicum, *J Bacteriol 183*, 4823-4838.

23. Lee, S. Y., Park, J. H., Jang, S. H., Nielsen, L. K., Kim, J., and Jung, K. S. (2008) Fermentative butanol production by Clostridia, *Biotechnol Bioeng 101*, 209-228.

24. Gheshlaghi, R., Scharer, J. M., Moo-Young, M., and Chou, C. P. (2009) Metabolic pathways of clostridia for producing butanol, *Biotechnol Adv 27*, 764-781.

25. Zhao, Y. S., Tomas, C. A., Rudolph, F. B., Papoutsakis, E. T., and Bennett, G. N. (2005) Intracellular butyryl phosphate and acetyl phosphate concentrations in Clostridium acetobutylicum and their implications for solvent formation, *Appl Environ Microb 71*, 530-537.

26. Bowles, L. K., and Ellefson, W. L. (1985) Effects of butanol on Clostridium acetobutylicum, *Appl Environ Microbiol 50*, 1165-1170.

27. Ezeji, T., Milne, C., Price, N. D., and Blaschek, H. P. (2010) Achievements and perspectives to overcome the poor solvent resistance in acetone and butanol-producing microorganisms, *Appl Microbiol Biotechnol 85*, 1697-1712.

28. Papoutsakis, E. T. (1984) Equations and calculations for fermentations of butyric acid bacteria, *Biotechnol Bioeng 26*, 174-187.

29. Edwards, J. S., and Palsson, B. O. (1999) Systems properties of the Haemophilus influenzae Rd metabolic genotype, *J Biol Chem 274*, 17410-17416.

30. Ogata, H., Goto, S., Sato, K., Fujibuchi, W., Bono, H., and Kanehisa, M. (1999) KEGG: Kyoto Encyclopedia of Genes and Genomes, *Nucleic Acids Res 27*, 29-34.

31. Karp, P. D., Ouzounis, C. A., Moore-Kochlacs, C., Goldovsky, L., Kaipa, P., Ahren, D., Tsoka, S., Darzentas, N., Kunin, V., and Lopez-Bigas, N. (2005) Expansion of the BioCyc collection of pathway/genome databases to 160 genomes, *Nucleic Acids Res 33*, 6083-6089.

32. Jankowski, M. D., Henry, C. S., Broadbelt, L. J., and Hatzimanikatis, V. (2008) Group contribution method for thermodynamic analysis of complex metabolic networks, *Biophys J 95*, 1487-1499.

33. Henry, C. S., Jankowski, M. D., Broadbelt, L. J., and Hatzimanikatis, V. (2006) Genome-scale thermodynamic analysis of Escherichia coli metabolism, *Biophys J 90*, 1453-1461.

34. Mahadevan, R. (2010) Constraint-Based Genome-Scale Models of Cellular Metabolism, In *The Metabolic Pathway Engineering Handbook* (Smolke, C. D., Ed.), Taylor & Francis Group, Boca Raton.

35. Yizhak, K., Benyamini, T., Liebermeister, W., Ruppin, E., and Shlomi, T. (2010) Integrating quantitative proteomics and metabolomics with a genome-scale metabolic network model, *Bioinformatics 26*, i255-260.

36. Price, N. D., Reed, J. L., Papin, J. A., Wiback, S. J., and Palsson, B. O. (2003) Network-based analysis of metabolic regulation in the human red blood cell, *J Theor Biol 225*, 185-194.

37. Varma, A., and Palsson, B. O. (1994) Metabolic Flux Balancing - Basic Concepts, Scientific and Practical Use, *Bio-Technol 12*, 994-998.

38. Schilling, C. H., Edwards, J. S., Letscher, D., and Palsson, B. O. (2000) Combining pathway analysis with flux balance analysis for the comprehensive study of metabolic systems, *Biotechnol Bioeng 71*, 286-306.

39. Reed, J. L., Vo, T. D., Schilling, C. H., and Palsson, B. O. (2003) An expanded genome-scale model of Escherichia coli K-12 (iJR904 GSM/GPR), *Genome Biol 4*, R54.

40. Bonarius, H. P. J., Schmid, G., and Tramper, J. (1997) Flux analysis of underdetermined metabolic networks: The quest for the missing constraints, *Trends Biotechnol 15*, 308-314.

41. Kauffman, K. J., Prakash, P., and Edwards, J. S. (2003) Advances in flux balance analysis, *Curr Opin Biotechnol 14*, 491-496.

42. Segre, D., Vitkup, D., and Church, G. M. (2002) Analysis of optimality in natural and perturbed metabolic networks, *Proc Natl Acad Sci U S A 99*, 15112-15117.

43. Shlomi, T., Berkman, O., and Ruppin, E. (2005) Regulatory on/off minimization of metabolic flux changes after genetic perturbations, *Proc Natl Acad Sci U S A 102*, 7695-7700.

44. Murabito, E., Simeonidis, E., Smallbone, K., and Swinton, J. (2009) Capturing the essence of a metabolic network: a flux balance analysis approach, *J Theor Biol 260*, 445-452.

45. Smallbone, K., and Simeonidis, E. (2009) Flux balance analysis: a geometric perspective, *J Theor Biol 258*, 311-315.

46. Burgard, A. P., Pharkya, P., and Maranas, C. D. (2003) Optknock: a bilevel programming framework for identifying gene knockout strategies for microbial strain optimization, *Biotechnol Bioeng 84*, 647-657.

47. Rocha, I., Maia, P., Evangelista, P., Vilaca, P., Soares, S., Pinto, J. P., Nielsen, J., Patil, K. R., Ferreira, E. C., and Rocha, M. (2010) OptFlux: an open-source software platform for in silico metabolic engineering, *BMC Syst Biol 4*, 45.

48. Kim, J., and Reed, J. L. (2010) OptORF: Optimal metabolic and regulatory perturbations for metabolic engineering of microbial strains, *BMC Syst Biol 4*, 53.

49. Price, N. D., Reed, J. L., and Palsson, B. O. (2004) Genome-scale models of microbial cells: evaluating the consequences of constraints, *Nat Rev Microbiol 2*, 886-897.

50. Kim, H. U., Kim, T. Y., and Lee, S. Y. (2010) Genome-scale metabolic network analysis and drug targeting of multi-drug resistant pathogen Acinetobacter baumannii AYE, *Mol Biosyst 6*, 339-348.

51. Plata, G., Hsiao, T. L., Olszewski, K. L., Llinas, M., and Vitkup, D. (2010) Reconstruction and flux-balance analysis of the Plasmodium falciparum metabolic network, *Mol Syst Biol 6*, 408.

52. Blandin, S., Moita, L. F., Kocher, T., Wilm, M., Kafatos, F. C., and Levashina, E. A. (2002) Reverse genetics in the mosquito Anopheles gambiae: targeted disruption of the Defensin gene, *Embo Reports 3*, 852-856.

53. Senger, R. S., and Papoutsakis, E. T. (2008) Genome-scale model for Clostridium acetobutylicum: Part II. Development of specific proton flux states and numerically determined sub-systems, *Biotechnol Bioeng 101*, 1053-1071.

54. Casey, J. R., Grinstein, S., and Orlowski, J. (2010) Sensors and regulators of intracellular pH, *Nat Rev Mol Cell Biol 11*, 50-61.

55. Husemann, M. H. W., and Papoutsakis, E. T. (1989) Comparison between Invivo and Invitro Enzyme-Activities in Continuous and Batch Fermentations of Clostridium-Acetobutylicum, *Appl Microbiol Biot 30*, 585-595.

56. Szegezdi, J., and Csizmadia, F. (2004) Prediction of distribution coefficient using microconstants., *Abstr Pap Am Chem S 227*, U1019-U1019.

57. Szegezdi, J., and Csizmadia, F. (2007) A method for calculating the pKa values of small and large molecules, In *American Chemical Society Spring Meeting*.

58. Harris, D. C. (1995) *Quantitative Chemical Analysis*, 4 ed., W.H. Freeman and Company, New York.

59. Kell, D. B., Peck, M. W., Rodger, G., and Morris, J. G. (1981) On the permeability to weak acids and bases of the cytoplasmic membrane of Clostridium pasteurianum, *Biochem Biophys Res Commun 99*, 81-88.

60. Law, C. J., Maloney, P. C., and Wang, D. N. (2008) Ins and outs of major facilitator superfamily antiporters, *Annu Rev Microbiol 62,* 289-305.

61. Senger, R. S., and Papoutsakis, E. T. (2008) Genome-scale model for Clostridium acetobutylicum: Part I. Metabolic network resolution and analysis, *Biotechnol Bioeng 101*, 1036-1052.

62. Desai, R. P., Nielsen, L. K., and Papoutsakis, E. T. (1999) Stoichiometric modeling of Clostridium acetobutylicum fermentations with non-linear constraints, *J Biotechnol 71*, 191-205.

63. Lee, J., Yun, H., Feist, A. M., Palsson, B. O., and Lee, S. Y. (2008) Genome-scale reconstruction and in silico analysis of the *Clostridium acetobutylicum* ATCC 824 metabolic network, *Appl Microbiol Biotechnol 80*, 849-862.

64. Fond, O., Mattaammouri, G., Petitdemange, H., and Engasser, J. M. (1985) The Role of Acids on the Production of Acetone and Butanol by Clostridium-Acetobutylicum, *Appl Microbiol Biot 22*, 195-200.

65. Datta, R., and Zeikus, J. G. (1985) Modulation of acetone-butanol-ethanol fermentation by carbon monoxide and organic acids, *Appl Environ Microbiol 49*, 522-529.

66. Zhang, H., Bruns, M. A., and Logan, B. E. (2006) Biological hydrogen production by Clostridium acetobutylicum in an unsaturated flow reactor, *Water Res 40*, 728-734.

67. Kim, B. H., Bellows, P., Datta, R., and Zeikus, J. G. (1984) Control of Carbon and Electron Flow in Clostridium acetobutylicum Fermentations: Utilization of Carbon Monoxide to Inhibit Hydrogen Production and to Enhance Butanol Yields, *Appl Environ Microbiol 48*, 764-770.

68. Chen, J. S., Toth, J., and Kasap, M. (2001) Nitrogen-fixation genes and nitrogenase activity in Clostridium acetobutylicum and Clostridium beijerinckii, *J Ind Microbiol Biotechnol 27*, 281-286.

69. Chen, J. S., and Johnson, J. L. (1993) Molecular biology of nitrogen fixation in the clostridia, *Biotechnology 25*, 371-392.

70. Desai, R. P., Nielsen, L. K., and Papoutsakis, E. T. (1999) Stoichiometric modeling of Clostridium acetobutylicum fermentations with non-linear constraints, *Journal of Biotechnology 71*, 191-205.

71. Amador-Noguez, D., Feng, X. J., Fan, J., Roquet, N., Rabitz, H., and Rabinowitz, J. D. (2010) Systems-level metabolic flux profiling elucidates a complete, bifurcated tricarboxylic acid cycle in Clostridium acetobutylicum, *J Bacteriol 192*, 4452-4461.

72. Crown, S. B., Indurthi, D. C., Ahn, W. S., Choi, J., Papoutsakis, E. T., and Antoniewicz, M. R. (2011) Resolving the TCA cycle and pentose-phosphate pathway of Clostridium acetobutylicum ATCC 824: Isotopomer analysis, in vitro activities and expression analysis, *Biotechnol J 6*, 300-305.

73. Calhoun, M. W., Oden, K. L., Gennis, R. B., de Mattos, M. J., and Neijssel, O. M. (1993) Energetic efficiency of Escherichia coli: effects of mutations in components of the aerobic respiratory chain, *J Bacteriol 175*, 3020-3025.

74. Noguchi, Y., Nakai, Y., Shimba, N., Toyosaki, H., Kawahara, Y., Sugimoto, S., and Suzuki, E. (2004) The energetic conversion competence of Escherichia coli during aerobic respiration studied by 31P NMR using a circulating fermentation system, *J Biochem 136*, 509-515.

75. Taymaz-Nikerel, H., Borujeni, A. E., Verheijen, P. J., Heijnen, J. J., and van Gulik, W. M. (2010) Genome-derived minimal metabolic models for Escherichia coli MG1655 with estimated in vivo respiratory ATP stoichiometry, *Biotechnol Bioeng 107*, 369-381.

76. Famili, I., Forster, J., Nielsen, J., and Palsson, B. O. (2003) Saccharomyces cerevisiae phenotypes can be predicted by using constraint-based analysis of a genome-scale reconstructed metabolic network, *Proc Natl Acad Sci U S A 100*, 13134-13139.

77. Feist, A. M., Henry, C. S., Reed, J. L., Krummenacker, M., Joyce, A. R., Karp, P. D., Broadbelt, L. J., Hatzimanikatis, V., and Palsson, B. O. (2007) A genome-scale metabolic reconstruction for Escherichia coli K-12 MG1655 that accounts for 1260 ORFs and thermodynamic information, *Mol Syst Biol 3*, 121.

78. Galkin, A. S., Grivennikova, V. G., and Vinogradov, A. D. (1999) -->H+/2e- stoichiometry in NADH-quinone reductase reactions catalyzed by bovine heart submitochondrial particles, *FEBS Lett 451*, 157-161.

79. Falk-Krzesinski, H. J., and Wolfe, A. J. (1998) Genetic analysis of the nuo locus, which encodes the proton-translocating NADH dehydrogenase in Escherichia coli, *J Bacteriol 180*, 1174-1184.

80. Torres-Bacete, J., Nakamaru-Ogiso, E., Matsuno-Yagi, A., and Yagi, T. (2007) Characterization of the NuoM (ND4) subunit in Escherichia coli NDH-1: conserved charged residues essential for energy-coupled activities, *J Biol Chem 282*, 36914-36922.

81. Kao, M. C., Nakamaru-Ogiso, E., Matsuno-Yagi, A., and Yagi, T. (2005) Characterization of the membrane domain subunit NuoK (ND4L) of the NADH-quinone oxidoreductase from Escherichia coli, *Biochemistry 44*, 9545-9554.

82. Brown, T. R., Ugurbil, K., and Shulman, R. G. (1977) 31P nuclear magnetic resonance measurements of ATPase kinetics in aerobic Escherichia coli cells, *Proc Natl Acad Sci U S A 74*, 5551-5553.

83. Sheldon, J. G., Williams, S. P., Fulton, A. M., and Brindle, K. M. (1996) 31P NMR magnetization transfer study of the control of ATP turnover in Saccharomyces cerevisiae, *Proc Natl Acad Sci U S A 93*, 6399-6404.

3. Materials and Methods

3.1. Creating a new database of chemical compounds for genome-scale modeling

Genome-scale models are comprised of compounds and reactions that are given unique identifiers to facilitate computer programming and matrix formation. Different research groups commonly use different sets of identifiers, making comparisons between models very difficult. A database of compound information was created to link and unify all information related to chemical compounds used in genome-scale models. Metabolic information retrieved for entries in the compound database included: (i) compound identifiers (IDs) from KEGG (e.g.,C00001) and BiGG (e.g., h2o) databases, (ii) metabolite names, (iii) formulas, (iv) weights, and (v) formal charges at pH 7. Metabolite entries from other models and databases were combined into the same compound entry in this database by performing cross-checks between information. In particular, ".mol" files for all known compounds were extracted from the KEGG database. A ".mol" file contains information about (i) atoms, (ii) bonds, (iii) connectivity, and (iv) internal coordinates of a molecule. An example of a ".mol" file for pyruvate is given as Fig. 3.1. These ".mol" files were used for calculating pK_a values and the standard Gibbs free energy of formation $\left(\Delta G^0_{formation}\right)$ values for each compound available in the Kyoto Encyclopedia of Genes and Genomes (KEGG) database (*1*). The pK_a values were calculated from ".mol" files using the Marvin program from ChemAxon (*2*). All pK_a values were calculated according to a temperature of 47°C and pressure of 1 atm. A MATLAB code was written that automatically performed these calculations by extracting ".mol" files one by one from KEGG and running Marvin as a stand-alone program for each of the 14,050 entries. In the same way, the ".mol" files were also used to calculate the $\Delta G^0_{formation}$ values using a group contribution method

(GCM) thermodynamic calculator (*3*). The GCM program calculates $\Delta G^0_{formation}$ values based on the molecular substructure groups that make up a molecule.

```
C3H6O3
APtclcactv06101115253D 0   0.00000     0.00000     1

 12 11  0  0  0  0  0  0  0  0999 V2000
    1.2238   -1.3378   -0.4611 C   0  0  0  0  0  0  0  0  0  0  0  0
    0.7085   -0.2031    0.4264 C   0  0  0  0  0  0  0  0  0  0  0  0
    1.5245    0.9552    0.2406 O   0  0  0  0  0  0  0  0  0  0  0  0
   -0.7151    0.1202    0.0524 C   0  0  0  0  0  0  0  0  0  0  0  0
   -0.9858    1.1994   -0.4187 O   0  0  0  0  0  0  0  0  0  0  0  0
   -1.6824   -0.7908    0.2426 O   0  0  0  0  0  0  0  0  0  0  0  0
    2.2535   -1.5716   -0.1906 H   0  0  0  0  0  0  0  0  0  0  0  0
    0.6014   -2.2212   -0.3194 H   0  0  0  0  0  0  0  0  0  0  0  0
    1.1838   -1.0288   -1.5057 H   0  0  0  0  0  0  0  0  0  0  0  0
    0.7485   -0.5120    1.4710 H   0  0  0  0  0  0  0  0  0  0  0  0
    1.4612    1.1947   -0.6941 H   0  0  0  0  0  0  0  0  0  0  0  0
   -2.5959   -0.5833    0.0026 H   0  0  0  0  0  0  0  0  0  0  0  0
  1  2  1  0  0  0  0
  2  3  1  0  0  0  0
  2  4  1  0  0  0  0
  4  5  2  0  0  0  0
  4  6  1  0  0  0  0
  1  7  1  0  0  0  0
  1  8  1  0  0  0  0
  1  9  1  0  0  0  0
  2 10  1  0  0  0  0
  3 11  1  0  0  0  0
  6 12  1  0  0  0  0
M  END
$$$$
```

Fig. 3.1. The ".mol" file for pyruvate downloaded from the KEGG database.

3.2. Construction of the new *C. acetobutylicum* model, *iMM864*

A new genome-scale model for *C. acetobutylicum* ATCC 824 was created using the *iRS552* model (*4*, *5*) as a base. The following modifications to the *iRS552* model were made to create the *iMM864* model: (i) full pH balancing using pK_a values for all metabolites, (ii) compartmentalizing metabolites, (iii) changing the metabolite identification system in use, (iv) adding new reactions, and (v) modifying bounds and reversibility of reactions based on thermodynamic calculations (*3*). In the original *iRS552* model, compartmentalization was not considered and transport reactions were treated as "exchange reactions." Ultimately, this meant

chemical reactions could only occur inside the cell and not in the extracellular environment. The system boundary was the membrane of the cell itself. As *C. acetobutylicum* is a gram-positive bacterium, the model only needs two compartments: (i) the cytosol and (ii) the extracellular environment. Thus, compartmentalization was considered by adding '[c]' and '[e]' after metabolite identifiers (IDs) for those in the "cytosolic" and "extracellular" compartments, respectively. Fig. 3.2 provides an example of butanol transport reaction across the cell membrane from the cytoplasm [c] to the extracellular environment [e]. The transport reaction is represented in this figure using compound IDs and compartmentalization. Fig. 3.3 shows how this transport reaction is represented in the stoichiometric matrix. These updates allowed transport reactions to exchange metabolites between the cytosolic and extracellular compartments. This put the system boundary around the extracellular media instead of the cell itself. To complete flux balancing, "exchange reactions" were added that allowed all metabolites that crossed the cell membrane to be exported out of the system boundary. This formalism for flux balance analysis has existed since the first genome-scale models were created (*6*).

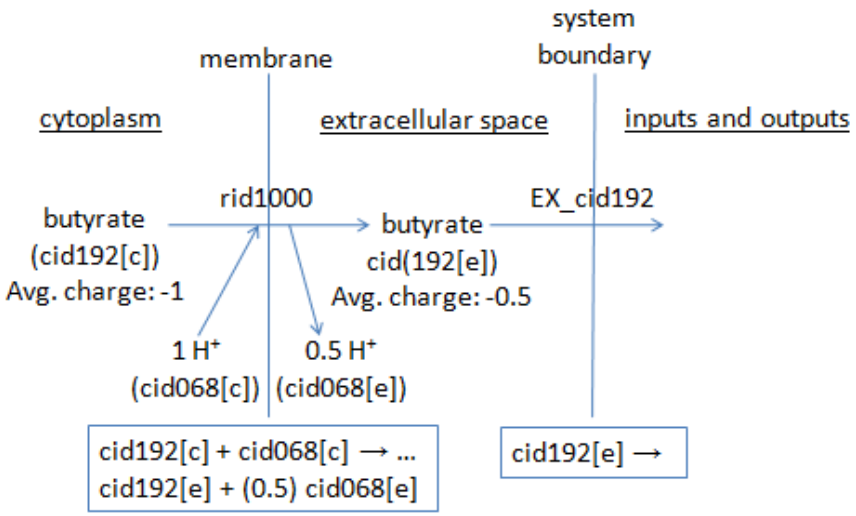

Fig 3.2. Example transport reaction of butyrate being excreted from the cell cytoplasm [c] into the extracellular space [e] (i.e., the culture media), and exchange reaction for butyrate.

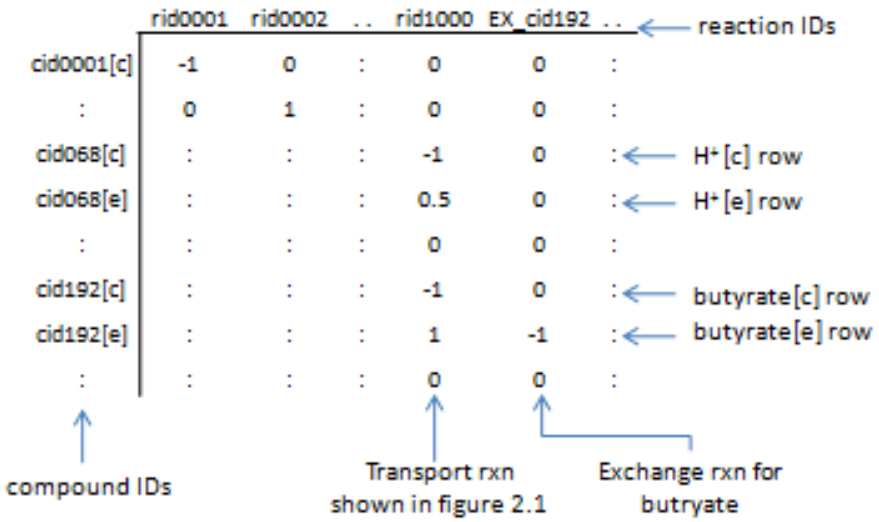

Fig 3.3. Representation of the reactions of Fig. 3.2 in the stoichiometric matrix.

To build the *iMM864* model, 230 new reactions occurring in the cytoplasm were added to the *iRS552* model. These new reactions were found as recent updates to the KEGG database (*1*), as well as from new insights provided by literature, including updates on central carbon metabolism (*7*, *8*). Metabolites involved in these reactions were added to the compound database and metabolite IDs were synchronized in an automated manner. Duplicate IDs in the database and in the new reactions were identified manually and updated.

Constraints in the *iMM864* model were modified from the *iRS552* model according to a thermodynamic analysis. The standard Gibbs free energy of reaction ($\Delta G^0_{reaction}$) was calculated from the $\Delta G^0_{formation}$ values of reactants and products for each reaction. The method described by Henry et al. (*9*) was used to determine the possible range of $\Delta G'_{reaction}$ (which differ from the standard $\Delta G^0_{reaction}$) values that each reaction could have. Ranges of $\Delta G'_{reaction}$ values were determined, since the $\Delta G'_{reaction}$ is a function of metabolite concentrations. To do this, minimum and maximum possible $\Delta G'_{reaction}$ values were calculated given uncertainties in metabolite

concentrations. Calculations included the minimum and maximum metabolic concentrations of 20 mM and 10 μM, respectively, for reactants and products. This analysis was used to determine reaction reversibility constraints. Reactions with only negative possible $\Delta G'_{reaction}$ values (given metabolite concentrations of 20 mM and 10 μM) are assumed to only progress in the "forward" direction, those with only positive values are assumed to only progress in the "reverse" direction. Those reactions that included both positive and negative values in their range of $\Delta G'_{reaction}$ values were assumed "reversible" reactions (may proceed in either direction). A summary of these thermodynamic rules to determine reaction reversibility is shown in Table 3.1. Several reactions of the *iRS552* model were found to have reversibility constraints inconsistent with the thermodynamic calculations. Constraints for these reactions were then modified manually, while also taking into account essentialities and known pathway directions.

Table 3.1. Example of reaction reversibilities using $\Delta G'_{reaction}$ calculations.

$\Delta G'_{rxn}$ conditions	Reaction direction
$\Delta G'_{rxn,max} > 0$ and $\Delta G'_{rxn,min} < 0$	$A + B \leftrightarrow C + D$
$\Delta G'_{rxn,max} < 0$ and $\Delta G'_{rxn,min} < 0$	$A + B \rightarrow C + D$
$\Delta G'_{rxn,max} > 0$ and $\Delta G'_{rxn,min} > 0$	$A + B \leftarrow C + D$

3.3. Proton balancing algorithm

A novel proton balancing algorithm was developed using pK_a information for all metabolites in the cell. This method modifies the stoichiometry of protons in each metabolic reaction according to user-specified pH values for each of the different compartments. The algorithm calculates average charges for all metabolites given pK_a values and pH input. This allows precise proton balancing for each reaction and across membranes, where pH conditions

are often different. As an example, the monoprotic hydrofluoric acid (HF) dissociates partially in water to yield F^- and H^+ ions, while the protonated HF species remains in solution as well (depending on the pH). The dissociation constant (K_a) of HF is $6.76 * 10^{-4}$ M at a temperature of 25°C and pressure of 1 atm. The dissociation constant is also an equilibrium constant and is described by Eq. 3.1.

$$K_a = \frac{[H^+][F^-]}{[HF]} \qquad Eq. 3.1$$

So, the relative amount of each species can be calculated given the pH ($pH = -log([H^+])$. For the above example, an input pH of 4, yields $[H^+]=10^{-4}$ M. This yields the following relationship between protonated and unprotonated fluorine.

$$\frac{[F^-]}{[HF]} = \frac{K_a}{[H^+]} = \frac{6.76*10^{-4}}{10^{-4}} = 6.76 \qquad Eq. 3.2$$

For every 1 M of undissociated HF present in solution, there are 6.76 M of dissociated F^-. This also means that, for fluoride, 87% [(6.76 M HF) / (1 M F^- + 6.76 M HF)] will be in its deprotonated form (which carries a -1 charge). The remaining 13% will be in the protonated (HF) form (which carries a neutral charge). So, the average charge of this species at the specified pH is calculated as shown in Eq. 3.3.

$$0.87 * (-1) + 0.13 * (0) = -0.87 \qquad Eq. 3.3$$

A more complex example involves the molecule AH_2, which can be protonated (or deprotonated) to yield the five species: (i) AH_4^{2+}, (ii) AH_3^+, (iii) AH_2, (iv) AH^-, and (v) A^{2-}. With this, it will have the following dissociation constants: (i) K_{b2}, (ii) K_{b1}, (iii) K_{a1}, and (iv) K_{b2}. The basic dissociation constants (K_{b1} and K_{b2}) can be inverted to yield K_{a-1} and K_{a-2}.

$$K_{a-2} = \frac{[AH_3^+][H^+]}{[AH_4^{2+}]}$$

$$K_{a-1} = \frac{[AH_2][H^+]}{[AH_3^+]}$$

$$K_{a1} = \frac{[AH^-][H^+]}{[AH_2]}$$

$$K_{a2} = \frac{[A^{2-}][H^+]}{[AH^-]} \qquad Eq.3.4$$

The relative composition (R) of each species is used to find the percent composition of each species. In general, it is calculated using Eq. 3.5 (*10*).

$$R_1 = [H^+]^{n-1}$$

$$R_{1+i} = R_i * \frac{K_{a_i}}{[H^+]} \qquad Eq.3.5$$

Here, R_1 is the relative composition of the most protonated species (e.g., AH_4^{2+}), n is the total number of ionized species (e.g., 5 for the above example), R_{1+i} is the relative composition of the species that contains 'i' less protons than that of the most protonated species, and K_{ai} is the i^{th} K_a value when K_a values are ordered from most basic to most acidic. Using the example of AH_2, the relative composition for each of its species are as follows:

$$R_1([AH_4^{2+}]) = [H^+]^4$$

$$R_2([AH_3^+]) = K_{a2} * [H^+]^3$$

$$R_3([AH_2]) = K_{a1} * K_{a2} * [H^+]^2$$

$$R_4([AH^-]) = K_{a-1} * K_{a1} * K_{a2} * [H^+]$$

$$R_5([A^{2-}]) = K_{a-2} * K_{a-1} * K_{a1} * K_{a2} \qquad Eq.3.6$$

The percent composition (P_i) of species (*i*) can be calculated from the relative composition of that species (R_i) and the relative compositions of all *n* species, as shown in Eq. 3.7.

$$P_i = \frac{R_i}{\sum_{a=1}^{n} R_a} * 100 \qquad Eq.3.7$$

Finally, the average charge of a metabolite (C) is calculated by the Eq. 3.8, where C_i is the charge of species i.

$$\mathrm{C} = \sum_{i=1}^{n} \left(\frac{P_i}{100} * C_i \right) \qquad Eq. 3.8$$

Once the average charge of each species is calculated, the algorithm modifies the proton stoichiometry of all reactions through charge balancing. To do this, reactions are categorized into "transport reactions" and "non-transport reactions." A transport reaction is one that crosses a membrane. This is an important distinction because often the pH is different on either side of a biological membrane in a cell. Thus, transport reactions are balanced differently from non-transport reactions. Reactions involving metabolites in only one compartment (non-transport reactions) are charge balanced easily, and only the stoichiometric coefficient of protons (in the appropriate compartment) must be modified in the stoichiometric matrix. The following example involving the reaction catalyzed by the pyruvate kinase enzyme is presented below.

$$ATP + Pyruvate + H_2O \leftrightarrow AMP + Phosphoenolpyruvate + \cdots$$
$$Orthophosphate + H^+ \qquad Eq. 3.9$$

The average charge calculated for each metabolite is shown in Table 3.2 for two different pH values.

Table 3.2. Average charges for a reaction catalyzed by a pyruvate kinase.

Metabolite	**Average charge (pH=5.5)**	**Average charge (pH=7.2)**
ATP	-3.0	-3.4
Pyruvate	-1.0	-1.0
H2O	0.0	0.0
AMP	-1.1	-1.9
Phosphoenolpyruvate	-2.2	-2.9
Orthophosphate	-1.6	-1.0
H^+	1.0	1.0
Σ reactants	-4	-4.4
Σ products	-3.9	-4.8
Δ(Σ react. - Σ prod.)	-0.1	0.4

Given a pH of 5.5, the additional H^+ that must be added to the right-hand side of Eq. 3.9 to complete the charge balancing between reactants and products is calculated as follows (using values from Table 3.2 and metabolites from Eq. 3.9).

$$(-3.0 - 1.0 + 0) - (-1.1 - 2.2 - 1.6 + 1) = -0.1 \qquad Eq.\,3.10$$

So, the proton balanced final reaction at pH 5.5 is shown in Eq. 3.11.

$$ATP + Pyruvate + H_2O \leftrightarrow AMP + Phosphoenolpyruvate + \cdots$$
$$+ Orthophosphate + 0.9H^+ \qquad Eq.\,3.11$$

Similarly, at pH 7.2, the additional H^+ to add on the right hand side is calculated as follows.

$$(-3.4 - 1.0) - (-1.9 - 2.9 - 1.0 + 1) = -0.4 \qquad Eq.\,3.12$$

The proton balanced equation at pH 7.2 is given in Eq. 3.13. This is significantly different from the balanced equation at pH 5.5 (Eq. 3.11).

$$ATP + Pyruvate + H_2O \leftrightarrow AMP + Phosphoenolpyruvate + \cdots$$
$$Orthophosphate + 0.6H^+ \qquad Eq.\,3.13$$

Proton balancing for membrane transport reactions is a much more complex process. In this case, it is likely that more than one row of the stoichiometric matrix must be altered (not just for protons in one compartment as shown in Eqs. 3.11 and 3.13). Proton balancing in transport reactions may be further complicated by the following possibilities: (i) protons may be transported themselves via symport or antiport mechanisms, or (ii) the transport mechanism may be selective for a species of a specific charge. To accommodate this, transport reactions were further categorized into those that are "selective" in terms of species charge, and those that are "non-selective." The "non-selective" transport mechanisms are assumed to be able to transport metabolites in all possible states of protonation (or deprotonation). The "selective" transport reactions, on the other hand, are able to transport only species that have a specific charge. For example, diffusion across a cell membrane only occurs with molecules of neutral charge. So a metabolite involved in this transport reaction must first be protonated (or deprotonated) to its neutrally charged state before diffusing. The difference between these two reaction mechanisms significantly affects the total number of protons that move across the cell membrane along with the metabolite.

Transport reactions that are labeled as "selective" towards a certain species charge are balanced according to the difference between (i) the average charge in the respective compartment and (ii) the charge that the transporter is selective towards. Transport reactions are labeled in the reaction identification string by having "_S" along with the charge specificity. The algorithm checks reaction identification for this specificity identifier before proton-balancing a reaction. An example of charge balancing a "selective" transport reaction is presented in Eqs. 3.14 and 3.15. This example uses transport of a metabolite A, in which the average charge of A in both compartments is -1 and only the neutrally charged species is transported. The

extracellular [e] and cytoplasm [c] compartments are used in this example. The unbalanced reaction is given in Eq. 3.14.

$$A^{-1}[e] \rightarrow A^{-1}[c] \qquad Eq.3.14$$

The charge balanced form of this transport reaction is shown as Eq. 3.15.

$$A^{-1}[e] + H^{+}[e] \rightarrow A^{-1}[c] + H^{+}[c] \qquad Eq.3.15$$

This charge balancing procedure results in the net transport of one proton from the extracellular [e] environment to the cytoplasm [c]. This does not occur in the unbalanced reaction (Eq. 3.14). In the charge balancing procedure, it is assumed that the metabolite is protonated (or deprotonated) to the species that the transporter is selective towards. This metabolite then moves into the other compartment and is protonated (or deprotonated) according to the pH in that compartment. Reaction direction in this case makes no difference in the charge balanced equation.

For the case of "non-selective" transport reactions, it is assumed that metabolites are readily transported and then protonated (or deprotonated) depending on the pH of the new compartment (not the compartment where they originated). The strategy developed for these reactions was to split the reaction into simpler "sub-reactions," and then proton balance each sub-reaction to determine the final proton stoichiometry in the total reaction. Because these transport mechanisms have no specificity in terms of protonated (or deprotonated) species, only the stoichiometry of protons in the destination compartment must be modified. Proton balancing for all "sub-reactions" is done in the same way. In mathematical terms, the number of protons that are added to the compartment containing the product is calculated by subtracting the average charges of the products from the average charges of the substrates. The following rules have

been developed for forming "sub-reactions", and examples are given for each of the rules listed below.

1) Product metabolites are matched with substrate metabolites. This is shown in Eqs. 3.16 and 3.17 and is important for keeping an antiporter or symporter mechanism in place.

$$A[e] + B[c] \rightarrow A[c] + B[e] \qquad Eq. 3.16$$

This transport reaction is split into the following "sub-reactions."

a) $A[e] \rightarrow \mathrm{A[c]}$

b) $B[c] \rightarrow \mathrm{B[e]}$ Eq. 3.17

Most transport reactions involve only the transport of a metabolite without modifying it, so this step is used by itself to assess most transport reactions. However, more complicated reactions exist in which a metabolite is altered (i.e. phosphorylated) while being transported, so the other rules have been created for those cases.

2) When a chemical reaction takes place in a membrane transporter, the reaction is split into separate "sub-reactions." These reactions are identified by the algorithm by first checking if substrates are involved in one compartment, while a product is involved in another. The following example in Eq. 3.18 is presented for this case.

$$A[c] + B[c] \rightarrow C[c] + D[e] \qquad Eq. 3.18$$

The reaction is split into the "sub-reactions" given as Eqs. 3.19 and 3.20. Product D is assumed to be made in the cytoplasm and then exported into the extracellular environment.

$$A[c] + B[c] \rightarrow C[c] + D[c] \qquad Eq. 3.19$$

$$D[c] \rightarrow D[e] \qquad Eq. 3.20$$

From here, Eq. 3.19 is charge-balanced within the single compartment and Eq. 3.20 is balanced according to Rule 1 (see above). To complete the charge balancing, protons added to balance Eqs. 3.19 and 3.20 are then transferred to Eq. 3.18.

3) When all products of the transporter reaction are in the same compartment, the reaction is balanced easily. An example of this scenario is shown in Eq. 3.21. It does not matter which compartments the substrates are in, so the reaction can be balanced as though it is not a transport reaction, as long as the average charge for A[e] is calculated from the pH in the [e] compartment.

$$A[e] + B[c] \rightarrow A[c] + D[c] \qquad Eq. 3.21$$

4) Any remainder of the reaction not covered by the previous rules is split according to the compartments of reactants and products. Reactions covered by this final rule are proton-balanced as though they consist of separate reactions in different compartments, with no net charge moving across the membrane.

All "non-selective" transport reactions must be constrained as "irreversible" in order to preserve accuracy of the proton balancing, since the resulting proton stoichiometry is affected by reaction direction. Because of this requirement, the algorithm has been fitted with the option of creating a copy of a "non-selective" transport reaction that operates in reverse whenever it encounters one that is reversible. When using this option, however, reaction flux may flow "in" through one transporter and "out" through the other simultaneously. The only way to resolve this network singularity is to minimize the total flux of the system or constrain one of the reaction directions to zero flux.

How to identify transport reactions as "selective" or "non-selective" must be determined experimentally. From a genome-scale modeling perspective, it is not known whether transport reactions that have not been studied experimentally should be treated as "selective" or "non-selective." It is recommended that future simulations determine the overall impact of treating all transport reactions as "selective" or "non-selective.".

The following examples are presented detailing the use of this algorithm for "non-selective" transport reactions in the *E. coli* K12 MG1655 *iAF1260* model (*6*). The formalism for identifying compounds and reactions in the *iAF1260* model is used in the following examples.

Reaction NO3R1bpp: catalyzed by Nitrate reductase

$$no3[p] + q8h\,[c] \rightarrow h2o[p] + no2[p] + q8[c] \qquad Eq.\,3.22$$

Table 3.3. Compounds and average charges of NO3R1bpp.

Compound ID	Compound Name	Average Charge (pH 7)
$no3[p]$	Nitrate	-1
$q8h2[c]$	Ubiquinol	0
$h2o[p]$	Water	0
$no2[p]$	Nitrite	-0.9998
$q8[c]$	Ubiquinone	0

Since none of the compounds on the product side match any on the substrate side, the reaction is split into "sub-reactions" according to the different compartments (Rule 4). Then the reaction in each compartment is charge balanced as shown in Table 3.4.

Table 3.4. Sub-reactions and proton balancing for NO3R1bpp.

Compartment	Reaction	Proton Balancing
[p]	$no3 \rightarrow h2o + no2$	H^+ added: -1 – (-0.9998) = -0.0002
[c]	$q8h2 \rightarrow q8$	H^+ added: 0 – 0 = 0

Since the number of protons added to the [p] compartment is negative, they are added to the reactants side of the equation. This yields the final proton balanced reaction, shown as Eq. 3.23.

$$no3[p] + q8h2[c] + 0.0002\, h[p] \rightarrow h2o[p] + no2[p] + q8[c] \qquad Eq.3.23$$

The overall transport mechanism of 2 protons and 2 electrons going from the cytosol into the periplasm is kept intact.

Reaction GAM6Pt6_2pp: catalyzed by glucosamine 6-phosphate, phosphate antiporter

$$Gam6p[p] + (2)pi[c] \rightarrow gam6p[c] + (2)pi[p] \qquad Eq.3.24$$

Table 3.5. Compounds and average charges of GAM6Pt6_2pp.

Compound ID	Compound Name	Average Charge (pH 7)
$gam6p[p]$	Glucosamine 6-phosphate	-1.5
$pi[c]$	Orthophosphate	-2
$gam6p[c]$	Glucosamine 6-phosphate	-1
$pi[p]$	Phosphate	-2

In this example, metabolites are matched on either side of the reaction, yielding two "sub-reactions" from Rule 1. These reactions and proton balancing for each is given in Table 3.6.

Table 3.6. Sub-reactions and proton balancing for GAM6Pt6_2pp.

Reaction	Proton Balancing
$gam6p[p] \rightarrow gam6p[c]$	H^+ added: -1.5 – (-1) = -0.5
$(2)pi[c] \rightarrow (2)pi[p]$	H^+ added: 2*(-2) – 2*(-2) = 0

The charge balancing of the first "sub-reaction" yields 0.5 protons should be added to the reactant side of the equation. However, the "non-selective" approach adds these to the [c] compartment, and the "selective" approach adds these to the [p] compartment. This is a good example of where "selective" and "non-selective" approaches can lead to ambiguous results. If the "non-selective" approach is taken, protons are added to the left-hand side in the [c] compartment, yielding the final reaction in Eq. 3.25. Proton antiporters are balanced the same way. Simulation studies were designed to reveal the impact of the questions that arise from this example.

$$gam6p[p] + (2)pi[c] + 0.5\, h[c] \rightarrow gam6p[c] + (2)pi[p] \qquad Eq.\,3.25$$

Reaction MPTG: catalyzed by murein polymerizing transglycosylase

$$(2)uaagmda[c] \rightarrow (2)h[c] + murein5p5p[p] + (2)udcpdp[c] \qquad Eq.\,3.26$$

Table 3.7. Compounds and average charges for MPTG.

Compound ID	Compound Name	Average Charge (pH 7)
$uaagmda[c]$	Peptidoglycan Unit (tv)	-4
$h[c]$	Proton	1
$murein5p5p[p]$	GlcNac-MurNac-pentapeptide (x2)	-4
$murein5p5p[c]$	GlcNac-MurNac-pentapeptide (x2)	-3
$udcpdp[c]$	Undecaprenyl diphosphate	-3

Here, Rule 2 is used to break the reaction into the following "sub-reactions" given in Table 3.8. In this example, the product "murein5p5p" is synthesized in the [c] compartment then transported to the [p] compartment.

Table 3.8. Sub-reactions and proton balancing for MPTG.

Reaction	Proton Balancing
$(2)uaagmda[c] \rightarrow\ (2)\ h[c]\ +\ murein5p5p[c]\ +\ (2)\ udcpdp[c]$	H^+ added to [c]: -8 – (2*1-3-6) = -1
murein5p5p[c] → murein5p5p[p]	H^+ added to [p]: -3 – (-4) = 1

In the first "sub-reaction," a proton is added to the [c] compartment on the reactant side of the equation. This cancels with one of the protons in the [c] compartment on the product side. The second "sub-reaction" is balanced by adding a proton in the [p] compartment to the product side. This result is returned regardless of whether the "selective" or "non-selective" approach is used. Combining the "sub-reactions" gives the final reaction as Eq. 3.27.

$$(2)uaagmda[c] \rightarrow\ h[p] +\ h[c] + murein5p5p[p] +\ (2)udcpdp[c] \qquad Eq.\,3.27$$

3.4. Constraining reaction ratios

A novel method for constraining reaction flux ratios in a metabolic network was developed. The overall objective of this method is to provide a solution for singularities in a reaction network (where the use of one metabolic pathway yields the overall same result as the use of another)This method is best described by example. The Papoutsakis Lab (*11*) found that the rates of butyrate and acetate re-uptake by *C. acetobutylicum* were related by the ratio given in Eq. 3.28.

$$\frac{rBYUP}{rACUP} = 0.315\frac{[butyrate]_{ext}}{[acetate]_{ext}} \qquad Eq.\,3.28$$

This equation states that the ratio of flux of butyrate re-uptake (rBYUP) to that of acetate re-uptake (rACUP) is proportional to the ratio of the extracellular butyrate to acetate concentrations. This ratio is critical for defining *C. acetobutylicum* metabolism during solventogenesis. In this research, a novel method was developed to add Eq. 3.28 to the stoichiometric matrix. Since $S \cdot v = 0$, the flux ratio was re-arranged and set equal to zero, as shown in Eq. 3.29.

$$rBYUP - \left(\frac{0.315[butyrate]_{ext}}{[acetate]_{ext}}\right) rACUP = 0 \qquad Eq.\,3.29$$

In this form, the flux ratio can be added directly to the stoichiometric matrix. This addition requires a new row in the stoichiometric matrix as shown in Fig. 3.4.

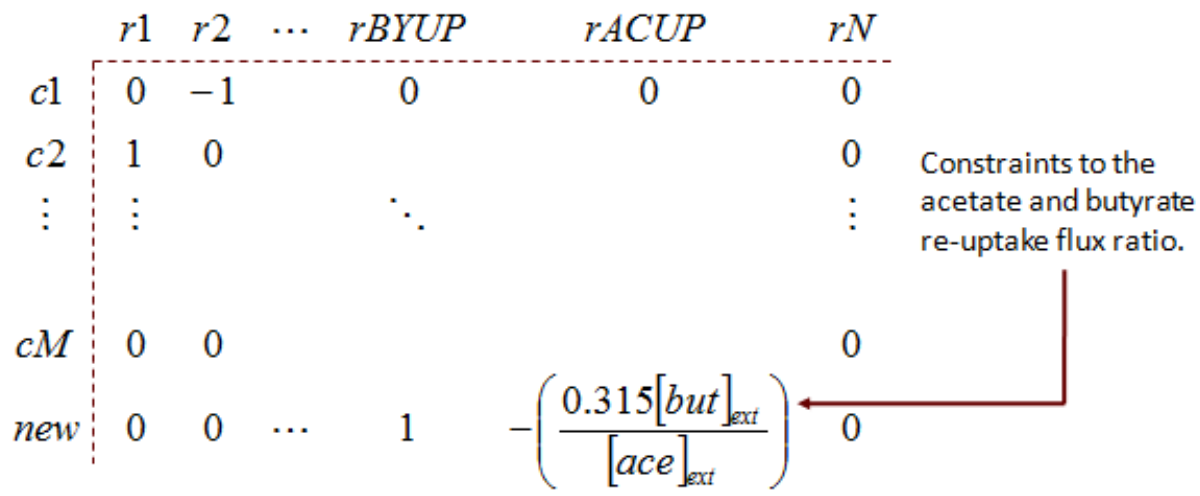

Fig. 3.4. Addition of the flux ratio constraints for acetate and butyrate re-uptake into a stoichiometric matrix of a genome-scale model.

This method was used to constrain the specific proton flux and the P/O ratio in relevant *in silico* simulations, as well as ratios between a few other reactions in other simulations. The

specific proton flux is defined as the net number of protons being transported across the cellular membrane. Many transport reactions are involved in determining the specific proton flux. So, constraining it to a particular value is not straightforward. However, the specific proton flux has shown to dramatically impact results of a genome-scale model (5). In general, the specific proton flux is positive for a net uptake of protons and negative for a net secretion of protons. It is defined by Eq. 3.30, where SPF is the specific proton flux. Here, P_i is the stoichiometry of protons in a transport reaction, and $v_{p,i}$ is the flux of that reaction.

$$SPF = \sum_{i=1}^{j} P_i v_i \qquad Eq.\,3.30$$

This equation is re-arranged and set equal to zero, as shown in Eq. 3.31.

$$P_1 v_{p,1} + P_2 v_{p,2} + \cdots + P_2 v_{p,2} - SPF = 0 \qquad Eq.\,3.31$$

To add Eq. 3.30 to the stoichiometric matrix, a new row and a new column must be added. This is shown in Fig. 3.5. To then specify the value of the specific proton flux, the flux through the new reaction (column) is constrained to the desired value.

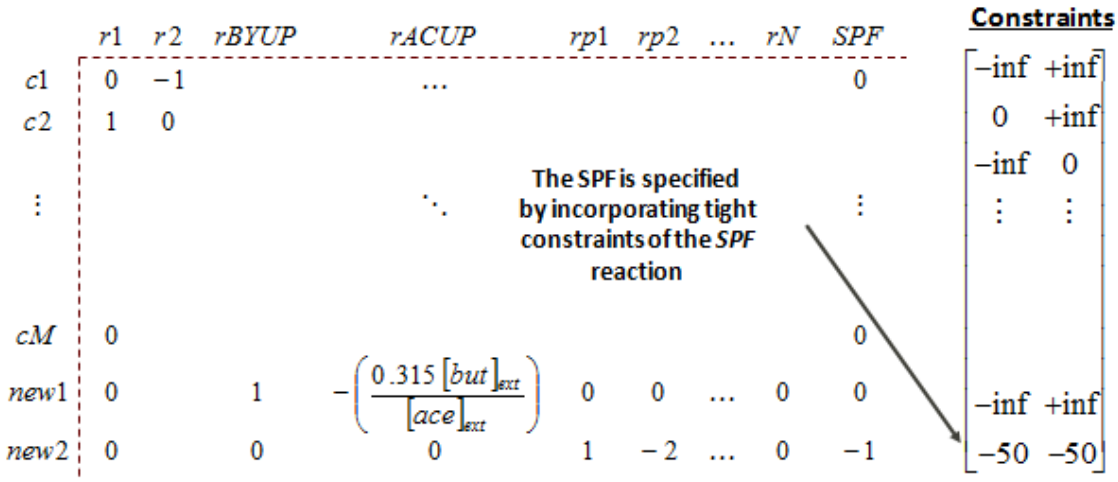

Fig. 3.5. The stoichiometric matrix containing flux ratio and specific proton flux constraints.

Flux constraints were also applied for the P/O ratio in *E. coli* K12 and for other specific "branch points" in clostridial metabolism. The P/O ratio was defined as the amount of ATP being produced via phosphorylation divided by the consumption of oxygen (or flux going through the oxygen exchange reaction). Specific branch points in clostridial metabolism included: (i) the diversion of flux to produce acetate or butyrate, (ii) hydrogen production or NAD(P) recycling, (iii) nitrogen uptake mechanisms, and (iv) usage of the TCA cycle.

3.5. Methods of flux balance analysis

Simulations were performed for the *in silico* organisms *iAF1260* (*E. coli* K12 MG1655) (*6*), *iRS552* (*C. acetobutylicum* ATCC 842) (*4*), and *iMM864* (*C. acetobutylicum*) (developed in this research). All model simulations were performed using the COBRA Toolbox (*8*) and GLPK linear programming open-source software (http://www.gnu.org/s/glpk/) in the MATLAB programming environment. All simulations were made using flux balance analysis (FBA) with maximized cell growth as the objective function. The minimization of total flux was set as a secondary objective. Phase plane analyses and other three-dimensional plots were made by setting two separate independent variables (reaction fluxes, ratios, or pH conditions) to specified values. Growth or the efflux through an exchange reaction from a resulting FBA was plotted as the dependent variable. Three-dimensional data were visualized on contour plots. Two-dimensional plots, including robustness analyses, were made in the same way with the exception of having only one independent variable, and being visualized as linear graphs.

3.6. Experimental *E. coli* gene knockout

A gene knockout of *ndh* was performed with the *E. coli* BL-21 strain to study the effects of a forcibly increased P/O ratio on growth and acetate production. The *ndh* gene encodes one of two NADH dehydrogenases that *E. coli* uses in its electron transport chain. The one encoded by *ndh* does not contribute to the proton motive force. Overall, a knockout of *ndh* should result in a higher P/O ratio, possibly at the expense of decreasing the growth rate due to less cycling of NADH to NAD+. Knockouts were performed using the TargeTron commercial gene knockout kit (Sigma) according to the manufacturer's protocol. Successful knockouts were examined at the molecular level using colony PCR. They were also tested for growth defects using a Synergy H4 Hybrid Reader (Biotek). It is recognized this knockout strain is available and can be purchased from several collections. This procedure provided substantial laboratory training to a project that was dominated by computational research.

3.7. References

1. Ogata, H., Goto, S., Sato, K., Fujibuchi, W., Bono, H., and Kanehisa, M. (1999) KEGG: Kyoto Encyclopedia of Genes and Genomes, *Nucleic Acids Res 27,* 29-34.
2. Szegezdi, J., and Csizmadia, F. (2004) Prediction of distribution coefficient using microconstants., *Abstr Pap Am Chem S 227,* U1019-U1019.
3. Jankowski, M. D., Henry, C. S., Broadbelt, L. J., and Hatzimanikatis, V. (2008) Group contribution method for thermodynamic analysis of complex metabolic networks, *Biophys J 95,* 1487-1499.

4. Senger, R. S., and Papoutsakis, E. T. (2008) Genome-scale model for Clostridium acetobutylicum: Part I. Metabolic network resolution and analysis, *Biotechnol Bioeng 101*, 1036-1052.

5. Senger, R. S., and Papoutsakis, E. T. (2008) Genome-scale model for Clostridium acetobutylicum: Part II. Development of specific proton flux states and numerically determined sub-systems, *Biotechnol Bioeng 101*, 1053-1071.

6. Feist, A. M., Henry, C. S., Reed, J. L., Krummenacker, M., Joyce, A. R., Karp, P. D., Broadbelt, L. J., Hatzimanikatis, V., and Palsson, B. O. (2007) A genome-scale metabolic reconstruction for Escherichia coli K-12 MG1655 that accounts for 1260 ORFs and thermodynamic information, *Mol Syst Biol 3*, 121.

7. Amador-Noguez, D., Feng, X. J., Fan, J., Roquet, N., Rabitz, H., and Rabinowitz, J. D. (2010) Systems-level metabolic flux profiling elucidates a complete, bifurcated tricarboxylic acid cycle in Clostridium acetobutylicum, *J Bacteriol 192*, 4452-4461.

8. Crown, S. B., Indurthi, D. C., Ahn, W. S., Choi, J., Papoutsakis, E. T., and Antoniewicz, M. R. (2011) Resolving the TCA cycle and pentose-phosphate pathway of Clostridium acetobutylicum ATCC 824: Isotopomer analysis, in vitro activities and expression analysis, *Biotechnol J 6*, 300-305.

9. Henry, C. S., Jankowski, M. D., Broadbelt, L. J., and Hatzimanikatis, V. (2006) Genome-scale thermodynamic analysis of Escherichia coli metabolism, *Biophys J 90*, 1453-1461.

10. Harris, D. C. (1995) *Quantitative Chemical Analysis*, 4 ed., W.H. Freeman and Company, New York.

11. Desai, R. P., Nielsen, L. K., and Papoutsakis, E. T. (1999) Stoichiometric modeling of Clostridium acetobutylicum fermentations with non-linear constraints, *J Biotechnol 71*, 191-205.

4. Results and Discussion

4.1. The new genome-scale model of Clostridium acetobutylicum, iMM864

The *iMM864* genome-scale model of *C. acetobutylicum* ATCC 824 was constructed using the previously published *iRS552* model (*1*, *2*) as a base. An additional 218 reactions were added to the *iRS552* model from the KEGG database. All transport reactions (a total of 80) from the *iRS552* model were included in the *iMM864* model. Exchange reactions (56 total) were created for extracellular metabolites and the "biomass" metabolite. Three vital reactions were added based on recent ^{13}C metabolic flux analysis findings for the TCA cycle (*3*, *4*) and the metabolic pathways involving glycine, serine, and threonine biosynthesis (*3*): (i) the formation of citrate catalyzed by a Re-citrate synthase, allowing for acetyl-coA and oxaloacetate to enter the oxidative TCA pathway and lead to L-glutamate, (ii) a lumped reaction allowing for glycine and tetrahydrofolate to produce methylene-tetrahydrofolate ,oxidized NAD^+, ammonia, and carbon dioxide, (iii) and succinate export across the cell membrane. An additional metabolite exchange reaction was then added for succinate. The entire *iMM864* genome-scale model of *C. acetobutylicum* is included as Appendix 1.

From the thermodynamic analysis using the group contribution method (GCM) (*5*) for reaction reversibility, 41 reactions that had been constrained irreversible in the *iRS552* model were deemed to be reversible, 3 irreversible reactions were constrained to be irreversible in the opposite direction, and 49 reversible reactions were constrained to be irreversible. Even with these new thermodynamic constraints, flux "loops" (or futile cycles) existed in the model that allowed flux to bypass expected pathways, resulting in production of acids and solvents that did not fit experimental observations. Additional constraints were added manually to correct these

futile cycles. The final set of constraints, in addition to the thermodynamic results and reversibility constraints, are also included in Appendix 1. The standard Gibb's free energy of formation for each compound in the *iMM864* model is given in Appendix 2.

Overall, the new *iMM864* genome-scale model contains 719 metabolites, 504 genes, and 846 reactions. A summary of these reactions and comparison to the *iRS552* model are shown in Fig. 4.1. Some reactions are still isolated or completely "blocked-off," meaning flux is not able to go through them. These reactions are referred to as "other blocked" in Fig. 4.1. Other reactions have been blocked as a result of the constraints placed on the model. These constraints have either been placed on the reactions themselves to not carry flux or on reactions that precede it in the metabolic pathway. These reactions are called "blocked by constraints" in Fig. 4.1. All reactions that are used in a particular pathway are referred to as "non-redundant" reactions in Fig. 4.1. Because of tighter constraints being issued, some pathways have fewer reactions in use in the new *iMM864* model, as compared to *iRS552*. A fully reduced version of *iMM864*, containing only non-blocked pathways (642 reactions total), is also available as *iMM642*.

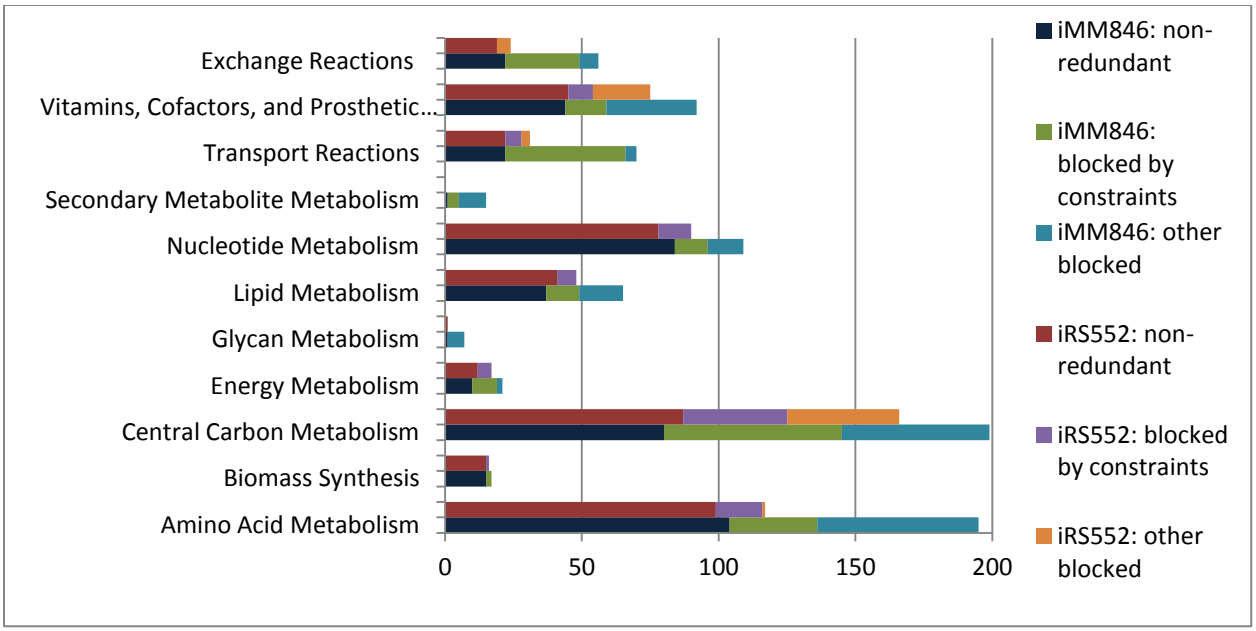

Fig. 4.1. Summary of reactions (non-redundant, those blocked by constraints, and other blocked reactions) in iRS552 and iMM864.

4.2. *In silico* simulations of the *iMM864* and *iRS552* models

To predict and study the metabolic programs of acidogenesis and solventogenesis (and the transition between them) in *C. acetobutylicum*, simulations of metabolic flux using flux balance analysis (FBA) were generated with the specific proton flux (SPF) as the independent variable. The SPF is the rate at which protons enter or leave the cell through the many transport reactions available. A negative value of SPF means protons are leaving the cell, while a positive SPF correlates to proton uptake. Simulations for growth of *C. acetobutylicum* on glucose as the sole carbon source (uptake constrained to 10 $\frac{mmol}{h \cdot gDCW}$) with the original *iRS552* model are shown in Fig. 4.2. With this model, the growth rate remained unaffected throughout the range of SPF studied, and acetate production accounted for the differences in the SPF. It is noted that several more constraints than the glucose uptake rate were required of the *iRS552* model to effectively capture phenotypic traits. These additional constraints were fully disclosed (*1*, *2*). However, in

the updated *C. acetobutylicum* model (*iMM864*), it is desired to (i) effectively distinguish between acids and solvents production based on SPF, (ii) determine the partition between acetate/butyrate and acetone/butanol production, and (iii) examine the impact of the pH gradients across the cell membrane. In the case of the *iRS552* model, greater acetate production occurs at more negative SPF values, as shown in Fig. 4.2. Thus, the SPF may be used to predict acidogenic phenotypes. The acetate production may be seen as representing the production of weak acids (acetate, butyrate, and lactate) in general. Why acetate was the only weak acid produced in these simulations can be explained. As shown in Fig. 2.3, the production of acetate from acetyl-CoA regenerates ATP, while the production of butyrate from acetyl-CoA regenerates the same amount of ATP but also converts NADH to NAD^+. Because butyrate was not produced in these simulations, the *iRS552* model must contain a futile cycle or "loop" that artificially balances NAD(P)/NAD(P)H. This is confirmed by the production of hydrogen (H_2), which was zero in this simulation (Fig. 4.2). As shown in Fig. 2.3, the oxidation of ferredoxin accompanies hydrogen production and is a highly active pathway in clostridial metabolism. This supports the hypothesis of a futile cycle balancing NAD(P)/NAD(P)H. The linear programming optimization procedure used to perform these simulations was given the objective to maximize the cellular growth rate and a second objective of minimizing total flux. So the shortest pathways possible will always be used over longer pathways. Thus, production of acetate to generate ATP and balancing of NAD^+/NADH through a futile cycle will be preferred to butyrate production. With the exception of lactate production, the production of acetate requires the shortest pathway compared to those of all other weak acids produced by *C. acetobutylicum*. Lactate was not produced by the *iRS552* model in this case because it yields no ATP regeneration, unlike the production of acetate.

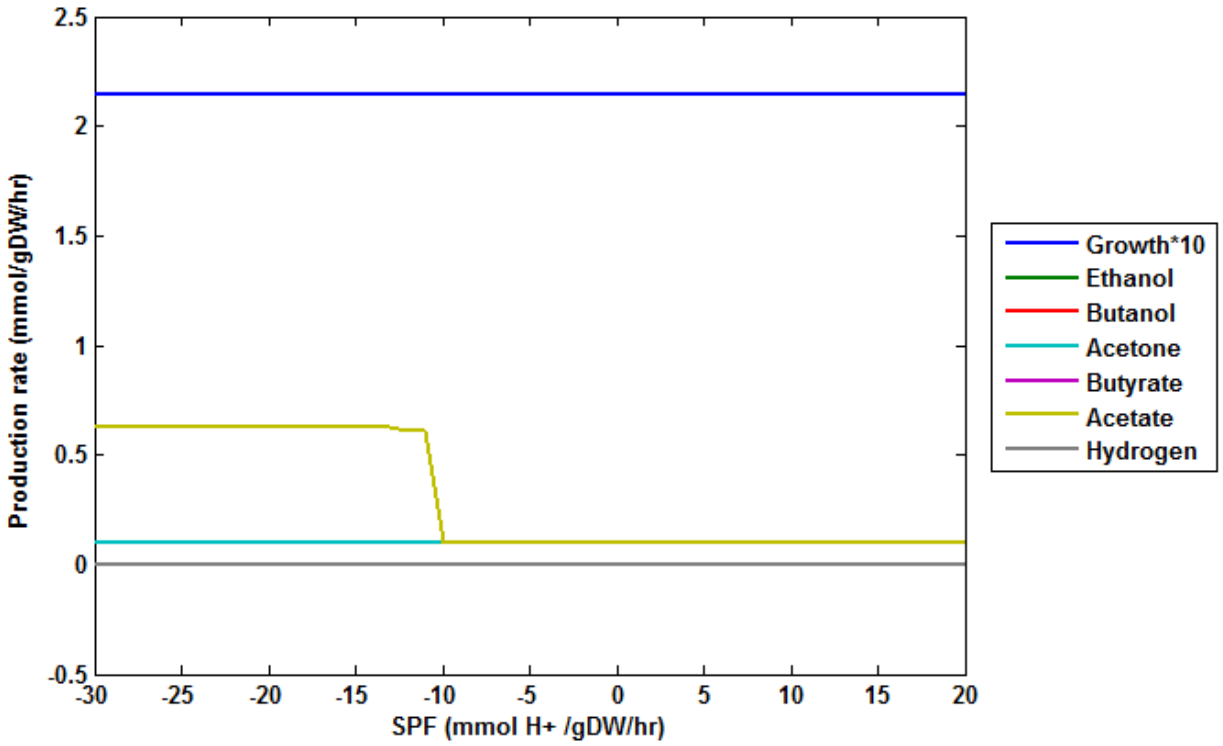

Fig. 4.2. Production rates and growth as a function of the SPF using the *iRS552* model. Glucose uptake was constrained to 10 $\frac{mmol}{h \cdot gDCW}$ and the re-uptake of acids was constrained to zero.

Simulations with varied SPF for the *iMM864* model with glucose as the sole carbon source and a constrained uptake of 10 $\frac{mmol}{h \cdot gDCW}$ are shown in Fig. 4.3. The maximum growth rate is correctly predicted to correlate with a negative SPF. This is accompanied by high levels of acid production and is characteristic of exponential growth of the culture. The growth rate decreases at either extreme of the SPF range viewed. This is also characteristic of observed culture behavior (*2*). The new *iMM864* model also predicts the onset of solventogenesis to correlate with more positive SPF values, even with glucose being the sole carbon source and weak acids re-uptake constrained to zero. In much the same way that acetate production is representative of all weak acid production, acetone production is representative of all solvent production here. Acetone production, however, is associated with the simultaneous re-uptake of acetate, so it may

also be seen as a mechanism for the cell to control its SPF. The fact that butyrate and butanol production are not observed in these simulation results suggests that correct balancing of NAD(P)/NAD(P)H remains an issue of concern when only glucose uptake is constrained. Although in small quantities, butyrate is produced at extremely negative SPF values. This most likely means that the cell needs to balance excessive amounts of NAD(P)H under these conditions, causing it to use longer pathways to produce butyrate. Hydrogen production in these simulations is erroneous, however, as high hydrogen production should correlate with high acid production (*6, 7*). However, an incorrect hydrogen result confirms that NAD(P)/NAD(P)H balancing still needs to be addressed in the model. This simulation has also revealed that *C. acetobutylicum* has the metabolic capacity to produce solvents during growth on glucose as the sole carbon source. Regulatory constraints (which are not accounted for in *iMM864*) most likely prevent that from happening, as solventogenesis leads to lower growth rates.

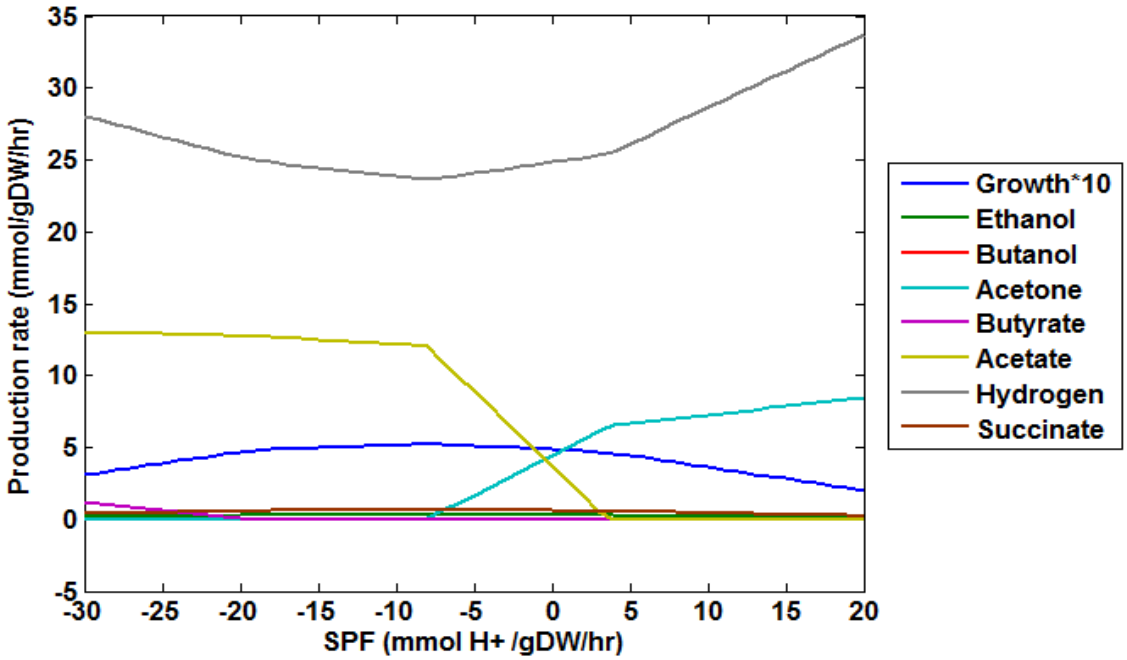

Fig. 4.3. Production rates and growth vs. SPF in *iMM864* with no uptake of acids.

In contrast to acid production during exponential growth (acidogenesis), solventogenesis is associated with the uptake of not only glucose, but also the weak acids (acetate and butyrate) it had secreted previously. The *iRS552* model was simulated with arbitrarily constrained acid re-uptake rates of 2 $\frac{mmol}{h \cdot gDCW}$ for acetate and 6 $\frac{mmol}{h \cdot gDCW}$ for butyrate. Simulation results are presented in Fig. 4.4 and show the production of solvents (butanol and acetone). The growth rate and the production of butanol and acetone remain constant throughout the range of SPF viewed at. In fact, the production of all metabolites remained unaffected when the SPF was varied. This would indicate that the model is not properly proton balanced, or a futile cycle is allowing for protons to be created or consumed. In terms of the fermentation pathway, all of the consumption of butyrate is going towards the production of both acetone and butanol, while the consumption of acetate fuels the production of only acetone. Still, no hydrogen is produced because of futile cycles oxidizing excess NADH.

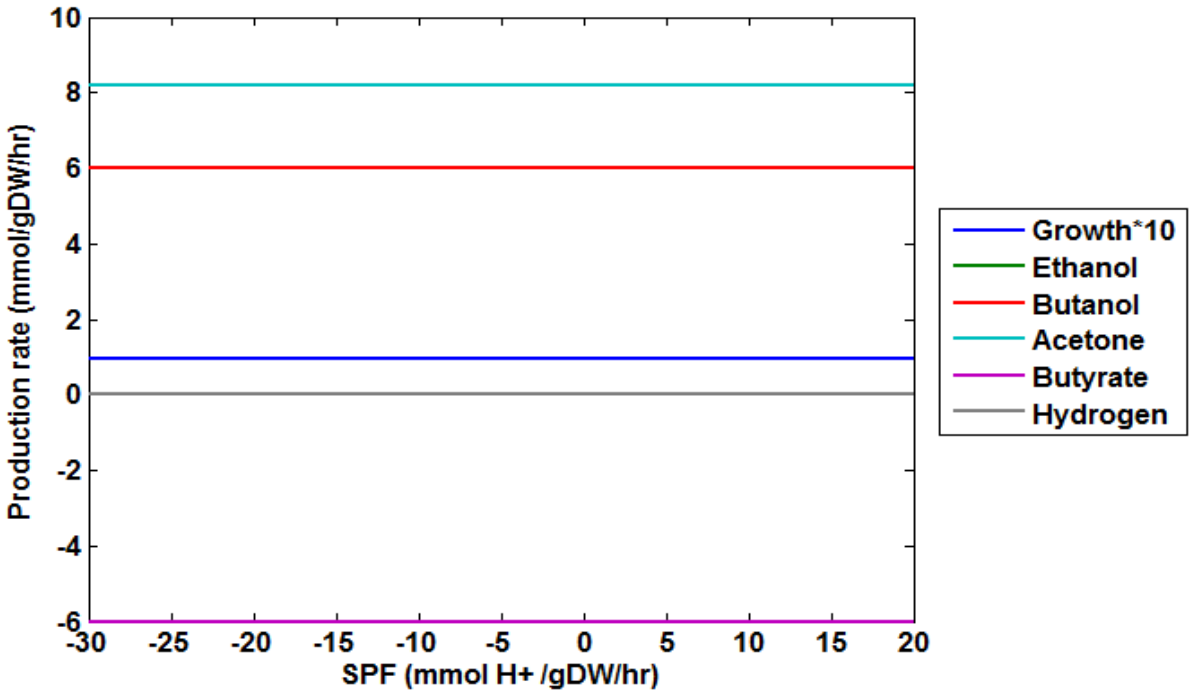

Fig. 4.4. Production rates and growth as a function of the SPF using the *iRS552* model with the re-uptake fluxes of acetate and butyrate constrained to 2 and 6 $\frac{mmol}{h \cdot gDCW}$, respectively.

The *iMM864* model was also simulated with the added re-uptake constraints of acetate and butyrate being 6 and 2 $\frac{mmol}{h \cdot gDCW}$ respectively, while keeping glucose uptake constant at 10 $\frac{mmol}{h \cdot gDCW}$. Results are shown in Fig. 4.5. These simulations are more characteristic of solventogenic phenotypes, with the production of either butanol or acetone. It appears that all butyrate re-uptake goes directly to butanol production, while acetone is produced from both acetate and glucose. Solventogenesis is also accompanied by lower growth rates. The major flaws observed in this simulation include the fact that ethanol is not produced, and that hydrogen is produced at greater rates as the SPF increases. However, experimental observations contradict these simulations (*6*). This is further indicative of NAD(P)/NAD(P)H balancing issues and possibly of constraints needed at critical "branch points" or "nodes" in clostridial metabolism.

Another flaw with these simulations is that butanol production continues to stay constant throughout negative SPF values. Studies indicate that butanol production is only observed at more positive SPF values (*2*). However, the re-uptake constraint imposed in this simulation required solvent production during all phases of growth. Thus, an additional constraint is needed to relate the re-uptake flux of acetate and butyrate to the SPF.

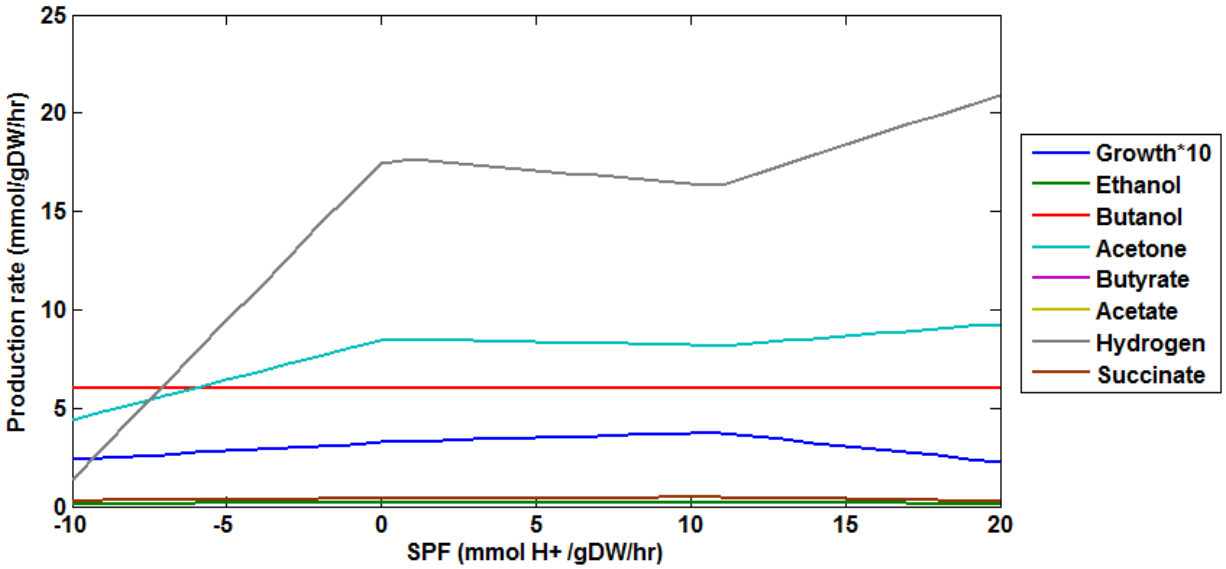

Fig. 4.5. Production rates and growth as a function of the SPF using the *iMM864* model with the re-uptake fluxes of acetate and butyrate constrained to 2 and 6 $\frac{mmol}{h \cdot gDCW}$, respectively.

In order to generate a more complete picture of metabolism by modeling acidogenesis and solventogenesis, acetate and butyrate production and re-uptake fluxes should not be arbitrarily constrained to particular values. In the following simulations, these re-uptake rates were left completely unconstrained. These simulations with the *iMM864* model are provided in Fig. 4.6. When these conditions were enforced with the *iRS552* model, the simulation results were identical to those in Fig. 4.2. These simulations best reveal the new capabilities of the *iMM864* model in terms of predicting the end of acidogenesis and exponential growth and the onset of solventogenesis. However, as noted previously, additional strategies are required to

ensure effective balancing of NAD(P)/NAD(P)H to produce acetate/butyrate and acetone/butanol simultaneously under conditions in which only glucose uptake is constrained.

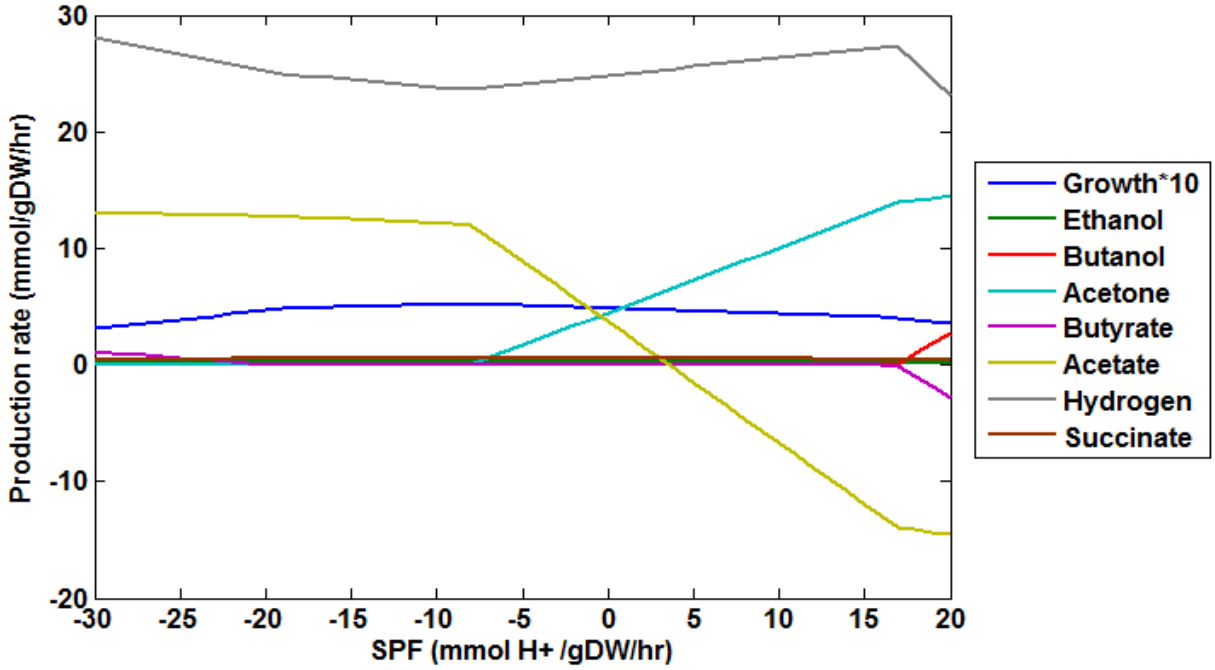

Fig. 4.6. Growth and production using the *iMM864* model during growth on glucose (constrained to 10 $\frac{mmol}{h \cdot gDCW}$) with unconstrained acetate and butyrate production and re-uptake.

In these preliminary simulations with the *iMM864* model, hydrogen production seemed to be the most flawed of all products being investigated, so it was studied in more detail. However, comparisons with the *iRS552* model showed superior performance from this expanded model with thermodynamic constraints. The simulations with constrained glucose uptake and unconstrained acetate and butyrate re-uptake, shown in Fig. 4.7, reveal hydrogen production values that are consistent with what is observed experimentally. Greater solvent production is correlated with lower hydrogen production, while greater acid production is observed with higher hydrogen production (*6*, *7*). This is further explained by the picture of preliminary clostridial metabolism shown in Fig. 2.3. Ferredoxin is reduced as pyruvate is converted to acetyl-CoA. It is then re-oxidized by competing pathways, one regenerates NAD(P)H and the

other produces hydrogen. Acetyl-CoA is converted to acetate to generate ATP. It is converted to ethanol to produce NAD^+, and conversion to butyrate produces both ATP and NAD^+. During acidogenesis, all acetyl-CoA is generated from pyruvate. This results in a high production of hydrogen to reduce the ferredoxin required of this conversion. During solventogenesis, however, acetyl-CoA is produced from the re-uptake of acetate and from conversion of pyruvate. Re-uptake of butyrate yields butyryl-CoA. Thus, the conversion of pyruvate to acetyl-CoA is not required to satisfy all of the ATP and NAD(P)/NAD(P)H balancing of the cell. This results in a diminished flux of pyruvate to acetyl-CoA and is accompanied by a lower production rate of hydrogen. In addition, with lower amounts of hydrogen being produced, higher amounts of NADH are available for the production of both acids and solvents. In Fig. 4.7, ethanol is seen as characteristic of total solvent production, which may be explained by the fact that no constraints were placed on the SPF or NAD(P)/NAD(P)H balancing. Of the ABE solvents, ethanol is the only one not connected with the re-uptake of one of the acids produced from fermentation.

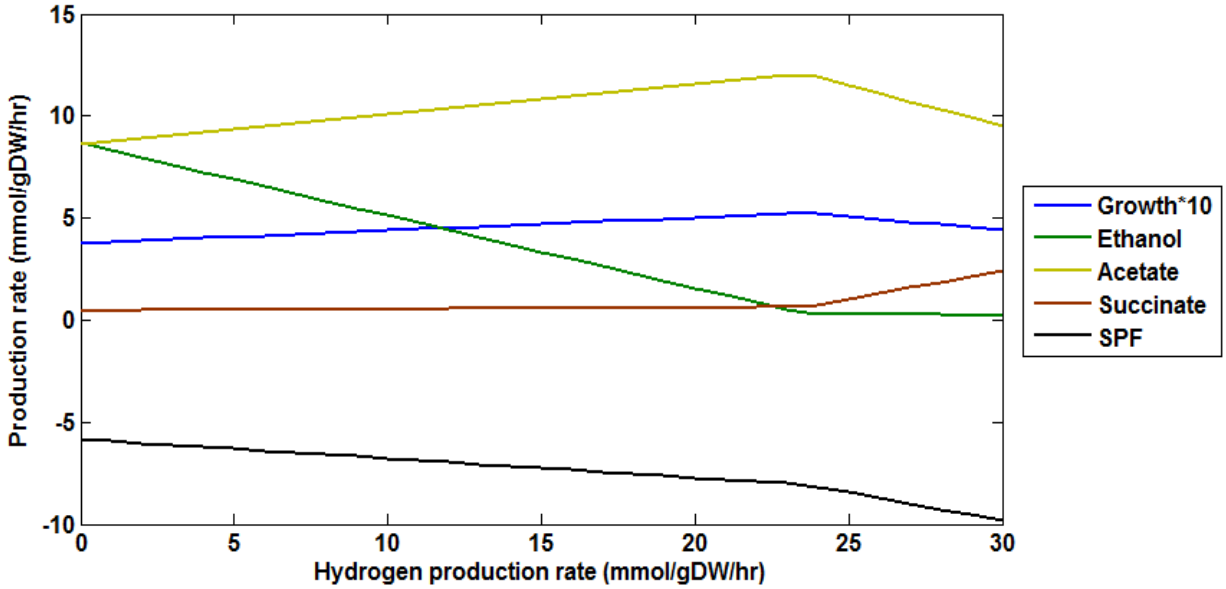

Fig. 4.7. Growth and production of acids and solvents vs. hydrogen production in *iMM864* during growth on glucose (constrained to 10 $\frac{mmol}{h \cdot gDCW}$).

4.3. Applying ratio constraints to find correct metabolic phenotypes

The previous simulations have shown that without the proper constraints, it is difficult to effectively model the metabolism of *C. acetobutylicum*. Traditionally, constraints are applied to the uptake of a carbon source (e.g., glucose) or the secretion of a product (e.g., acetate, butyrate, etc.). These constraints often consist of an upper and lower limit for flux for a reaction or transport of a metabolite across a membrane. Here, a novel method of constraints is explored using flux ratios. Ratio constraints are placed with the assumption that the flux going through one pathway or set of reactions is proportional to the flux going through another pathway. They can thus be used to force flux through pathways unused as predicted by conventional optimization algorithms. This is particularly useful at metabolic branch-points. One primary example is the direction acetyl-CoA flows in Fig. 2.3. In a physiological sense, enzymes may be produced by the cell in ratios to one another under certain conditions, based on the strengths of their promoters or ribosome binding sites. Such is the case with the thiolase enzyme (THL in Fig. 2.3). The thioloase promoter is reported to be very strong and is used as a clostridial promoter for over-expressions in metabolic engineering strategies (*8, 9*). This enzyme provides flux to convert acetyl-CoA along the longer metabolic pathway to produce butyrate and butanol, as opposed to the shorter conversions to acetate and ethanol. The simulations in this section have been made in an attempt to identify ratio constraints that ultimately provide for more accurate representations of the metabolism in *C. acetobutylicum.* Correct production of hydrogen and a distribution between acetate/butyrate and acetone/butanol were sought by this strategy.

In order to better characterize the production of acids or solvents, a ratio constraint was placed on fluxes in fermentation going from acetyl-CoA, a pivotal "branch-point" or "node" in the pathway (see Fig. 2.3). The ratio constraint was placed so that flux going through the reaction

catalyzed by the thiolase (THL) enzyme will be twice that of the flux going from acetyl-CoA to acetyl phosphate (towards acetate production) and acetaldehyde (towards ethanol production). Simulations from this ratio constraint (results not shown) were flawed, with notably large amounts of succinate being produced (which is uncharacteristic) to offset the SPF. So, succinate production was included in the denominator of the ratio (named 2Thl:1PtaAcetSuc). However, results from these simulations showed that excessive amounts of acetone were produced in relation to butyrate and butanol. This would indicate that large amounts of acetate were simultaneously secreted and re-consumed. So, another constraint (termed >2hbcoa:aacet) was placed to force flux going through the conversion of acetoacetyl-CoA to hydroxybutyryl-CoA (towards production of butyrate and butanol) to be at least twice that of the fluxes converting acetoacetyl-CoA to acetoacetate (towards production of acetone), which rely on the reuptake of acetate or butyrate. These two ratio constraints are termed (2Thl:PtaAcetSuc|>2hbcoa:aacet). Simulations with these ratio constraints and glucose as the sole carbons source (constrained to 10 $\frac{mmol}{h \cdot gDCW}$) are shown in Fig. 4.8. Simulations allowing unconstrained acetate and butyrate re-uptake (with constrained glucose uptake) are shown in Fig. 4.9. These results are shown as a function of hydrogen production in Fig. 4.10. In these simulations, the production of acetone, butanol, and ethanol are all seen during solventogenesis, while the production of acetate and butyrate both occur during acidogenesis. To achieve this result, only flux ratios for internal enzymes were used instead of artificially constraining the production of each product individually. This is a novel development that may have profound impacts on genome-scale modeling and identifying metabolic engineering targets.

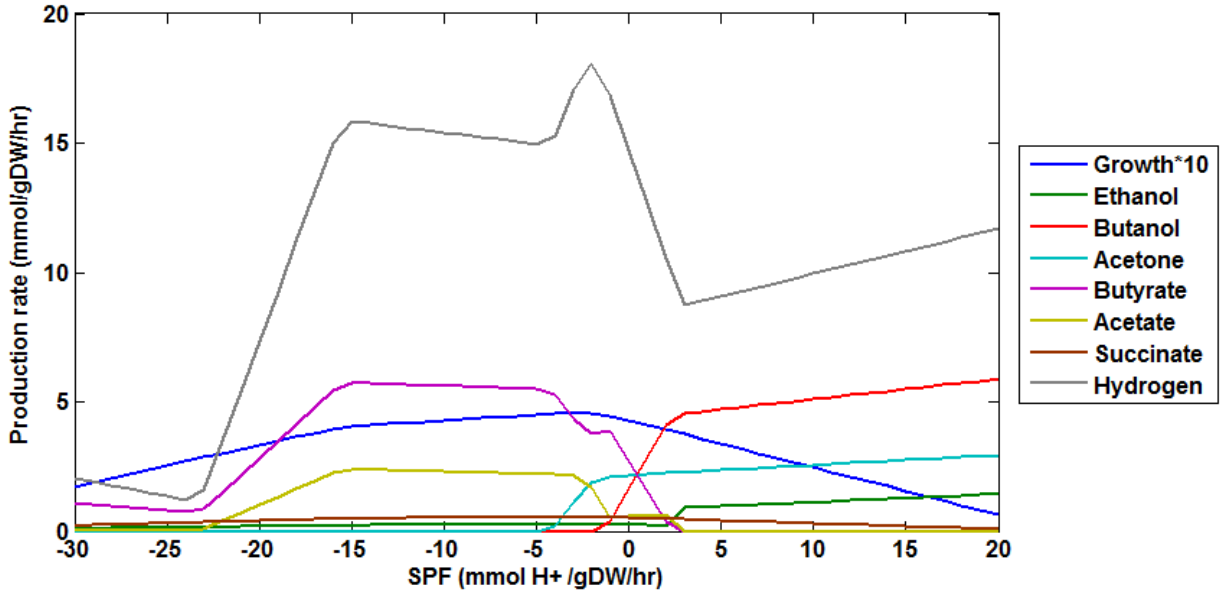

Fig. 4.8. Using the *2Thl:PtaAcetSuc|>2hbcoa:aacet* flux ratio constraints in the *iMM864* model. Simulations show growth and production as a function of SPF with constrained glucose uptake ($10\ \frac{mmol}{h \cdot gDCW}$) as sole carbon source.

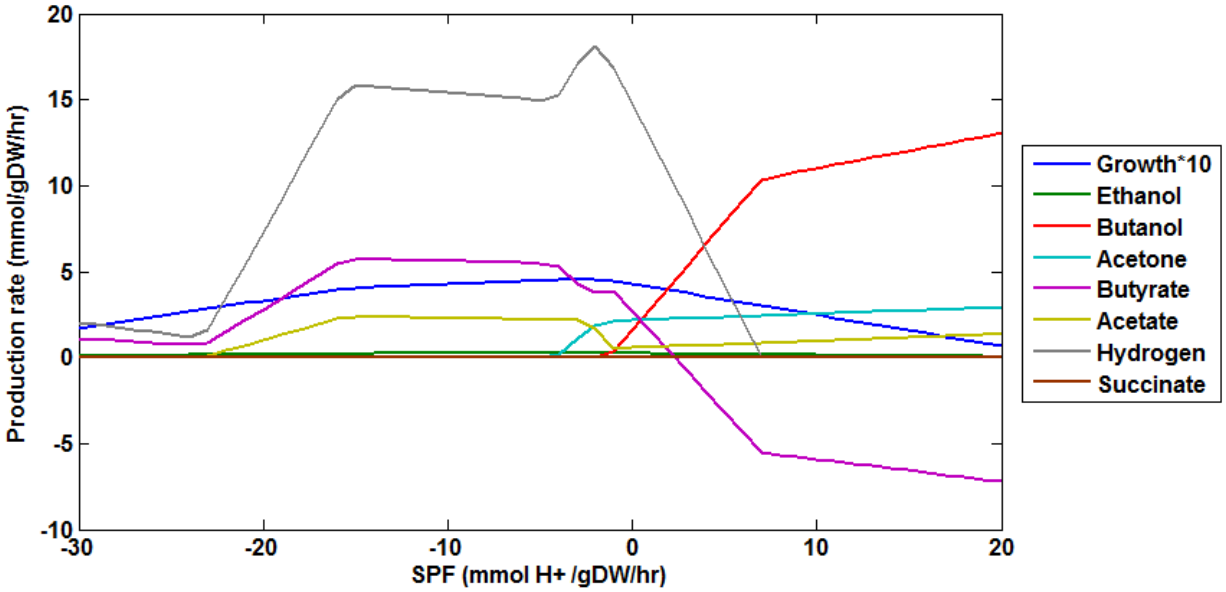

Fig. 4.9. Using the *2Thl:PtaAcetSuc|>2hbcoa:aacet* flux ratio constraints in the *iMM864* model. Simulations show growth and production as a function of SPF with constrained glucose uptake ($10\ \frac{mmol}{h \cdot gDCW}$) and unconstrained acetate and butyrate production and re-uptake.

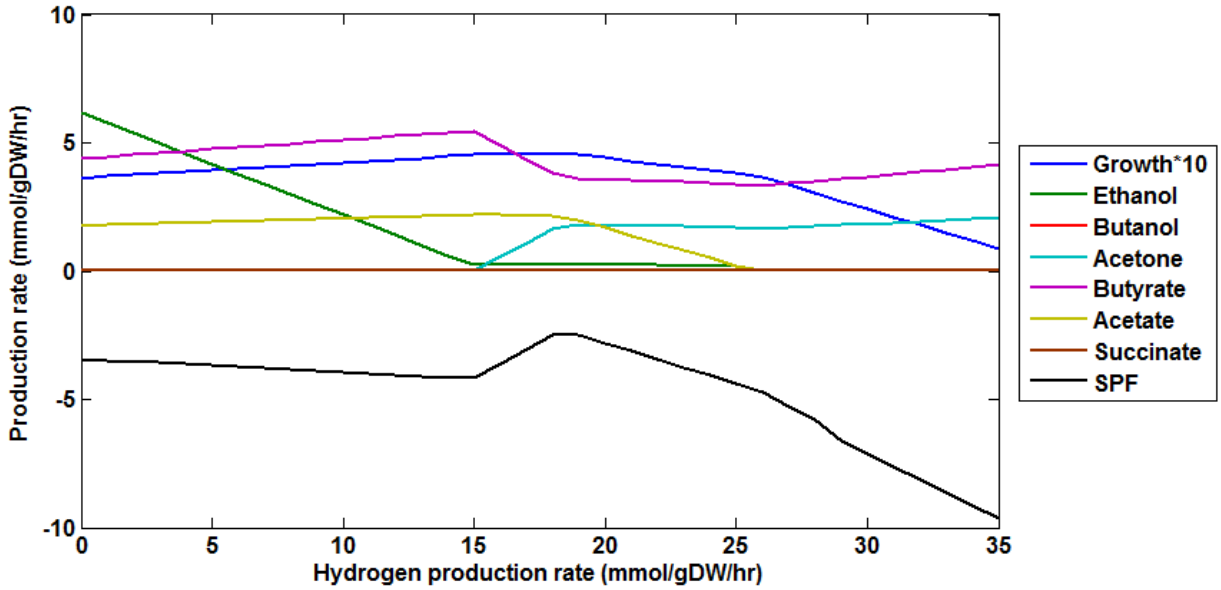

Fig. 4.10. Simulation results of Fig. 4.9 shown as a function of hydrogen production.

To visualize what happens when one of these ratios is varied, the Thl:PtaAcetSuc ratio was changed from 2 to 4. The new constraint of 4Thl:1PtaAcetSuc|>2hbcoa:aacet was used to provide the simulations shown in Fig. 4.11 (with constrained glucose uptake as the sole carbon substrate) and Fig. 4.12 (with constrained glucose uptake and unconstrained acetate and butyrate re-uptake). Ethanol production is shown to decrease substantially with this new ratio, while the ratio of butanol to acetone production remains unaffected. The butyrate to acetate production ratio is increased. Therefore, varying the Thl:PtaAcetSuc ratio clearly affects the ratios of ABE products and the ratio of acetate to butyrate. In fact, these results coincide well with experimental studies that have already been conducted on over-expressing the thiolase enzyme. This over-expression, in synchrony with over-expression of other genes, leads to greater butyrate production, and lower production of acetate and ethanol (*10*). Another result to note, with Fig 4.12, is that the cell uptakes both acetate and butyrate during solventogenesis instead butyrate alone, which was seen in previous simulations with unconstrained acetate and butyrate uptake.

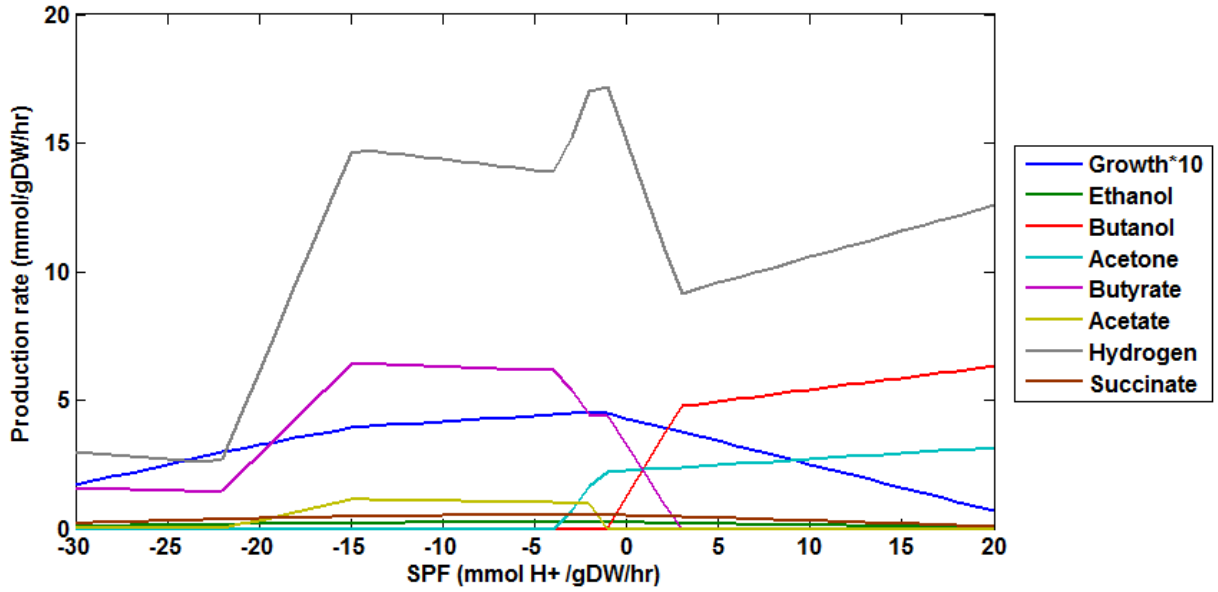

Fig. 4.11. Using the *4Thl:PtaAcetSuc|>2hbcoa:aacet* flux ratio constraints in the *iMM864* model. Simulations show growth and production as a function of SPF with constrained glucose uptake ($10\ \frac{mmol}{h \cdot gDCW}$) as sole carbon source.

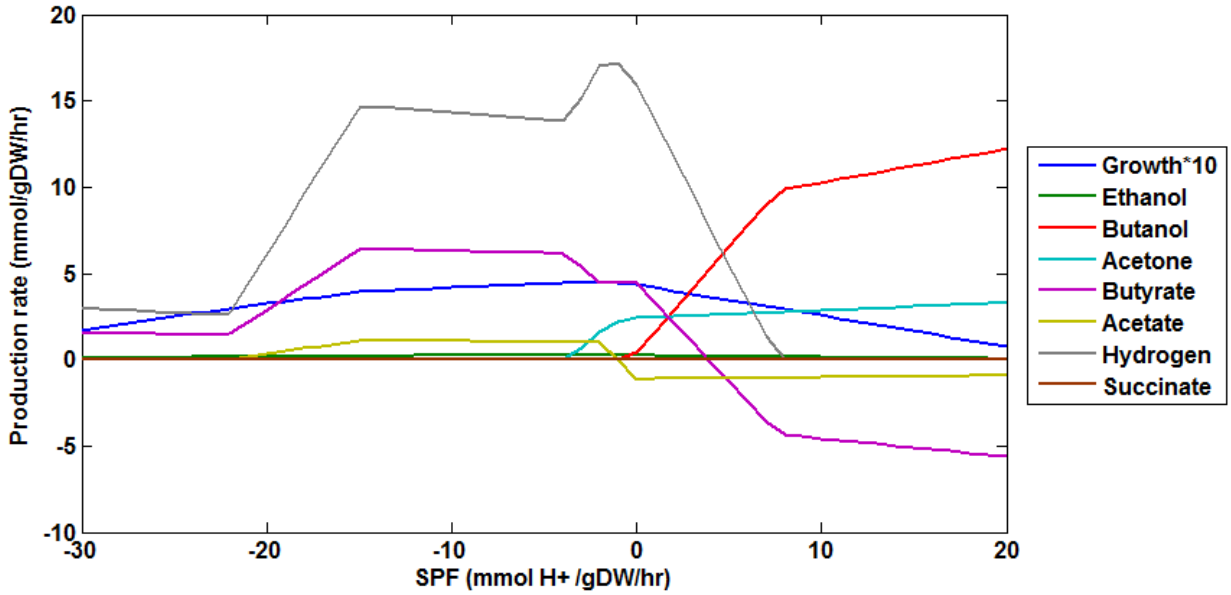

Fig. 4.12. Using the *4Thl:PtaAcetSuc|>2hbcoa:aacet* flux ratio constraints in the *iMM864* model. Simulations show growth and production as a function of SPF with constrained glucose uptake ($10\ \frac{mmol}{h \cdot gDCW}$) and unconstrained acetate and butyrate production and re-uptake.

Another flux ratio constraint of interest is the ratio of the number of electrons going from reduced ferredoxin (during its oxidation) towards hydrogen production per the total number of electrons donated to all molecules (including hydrogen). As seen in Fig. 2.3, these electrons can also be used to regenerate NAD(P)H during ferredoxin oxidation. Using a ratio of 0.4 gave comprehensive results in terms of the production of various products in relation to hydrogen production. Results are shown in Fig. 4.13. When this ratio constraint is applied, the cell must produce some amount of hydrogen, or else it will not be able to grow. Here, butanol production is produced in higher quantities when hydrogen production is very low. Experimental data support this simulation result, as butanol and total solvent production is highest at low rates of hydrogen production (*7, 11*). Also, just like the simulations with only the *2Thl:PtaAcetSuc|>2hbcoa:aacet* constraint (Fig. 4.10), these simulations show that the cell has the metabolic capability to produce almost 4 moles of hydrogen for every mole of glucose consumed, its theoretical hydrogen production limit (*6*).

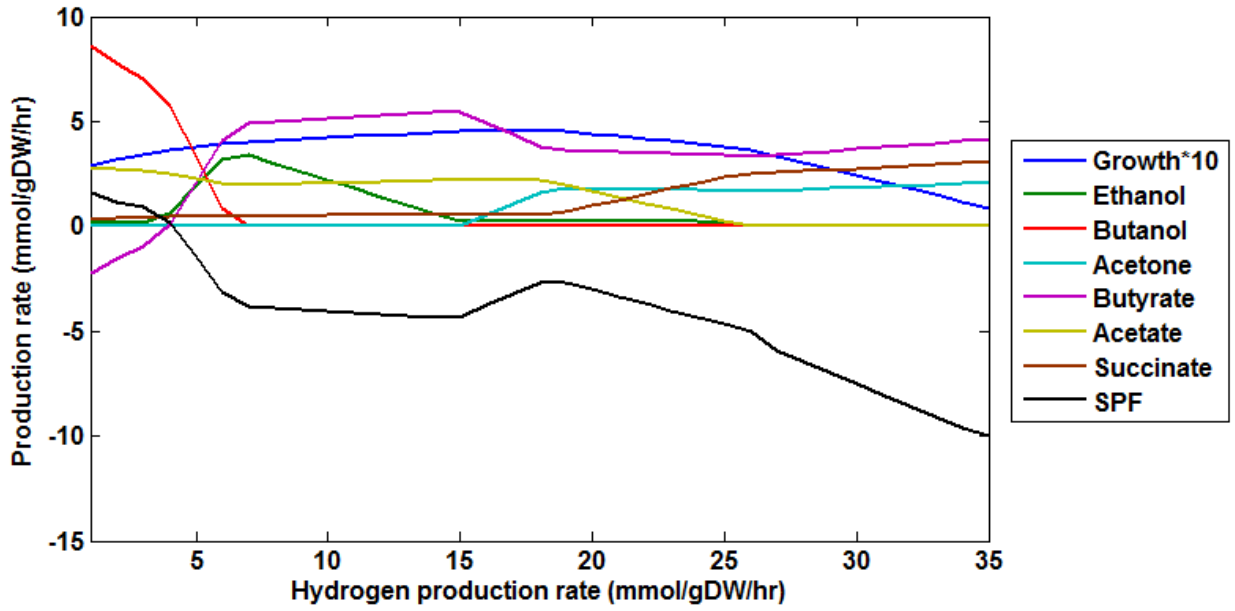

Fig. 4.13. Using the *2Thl:PtaAcetSuc|>2hbcoa:aacet|0.4fd:H* flux ratio constraints with the *iMM864* model. Simulations show growth and production as a function of hydrogen production with constrained glucose uptake (10 $\frac{mmol}{h \cdot gDCW}$) and unconstrained acetate and butyrate production and re-uptake.

4.4. Proton-balancing simulations

Increased solvents production during growth on glucose as the sole carbon source was not revealed by varying the SPF in the initial simulations of *iRS552* (Fig. 4.2). So, an effort was made to see if properly proton-balancing a compartmentalized version of this model would yield different results. The simulations were thus repeated, while proton-balancing the model to an intracellular and extracellular pH of 7. The acidic and basic pKa values for every compound in the *iMM864* model are given in Appendix 2. Results of this effort are shown in Fig. 4.14. As indicated by these simulations, properly proton-balancing the model effectively links acetone production to solventogenic growth in this model at positive SPF values. In this round of simulations, however, hydrogen production is erroneous, as it is shown to increase during

solventogenesis to extremely high values. However, the utility and influence of proper proton balancing is shown in this simple example.

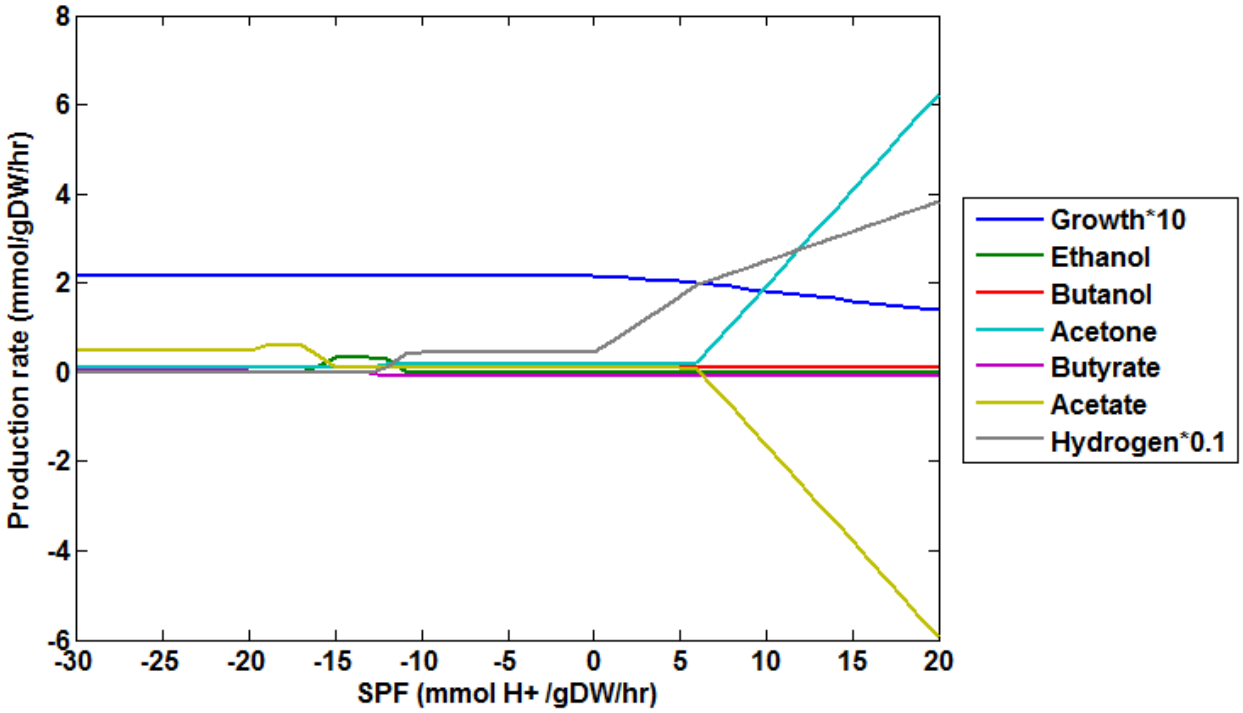

Fig. 4.14. *iRS552* proton balanced to an extracellular and intracellular pH of 7. Growth on glucose and unconstrained acetate and butyrate uptake/production and production rates are plotted as a function of SPF.

The effects of changing the extracellular pH and SPF (while keeping intracellular pH constant at 7) in the *iMM864* model are shown in Fig. 4.15 (for growth rate), Fig. 4.16 (for total solvent production), and Fig. 4.17 (for total acid production). In these simulations, butyrate and acetate exchange fluxes were unconstrained, so the cell was allowed to produce or re-uptake the acids at unconstrained rates. An interesting phenomenon is observed as the pH decreases. The maximum growth rate moves slightly toward more positive SPF values (Fig. 4.15). This may be due to the fact that more of the secreted acids will be in the protonated form as extracellular pH is lower. So, as the extracellular pH decreases, the secretion of acids by the cell has less of an effect on the pH of the extracellular environment. This curvature also occurs with total acids

production and total solvents production, as seen in Fig. 4.16 and Fig 4.17. Proton balancing the model to varying extracellular pH values does not predict the onset of acidogenesis, as the maximum growth rate always occurs with acidogenic phenotypes. However, these results may be expected, since the growth (and glucose uptake) of *C. acetobutylicum* decreases as it switches into solventogenesis. These simulations reveal that the cell has the capability (stoichiometrically) to continue producing acids with extracellular pH conditions as low as 4.5, and that this would result in a more optimal growth rate. However, the cell "chooses" to produce solvents instead at lower extracellular pH conditions. This raises the question of whether or not the cell always chooses a phenotype resulting in an optimal growth rate. These simulations provide more evidence that *C. acetobutylicum* has evolved the capacity to undergo solventogenesis as a means to increase the pH to reduce the toxic effects of low pH. This would also explain why the onset of solventogenesis can be predicted only once constraints on the SPF are in place.

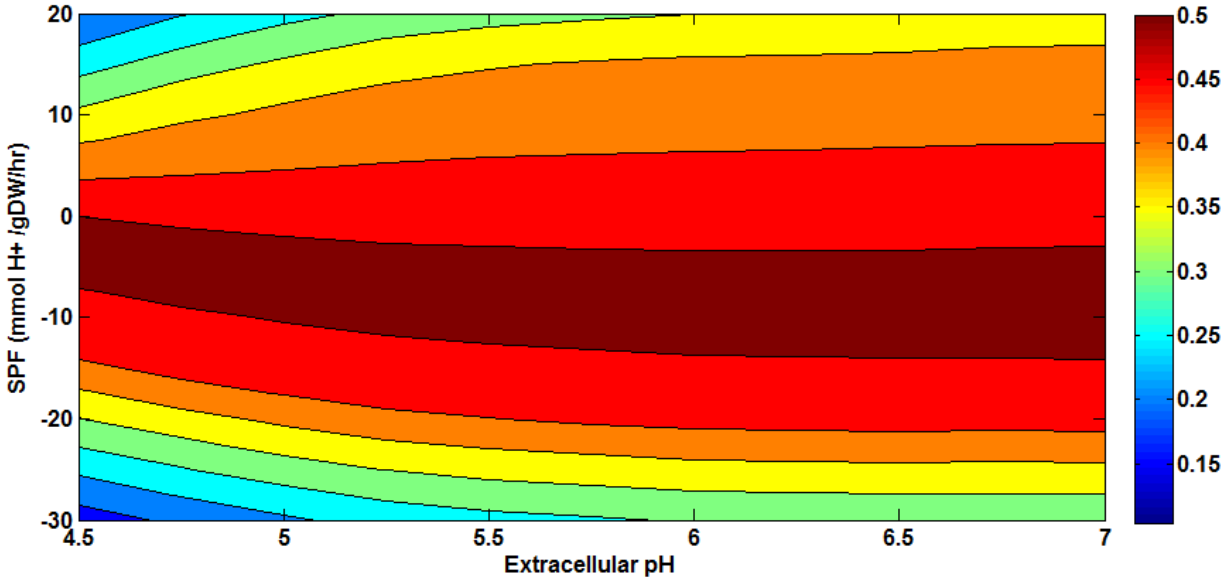

Fig. 4.15. Growth rate (hr^{-1}) as a function of extracellular pH and SPF in *iMM864*. Intracellular pH was kept constant at 7, glucose consumption was constrained to 10 $\frac{mmol}{h \cdot gDCW}$, and acetate and butyrate production and re-uptake were left unconstrained.

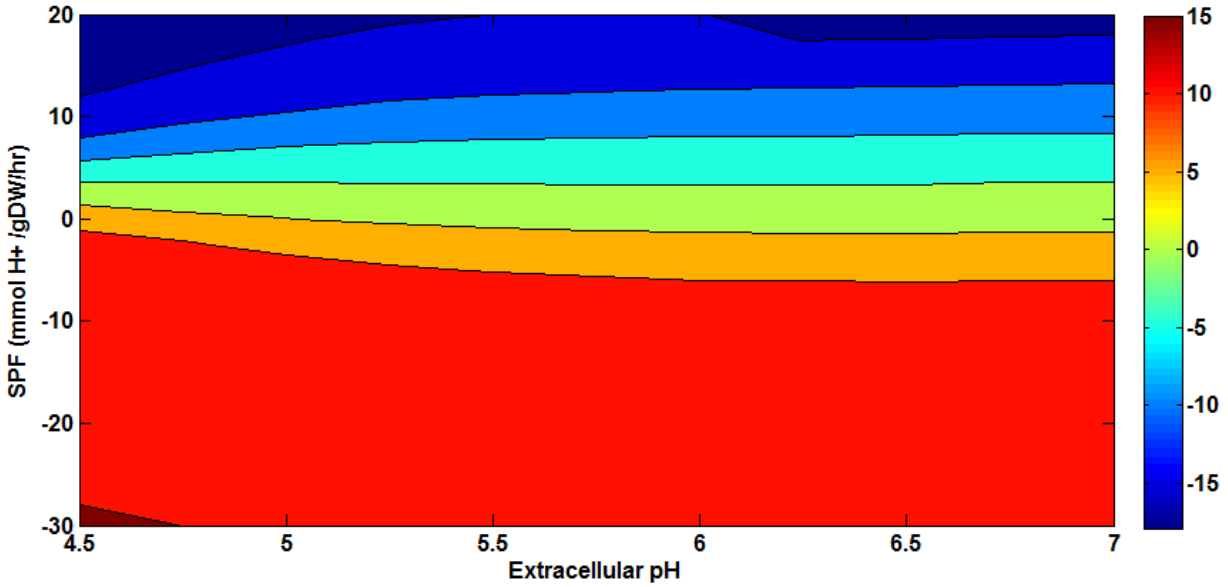

Fig. 4.16. Total acid production (acetate, butyrate, lactate, and succinate) ($\frac{mmol}{h \cdot gDCW}$) as a function of extracellular pH and SPF in iMM864. Intracellular pH was kept constant at 7, glucose consumption was constrained to 10 $\frac{mmol}{h \cdot gDCW}$, and acetate and butyrate production and re-uptake were left unconstrained. Negative values indicate consumption.

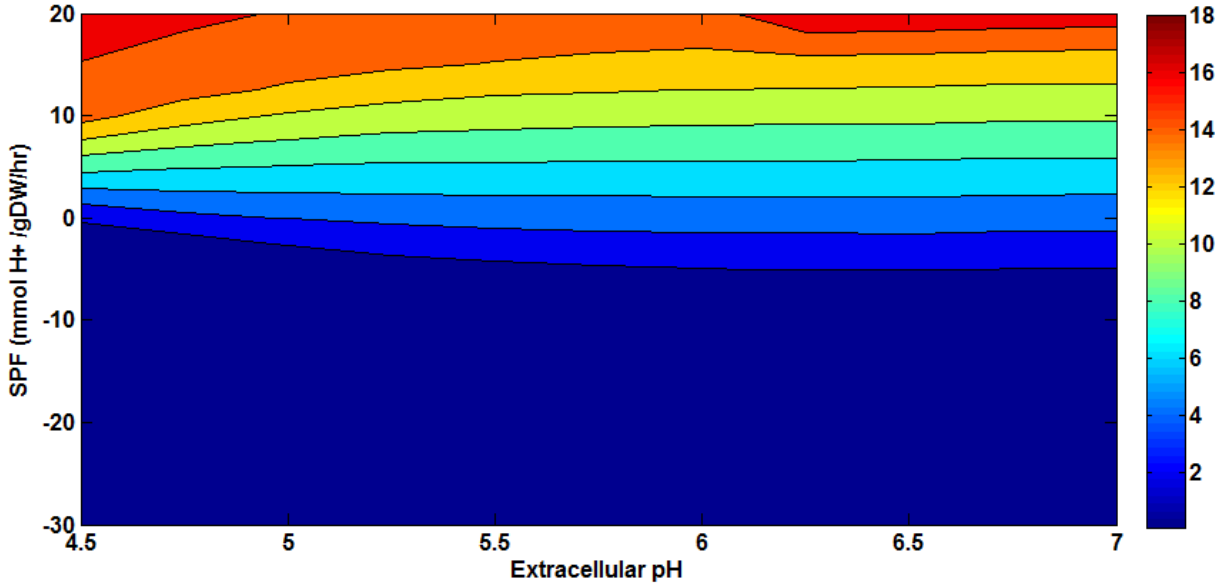

Fig. 4.17. Total solvent production (butanol, acetone, ethanol, and acetoin) ($\frac{mmol}{h \cdot gDCW}$) as a function of extracellular pH and SPF in *iMM864*. Intracellular pH was kept constant at 7, glucose consumption was constrained to 10 $\frac{mmol}{h \cdot gDCW}$, and acetate and butyrate production and re-uptake were left unconstrained.

These simulations were repeated with an un-proton-balanced version of the *iMM864* model in an effort to reveal more effects of proton balancing on a genome-scale model. These simulations are shown in Fig. 4.18 (for growth rate), Fig. 4.19 (for total solvent production), and Fig. 4.20 (for total acid production). Obviously, none of the conditions change as pH is varied, and maximum growth rate here actually occurs with solventogenic phenotypes, which contradicts all previous observations. Also, the growth rate changes only slightly with varying constraints on the SPF. Although the onset of solventogenesis was not predicted when the model is proton-balanced in Fig. 4.15-17, these new simulations reveal the necessity of having the genome-scale model properly proton balanced.

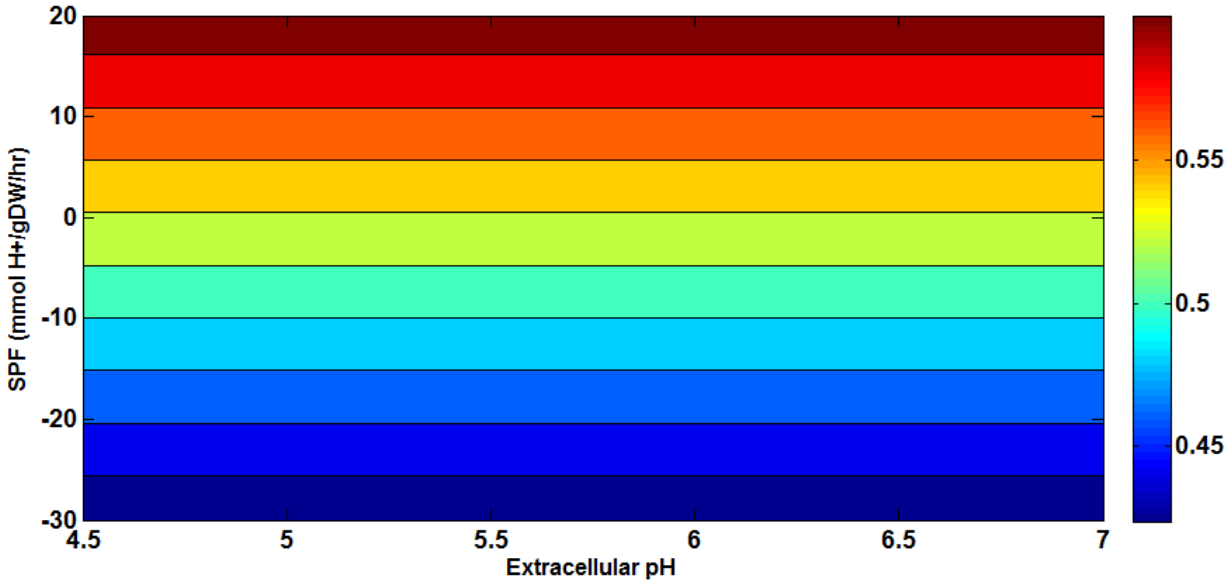

Fig. 4.18. Growth rate (hr^{-1}) as a function of extracellular pH and SPF in an un-proton-balanced version of *iMM864*. Glucose consumption was constrained to 10 $\frac{mmol}{h \cdot gDCW}$, and acetate and butyrate production and re-uptake were left unconstrained.

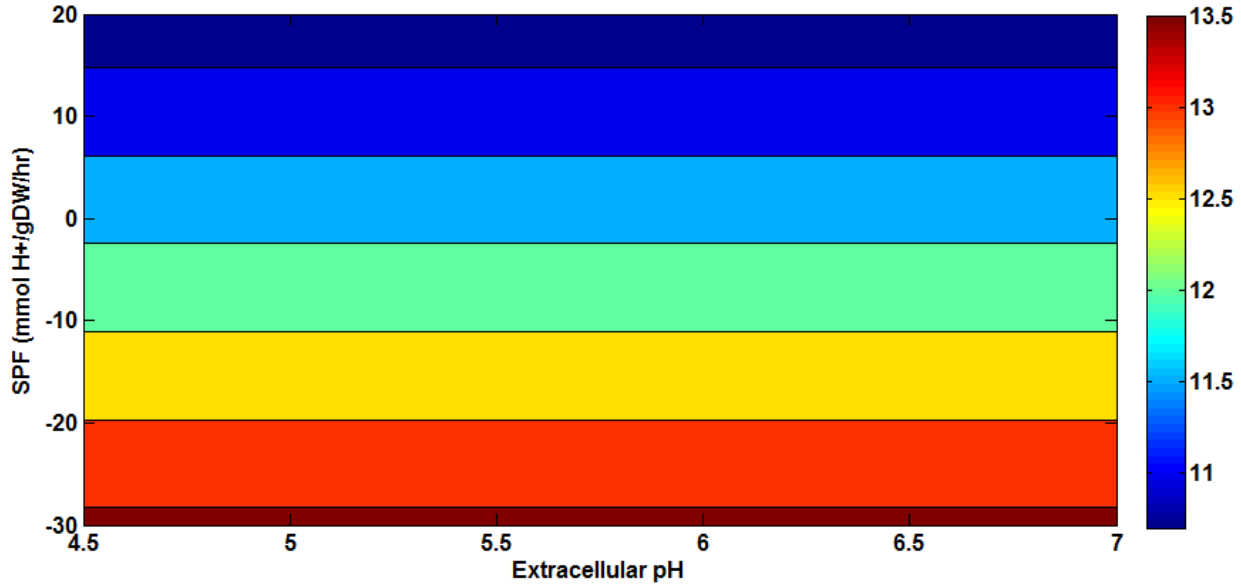

Fig. 4.19. Total acid production (acetate, butyrate, lactate, and succinate) ($\frac{mmol}{h \cdot gDCW}$) as a function of extracellular pH and SPF in an un-proton-balanced version of *iMM864*. Glucose consumption was constrained to 10 $\frac{mmol}{h \cdot gDCW}$, and acetate and butyrate production and re-uptake were left unconstrained.

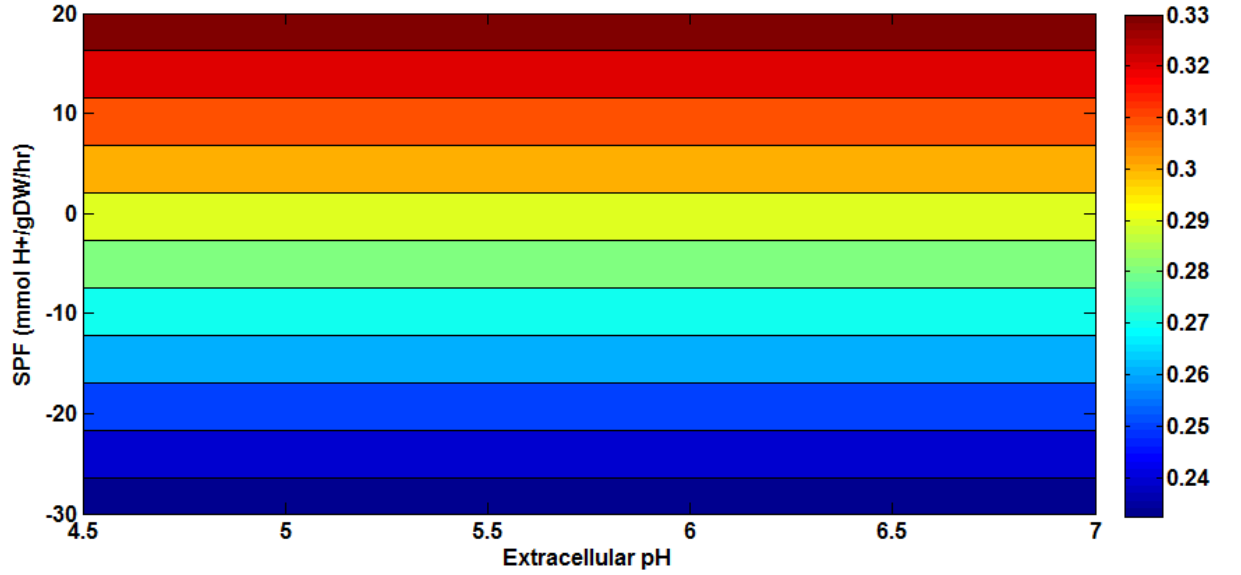

Fig. 4.20. Total solvent production (butanol, acetone, ethanol, and acetoin) ($\frac{mmol}{h \cdot gDCW}$) as a function of extracellular pH and SPF in an un-proton-balanced version of *iMM864*. Glucose consumption was constrained to 10 $\frac{mmol}{h \cdot gDCW}$, and acetate and butyrate production and re-uptake were left unconstrained.

4.4. *In silico* simulations of the *iAF1260* model for *E. coli* K12

The relationship between acetate productivity and growth was investigated by employing flux ratio constraints in the *iAF1260* genome-scale model for *E. coli* K12 MG1655 (*12*). Both the P/O ratio and the specific proton flux were constrained using a flux ratio to specified values and (i) acetate production and (ii) the specific growth rate were calculated. Constraints related to glucose minimal media were used (with maximum uptakes for glucose and oxygen of 8 and 18.5 $\frac{mmol}{h \cdot gDCW}$, respectively). A ratio constraint, instead of using the proton exchange reaction was used instead. When the proton exchange reaction is constrained, all of the transport reactions are taken into account. This led to erroneous results (not shown) with more acetate production occurring at more positive SPF values. Using the ratio constraint instead allowed for the constraining of only certain major transport reactions involved with generating the SPF. Results are shown in Figs. 4.21 and Fig. 4.22, respectively.

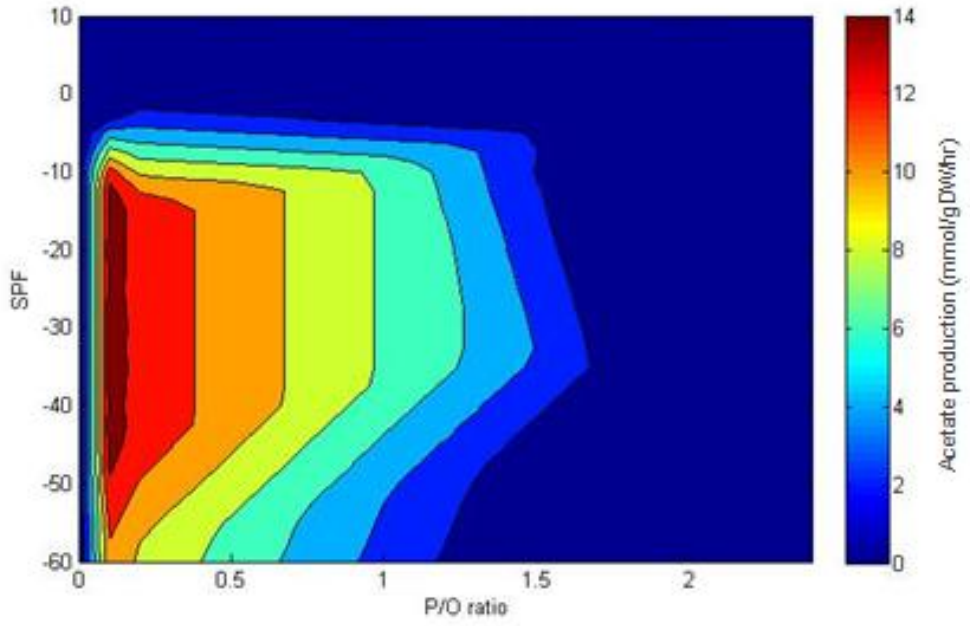

Fig. 4.21. Acetate production predicted by the *iAF1260* model as a function of the P/O ratio and the SPF.

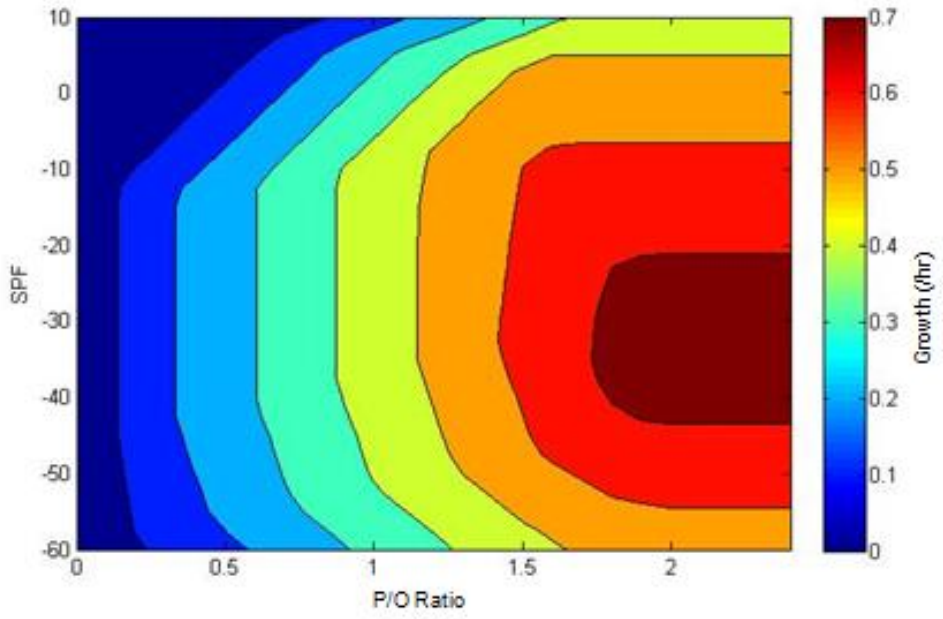

Fig. 4.22. Growth of *E. coli* K12 MG1655 predicted by the *iAF1260* model as a function of the P/O ratio and the SPF.

According to genome-scale model simulations, the maximum acetate production occurs at low P/O ratios, while maximum growth occurs at higher P/O ratios. Maximum acetate production and growth is predicted at an SPF of -30 $\frac{mmol\ H^+}{h \cdot gDCW}$. These simulations also indicate that if *E. coli* K12 cells were to grow as efficiently as possible (high P/O ratio), they would produce no acetate. Experimentally, this does not happen with the wild-type, as typical P/O ratios associated with growth in *E. coli* K12 are in the range of 1.4 to 1.5. It can then be concluded that there is some metabolic flux going through the less efficient NADH-2 and cytochrome *bd* complexes, diverting flux from NADH-1 and cytochrome *bo* enzymes. This, in turn, reduces the proton motive force created through the electron transport chain, and ATP production from the ATP synthase. The cell then needs another means of producing ATP, and this is done by producing acetate. From a metabolic engineering perspective, these simulations suggest that gene knockouts disrupting the NADH-1 and/or cytochrome *bo* proteins would result in increased

acetate production. If acetate is an undesired byproduct, however, its production may be reduced or even eliminated by conducting gene knockouts that disrupt the NADH-2 and/or cytochrome *bd* proteins. Its production may also be reduced by over-expressing NADH-1 and/or the cytochrome *bo* proteins.

Another possible reason that *E. coli* K12 relies on less-efficient proton motive force-generating components is that the more efficient components carry-out reactions with slower kinetic rates. So, conducting *in silico* gene knockouts may differ from what is expected as shown in these simulations. Knocking-out genes encoding for the NADH-2 and cytochrome *bd* proteins may end up decreasing the growth rate, even though the cells will be utilizing oxygen more efficiently. This knockout procedure may present a bottleneck to overall cellular metabolism by increasing the burden on NADH-1 and cytochrome *bo* to oxidize NADH. The only possible way that this can be reflected in simulations using a genome-scale model would be to place additional proper constraints on reactions catalyzed by NADH-1 and cytochrome *bo*. *In vivo* tests (Fig. 4.23) revealed that a knockout of the *ndh* gene (encoding for NADH-1) results in a distortion of the growth rate, especially with an increase in the amount of time the culture spends in the lag phase of growth. This provides further evidence that the NADH-2 protein is needed in order to oxidize excess amounts of NADH not oxidized by the NADH-1 complex.

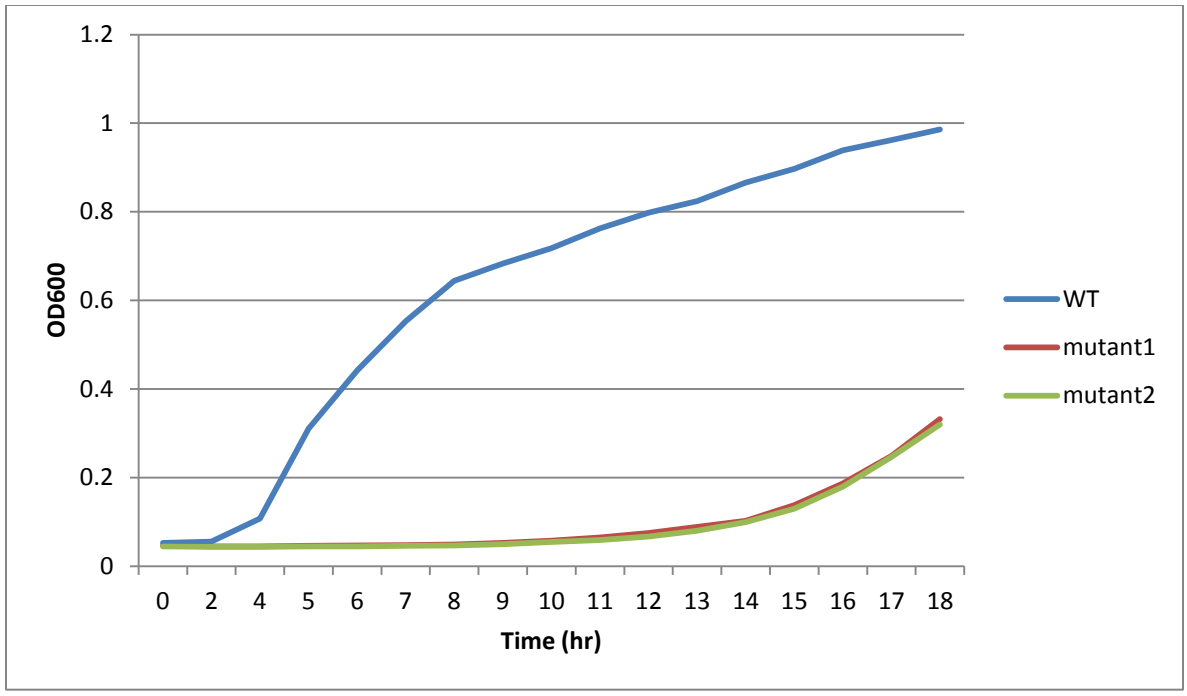

Fig. 4.23. Growth of wild-type *E. coli* BL-21 compared to growth of *Δndh* mutants.

4.5. References

1. Senger, R. S., and Papoutsakis, E. T. (2008) Genome-scale model for Clostridium acetobutylicum: Part I. Metabolic network resolution and analysis, *Biotechnol Bioeng 101*, 1036-1052.

2. Senger, R. S., and Papoutsakis, E. T. (2008) Genome-scale model for Clostridium acetobutylicum: Part II. Development of specific proton flux states and numerically determined sub-systems, *Biotechnol Bioeng 101*, 1053-1071.

3. Amador-Noguez, D., Feng, X. J., Fan, J., Roquet, N., Rabitz, H., and Rabinowitz, J. D. (2010) Systems-level metabolic flux profiling elucidates a complete, bifurcated tricarboxylic acid cycle in Clostridium acetobutylicum, *J Bacteriol 192*, 4452-4461.

4. Crown, S. B., Indurthi, D. C., Ahn, W. S., Choi, J., Papoutsakis, E. T., and Antoniewicz, M. R. (2011) Resolving the TCA cycle and pentose-phosphate pathway of Clostridium

acetobutylicum ATCC 824: Isotopomer analysis, in vitro activities and expression analysis, *Biotechnol J 6*, 300-305.

5. Jankowski, M. D., Henry, C. S., Broadbelt, L. J., and Hatzimanikatis, V. (2008) Group contribution method for thermodynamic analysis of complex metabolic networks, *Biophys J 95*, 1487-1499.

6. Zhang, H., Bruns, M. A., and Logan, B. E. (2006) Biological hydrogen production by Clostridium acetobutylicum in an unsaturated flow reactor, *Water Res 40*, 728-734.

7. Kim, B. H., Bellows, P., Datta, R., and Zeikus, J. G. (1984) Control of Carbon and Electron Flow in Clostridium acetobutylicum Fermentations: Utilization of Carbon Monoxide to Inhibit Hydrogen Production and to Enhance Butanol Yields, *Appl Environ Microbiol 48*, 764-770.

8. Wiesenborn, D. P., Rudolph, F. B., and Papoutsakis, E. T. (1988) Thiolase from Clostridium acetobutylicum ATCC 824 and Its Role in the Synthesis of Acids and Solvents, *Appl Environ Microbiol 54*, 2717-2722.

9. Ansorge-Schumacher, M. B., Klein, M., Fritsch, M., and Hartmeier, W. (2010) Influence of hydrogenase overexpression on hydrogen production of Clostridium acetobutylicum DSM 792, *Enzyme Microb Tech 46*, 384-390.

10. Sillers, R., Al-Hinai, M. A., and Papoutsakis, E. T. (2009) Aldehyde-alcohol dehydrogenase and/or thiolase overexpression coupled with CoA transferase downregulation lead to higher alcohol titers and selectivity in Clostridium acetobutylicum fermentations, *Biotechnol Bioeng 102*, 38-49.

11. Datta, R., and Zeikus, J. G. (1985) Modulation of acetone-butanol-ethanol fermentation by carbon monoxide and organic acids, *Appl Environ Microbiol 49*, 522-529.

12. Feist, A. M., Henry, C. S., Reed, J. L., Krummenacker, M., Joyce, A. R., Karp, P. D., Broadbelt, L. J., Hatzimanikatis, V., and Palsson, B. O. (2007) A genome-scale metabolic reconstruction for Escherichia coli K-12 MG1655 that accounts for 1260 ORFs and thermodynamic information, *Mol Syst Biol 3*, 121.

5. Conclusions and Recommendations

5.1. Conclusions

The research presented in this thesis focused on creating an updated genome-scale model for the butanol-producer *C. acetobutylicum* using a newly constructed genome-scale model database. Then this model was used to prepare simulations that can eventually be used to provide metabolic engineering strategies. The necessity of having a genome-scale model properly proton-balanced was proven. The capabilities of proton-balancing for different pH conditions, as well as adding ratio constraints for models of *C. acetobutylicum*, were also probed. Since the metabolism of *C. acetobutylicum* is biphasic (acidogenic and solventogenic) according to pH conditions, the combination of proton balancing the model and setting SPF constraints yielded simulation results qualitatively similar to what has been observed in published experimental results. In doing so, however, the production of one acid or solvent seemed to be representative for the production of all weak acids or all solvents. Imposing proper flux ratio constraints on reactions at "branch points" or "nodes" in the metabolic network changed simulations to appear closer to what was observed experimentally. The concept of the flux ratio constraint at a critical "branch point" or "node" in the metabolic network to result in the production of multiple metabolites that match experimental observations is novel. In previous approaches, researchers have constrained the production of individual metabolites (e.g., acetate, butyrate, etc.) individually to achieve a desired result. In retrospect, the following strategies were imperative for modeling the metabolism of *C. acetobutylicum*: (1) proton-balancing, (2) constraining the SPF, and (3) enforcing proper flux ratio constraints. The new *iMM864* genome-

scale model has shown to be superior to the first published genome-scale model of *C. acetobutylicum* in its ability to predict metabolism qualitatively.

Implementing a flux ratio constraint for the overall aerobic efficiency in *E. coli* K12 MG1655 was explored to illuminate relationships between (1) the P/O ratio, (2) the SPF, (3) the growth rate, and (4) the production of acetate. The simulations revealed that larger amounts of acetate are produced at low P/O ratios, while higher growth rates correlate to higher P/O ratios. Experimental observations show greater acetate production coincides with lower growth rates. However, *E. coli* K12, with glucose as the sole carbon source, tends to grow, in the laboratory, with a P/O ratio of 1.4 to 1.5 (*1*), which does not (theoretically) maximize its growth rate. This is most likely due to slower enzyme kinetics with the more efficient (in terms of oxygen consumption and proton efflux) NADH dehydrogenase and cytochrome oxidase proteins. Experimental results of the *E. coli* K12 *Δndh* knockout mutant reinforced this conclusion in that a knockout of the less efficient NADH dehydrogenase resulted in major growth deficiency.

5.2. Recommendations

The development of the proton-balancing algorithm has yielded more insights and questions to be answered in terms of the selectivity of transporter proteins towards the charge of their substrates. Not much research has been conducted on this topic, although evidence has been presented for various types of transport mechanisms being selective to the degree of protonation that the substrate is in (*2, 3*). This impacts the overall transport of protons across the membrane along with molecules transported either through diffusion or through a transporter protein. Because assumptions had to be made for the simulations in this study, further insight into this

aspect of membrane transport may yield possibly more accurate proton balancing for transport reactions.

Construction of an updated model for *C. acetobutylicum* has not only revealed new insights into its metabolism, but it has also generated new questions to be answered. The biomass constituting equation, defined as the RNA, DNA, protein, lipid, cell wall, and solute pool composition, is an important feature of a genome-scale model. Because the exact make-up of the biomass of *C. acetobutylicum* is not known, parts of the biomass constituting equation were based off of data for another organism, *S. aureus* N315 (*3*). The actual composition of the biomass of *C. acetobutylicum* may differ from that of *S. aureus*. Experimental studies using HPLC/MS and GC/MS may help determine the exact biomass constituting equation. What complicates this further, however, is the fact that cell composition may change as conditions vary, for instance with acidogenic and solventogenic phenotypes. Using a dynamic biomass constituting equation, rather than a static one, may solve this problem.

One major problem remains unanswered with regards to the metabolism in *C. acetobutylicum*. C^{13} analyses have revealed that it has a bifurcated TCA cycle leading to the production of succinate (*4*, *5*). What happens to succinate, however, is not known. Succinate is known to be secreted into the extracellular media only in small quantities (on a scale of one thousandth that of acid production) (*4*). The results in all simulations with the *iMM864* model indicate that it must be secreted at notable quantities, on a scale of almost one tenth of acid production. This could mean that *C. acetobutylicum* has developed a means for consuming succinate, and may actually incorporate it into its biomass rather than just secrete it as a by-product. To test this hypothesis, C^{13} analyses may be done by growing *C. acetobutylicum* in media containing C^{13}-labeled succinate.

The *iMM864* model still has yet to be fine-tuned to fit experimental data. The simulations provided in this research provided for mostly qualitative comparisons for what is seen experimentally. However, adjusting the flux ratio constraints to fit experimental data has not been done and may require additional flux ratios. None of these flux ratios have been measured experimentally, so the true validity of this constraint has yet to be verified. Although, this method did show to approximate experimental results when the thiolase enzyme was over-expressed in *C. acetobutylicum.* More advanced C^{13} analyses may be used to experimentally validate intracellular flux ratios, while SPF can be found by measuring how quickly *C. acetobutylicum* growth changes the pH under various conditions.

More simulations can always be done with the *iMM864* model, as well as proton balancing in general, not only to validate the model and constraints, but also to model *C. acetobutylicum* metabolism. The research in this work did not provide simulations for *C. acetobutylicum* growing under conditions promoting nitrogen fixation. Previous research has revealed certain aspects of the metabolism of *C. acetobutylicum* while it undergoes nitrogen fixation. Also, no simulations were performed comparing the effects of leaving all transport reactions labeled as "non-selective" for proton balancing. Such a comparison could yield more insight into the actual transport mechanism with regards to proton balancing. While the effects of changing extracellular pH were modeled while keeping intracellular pH constant, the effect of changing intracellular pH has also not been shown. Most gram-negative bacteria keep their intracellular pH constant, while gram-positive bacteria (including clostridia) can vary their intracellular pH as their surroundings change. These simulations may also be used to determine the optimum intracellular pH, while disregarding the effects of pH on enzyme kinetics.

5.3. References

1. Noguchi, Y., Nakai, Y., Shimba, N., Toyosaki, H., Kawahara, Y., Sugimoto, S., and Suzuki, E. (2004) The energetic conversion competence of Escherichia coli during aerobic respiration studied by 31P NMR using a circulating fermentation system, *J Biochem 136*, 509-515.
2. Law, C. J., Maloney, P. C., and Wang, D. N. (2008) Ins and outs of major facilitator superfamily antiporters, *Annu Rev Microbiol 62*, 289-305.
3. Senger, R. S., and Papoutsakis, E. T. (2008) Genome-scale model for Clostridium acetobutylicum: Part I. Metabolic network resolution and analysis, *Biotechnol Bioeng 101*, 1036-1052.
4. Amador-Noguez, D., Feng, X. J., Fan, J., Roquet, N., Rabitz, H., and Rabinowitz, J. D. (2010) Systems-level metabolic flux profiling elucidates a complete, bifurcated tricarboxylic acid cycle in Clostridium acetobutylicum, *J Bacteriol 192*, 4452-4461.
5. Crown, S. B., Indurthi, D. C., Ahn, W. S., Choi, J., Papoutsakis, E. T., and Antoniewicz, M. R. (2011) Resolving the TCA cycle and pentose-phosphate pathway of Clostridium acetobutylicum ATCC 824: Isotopomer analysis, in vitro activities and expression analysis, *Biotechnol J 6*, 300-305.

Appendix A. *iMM864* with reversibility information

Constraint Notes:			
d = determined by thermodynamics	df = constrained forward by thermodynamics	dr = constrained reverse by thermodynamics	tca = determined from fluxomics

Reaction ID	Pathway	Locus number	Stoichoimetric Equation	Lower Bound	Upper Bound	Constraint Notes	Minimum ΔG (kcal/mol)	Maximum ΔG (kcal/mol)
R00344	Alanine and aspartate metabolism	CAC2660	ATP[c] + Pyruvate[c] + HCO3-[c] -> ADP[c] + Orthophosphate[c] + Oxaloacetate[c] + 0.62 H+[c]	0	1000	tca	-13.800	30.712
R00355	Alanine and aspartate metabolism	CAC1001|CAC1819|CAC2832	2-Oxoglutarate[c] + L-Aspartate[c] <=> L-Glutamate[c] + Oxaloacetate[c] + 0.01 H+[c]	-1000	1000	d	-10.636	10.636
R00401	Alanine and aspartate metabolism	CAC0492|CAC3331	L-Alanine[c] <=> D-Alanine[c]	-1000	1000		-5.620	5.620
R00485	Alanine and aspartate metabolism	CAC1714	H2O[c] + L-Asparagine[c] -> NH3[c] + L-Aspartate[c]	0	1000	df	-16.022	6.576
R00489	Alanine and aspartate metabolism	CAC2916	L-Aspartate[c] + 2.41 H+[c] -> CO2[c] + beta-Alanine[c]	0	1000		-25.472	-8.897
R00490	Alanine and aspartate metabolism	CAC0274|CAC1652	NH3[c] + Fumarate[c] <- L-Aspartate[c] + 0.98 H+[c]	-1000	0	dr	1.073	18.475
R00578	Alanine and aspartate metabolism	CAC2243	H2O[c] + ATP[c] + L-Aspartate[c] + L-Glutamine[c] -> Diphosphate[c] + AMP[c] + L-Glutamate[c] + 1.23 H+[c] + L-Asparagine[c]	0	1000		-35.327	18.841
R00908	Alanine and aspartate metabolism	CAC0368|CAC1427	2-Oxoglutarate[c] + beta-Alanine[c] <=> L-Glutamate[c] + 1.42 H+[c] + 3-Oxopropanoate[c]	-1000	1000		-11.492	9.492
R01083	Alanine and aspartate metabolism	CAC1821	"N6-(1,2-Dicarboxyethyl)-AMP"[c] <=> AMP[c] + 0.01 H+[c] + Fumarate[c]	-1000	1000		-12.728	18.279
R01086	Alanine and aspartate metabolism	CAC0974	2.97 H+[c] + N-(L-Arginino)succinate[c] <=> L-Arginine[c] + Fumarate[c]	-1000	1000		NaN	NaN
R01135	Alanine and aspartate metabolism	CAC3593	GTP[c] + L-Aspartate[c] + IMP[c] -> Orthophosphate[c] + GDP[c] + 0.51 H+[c] + "N6-(1,2-Dicarboxyethyl)-AMP"[c]	0	1000		-16.723	33.075
R01397	Alanine and aspartate metabolism	CAC2653|CAC2654	L-Aspartate[c] + 0.36 H+[c] + Carbamoyl phosphate[c] <=> Orthophosphate[c] + N-Carbamoyl-L-aspartate[c]	-1000	1000		-9.818	13.390
R01954	Alanine and aspartate metabolism	CAC0973	ATP[c] + L-Aspartate[c] + L-Citrulline[c] <=> Diphosphate[c] + AMP[c] + 1.21 H+[c] + N-(L-Arginino)succinate[c]	-1000	1000		NaN	NaN
R07255	Alanine and aspartate metabolism	Unassigned	H+[c] + 3-Oxopropanoate[c] -> CO2[c] + Acetaldehyde[c]	0	1000		-26.571	-10.118
R00150	Arginine and proline metabolism	Unassigned	ATP[c] + CO2[c] + NH3[c] <=> ADP[c] + 1.86 H+[c] + Carbamoyl phosphate[c]	-1000	1000	d	-6.490	33.559
R00551	Arginine and proline metabolism	CAC1054	H2O[c] + L-Arginine[c] <=> L-Ornithine[c] + 0.11 H+[c] + Urea[c]	-1000	1000		NaN	NaN
R00667	Arginine and proline metabolism	Unassigned	2-Oxoglutarate[c] + L-Ornithine[c] <0> L-Glutamate[c] + 2.88 H+[c] + L-Glutamate 5-semialdehyde[c]	0	0		-12.100	10.100
R01248	Arginine and proline metabolism	CAC3252	NAD+[c] + L-Proline[c] <0> NADH[c] + 1.31 H+[c] + (S)-1-Pyrroline-5-carboxylate[c]	0	0		-29.259	18.150
R01251	Arginine and proline metabolism	CAC3252	NADP+[c] + L-Proline[c] <- NADPH[c] + 1.31 H+[c] + (S)-1-Pyrroline-5-carboxylate[c]	-1000	0		-29.232	18.123
R01398	Arginine and proline metabolism	CAC0316	L-Ornithine[c] + Carbamoyl phosphate[c] <=> Orthophosphate[c] + 2.52 H+[c] + L-Citrulline[c]	-1000	1000		-10.313	13.885
R07358	Arginine and proline metabolism	Unassigned	H2O[c] + (S)-1-Pyrroline-5-carboxylate[c] <- N-Acetyl-L-glutamate 5-semialdehyde[c]	-1000	0		-29.698	-11.319
R02869	B-alanine metabolism	Unassigned	Spermidine[c] + S-Adenosylmethioninamine[c] <=> 1.03 H+[c] + 5-Methylthioadenosine[c] + Spermine[c]	-1000	1000		-24.044	14.704
R02473	Beta-alanine metabolism	CAC2915	ATP[c] + beta-Alanine[c] + (R)-Pantoate[c] <=> Diphosphate[c] + AMP[c] + 1.63 H+[c] + Pantothenate[c]	-1000	1000		-38.472	6.332
R00483	Cyanoamino acid metabolism	Unassigned	ATP[c] + NH3[c] + L-Aspartate[c] -> Diphosphate[c] + AMP[c] + 1.21 H+[c] + L-Asparagine[c]	0	1000		-25.912	18.872
R00945	Cyanoamino acid metabolism	CAC2264	H2O[c] + Glycine[c] + "5,10-Methylenetetrahydrofolate"[c] <=> L-Serine[c] + 0.01 H+[c] + Tetrahydrofolate[c]	-1000	1000		-15.506	24.529
R00586	Cysteine metabolism	CAC0687	Acetyl-CoA[c] + L-Serine[c] -> CoA[c] + O-Acetyl-L-serine[c]	0	1000		NaN	NaN
R00782	Cysteine metabolism	CAC0391	H2O[c] + 0.3 H+[c] + L-Cysteine[c] -> NH3[c] + Pyruvate[c] + Hydrogen sulfide[c]	0	1000	df	-24.704	2.517
R00897	Cysteine metabolism	CAC0931|CAC2235	Hydrogen sulfide[c] + O-Acetyl-L-serine[c] -> Acetate[c] + 0.31 H+[c] + L-Cysteine[c]	0	1000		-14.788	7.940
R01148	D-alanine metabolism	CAC0792	2-Oxoglutarate[c] + D-Alanine[c] <=> Pyruvate[c] + 0.02 H+[c] + D-Glutamate[c]	-1000	1000		-10.554	10.554
R01150	D-alanine metabolism	CAC2895	ATP[c] + 0.47 H+[c] + 2 D-Alanine[c] <=> ADP[c] + Orthophosphate[c] + D-Alanyl-D-alanine[c]	-1000	1000		-27.562	17.334
R02459	D-arginine and D-ornithine metabolism	CAC0792	L-Ornithine[c] + 2-Oxo acid[c] <=> Amino acid[c] + 5-Amino-2-oxopentanoic acid|5-Amino-2-oxopentanoic acid|5-Amino-2-oxopentanoate|2-Oxo-5-amino-pentanoate|2-Oxo-5-aminopentanoate|alpha-Keto-delta-aminopentanoate|2-Oxo-5-aminovalerate[c]	-1000	1000		NaN	NaN
R02924	D-arginine and D-ornithine metabolism	CAC0792	L-Arginine[c] + 2-Oxo acid[c] <=> Amino acid[c] + 5-Guanidino-2-oxopentanoate|5-Guanidino-2-oxopentanoate|5-Guanidino-2-oxo-pentanoate|2-Oxo-5-guanidinopentanoate|2-Oxo-5-guanidino-pentanoate|2-Oxoarginine[c]	-1000	1000		NaN	NaN
R00260	D-glutamine and D-glutamate metabolism	CAC3250	L-Glutamate[c] <=> D-Glutamate[c]	-1000	1000	d	-5.804	5.804
R02783	D-glutamine and D-glutamate metabolism	CAC3194	ATP[c] + 0.48 H+[c] + D-Glutamate[c] + UDP-N-acetylmuramoyl-L-alanine[c] -> ADP[c] + Orthophosphate[c] + UDP-N-acetylmuramoyl-L-alanyl-D-glutamate[c]	0	1000		-32.268	22.040
R03193	D-glutamine and D-glutamate metabolism	CAC3225	ATP[c] + L-Alanine[c] + 0.46 H+[c] + UDP-N-acetylmuramate[c] -> ADP[c] + Orthophosphate[c] + UDP-N-acetylmuramoyl-L-alanine[c]	0	1000		-31.554	21.326
R00114	Glutamate metabolism	CAC0764|CAC1673|CAC1674	NADP+[c] + 2 L-Glutamate[c] <- NADPH[c] + 2-Oxoglutarate[c] + L-Glutamine[c]	-1000	0		-27.628	28.739
R00248	Glutamate metabolism	CAC0737	H2O[c] + NADP+[c] + L-Glutamate[c] <- NADPH[c] + NH3[c] + 2-Oxoglutarate[c] + 0.01 H+[c]	-1000	0	d	-32.222	23.887
R00253	Glutamate metabolism	CAC2658	ATP[c] + NH3[c] + L-Glutamate[c] -> ADP[c] + Orthophosphate[c] + L-Glutamine[c] + 0.51 H+[c]	0	1000		-14.970	29.842
R00257	Glutamate metabolism	CAC1050|CAC1782	H2O[c] + ATP[c] + L-Glutamine[c] + Deamino-NAD+[c] -> NAD+[c] + Diphosphate[c] + AMP[c] + L-Glutamate[c] + 1.22 H+[c]	0	1000		-41.380	24.894
R00575	Glutamate metabolism	CAC2644|CAC2645	H2O[c] + 2 ATP[c] + L-Glutamine[c] + HCO3-[c] -> 2 ADP[c] + Orthophosphate[c] + L-Glutamate[c] + 1.51 H+[c] + Carbamoyl phosphate[c]	0	1000		-41.634	38.180
R01072	Glutamate metabolism	CAC1392	Diphosphate[c] + L-Glutamate[c] + 1.38 H+[c] + 5-Phosphoribosylamine[c] <=> H2O[c] + L-Glutamine[c] + 5-Phospho-alpha-D-ribose 1-diphosphate[c]	-1000	1000		-15.273	20.559
R01231	Glutamate metabolism	CAC2700	H2O[c] + ATP[c] + L-Glutamine[c] + Xanthosine 5-phosphate[c] -> Diphosphate[c] + AMP[c] + L-Glutamate[c] + 2.21 H+[c] + GMP[c]	0	1000		-24.396	35.290
R00220	Glycine and serine and threonine metabolism	CAC0673|CAC0674	L-Serine[c] + 0.98 H+[c] -> NH3[c] + Pyruvate[c]	0	1000	df	-28.539	-12.190
R00480	Glycine and serine and threonine metabolism	CAC0278|CAC1810	ATP[c] + L-Aspartate[c] + 0.19 H+[c] <=> ADP[c] + 4-Phospho-L-aspartate[c]	-1000	1000		-24.586	10.786
R00582	Glycine and serine and threonine metabolism	Unassigned	H2O[c] + 0.27 H+[c] + O-Phospho-L-serine[c] <=> Orthophosphate[c] + L-Serine[c]	-1000	1000		-3.625	18.051
R00751	Glycine and serine and threonine metabolism	CAC3420	L-Threonine[c] -> Glycine[c] + Acetaldehyde[c]	0	1000		-9.681	6.972

R01388	Glycine and serine and threonine metabolism	CAC2945	NAD+[c] + D-Glycerate[c] <- NADH[c] + H+[c] + Hydroxypyruvate[c]	-1000	0		-21.823	25.134
R01466	Glycine and serine and threonine metabolism	CAC0999	H2O[c] + 0.04 H+[c] + O-Phospho-L-homoserine[c] <=> Orthophosphate[c] + L-Threonine[c]	-1000	1000		-5.538	16.344
R01513	Glycine and serine and threonine metabolism	CAC0015|CAC0089	NAD+[c] + 3-Phospho-D-glycerate[c] <=> NADH[c] + 1.1 H+[c] + 3-Phosphonooxypyruvate[c]	-1000	1000		-21.821	25.132
R01771	Glycine and serine and threonine metabolism	CAC1235	ATP[c] + L-Homoserine[c] <=> ADP[c] + 0.56 H+[c] + O-Phospho-L-homoserine[c]	-1000	1000		-22.185	13.185
R01773	Glycine and serine and threonine metabolism	CAC0998	NAD+[c] + L-Homoserine[c] <0> NADH[c] + H+[c] + L-Aspartate 4-semialdehyde[c]	0	0		-22.849	24.160
R01775	Glycine and serine and threonine metabolism	CAC0998	NADP+[c] + L-Homoserine[c] <=> NADPH[c] + H+[c] + L-Aspartate 4-semialdehyde[c]	-1000	1000	d	-22.821	24.132
R02291	Glycine and serine and threonine metabolism	CAC0022|CAC0568	NADP+[c] + Orthophosphate[c] + L-Aspartate 4-semialdehyde[c] <=> NADPH[c] + 1.28 H+[c] + 4-Phospho-L-aspartate[c]	-1000	1000		-35.656	15.884
R02528	Glycine and serine and threonine metabolism	CAC3298|CAC3299	NADPH[c] + H+[c] + Methylglyoxal[c] <=> NADP+[c] + Hydroxyacetone[c]	-1000	1000		NaN	NaN
R04173	Glycine and serine and threonine metabolism	Unassigned	2-Oxoglutarate[c] + O-Phospho-L-serine[c] <0> L-Glutamate[c] + 0.07 H+[c] + 3-Phosphonooxypyruvate[c]	0	0		-10.608	10.608
R01071	Histidine metabolism	CAC0936	Diphosphate[c] + 0.37 H+[c] + 1-(5-Phospho-D-ribosyl)-ATP[c] <=> ATP[c] + 5-Phospho-alpha-D-ribose 1-diphosphate[c]	-1000	1000		-12.598	27.958
R01163	Histidine metabolism	CAC0937	H2O[c] + 2 NAD+[c] + L-Histidinal[c] <=> 2 NADH[c] + 3.86 H+[c] + L-Histidine[c]	-1000	1000		-37.635	47.629
R01168	Histidine metabolism	Unassigned	0.98 H+[c] + L-Histidine[c] -> NH3[c] + Urocanate[c]	0	1000	df	-23.415	-2.674
R02287	Histidine metabolism	Unassigned	H2O[c] + N-Formimino-L-glutamate[c] <- L-Glutamate[c] + Formamide[c]	-1000	0	dr	16.117	41.417
R02288	Histidine metabolism	Unassigned	H2O[c] + 4-Imidazolone-5-propanoate[c] -> 0.2 H+[c] + N-Formimino-L-glutamate[c]	0	1000	df	-35.739	-9.887
R02914	Histidine metabolism	Unassigned	0.8 H+[c] + 4-Imidazolone-5-propanoate[c] <=> H2O[c] + Urocanate[c]	-1000	1000		-11.886	8.303
R03012	Histidine metabolism	CAC0937	NAD+[c] + L-Histidinol[c] <=> NADH[c] + 1.29 H+[c] + L-Histidinal[c]	-1000	1000		-23.231	24.542
R03013	Histidine metabolism	CAC2727	H2O[c] + 1.31 H+[c] + L-Histidinol phosphate[c] <=> Orthophosphate[c] + L-Histidinol[c]	-1000	1000		-5.399	19.825
R03243	Histidine metabolism	CAC1369|CAC3031	2-Oxoglutarate[c] + L-Histidinol phosphate[c] <=> L-Glutamate[c] + 0.22 H+[c] + 3-(Imidazol-4-yl)-2-oxopropyl phosphate[c]	-1000	1000		NaN	NaN
R03457	Histidine metabolism	CAC0938	D-erythro-1-(Imidazol-4-yl)glycerol 3-phosphate[c] <=> H2O[c] + 0.19 H+[c] + 3-(Imidazol-4-yl)-2-oxopropyl phosphate[c]	-1000	1000		NaN	NaN
R04035	Histidine metabolism	CAC0943	H2O[c] + 1-(5-Phospho-D-ribosyl)-ATP[c] <=> Diphosphate[c] + 1.26 H+[c] + Phosphoribosyl-AMP[c]	-1000	1000		-30.132	13.646
R04037	Histidine metabolism	CAC0942	H2O[c] + Phosphoribosyl-AMP[c] <=> 0.09 H+[c] + 5-(5-Phospho-D-ribosylaminoformimino)-1-(5-phosphoribosyl)-[c]	-1000	1000		-10.706	27.909
R04558	Histidine metabolism	Unassigned	L-Glutamate[c] + 0.9 H+[c] + D-erythro-1-(Imidazol-4-yl)glycerol 3-phosphate[c] + 1-(5-Phosphoribosyl)-5-amino-4-imidazolecarboxamide[c] <=> L-Glutamine[c] + N-(5-Phospho-D-1-ribulosylformimino)-5-amino-1-(5-phospho-D-[c]	-1000	1000		NaN	NaN
R04640	Histidine metabolism	CAC0940	0.17 H+[c] + 5-(5-Phospho-D-ribosylaminoformimino)-1-(5-phosphoribosyl)-[c] <=> N-(5-Phospho-D-1-ribulosylformimino)-5-amino-1-(5-phospho-D-[c]	-1000	1000		NaN	NaN
R00451	Lysine biosynthesis	CAC0608	3.9 H+[c] + "meso-2,6-Diaminoheptanedioate"[c] -> CO2[c] + L-Lysine[c]	0	1000		-26.380	-7.989
R02292	Lysine biosynthesis	CAC2378|CAC3600	Pyruvate[c] + L-Aspartate 4-semialdehyde[c] <=> 2 H2O[c] + "L-2,3-Dihydrodipicolinate"[c]	-1000	1000		NaN	NaN
R02734	Lysine biosynthesis	CAC2723	H2O[c] + "N-Succinyl-LL-2,6-diaminoheptanedioate"[c] <=> Succinate[c] + 0.96 H+[c] + "LL-2,6-Diaminoheptanedioate"[c]	-1000	1000		NaN	NaN
R02735	Lysine biosynthesis	CAC2624	"LL-2,6-Diaminoheptanedioate"[c] <=> "meso-2,6-Diaminoheptanedioate"[c]	-1000	1000		-6.780	6.780
R04198	Lysine biosynthesis	CAC2379	NAD+[c] + "2,3,4,5-Tetrahydrodipicolinate"[c] <0> NADH[c] + H+[c] + "L-2,3-Dihydrodipicolinate"[c]	0	0		NaN	NaN
R04199	Lysine biosynthesis	CAC2379	NADP+[c] + "2,3,4,5-Tetrahydrodipicolinate"[c] <=> NADPH[c] + H+[c] + "L-2,3-Dihydrodipicolinate"[c]	-1000	1000		NaN	NaN
R04365	Lysine biosynthesis	CAC2381	H2O[c] + Succinyl-CoA[c] + "2,3,4,5-Tetrahydrodipicolinate"[c] <=> CoA[c] + N-Succinyl-2-L-amino-6-oxoheptanedioate[c]	-1000	1000		NaN	NaN
R04475	Lysine biosynthesis	CAC2380	2-Oxoglutarate[c] + "N-Succinyl-LL-2,6-diaminoheptanedioate"[c] <=> L-Glutamate[c] + N-Succinyl-2-L-amino-6-oxoheptanedioate[c]	-1000	1000		NaN	NaN
R00177	Methionine metabolism	CAC2856	Orthophosphate[c] + Diphosphate[c] + S-Adenosyl-L-methionine[c] <- H2O[c] + ATP[c] + L-Methionine[c] + 1.09 H+[c]	-1000	0		-20.320	26.494
R00192	Methionine metabolism	Unassigned	H2O[c] + S-Adenosyl-L-homocysteine[c] + 0.02 H+[c] <=> L-Homocysteine[c] + Adenosine[c]	-1000	1000		-12.321	23.667
R00194	Methionine metabolism	CAC2117	H2O[c] + S-Adenosyl-L-homocysteine[c] + 0.03 H+[c] -> Adenine[c] + S-Ribosyl-L-homocysteine[c]	0	1000		NaN	NaN
R00650	Methionine metabolism	CAC3348	S-Adenosyl-L-methionine[c] + L-Homocysteine[c] <=> S-Adenosyl-L-homocysteine[c] + L-Methionine[c] + 2 H+[c]	-1000	1000		-22.669	15.437
R00946	Methionine metabolism	CAC0578	0.01 H+[c] + L-Homocysteine[c] + 5-Methyltetrahydrofolate[c] <=> L-Methionine[c] + Tetrahydrofolate[c]	-1000	1000		-24.026	11.214
R00999	Methionine metabolism	CAC0390|CAC0930	H2O[c] + 0.03 H+[c] + O-Succinyl-L-homoserine[c] <=> NH3[c] + Succinate[c] + 2-Oxobutanoate[c]	-1000	1000		-26.379	0.424
R01286	Methionine metabolism	CAC0391	H2O[c] + H+[c] + Cystathionine[c] -> NH3[c] + Pyruvate[c] + L-Homocysteine[c]	0	1000	df	-29.016	-0.367
R01291	Methionine metabolism	CAC2942	H2O[c] + 0.01 H+[c] + S-Ribosyl-L-homocysteine[c] <=> D-Ribose[c] + L-Homocysteine[c]	-1000	1000		NaN	NaN
R01777	Methionine metabolism	CAC1825	Succinyl-CoA[c] + L-Homoserine[c] <=> CoA[c] + 0.01 H+[c] + O-Succinyl-L-homoserine[c]	-1000	1000		NaN	NaN
R03260	Methionine metabolism	CAC0390|CAC0930	L-Cysteine[c] + O-Succinyl-L-homoserine[c] <=> Succinate[c] + 0.96 H+[c] + Cystathionine[c]	-1000	1000		-10.329	13.757
R00674	Phenylalanine and tyrosine and tryptophan biosynthesis	CAC3157|CAC3158	L-Serine[c] + 0.02 H+[c] + Indole[c] -> H2O[c] + L-Tryptophan[c]	0	1000		-25.643	1.749
R00694	Phenylalanine and tyrosine and tryptophan biosynthesis	CAC1001|CAC1819|CAC2832|CAC1369|CAC3031	L-Glutamate[c] + 0.02 H+[c] + Phenylpyruvate[c] <=> 2-Oxoglutarate[c] + L-Phenylalanine[c]	-1000	1000		-11.682	11.682
R00734	Phenylalanine and tyrosine and tryptophan biosynthesis	CAC1001|CAC1819|CAC2832|CAC1369|CAC3031	L-Glutamate[c] + 3-(4-Hydroxyphenyl)pyruvate[c] <=> 2-Oxoglutarate[c] + L-Tyrosine[c]	-1000	1000		-11.867	11.867
R00985	Phenylalanine and tyrosine and tryptophan biosynthesis	CAC3162|CAC3163	NH3[c] + Chorismate[c] -> H2O[c] + Pyruvate[c] + 0.98 H+[c] + Anthranilate[c]	0	1000		-49.440	-19.503
R00986	Phenylalanine and tyrosine and tryptophan biosynthesis	CAC3162|CAC3163	L-Glutamine[c] + Chorismate[c] -> Pyruvate[c] + L-Glutamate[c] + H+[c] + Anthranilate[c]	0	1000		-54.358	-24.031
R01073	Phenylalanine and tyrosine and tryptophan biosynthesis	CAC3161	Anthranilate[c] + 5-Phospho-alpha-D-ribose 1-diphosphate[c] <=> Diphosphate[c] + 0.38 H+[c] + N-(5-Phospho-D-ribosyl)anthranilate[c]	-1000	1000		-24.199	3.259
R01373	Phenylalanine and tyrosine and tryptophan biosynthesis	CAC0217	H+[c] + Prephenate[c] -> H2O[c] + CO2[c] + Phenylpyruvate[c]	0	1000	df	-60.142	-35.309
R01714	Phenylalanine and tyrosine and tryptophan biosynthesis	CAC0896	0.23 H+[c] + 5-O-(1-Carboxyvinyl)-3-phosphoshikimate[c] <=> Orthophosphate[c] + Chorismate[c]	-1000	1000		-19.037	2.120
R01715	Phenylalanine and tyrosine and tryptophan biosynthesis	CAC1234	Chorismate[c] -> Prephenate[c]	0	1000	df	-25.034	-8.326
R01728	Phenylalanine and tyrosine and tryptophan biosynthesis	CAC0893	NAD+[c] + Prephenate[c] -> NADH[c] + CO2[c] + 3-(4-Hydroxyphenyl)pyruvate[c]	0	1000	df	-60.923	-8.635

R01826	Phenylalanine and tyrosine and tryptophan biosynthesis	CAC0892	H2O[c] + Phosphoenolpyruvate[c] + 0.45 H+[c] + D-Erythrose 4-phosphate[c] <=> Orthophosphate[c] + 2-Dehydro-3-deoxy-D-arabino-heptonate 7-phosphate[c]	-1000	1000		NaN	NaN
R02340	Phenylalanine and tyrosine and tryptophan biosynthesis	CAC3157|CAC3158	0.04 H+[c] + D-Glyceraldehyde 3-phosphate[c] + Indole[c] <=> Indoleglycerol phosphate[c]	-1000	1000		-9.541	13.110
R02412	Phenylalanine and tyrosine and tryptophan biosynthesis	CAC0898	ATP[c] + Shikimate[c] <=> ADP[c] + 0.78 H+[c] + Shikimate 3-phosphate[c]	-1000	1000		-22.495	13.495
R02413	Phenylalanine and tyrosine and tryptophan biosynthesis	CAC0897	NADP+[c] + Shikimate[c] <=> NADPH[c] + H+[c] + 3-Dehydroshikimate[c]	-1000	1000		-27.517	19.888
R03083	Phenylalanine and tyrosine and tryptophan biosynthesis	CAC0894	0.16 H+[c] + 2-Dehydro-3-deoxy-D-arabino-heptonate 7-phosphate[c] <=> Orthophosphate[c] + 3-Dehydroquinate[c]	-1000	1000		NaN	NaN
R03084	Phenylalanine and tyrosine and tryptophan biosynthesis	CAC0899	3-Dehydroquinate[c] -> H2O[c] + 3-Dehydroshikimate[c]	0	1000	df	-22.584	-3.498
R03460	Phenylalanine and tyrosine and tryptophan biosynthesis	CAC0895	Phosphoenolpyruvate[c] + 0.4 H+[c] + Shikimate 3-phosphate[c] <=> Orthophosphate[c] + 5-O-(1-Carboxyvinyl)-3-phosphoshikimate[c]	-1000	1000		-2.072	22.724
R03508	Phenylalanine and tyrosine and tryptophan biosynthesis	CAC3160	H+[c] + 1-(2-Carboxyphenylamino)-1-deoxy-D-ribulose 5-phosphate[c] -> H2O[c] + CO2[c] + Indoleglycerol phosphate[c]	0	1000	df	-46.306	-19.925
R03509	Phenylalanine and tyrosine and tryptophan biosynthesis	CAC3159	0.09 H+[c] + N-(5-Phospho-D-ribosyl)anthranilate[c] <=> 1-(2-Carboxyphenylamino)-1-deoxy-D-ribulose 5-phosphate[c]	-1000	1000		-7.879	9.119
R01090	Valine and leucine and isoleucine biosynthesis	CAC1479	L-Glutamate[c] + 0.04 H+[c] + 4-Methyl-2-oxopentanoate[c] <=> 2-Oxoglutarate[c] + L-Leucine[c]	-1000	1000		-10.771	10.771
R01652	Valine and leucine and isoleucine biosynthesis	Unassigned	H+[c] + (2S)-2-Isopropyl-3-oxosuccinate[c] -> CO2[c] + 4-Methyl-2-oxopentanoate[c]	0	1000	df	-25.561	-8.808
R02199	Valine and leucine and isoleucine biosynthesis	CAC1479	2-Oxoglutarate[c] + L-Isoleucine[c] <=> L-Glutamate[c] + 0.05 H+[c] + (S)-3-Methyl-2-oxopentanoic acid[c]	-1000	1000		-10.771	10.771
R03968	Valine and leucine and isoleucine biosynthesis	CAC3172|CAC3173	0.07 H+[c] + (2S)-2-Isopropylmalate[c] <=> H2O[c] + 2-Isopropylmaleate[c]	-1000	1000		-11.886	5.703
R04001	Valine and leucine and isoleucine biosynthesis	CAC3172|CAC3173	0.07 H+[c] + "(2R,3S)-3-Isopropylmalate"[c] <=> H2O[c] + 2-Isopropylmaleate[c]	-1000	1000		-13.392	4.370
R04426	Valine and leucine and isoleucine biosynthesis	CAC3171	NAD+[c] + "(2R,3S)-3-Isopropylmalate"[c] <=> NADH[c] + 1.03 H+[c] + (2S)-2-Isopropyl-3-oxosuccinate[c]	-1000	1000		-21.883	25.194
R04440	Valine and leucine and isoleucine biosynthesis	CAC0091	NADP+[c] + "2,3-Dihydroxy-3-methylbutanoate"[c] + "(R)-2,3-Dihydroxy-3-methylbutanoate"[c] <- NADPH[c] + 3-Hydroxy-3-methyl-2-oxobutanoic acid[c]	-1000	0	dr	157.984	205.045
R04441	Valine and leucine and isoleucine biosynthesis	CAC3170|CAC3604	H+[c] + "2,3-Dihydroxy-3-methylbutanoate"[c] + "(R)-2,3-Dihydroxy-3-methylbutanoate"[c] <- H2O[c] + 3-Methyl-2-oxobutanoic acid[c]	-1000	0	dr	143.590	165.316
R04672	Valine and leucine and isoleucine biosynthesis	CAC3169|CAC3176|CAC3652	Thiamin diphosphate[c] + 2-Acetolactate[c] <=> Pyruvate[c] + 2-(alpha-Hydroxyethyl)thiamine diphosphate[c]	-1000	1000		NaN	NaN
R04673	Valine and leucine and isoleucine biosynthesis	CAC3169|CAC3176|CAC3652	2-Oxobutanoate[c] + 2-(alpha-Hydroxyethyl)thiamine diphosphate[c] <=> Thiamin diphosphate[c] + (S)-2-Aceto-2-hydroxybutanoate[c]	-1000	1000		NaN	NaN
R05068	Valine and leucine and isoleucine biosynthesis	CAC0091	NADP+[c] + "2,3-Dihydroxy-3-methylpentanoate"[c] <=> NADPH[c] + H+[c] + (R)-3-Hydroxy-3-methyl-2-oxopentanoate[c]	-1000	1000		-21.839	25.150
R05069	Valine and leucine and isoleucine biosynthesis	CAC0091	(S)-2-Aceto-2-hydroxybutanoate[c] <=> (R)-3-Hydroxy-3-methyl-2-oxopentanoate[c]	-1000	1000		-3.369	8.289
R05070	Valine and leucine and isoleucine biosynthesis	CAC3170|CAC3604	"2,3-Dihydroxy-3-methylpentanoate"[c] -> H2O[c] + (S)-3-Methyl-2-oxopentanoic acid[c]	0	1000	df	-19.672	-2.951
R05071	Valine and leucine and isoleucine biosynthesis	CAC0091	2-Acetolactate[c] <=> 3-Hydroxy-3-methyl-2-oxobutanoic acid[c]	-1000	1000		-3.346	8.266
R07399	Valine and leucine and isoleucine biosynthesis	Unassigned	H2O[c] + Pyruvate[c] + Acetyl-CoA[c] <=> CoA[c] + 0.98 H+[c] + (R)-2-Methylmalate[c]	-1000	1000		NaN	NaN
R00357	alanine, aspartate and glutamate metabolism	Unassigned	H2O[c] + Oxygen[c] + L-Aspartate[c] + 0.97 H+[c] -> NH3[c] + H2O2[c] + Oxaloacetate[c]	0	1000	df	-47.100	-15.526
R01648	alanine, aspartate and glutamate metabolism|butanoate metabolism	Unassigned	2-Oxoglutarate[c] + 4-Aminobutanoate[c] <=> L-Glutamate[c] + 1.7 H+[c] + Succinate semialdehyde[c]	-1000	1000		-11.572	9.572
R00093	alanine, aspartate and glutamate metabolism|nitrogen metabolism	Unassigned	NAD+[c] + 2 L-Glutamate[c] <- NADH[c] + 2-Oxoglutarate[c] + L-Glutamine[c]	-1000	0		-27.656	28.767
R00471	arginine and proline metabolism	Unassigned	4-Hydroxy-2-oxoglutarate[c] <=> Pyruvate[c] + Glyoxylate[c]	-1000	1000		-9.242	6.533
R03291	arginine and proline metabolism	CAC3252	NAD+[c] + trans-4-Hydroxy-L-proline[c] <- NADH[c] + 1.04 H+[c] + L-1-Pyrroline-3-hydroxy-5-carboxylate[c]	-1000	0		-29.231	18.122
R03293	arginine and proline metabolism	CAC3252	NADP+[c] + trans-4-Hydroxy-L-proline[c] <- NADPH[c] + 1.04 H+[c] + L-1-Pyrroline-3-hydroxy-5-carboxylate[c]	-1000	0		-29.203	18.094
R05052	arginine and proline metabolism	Unassigned	2-Oxoglutarate[c] + L-erythro-4-Hydroxyglutamate[c] <=> L-Glutamate[c] + 4-Hydroxy-2-oxoglutarate[c]	-1000	1000		NaN	NaN
R05053	arginine and proline metabolism	CAC0792	D-Aspartate[c] + 4-Hydroxy-2-oxoglutarate[c] <=> Oxaloacetate[c] + 0.01 H+[c] + L-erythro-4-Hydroxyglutamate[c]	-1000	1000		NaN	NaN
R00178	arginine and proline metabolism|cysteine and methionine metabolism	CAC2601	S-Adenosyl-L-methionine[c] + H+[c] <=> CO2[c] + S-Adenosylmethioninamine[c]	-1000	1000		-22.651	16.471
R01920	arginine and proline metabolism|cysteine and methionine metabolism|glutathione metabolism	CAC2602	Putrescine[c] + S-Adenosylmethioninamine[c] <=> 1.03 H+[c] + 5-Methylthioadenosine[c] + Spermidine[c]	-1000	1000		-23.709	14.369
R04949	cyanoamino acid metabolism	Unassigned	H2O[c] + Cyanoglycoside[c] <=> D-Glucose[c] + Cyanohydrin[c]	-1000	1000		NaN	NaN
R00590	cysteine and methionine metabolism	Unassigned	L-Serine[c] <=> H2O[c] + 2-Aminoacrylate|2-Aminoacrylate|Dehydroalanine[c]	-1000	1000		-14.024	3.161
R00896	cysteine and methionine metabolism	Unassigned	2-Oxoglutarate[c] + L-Cysteine[c] <=> L-Glutamate[c] + 0.01 H+[c] + Mercaptopyruvate[c]	-1000	1000		-11.369	11.369
R01287	cysteine and methionine metabolism	Unassigned	Hydrogen sulfide[c] + O-Acetyl-L-homoserine[c] -> Acetate[c] + 0.3 H+[c] + L-Homocysteine[c]	0	1000		-14.826	7.978
R01288	cysteine and methionine metabolism	Unassigned	Hydrogen sulfide[c] + O-Succinyl-L-homoserine[c] <=> Succinate[c] + 0.25 H+[c] + L-Homocysteine[c]	-1000	1000		-13.243	9.475
R01401	cysteine and methionine metabolism	Unassigned	H2O[c] + 0.01 H+[c] + 5-Methylthioadenosine[c] <=> Adenine[c] + 5-Methylthio-D-ribose[c]	-1000	1000		NaN	NaN
R02026	cysteine and methionine metabolism	Unassigned	H+[c] + Thiosulfate[c] + Thioredoxin[c] + O-Acetyl-L-homoserine[c] -> Acetate[c] + Sulfite[c] + L-Homocysteine[c] + Thioredoxin disulfide[c]	0	1000		NaN	NaN
R02408	cysteine and methionine metabolism	Unassigned	H2O[c] + 0.99 H+[c] + L-Cystine[c] <=> NH3[c] + Pyruvate[c] + Thiocysteine[c]	-1000	1000		NaN	NaN
R02433	cysteine and methionine metabolism	Unassigned	2-Oxoglutarate[c] + L-Cysteate[c] <=> L-Glutamate[c] + 3-Sulfopyruvate|3-Sulfopyruvate|3-Sulfopyruvic acid[c]	-1000	1000		NaN	NaN
R02619	cysteine and methionine metabolism	Unassigned	2-Oxoglutarate[c] + 3-Sulfino-L-alanine[c] <=> L-Glutamate[c] + 3-Sulfinylpyruvate[c]	-1000	1000		NaN	NaN
R03104	cysteine and methionine metabolism	Unassigned	NAD+[c] + 3-Mercaptolactate[c] <=> NADH[c] + H+[c] + Mercaptopyruvate[c]	-1000	1000		-21.944	25.255
R03217	cysteine and methionine metabolism	Unassigned	L-Cysteine[c] + O-Acetyl-L-homoserine[c] -> Acetate[c] + 1.01 H+[c] + Cystathionine[c]	0	1000		-11.903	12.251
R04858	cysteine and methionine metabolism	Unassigned	S-Adenosyl-L-methionine[c] + DNA cytosine[c] <=> S-Adenosyl-L-homocysteine[c] + DNA 5-methylcytosine[c]	-1000	1000		NaN	NaN
R04859	cysteine and methionine metabolism	Unassigned	H+[c] + Thiosulfate[c] + Thioredoxin[c] + O-Acetyl-L-serine[c] -> Acetate[c] + Sulfite[c] + L-Cysteine[c] + Thioredoxin disulfide[c]	0	1000		NaN	NaN
R00274	glutathione metabolism	Unassigned	H2O2[c] + 2 Glutathione[c] -> 2 H2O[c] + Glutathione disulfide[c]	0	1000	df	-96.744	-51.548

R00894	glutathione metabolism	CAC1539	ATP[c] + L-Glutamate[c] + 0.47 H+[c] + L-Cysteine[c] <=> ADP[c] + Orthophosphate[c] + gamma-L-Glutamyl-L-cysteine[c]	-1000	1000		-27.696	17.468
R08359	glutathione metabolism	CAC2602	S-Adenosylmethioninamine[c] + Cadaverine[c] <=> 1.03 H+[c] + 5-Methylthioadenosine[c] + Aminopropylcadaverine[c]	-1000	1000		-23.746	14.406
R06171	glycine, serine and threonine metabolism	CAC3420	L-Allothreonine[c] -> Glycine[c] + Acetaldehyde[c]	0	1000		-9.681	6.972
R02722	glycine, serine and threonine metabolism|phenylalanine, tyrosine and tryptophan biosynthesis	Unassigned	L-Serine[c] + Indoleglycerol phosphate[c] -> H2O[c] + L-Tryptophan[c] + 0.02 H+[c] + D-Glyceraldehyde 3-phosphate[c]	0	1000		-29.746	2.283
R01221	glycine, serine and threonine metabolism	Unassigned	NAD+[c] + Glycine[c] + 0.98 H+[c] + Tetrahydrofolate[c] -> NADH[c] + CO2[c] + NH3[c] + "5,10-Methylenetetrahydrofolate"[c]	0	1000		-57.888	8.170
R01159	histidine metabolism	Unassigned	S-Adenosyl-L-methionine[c] + L-Histidine[c] <=> S-Adenosyl-L-homocysteine[c] + 2 H+[c] + N(pi)-Methyl-L-histidine[c]	-1000	1000		-16.557	22.137
R04467	lysine biosynthesis	Unassigned	2-Oxoglutarate[c] + "N6-Acetyl-LL-2,6-diaminoheptanedioate"[c] <=> L-Glutamate[c] + N-Acetyl-L-2-amino-6-oxopimelate[c]	-1000	1000		NaN	NaN
R02788	lysine biosynthesis|peptidoglycan biosynthesis	Unassigned	ATP[c] + 0.48 H+[c] + "meso-2,6-Diaminoheptanedioate"[c] + UDP-N-acetylmuramoyl-L-alanyl-D-glutamate[c] <=> ADP[c] + Orthophosphate[c] + "UDP-N-acetylmuramoyl-L-alanyl-D-gamma-glutamyl-meso-2,6-"[c]	-1000	1000		-33.322	23.094
R04617	lysine biosynthesis|peptidoglycan biosynthesis	CAC2128	ATP[c] + 0.45 H+[c] + D-Alanyl-D-alanine[c] + "UDP-N-acetylmuramoyl-L-alanyl-D-gamma-glutamyl-meso-2,6-"[c] <=> ADP[c] + Orthophosphate[c] + UDP-N-acetylmuramoyl-L-alanyl-D-glutamyl-6-carboxy-L-lysyl-D-alanyl-[c]	-1000	1000		-35.158	24.930
R00271	lysine biosynthesis|pyruvate metabolism	CAC0261	H2O[c] + Acetyl-CoA[c] + 2-Oxoglutarate[c] <=> CoA[c] + 0.98 H+[c] + "(R)-2-Hydroxybutane-1,2,4-tricarboxylate|(R)-2-Hydroxybutane-1,2,4-tricarboxylate|Homocitrate|Homocitric acid|3-Hydroxy-3-carboxyadipic acid|(R)-2-Hydroxy-1,2,4-butanetricarboxylic acid"[c]	-1000	1000		NaN	NaN
R00691	phenylalanine, tyrosine and tryptophan biosynthesis	Unassigned	1.02 H+[c] + L-Arogenate[c] -> H2O[c] + CO2[c] + L-Phenylalanine[c]	0	1000	df	-60.220	-35.232
R01582	phenylanine metabolism	CAC0792	2-Oxoglutarate[c] + L-Phenylalanine[c] <=> 0.02 H+[c] + Phenylpyruvate[c] + D-Glutamate[c]	-1000	1000		-11.682	11.682
R02252	phenylanine metabolism	CAC3371	NAD+[c] + Phenylpropanoate[c] <=> NADH[c] + H+[c] + trans-Cinnamate[c]	-1000	1000		-16.559	30.890
R03599	selenoamino acid metabolism	CAC3291	Reduced acceptor[c] + L-Selenocysteine[c] <=> L-Alanine[c] + Selenide[c] + Acceptor[c]	-1000	1000		NaN	NaN
R03601	selenoamino acid metabolism	Unassigned	O-Acetyl-L-serine[c] + Selenide[c] -> Acetate[c] + H+[c] + L-Selenocysteine[c]	0	1000		NaN	NaN
R04771	selenoamino acid metabolism	Unassigned	H2O[c] + ATP[c] + 0.1 H+[c] + L-Selenomethionine[c] <=> Orthophosphate[c] + Diphosphate[c] + Se-Adenosylselenomethionine[c]	-1000	1000		NaN	NaN
R04773	selenoamino acid metabolism	CAC2991	ATP[c] + tRNA(Met)[c] + L-Selenomethionine[c] <=> Diphosphate[c] + AMP[c] + Selenomethionyl-tRNA(Met)[c]	-1000	1000		NaN	NaN
R04927	selenoamino acid metabolism	CAC0104	AMP[c] + 2 Ferricytochrome c[c] + Selenite[c] <=> 2 Ferrocytochrome c[c] + Adenylylselenate|Adenylylselenate|Adenosine-5-phosphoselenate[c]	-1000	1000		NaN	NaN
R04928	selenoamino acid metabolism	CAC0103	ATP[c] + Adenylylselenate|Adenylylselenate|Adenosine-5-phosphoselenate[c] <=> ADP[c] + 0.91 H+[c] + 3-Phosphoadenylylselenate|3-Phosphoadenylylselenate|3-Phosphoadenosine-5-phosphoselanate[c]	-1000	1000		NaN	NaN
R04929	selenoamino acid metabolism	Unassigned	ATP[c] + Selenate|Selenate|Selenic acid[c] <=> Diphosphate[c] + 0.37 H+[c] + Adenylylselenate|Adenylylselenate|Adenosine-5-phosphoselenate[c]	-1000	1000		NaN	NaN
R04939	selenoamino acid metabolism	Unassigned	Se-Adenosylselenomethionine[c] + R[c] <=> Se-Adenosyl-L-selenohomocysteine[c] + CH3-R[c]	-1000	1000		NaN	NaN
R04941	selenoamino acid metabolism	Unassigned	H2O[c] + 0.99 H+[c] + L-Selenocystathionine[c] <=> NH3[c] + Pyruvate[c] + Selenohomocysteine[c]	-1000	1000		NaN	NaN
R04944	selenoamino acid metabolism	Unassigned	0.03 H+[c] + L-Selenocysteine[c] + O-Phosphorylhomoserine[c] <=> Orthophosphate[c] + L-Selenocystathionine[c]	-1000	1000		NaN	NaN
R04945	selenoamino acid metabolism	Unassigned	O-Acetyl-L-homoserine[c] + L-Selenocysteine[c] -> Acetate[c] + H+[c] + L-Selenocystathionine[c]	0	1000		NaN	NaN
R04946	selenoamino acid metabolism	Unassigned	O-Succinyl-L-homoserine[c] + L-Selenocysteine[c] <=> Succinate[c] + 0.95 H+[c] + L-Selenocystathionine[c]	-1000	1000		NaN	NaN
R00615	thiamine metabolism	CAC2665	H2O[c] + Thiamin diphosphate[c] -> Orthophosphate[c] + 0.91 H+[c] + Thiamin monophosphate[c]	0	1000		-13.685	19.111
R00616	thiamine metabolism	Unassigned	ATP[c] + Thiamin diphosphate[c] <=> ADP[c] + Thiamin triphosphate[c]	-1000	1000		-20.263	20.263
R04448	thiamine metabolism	CAC3096	ATP[c] + 5-(2-Hydroxyethyl)-4-methylthiazole[c] <=> ADP[c] + 0.67 H+[c] + 4-Methyl-5-(2-phosphoethyl)-thiazole[c]	-1000	1000		-22.814	13.814
R07459	thiamine metabolism	Unassigned	ATP[c] + C15810|C15810|Thiamine biosynthesis intermediate 1[c] <=> Diphosphate[c] + C15813|C15813|Thiamine biosynthesis intermediate 4[c]	-1000	1000		NaN	NaN
R07460	thiamine metabolism	Unassigned	L-Cysteine[c] + [Enzyme]-cysteine[c] <=> L-Alanine[c] + [Enzyme]-S-sulfanylcysteine[c]	-1000	1000		NaN	NaN
R07461	thiamine metabolism	Unassigned	[Enzyme]-S-sulfanylcysteine[c] + C15813|C15813|Thiamine biosynthesis intermediate 4[c] <=> C15814|C15814|Thiamine biosynthesis intermediate 5[c]	-1000	1000		NaN	NaN
R07462	thiamine metabolism	Unassigned	C15814|C15814|Thiamine biosynthesis intermediate 5[c] <=> C15815|C15815|Thiamine biosynthesis intermediate 6[c]	-1000	1000		NaN	NaN
R07464	thiamine metabolism	Unassigned	L-Tyrosine[c] + 1-Deoxy-D-xylulose 5-phosphate[c] + C15815|C15815|Thiamine biosynthesis intermediate 6[c] <=> 4-Methyl-5-(2-phosphoethyl)-thiazole[c]	-1000	1000		NaN	NaN
R07465	thiamine metabolism	Unassigned	L-Tyrosine[c] + Iminoglycine|Iminoglycine|Iminoacetic acid[c] + C15815|C15815|Thiamine biosynthesis intermediate 6[c] <=> 4-Methyl-5-(2-phosphoethyl)-thiazole[c]	-1000	1000		NaN	NaN
R03664	trypthophan metabolism	Unassigned	ATP[c] + L-Tryptophan[c] + 0.77 H+[c] + tRNA(Trp)[c] <=> Diphosphate[c] + AMP[c] + L-Tryptophanyl-tRNA(Trp)[c]	-1000	1000		NaN	NaN
R01645	tyrosine metabolism	CAC1343	4-Hydroxy-2-oxo-heptanedioate[c] <=> Pyruvate[c] + Succinate semialdehyde[c]	-1000	1000		NaN	NaN
R03943	tyrosine metabolism	Unassigned	S-Adenosyl-L-methionine[c] + N-Methyltyramine[c] <=> S-Adenosyl-L-homocysteine[c] + 2.01 H+[c] + Hordenine[c]	-1000	1000		-18.641	20.181
R04880	tyrosine metabolism	Unassigned	NAD+[c] + "3,4-Dihydroxyphenylethyleneglycol"[c] <=> NADH[c] + H+[c] + "3,4-Dihydroxymandelaldehyde"[c]	-1000	1000		NaN	NaN
R03656	valine, leucine and isoleucine biosynthesis	CAC3038	ATP[c] + 0.74 H+[c] + L-Isoleucine[c] + tRNA(Ile)[c] <=> Diphosphate[c] + AMP[c] + L-Isoleucyl-tRNA(Ile)[c]	-1000	1000		NaN	NaN
R03657	valine, leucine and isoleucine biosynthesis	CAC0646	ATP[c] + 0.75 H+[c] + L-Leucine[c] + tRNA(Leu)[c] <=> Diphosphate[c] + AMP[c] + L-Leucyl-tRNA[c]	-1000	1000		NaN	NaN
R03665	valine, leucine and isoleucine biosynthesis	CAC2399	ATP[c] + 0.75 H+[c] + L-Valine[c] + tRNA(Val)[c] <=> Diphosphate[c] + AMP[c] + L-Valyl-tRNA(Val)[c]	-1000	1000		NaN	NaN
R00131	Biomass synthesis and maintenance	Unassigned	H2O[c] + 1.97 H+[c] + Urea[c] -> CO2[c] + 2 NH3[c]	0	1000		-43.269	-15.486
R00188	Biomass synthesis and maintenance	Unassigned	H2O[c] + "Adenosine 3,5-bisphosphate"[c] + 0.4 H+[c] -> Orthophosphate[c] + AMP[c]	0	1000		-10.486	24.912
R00437_R00440_B	Biomass synthesis and maintenance	Unassigned	0.25 ADP[c] + 0.25 UDP[c] + 0.25 GDP[c] + 0.25 CDP[c] -> Orthophosphate[c] + RNA[c]	0	1000		NaN	NaN

R07224_B	Biomass synthesis and maintenance	Unassigned	0.041 L-Glutamate[c] + 0.0596 Glycine[c] + 0.0635 L-Alanine[c] + 0.0743 L-Lysine[c] + 0.0575 L-Aspartate[c] + 0.0345 L-Arginine[c] + 0.0641 L-Glutamine[c] + 0.0605 L-Serine[c] + 0.0261 L-Methionine[c] + 0.0129 L-Tryptophan[c] + 0.0443 L-Phenylalanine[c] + 0.0385 L-Tyrosine[c] + 0.00619 L-Cysteine[c] + 0.0902 L-Leucine[c] + 0.023 L-Histidine[c] + 0.0318 L-Proline[c] + 0.0559 L-Asparagine[c] + 0.00735 Thymine[c] + 0.0663 L-Valine[c] + 0.0572 L-Threonine[c] + 0.0849 L-Isoleucine[c] -> Protein[c]	0	1000		NaN	NaN
R07225_B	Biomass synthesis and maintenance	Unassigned	0.336 dATP[c] + 0.336 dGTP[c] + 0.164 dCTP[c] + 0.164 dTTP[c] -> Diphosphate[c] + DNA[c]	0	1000		NaN	NaN
R07226_B	Biomass synthesis and maintenance	Unassigned	0.25 ATP[c] + 0.25 GTP[c] + 0.25 CTP[c] + 0.25 UTP[c] -> Diphosphate[c] + RNA[c]	0	1000		NaN	NaN
R07227_B	Biomass synthesis and maintenance	Unassigned	0.000201 ATP[c] + 0.0036 NAD+[c] + 8.29e-005 NADH[c] + 0.000617 NADPH[c] + 0.000219 NADP+[c] + 0.25 Orthophosphate[c] + 0.001 CoA[c] + 0.000168 FAD[c] + 8.3e-005 Acetyl-CoA[c] + 0.132 L-Glutamate[c] + 0.119 D-Glucose[c] + 0.01 Glycine[c] + 0.029 L-Alanine[c] + 0.01 L-Lysine[c] + 0.15 L-Aspartate[c] + 0.0072 L-Arginine[c] + 0.002 L-Glutamine[c] + 0.019 L-Serine[c] + 0.0056 L-Methionine[c] + 0.001 L-Phenylalanine[c] + 0.0056 L-Leucine[c] +	0	1000		NaN	NaN
R07228_B	Biomass synthesis and maintenance	Unassigned	0.497 "Phosphatidylglycerol (didodecanoyl, n-C12:0)"[c] + 0.207 "1,2-Diacyl-sn-glycerol"[c] + 0.083 Menaquinone[c] + 0.0125 "3-D-Glucosyl-1,2-diacylglycerol"[c] + 0.0623 3-Phosphatidyl-1-(3-O-L-lysyl)glycerol[c] + 0.0622 "cardiolipin (tetradodecanoyl, n-C12:0)"[c] + 0.0747 Diglucosyl-diacylglycerol[c] -> Generic lipid content[c]	0	1000		NaN	NaN
R07229_B	Biomass synthesis and maintenance	Unassigned	0.95 Crosslinked peptideglycan[c] + 0.05 Wall Teichoic acid[c] -> Cell Wall[c]	0	1000		NaN	NaN
R07230_B	Biomass synthesis and maintenance	Unassigned	40 H2O[c] + 40 ATP[c] + 3.1 Protein[c] + 0.06 DNA[c] + 4e-005 Lipoteichoic acid[c] + 0.092 Cell Wall[c] + 0.251 Fatty acids[c] + 0.00102 Generic lipid content[c] + 0.001 Granulose[c] + 0.557 Pool Solutes[c] + 0.238 RNA[c] -> 40 ADP[c] + 40 Orthophosphate[c] + Biomass[c]	0	1000		NaN	NaN
R07274_B	Biomass synthesis and maintenance	Unassigned	H2O[c] + ADP[c] <0> Orthophosphate[c] + AMP[c] + 1.09 H+[c]	0	0		-14.983	20.409
R07276_B	Biomass synthesis and maintenance	Unassigned	H2O[c] + Diphosphate[c] -> 2 Orthophosphate[c] + 0.4 H+[c]	0	1000		2.223	25.115
R07296_B	Biomass synthesis and maintenance	Unassigned	UDP-N-acetyl-D-glucosamine[c] + CDP-glycerol[c] <=> Wall Teichoic acid[c]	-1000	1000		NaN	NaN
R07297_B	Biomass synthesis and maintenance	Unassigned	D-Alanine[c] + "Phosphatidylglycerol (didodecanoyl, n-C12:0)"[c] + Glycerophosphoglycoglycerolipid[c] <=> Lipoteichoic acid[c]	-1000	1000		NaN	NaN
R07312_B	Biomass synthesis and maintenance	Unassigned	H2O[c] + CO2[c] <0> 0.9 H+[c] + HCO3-[c]	0	0	d	-11.572	9.886
R07370_B	Biomass synthesis and maintenance	Unassigned	Hexadecanoic acid[c] -> Fatty acids[c]	0	1000		NaN	NaN
R07371_B	Biomass synthesis and maintenance	Unassigned	1000 ADP-glucose[c] -> 1000 ADP[c] + Granulose[c]	0	1000		NaN	NaN
R00415	Aminosugars metabolism	CAC3222	UTP[c] + 0.48 H+[c] + N-Acetyl-D-glucosamine 1-phosphate[c] -> Diphosphate[c] + UDP-N-acetyl-D-glucosamine[c]	0	1000		-16.153	18.293
R00660	Aminosugars metabolism	CAC2862|CAC3539	UDP-N-acetyl-D-glucosamine[c] + Phosphoenolpyruvate[c] + 0.38 H+[c] -> Orthophosphate[c] + UDP-N-acetyl-3-(1-carboxyvinyl)-D-	0	1000		-8.053	28.705
R00765	Aminosugars metabolism	CAC0187	H2O[c] + 0.99 H+[c] + D-Glucosamine 6-phosphate[c] <- NH3[c] + D-Fructose 6-phosphate[c]	-1000	0		-19.946	6.520
R00768	Aminosugars metabolism	CAC0158	L-Glutamine[c] + D-Fructose 6-phosphate[c] -> L-Glutamate[c] + 1.01 H+[c] + D-Glucosamine 6-phosphate[c]	0	1000		-11.415	15.395
R02059	Aminosugars metabolism	CAC0188	H2O[c] + N-Acetyl-D-glucosamine 6-phosphate[c] -> Acetate[c] + H+[c] + D-Glucosamine 6-phosphate[c]	0	1000		-7.337	19.911
R02060	Aminosugars metabolism	Unassigned	0.05 H+[c] + alpha-D-Glucosamine 1-phosphate[c] <=> D-Glucosamine 6-phosphate[c]	-1000	1000		NaN	NaN
R02086	Aminosugars metabolism	Unassigned	N-Acetyl-D-glucosamine 6-phosphate[c] <0> N-Acetyl-D-glucosamine 1-phosphate[c]	0	0		-9.047	9.047
R03191	Aminosugars metabolism	CAC0510	NAD+[c] + UDP-N-acetylmuramate[c] <0> NADH[c] + H+[c] + UDP-N-acetyl-3-(1-carboxyvinyl)-D-glucosamine[c]	0	0	dr	0.540	49.180
R03192	Aminosugars metabolism	CAC0510	NADP+[c] + UDP-N-acetylmuramate[c] <=> NADPH[c] + H+[c] + UDP-N-acetyl-3-(1-carboxyvinyl)-D-glucosamine[c]	-1000	1000	d	-15.781	37.312
R05332	Aminosugars metabolism	CAC3222	Acetyl-CoA[c] + 0.05 H+[c] + alpha-D-Glucosamine 1-phosphate[c] -> CoA[c] + N-Acetyl-D-glucosamine 1-phosphate[c]	0	1000		NaN	NaN
R02752	Ascorbate and aldarate metabolism	Unassigned	D-Glucarate[c] -> H2O[c] + 5-Dehydro-4-deoxy-D-glucarate[c]	0	1000	df	-21.677	-3.786
R02754	Ascorbate and aldarate metabolism	Unassigned	5-Dehydro-4-deoxy-D-glucarate[c] <=> Pyruvate[c] + 2-Hydroxy-3-oxopropanoate[c]	-1000	1000		-11.902	4.273
R03277	Ascorbate and aldarate metabolism	Unassigned	Pyruvate[c] + 2-Hydroxy-3-oxopropanoate[c] <- 2-Dehydro-3-deoxy-D-glucarate[c]	-1000	0		NaN	NaN
R07130	Ascorbate and aldarate metabolism	Unassigned	H2O[c] + 2-Dehydro-3-deoxy-D-glucarate[c] <- D-Glucarate[c]	-1000	0		NaN	NaN
R00238	Butanoate metabolism	CAC2873|CAP0078	2 Acetyl-CoA[c] <=> CoA[c] + Acetoacetyl-CoA[c]	-1000	1000		NaN	NaN
R01171	Butanoate metabolism	CAC2711	NAD+[c] + Butanoyl-CoA[c] <- NADH[c] + H+[c] + Crotonoyl-CoA[c]	-1000	0		NaN	NaN
R01172	Butanoate metabolism	CAP0035|CAP0162	NAD+[c] + CoA[c] + Butanal[c] <- NADH[c] + H+[c] + Butanoyl-CoA[c]	-1000	0		NaN	NaN
R01174	Butanoate metabolism	CAC3076	Orthophosphate[c] + Butanoyl-CoA[c] <=> CoA[c] + 0.32 H+[c] + Butanoylphosphate[c]	-1000	1000		NaN	NaN
R01365	Butanoate metabolism	CAP0163|CAP0164	Butanoic acid[c] + Acetoacetyl-CoA[c] <0> 0.01 H+[c] + Butanoyl-CoA[c] + Acetoacetate[c]	0	0		NaN	NaN
R01688	Butanoate metabolism	CAC3075	ATP[c] + 0.15 H+[c] + Butanoic acid[c] <=> ADP[c] + Butanoylphosphate[c]	-1000	1000	d	-24.530	10.730
R01778	Butanoate metabolism	CAC2708	NAD+[c] + (S)-3-Hydroxybutanoyl-CoA[c] <- NADH[c] + H+[c] + Acetoacetyl-CoA[c]	-1000	0		NaN	NaN
R03026	Butanoate metabolism	Unassigned	(S)-3-Hydroxybutanoyl-CoA[c] <=> H2O[c] + Crotonoyl-CoA[c]	-1000	1000		NaN	NaN
R03027	Butanoate metabolism	CAC2712	(R)-3-Hydroxybutanoyl-CoA[c] <0> H2O[c] + Crotonoyl-CoA[c]	0	0		NaN	NaN
R03276	Butanoate metabolism	Unassigned	(S)-3-Hydroxybutanoyl-CoA[c] <=> (R)-3-Hydroxybutanoyl-CoA[c]	-1000	1000		NaN	NaN
R03544	Butanoate metabolism	CAC3298|CAC3299	NADH[c] + H+[c] + Butanal[c] <=> NAD+[c] + 1-Butanol[c]	-1000	1000	d	-35.972	6.472
R03545	Butanoate metabolism	CAC3298|CAC3299	NADPH[c] + H+[c] + Butanal[c] <0> NADP+[c] + 1-Butanol[c]	0	0		-24.099	22.788
R00226	C5-branched dibasic acid metabolism	Unassigned	CO2[c] + 2-Acetolactate[c] <- 2 Pyruvate[c] + H+[c]	-1000	0	dr	9.266	30.854
R02948	C5-branched dibasic acid metabolism	Unassigned	H+[c] + 2-Acetolactate[c] -> CO2[c] + Acetoin[c]	0	1000	df	-24.017	-7.512
R03896	C5-branched dibasic acid metabolism	Unassigned	0.04 H+[c] + (R)-2-Methylmalate[c] <=> H2O[c] + 2-Methylmaleate[c]	-1000	1000		-11.767	5.584
R00342	Citrate Cycle (TCA Cycle)	CAC0566	NAD+[c] + (S)-Malate[c] <- NADH[c] + Oxaloacetate[c] + 1.01 H+[c]	-1000	0	tca	-21.824	25.136
R00709	Citrate Cycle (TCA Cycle)	CAC0972	NAD+[c] + Isocitrate[c] -> NADH[c] + CO2[c] + 2-Oxoglutarate[c] + 0.02 H+[c]	0	1000	tca	-41.324	10.266
R01082	Citrate Cycle (TCA Cycle)	CAC3090|CAC3091	(S)-Malate[c] -> H2O[c] + 0.01 H+[c] + Fumarate[c]	0	1000	tca	-12.554	4.651
R01197	Citrate Cycle (TCA Cycle)	CAC2458|CAC2459	CoA[c] + 2-Oxoglutarate[c] + Oxidized ferredoxin[c] -> CO2[c] + H+[c] + Succinyl-CoA[c] + Reduced ferredoxin[c]	0	1000	tca	NaN	NaN
R01324	Citrate Cycle (TCA Cycle)	CAC0971	Citrate[c] -> Isocitrate[c]	0	1000	tca	-4.456	7.296
R01325	Citrate Cycle (TCA Cycle)	CAC0971	H2O[c] + cis-Aconitate[c] <- 0.01 H+[c] + Citrate[c]	-1000	0	tca	-5.715	11.897

R01900	Citrate Cycle (TCA Cycle)	CAC0971	0.01 H+[c] + Isocitrate[c] <- H2O[c] + cis-Aconitate[c]	-1000	0	tca	-13.300	4.277
R07353	Citrate Cycle (TCA Cycle)	CAC2229	CoA[c] + Succinate[c] + 2.96 H+[c] + Reduced ferredoxin[c] <- Succinyl-CoA[c] + Oxidized ferredoxin[c]	-1000	0	tca	NaN	NaN
R00405	Citrate Cycle (TCA Cycle)|Citrate cycle (TCA cycle)	Unassigned	ATP[c] + CoA[c] + Succinate[c] + 0.43 H+[c] <- ADP[c] + Orthophosphate[c] + Succinyl-CoA[c]	-1000	0	tca	NaN	NaN
R00351	Citrate cycle (TCA cycle)	Unassigned	CoA[c] + 0.98 H+[c] + Citrate[c] <- H2O[c] + Acetyl-CoA[c] + Oxaloacetate[c]	-1000	0	tca	NaN	NaN
R00408	Citrate cycle (TCA cycle)	Unassigned	FAD[c] + Succinate[c] + 0.44 H+[c] <- Fumarate[c] + FADH2[c]	-1000	0	tca	-13.466	34.366
R00883	Fructose and mannose metabolism	CAC2968|CAC3058|CAC3072	Orthophosphate[c] + GDP-mannose[c] -> GDP[c] + 0.61 H+[c] + D-Mannose 1-phosphate[c]	0	1000	tca	-30.767	6.715
R00885	Fructose and mannose metabolism	CAC2981|CAC3056	GTP[c] + 0.49 H+[c] + D-Mannose 1-phosphate[c] -> Diphosphate[c] + GDP-mannose[c]	0	1000	tca	-17.680	19.820
R01015	Fructose and mannose metabolism	CAC0711	D-Glyceraldehyde 3-phosphate[c] <=> 0.07 H+[c] + Glycerone phosphate[c]	-1000	1000		-6.861	3.941
R01070	Fructose and mannose metabolism	CAC0827|CAP0064	0.07 H+[c] + "D-Fructose 1,6-bisphosphate"[c] <=> Glycerone phosphate[c] + D-Glyceraldehyde 3-phosphate[c]	-1000	1000		-9.750	9.242
R01818	Fructose and mannose metabolism	CAC2337|CAC2981	D-Mannose 6-phosphate[c] <=> 0.01 H+[c] + D-Mannose 1-phosphate[c]	-1000	1000		-8.757	8.757
R01819	Fructose and mannose metabolism	CAC2918	D-Mannose 6-phosphate[c] <=> D-Fructose 6-phosphate[c]	-1000	1000		-9.382	7.602
R02071	Fructose and mannose metabolism	CAC0232	ATP[c] + D-Fructose 1-phosphate[c] -> ADP[c] + 0.85 H+[c] + "D-Fructose 1,6-bisphosphate"[c]	0	1000		-22.852	13.852
R02568	Fructose and mannose metabolism	CAC0827|CAP0064	0.01 H+[c] + D-Fructose 1-phosphate[c] <0> Glycerone phosphate[c] + D-Glyceraldehyde[c]	0	0	tca	-9.792	9.283
R02703	Fructose and mannose metabolism	CAC0157	NAD+[c] + D-Mannitol 1-phosphate[c] <=> NADH[c] + 1.1 H+[c] + D-Fructose 6-phosphate[c]	-1000	1000		-10.066	33.146
R04779	Fructose and mannose metabolism	CAC0517	ATP[c] + D-Fructose 6-phosphate[c] -> ADP[c] + 0.86 H+[c] + "D-Fructose 1,6-bisphosphate"[c]	0	1000		-22.852	13.852
R04780	Fructose and mannose metabolism	CAC1088|CAC1572	H2O[c] + 0.34 H+[c] + "D-Fructose 1,6-bisphosphate"[c] -> Orthophosphate[c] + D-Fructose 6-phosphate[c]	0	1000		-5.736	20.162
R02630	Fructose and mannose metabolism|amino sugar and nucleotide sugar metabolism|fructose and mannose metabolism	CAC1458|CAP0066|CAP0067|CAP0068	D-Mannose[c] + Protein N(pi)-phospho-L-histidine[c] <=> D-Mannose 6-phosphate[c] + Protein histidine[c]	-1000	1000		NaN	NaN
R05692	Fructose and mannose metabolism|amino sugar and nucleotide sugar metabolism|fructose and mannose metabolism	CAC2179	NADP+[c] + GDP-L-fucose[c] <=> NADPH[c] + H+[c] + GDP-4-dehydro-6-deoxy-D-mannose[c]	-1000	1000		NaN	NaN
R00867	Fructose and mannose metabolism|fructose and mannose metabolism	CAC0424|CAC1523	ATP[c] + D-Fructose[c] -> ADP[c] + 0.84 H+[c] + D-Fructose 6-phosphate[c]	0	1000		-22.885	13.885
R00888	Fructose and mannose metabolism|fructose and mannose metabolism	CAC2180	GDP-mannose[c] <=> H2O[c] + GDP-4-dehydro-6-deoxy-D-mannose[c]	-1000	1000		NaN	NaN
R02704	Fructose and mannose metabolism|fructose and mannose metabolism	CAC0154|CAC0156	Mannitol[c] + Protein N(pi)-phospho-L-histidine[c] <=> D-Mannitol 1-phosphate[c] + Protein histidine[c]	-1000	1000		NaN	NaN
R03232	Fructose and mannose metabolism|fructose and mannose metabolism	CAC0233|CAC0234	D-Fructose[c] + Protein N(pi)-phospho-L-histidine[c] <=> D-Fructose 1-phosphate[c] + Protein histidine[c]	-1000	1000		NaN	NaN
R03234	Fructose and mannose metabolism|fructose and mannose metabolism	CAC3298|CAC3299	NADP+[c] + Sorbitol 6-phosphate[c] <=> NADPH[c] + 1.11 H+[c] + Sorbose 1-phosphate[c]	-1000	1000		NaN	NaN
R00289	Galactose metabolism	CAC2250|CAC2335	UTP[c] + 0.49 H+[c] + D-Glucose 1-phosphate[c] -> Diphosphate[c] + UDP-glucose[c]	0	1000		-15.891	18.031
R00291	Galactose metabolism	CAC0794|CAC1429|CAC2334|CAC2960	UDP-D-galactose[c] <=> UDP-glucose[c]	-1000	1000		-13.322	13.322
R00502	Galactose metabolism	CAC2844|CAC2961	UTP[c] + 0.49 H+[c] + alpha-D-Galactose 1-phosphate[c] <=> Diphosphate[c] + UDP-D-galactose[c]	-1000	1000		-15.891	18.031
R00959	Galactose metabolism	CAC0484	0.01 H+[c] + D-Glucose 1-phosphate[c] <=> D-Glucose 6-phosphate[c]	-1000	1000		-8.757	8.757
R01069	Galactose metabolism	Unassigned	0.07 H+[c] + "D-Tagatose 1,6-bisphosphate"[c] <=> Glycerone phosphate[c] + D-Glyceraldehyde 3-phosphate[c]	-1000	1000		-9.750	9.242
R01092	Galactose metabolism	CAC2959	ATP[c] + D-Galactose[c] <=> ADP[c] + 0.85 H+[c] + alpha-D-Galactose 1-phosphate[c]	-1000	1000		-23.115	14.115
R01786	Galactose metabolism	CAC2613	ATP[c] + D-Glucose[c] -> ADP[c] + 0.84 H+[c] + D-Glucose 6-phosphate[c]	0	1000		-23.115	14.115
R03236	Galactose metabolism	CAC0517|CAC0232|CAC2951	ATP[c] + D-Tagatose 6-phosphate[c] -> ADP[c] + 0.86 H+[c] + "D-Tagatose 1,6-bisphosphate"[c]	0	1000		-22.852	13.852
R03237	Galactose metabolism	CAC0517	CTP[c] + D-Tagatose 6-phosphate[c] -> 0.87 H+[c] + CDP[c] + "D-Tagatose 1,6-bisphosphate"[c]	0	1000		-20.075	11.075
R03238	Galactose metabolism	CAC0517	UTP[c] + D-Tagatose 6-phosphate[c] -> UDP[c] + 0.87 H+[c] + "D-Tagatose 1,6-bisphosphate"[c]	0	1000		-20.000	11.000
R03239	Galactose metabolism	CAC0517	ITP[c] + D-Tagatose 6-phosphate[c] -> 0.87 H+[c] + IDP[c] + "D-Tagatose 1,6-bisphosphate"[c]	0	1000		-22.107	13.107
R03240	Galactose metabolism	CAC2953|CAC2954	D-Galactose 6-phosphate[c] <=> D-Tagatose 6-phosphate[c]	-1000	1000		-9.382	7.602
R03256	Galactose metabolism	CAC2963	H2O[c] + Lactose 6-phosphate[c] <=> beta-D-Glucose[c] + D-Galactose 6-phosphate[c]	-1000	1000		NaN	NaN
R00955	Galactose metabolism|amino sugar and nucleotide sugar metabolism|galactose metabolism	CAC2844|CAC2961	UDP-glucose[c] + alpha-D-Galactose 1-phosphate[c] <=> UDP-D-galactose[c] + D-Glucose 1-phosphate[c]	-1000	1000		-18.795	18.795
R00801	Galactose metabolism|galactose metabolism	CAC2891	H2O[c] + Sucrose[c] <=> D-Glucose[c] + D-Fructose[c]	-1000	1000		-19.079	12.853
R02410	Galactose metabolism|galactose metabolism	CAC0425	H2O[c] + Raffinose[c] <=> D-Fructose[c] + Melibiose[c]	-1000	1000		NaN	NaN
R03635	Galactose metabolism|galactose metabolism	CAC0425	H2O[c] + Stachyose[c] <=> D-Fructose[c] + D-Gal alpha 1->6D-Gal alpha 1->6D-Glucose[c]	-1000	1000		NaN	NaN
R04393	Galactose metabolism|galactose metabolism	CAC2964|CAC2965	Lactose[c] + Protein N(pi)-phospho-L-histidine[c] <=> Lactose 6-phosphate[c] + Protein histidine[c]	-1000	1000		NaN	NaN
R05570	Galactose metabolism|galactose metabolism	CAC2956|CAC2957|CAC2958	Galactitol[c] + Protein N(pi)-phospho-L-histidine[c] <=> Galactitol 1-phosphate[c] + Protein histidine[c]	-1000	1000		NaN	NaN
R08366	Galactose metabolism|galactose metabolism	CAC1457	N-Acetyl-D-galactosamine[c] + Protein N(pi)-phospho-L-histidine[c] <=> Protein histidine[c] + N-Acetyl-D-galactosamine 6-phosphate[c]	-1000	1000		NaN	NaN
R08367	Galactose metabolism|galactose metabolism	CAC1457	D-Galactosamine[c] + Protein N(pi)-phospho-L-histidine[c] <=> Protein histidine[c] + D-Galactosamine 6-phosphate[c]	-1000	1000		NaN	NaN
R00014	Glycolysis/Gluconeogenesis	CAP0025	CO2[c] + 2-(alpha-Hydroxyethyl)thiamine diphosphate[c] <- Pyruvate[c] + Thiamin diphosphate[c] + H+[c]	-1000	0		NaN	NaN
R00200	Glycolysis/Gluconeogenesis	CAC0518|CAC1036	ATP[c] + Pyruvate[c] <- ADP[c] + Phosphoenolpyruvate[c] + 0.9 H+[c]	-1000	0		-13.085	22.305
R00658	Glycolysis/Gluconeogenesis	CAC0713	2-Phospho-D-glycerate[c] <=> H2O[c] + Phosphoenolpyruvate[c]	-1000	1000		-13.831	2.968

R00703	Glycolysis/Gluconeogenesis	CAC0267|CAC3552	NAD+[c] + (S)-Lactate[c] <- NADH[c] + Pyruvate[c] + H+[c]	-1000	0		-21.814	25.125
R00754	Glycolysis/Gluconeogenesis	CAC3375|CAP0035|CAP0162	NAD+[c] + Ethanol[c] <=> NADH[c] + H+[c] + Acetaldehyde[c]	-1000	1000	d	-22.310	24.741
R00755	Glycolysis/Gluconeogenesis	CAP0025	Thiamin diphosphate[c] + Acetaldehyde[c] -> 2-(alpha-Hydroxyethyl)thiamine diphosphate[c]	0	1000		NaN	NaN
R01061	Glycolysis/Gluconeogenesis	CAC0709	NAD+[c] + Orthophosphate[c] + D-Glyceraldehyde 3-phosphate[c] -> NADH[c] + 1.32 H+[c] + 3-Phospho-D-glyceroyl phosphate[c]	0	1000		-35.658	15.886
R01512	Glycolysis/Gluconeogenesis	CAC0710	ATP[c] + 0.13 H+[c] + 3-Phospho-D-glycerate[c] <=> ADP[c] + 3-Phospho-D-glyceroyl phosphate[c]	-1000	1000	d	-24.543	10.743
R01515	Glycolysis/Gluconeogenesis	CAC2830	H2O[c] + 3-Phospho-D-glyceroyl phosphate[c] -> Orthophosphate[c] + 0.66 H+[c] + 3-Phospho-D-glycerate[c]	0	1000		-1.074	20.300
R01518	Glycolysis/Gluconeogenesis	CAC0167|CAC0712|CAC2741|CAC3021	0.14 H+[c] + 2-Phospho-D-glycerate[c] <=> 3-Phospho-D-glycerate[c]	-1000	1000		-5.321	5.321
R01600	Glycolysis/Gluconeogenesis	CAC2613	ATP[c] + beta-D-Glucose[c] -> ADP[c] + 0.84 H+[c] + beta-D-Glucose 6-phosphate[c]	0	1000		-23.115	14.115
R01602	Glycolysis/Gluconeogenesis	CAC1349	D-Glucose[c] <=> beta-D-Glucose[c]	-1000	1000		-8.866	8.866
R02739	Glycolysis/Gluconeogenesis	CAC2680	D-Glucose 6-phosphate[c] <=> beta-D-Glucose 6-phosphate[c]	-1000	1000	d	-8.757	8.757
R02740	Glycolysis/Gluconeogenesis	CAC2680	D-Glucose 6-phosphate[c] <=> D-Fructose 6-phosphate[c]	-1000	1000	d	-9.382	7.602
R03321	Glycolysis/Gluconeogenesis	CAC2680	beta-D-Glucose 6-phosphate[c] <=> D-Fructose 6-phosphate[c]	-1000	1000	d	-9.382	7.602
R04394	Glycolysis/Gluconeogenesis	CAC0570|CAC1354|CAC2995|CAC3427	Salicin[c] + Protein N(pi)-phospho-L-histidine[c] <=> Salicin 6-phosphate[c] + Protein histidine[c]	-1000	1000		NaN	NaN
R05132	Glycolysis/Gluconeogenesis	CAC0532|CAC0570|CAC1354|CAC2995|CAC3427	Arbutin[c] + Protein N(pi)-phospho-L-histidine[c] <=> Arbutin 6-phosphate[c] + Protein histidine[c]	-1000	1000		NaN	NaN
R05133	Glycolysis/Gluconeogenesis	CAC0743|CAC1408|CAC3426	H2O[c] + Arbutin 6-phosphate[c] <=> p-Benzenediol[c] + beta-D-Glucose 6-phosphate[c]	-1000	1000		-17.186	10.960
R05134	Glycolysis/Gluconeogenesis	CAC0743|CAC1408|CAC3426	H2O[c] + Salicin 6-phosphate[c] <=> beta-D-Glucose 6-phosphate[c] + Salicyl alcohol[c]	-1000	1000		NaN	NaN
R07159	Glycolysis/Gluconeogenesis	CAC2018	H2O[c] + D-Glyceraldehyde 3-phosphate[c] + Oxidized ferredoxin[c] -> 2.98 H+[c] + Reduced ferredoxin[c] + 3-Phospho-D-glycerate[c]	0	1000		NaN	NaN
R02738	Glycolysis/Gluconeogenesis|amino sugar and nucleotide sugar metabolism|glycolysis	CAC0570|CAC1354|CAC2995|CAC3425|CAC3427	D-Glucose[c] + Protein N(pi)-phospho-L-histidine[c] <=> D-Glucose 6-phosphate[c] + Protein histidine[c]	-1000	1000		NaN	NaN
R01058	Glycolysis/Gluconeogenesis|glycolysis	CAC3657	H2O[c] + NADP+[c] + D-Glyceraldehyde 3-phosphate[c] -> NADPH[c] + 1.98 H+[c] + 3-Phospho-D-glycerate[c]	0	1000		-26.009	25.463
R00013	Glycoxylate and dicarboxylate metabolism	Unassigned	2 Glyoxylate[c] + H+[c] -> CO2[c] + 2-Hydroxy-3-oxopropanoate[c]	0	1000		-30.671	-9.529
R00472	Glycoxylate and dicarboxylate metabolism	Unassigned	CoA[c] + 0.99 H+[c] + (S)-Malate[c] <- H2O[c] + Acetyl-CoA[c] + Glyoxylate[c]	-1000	0		NaN	NaN
R00717	Glycoxylate and dicarboxylate metabolism	CAC2945	NAD+[c] + Glycolate[c] <=> NADH[c] + Glyoxylate[c] + H+[c]	-1000	1000		-20.346	26.577
R00943	Glycoxylate and dicarboxylate metabolism	CAC2083|CAC3201	ATP[c] + Formate[c] + 0.47 H+[c] + Tetrahydrofolate[c] <=> ADP[c] + Orthophosphate[c] + 10-Formyltetrahydrofolate[c]	-1000	1000		-12.366	39.218
R01220	Glycoxylate and dicarboxylate metabolism	CAC2083	NADPH[c] + "5,10-Methenyltetrahydrofolate"[c] <=> NADP+[c] + "5,10-Methylenetetrahydrofolate"[c]	-1000	1000		-25.922	22.082
R01333	Glycoxylate and dicarboxylate metabolism	Unassigned	H2O[c] + NAD+[c] + Glycolaldehyde[c] <=> NADH[c] + 2 H+[c] + Glycolate[c]	-1000	1000		-9.678	37.321
R01393	Glycoxylate and dicarboxylate metabolism	Unassigned	H+[c] + Hydroxypyruvate[c] -> CO2[c] + Glycolaldehyde[c]	0	1000		-26.201	-10.168
R01665	Glycoxylate and dicarboxylate metabolism	CAC1848	ATP[c] + 0.57 H+[c] + dCMP[c] <=> ADP[c] + dCDP[c]	-1000	1000	d	-19.037	19.037
R01745	Glycoxylate and dicarboxylate metabolism	Unassigned	NAD+[c] + D-Glycerate[c] <0> NADH[c] + H+[c] + 2-Hydroxy-3-oxopropanoate[c]	0	0		-22.819	24.130
R01747	Glycoxylate and dicarboxylate metabolism	Unassigned	NADP+[c] + D-Glycerate[c] <=> NADPH[c] + H+[c] + 2-Hydroxy-3-oxopropanoate[c]	-1000	1000		-22.791	24.102
R01432	Pentose and glucuronate interconversions	Unassigned	D-Xylose[c] <=> D-Xylulose[c]	-1000	1000		-9.062	7.282
R01524	Pentose and glucuronate interconversions	Unassigned	NAD+[c] + D-Ribitol 5-phosphate[c] <0> NADPH[c] + 2.95 H+[c] + D-Ribulose 5-phosphate[c]	0	0	df	-236.873	-189.736
R01525	Pentose and glucuronate interconversions	Unassigned	NADP+[c] + D-Ribitol 5-phosphate[c] <=> NADPH[c] + 1.01 H+[c] + D-Ribulose 5-phosphate[c]	-1000	1000		-24.359	22.750
R01528	Pentose and glucuronate interconversions	Unassigned	NADP+[c] + 6-Phospho-D-gluconate[c] <0> NADPH[c] + CO2[c] + 0.05 H+[c] + D-Ribulose 5-phosphate[c]	0	0		-43.858	7.880
R01529	Pentose and glucuronate interconversions	CAC1730	D-Ribulose 5-phosphate[c] <=> D-Xylulose 5-phosphate[c]	-1000	1000		-6.111	6.111
R01541	Pentose and glucuronate interconversions	CAC0395|CAC2684	ATP[c] + 2-Dehydro-3-deoxy-D-gluconate[c] <=> ADP[c] + 0.7 H+[c] + 2-Dehydro-3-deoxy-6-phospho-D-gluconate[c]	-1000	1000		-22.241	13.241
R01639	Pentose and glucuronate interconversions	CAC2612	ATP[c] + D-Xylulose[c] <=> ADP[c] + 0.75 H+[c] + D-Xylulose 5-phosphate[c]	-1000	1000		-22.558	13.458
R01761	Pentose and glucuronate interconversions	CAC1342|CAC1346	L-Arabinose[c] <=> L-Ribulose[c]	-1000	1000		-9.062	7.282
R02439	Pentose and glucuronate interconversions	Unassigned	ATP[c] + L-Ribulose[c] <=> ADP[c] + 0.75 H+[c] + L-Ribulose 5-phosphate[c]	-1000	1000		-22.558	13.458
R02921	Pentose and glucuronate interconversions	Unassigned	CTP[c] + 0.38 H+[c] + D-Ribitol 5-phosphate[c] <=> Diphosphate[c] + CDP-ribitol[c]	-1000	1000		-13.970	16.110
R05605	Pentose and glucuronate interconversions	CAC0394|CAC2973	2-Dehydro-3-deoxy-6-phospho-D-gluconate[c] <=> Pyruvate[c] + 0.09 H+[c] + D-Glyceraldehyde 3-phosphate[c]	-1000	1000		-11.949	4.320
R05850	Pentose and glucuronate interconversions	CAC1341	L-Ribulose 5-phosphate[c] <=> D-Xylulose 5-phosphate[c]	-1000	1000		-6.111	6.111
R05338	Pentose and glucuronate interconversions|methane metabolism|pentose and glucuronate interconversions	CAC0396	Formaldehyde[c] + D-Ribulose 5-phosphate[c] <=> D-arabino-Hex-3-ulose 6-phosphate[c]	-1000	1000		-9.528	8.216
R05339	Pentose and glucuronate interconversions|methane metabolism|pentose and glucuronate interconversions	CAC0397	D-arabino-Hex-3-ulose 6-phosphate[c] <=> 0.09 H+[c] + D-Fructose 6-phosphate[c]	-1000	1000		-9.264	5.764
R01482	Pentose and glucuronate interconversions|pentose and glucuronate interconversions	CAC0692	D-Glucuronate[c] <=> D-Fructuronate[c]	-1000	1000		-9.353	7.573
R01540	Pentose and glucuronate interconversions|pentose and glucuronate interconversions	CAC0696	D-Altronate[c] -> H2O[c] + 2-Dehydro-3-deoxy-D-gluconate[c]	0	1000	df	-21.835	-3.628
R01542	Pentose and glucuronate interconversions|pentose and glucuronate interconversions	CAC0361	NAD+[c] + 2-Dehydro-3-deoxy-D-gluconate[c] <=> NADH[c] + H+[c] + "(4S)-4,6-Dihydroxy-2,5-dioxohexanoate"[c]	-1000	1000		-24.353	22.744
R01983	Pentose and glucuronate interconversions|pentose and glucuronate interconversions	CAC0692	D-Galacturonate[c] <=> D-Tagaturonate[c]	-1000	1000		-9.353	7.573
R02555	Pentose and glucuronate interconversions|pentose and glucuronate interconversions	CAC0695	NAD+[c] + D-Altronate[c] <=> NADH[c] + H+[c] + D-Tagaturonate[c]	-1000	1000		-26.398	21.289

R05606	Pentose and glucuronate interconversions|pentose and glucuronate interconversions	CAC1332	D-Mannonate[c] -> H2O[c] + 2-Dehydro-3-deoxy-D-gluconate[c]	0	1000	df	-21.835	-3.628
R01049	Pentose phosphate pathway	CAC0819|CAC3221	ATP[c] + D-Ribose 5-phosphate[c] -> AMP[c] + 0.84 H+[c] + 5-Phospho-alpha-D-ribose 1-diphosphate[c]	0	1000		-22.866	13.866
R01051	Pentose phosphate pathway	Unassigned	ATP[c] + D-Ribose[c] <=> ADP[c] + 0.84 H+[c] + D-Ribose 5-phosphate[c]	-1000	1000		-22.885	13.885
R01056	Pentose phosphate pathway	CAC0726|CAC1431|CAC2880	0.09 H+[c] + D-Ribose 5-phosphate[c] <=> D-Ribulose 5-phosphate[c]	-1000	1000		-6.750	7.990
R01066	Pentose phosphate pathway	CAC1545	0.05 H+[c] + 2-Deoxy-D-ribose 5-phosphate[c] -> Acetaldehyde[c] + D-Glyceraldehyde 3-phosphate[c]	0	1000		-12.270	6.501
R01538	Pentose phosphate pathway	Unassigned	D-Gluconic acid[c] <=> H2O[c] + 2-Dehydro-3-deoxy-D-gluconate[c]	-1000	1000		-21.835	-3.628
R01641	Pentose phosphate pathway	CAC0944|CAC1348	0.06 H+[c] + D-Ribose 5-phosphate[c] + D-Xylulose 5-phosphate[c] <=> D-Glyceraldehyde 3-phosphate[c] + Sedoheptulose 7-phosphate[c]	-1000	1000		-10.393	14.553
R01737	Pentose phosphate pathway	Unassigned	ATP[c] + D-Gluconic acid[c] -> ADP[c] + 0.71 H+[c] + 6-Phospho-D-gluconate[c]	0	1000		-22.428	13.428
R01827	Pentose phosphate pathway	CAC1347	D-Glyceraldehyde 3-phosphate[c] + Sedoheptulose 7-phosphate[c] <=> 0.06 H+[c] + D-Fructose 6-phosphate[c] + D-Erythrose 4-phosphate[c]	-1000	1000		-14.150	10.650
R01830	Pentose phosphate pathway	CAC0944|CAC1348	0.13 H+[c] + D-Fructose 6-phosphate[c] + D-Glyceraldehyde 3-phosphate[c] <=> D-Xylulose 5-phosphate[c] + D-Erythrose 4-phosphate[c]	-1000	1000		-10.320	13.820
R02035	Pentose phosphate pathway	Unassigned	H2O[c] + "D-Glucono-1,5-lactone 6-phosphate"[c] <0> 0.89 H+[c] + 6-Phospho-D-gluconate[c]	0	0		-1.277	18.500
R02736	Pentose phosphate pathway	Unassigned	NADP+[c] + beta-D-Glucose 6-phosphate[c] -> NADPH[c] + 0.97 H+[c] + "D-Glucono-1,5-lactone 6-phosphate"[c]	0	1000		-30.591	17.462
R02749	Pentose phosphate pathway	CAC2065	2-Deoxy-D-ribose 1-phosphate[c] <=> 0.06 H+[c] + 2-Deoxy-D-ribose 5-phosphate[c]	-1000	1000		-7.834	7.834
R08571	Pentose phosphate pathway|pentose phosphate pathway	CAC2018	H2O[c] + Oxidized ferredoxin[c] + D-Glyceraldehyde[c] <0> 3 H+[c] + Reduced ferredoxin[c] + D-Glycerate[c]	0	0		NaN	NaN
R01057	Pentose phosphate pathway|pentose phosphate pathway|purine metabolism	CAC2065	0.01 H+[c] + alpha-D-Ribose 1-phosphate[c] <=> D-Ribose 5-phosphate[c]	-1000	1000		-8.225	8.225
R00742	Propanoate metabolism	CAC3568|CAC3569|CAC3570	ADP[c] + Orthophosphate[c] + 0.62 H+[c] + Malonyl-CoA[c] <- ATP[c] + Acetyl-CoA[c] + HCO3-[c]	-1000	0		NaN	NaN
R01359	Propanoate metabolism	Unassigned	Acetate[c] + Acetoacetyl-CoA[c] <0> Acetyl-CoA[c] + Acetoacetate[c]	0	0		NaN	NaN
R01366	Propanoate metabolism	CAP0165	H+[c] + Acetoacetate[c] -> CO2[c] + Acetone[c]	0	1000		-30.065	-13.564
R00199	Pyruvate metabolism	CAC0534	H2O[c] + ATP[c] + Pyruvate[c] <=> Orthophosphate[c] + AMP[c] + Phosphoenolpyruvate[c] + 1.99 H+[c]	-1000	1000		-14.981	29.627
R00214	Pyruvate metabolism	CAC1589|CAC1596	NAD+[c] + (S)-Malate[c] <0> NADH[c] + CO2[c] + Pyruvate[c] + 0.01 H+[c]	0	0		-26.760	20.271
R00216	Pyruvate metabolism	CAC1589|CAC1596	NADP+[c] + (S)-Malate[c] <0> NADPH[c] + CO2[c] + Pyruvate[c] + 0.01 H+[c]	0	0		-26.732	20.243
R00228	Pyruvate metabolism	CAP0035|CAP0162	NAD+[c] + CoA[c] + Acetaldehyde[c] <- NADH[c] + Acetyl-CoA[c] + H+[c]	-1000	0		NaN	NaN
R00230	Pyruvate metabolism	CAC1742	Orthophosphate[c] + Acetyl-CoA[c] -> CoA[c] + 0.31 H+[c] + Acetyl phosphate[c]	0	1000		NaN	NaN
R00315	Pyruvate metabolism	CAC1743	ATP[c] + Acetate[c] + 0.16 H+[c] <=> ADP[c] + Acetyl phosphate[c]	-1000	1000	d	-23.028	12.308
R00317	Pyruvate metabolism	CAC2830	H2O[c] + Acetyl phosphate[c] <0> Orthophosphate[c] + Acetate[c] + 0.69 H+[c]	0	0		-2.734	18.880
R00704	Pyruvate metabolism	CAC1543|CAC2691	NAD+[c] + (R)-Lactate[c] <- NADH[c] + Pyruvate[c] + H+[c]	-1000	0		-21.814	25.125
R01016	Pyruvate metabolism	CAC1604	0.33 H+[c] + Glycerone phosphate[c] <=> Orthophosphate[c] + Methylglyoxal[c]	-1000	1000		-13.971	2.234
R01213	Pyruvate metabolism	CAC0273|CAC3174	CoA[c] + 0.97 H+[c] + (2S)-2-Isopropylmalate[c] <- H2O[c] + Acetyl-CoA[c] + 3-Methyl-2-oxobutanoic acid[c]	-1000	0		NaN	NaN
R01450	Pyruvate metabolism	Unassigned	(S)-Lactate[c] <=> (R)-Lactate[c]	-1000	1000		-5.211	5.211
R02947	Pyruvate metabolism	CAC2697	H+[c] + 2-Acetolactate[c] -> CO2[c] + Acetoin[c]	0	1000	df	-24.017	-7.512
R00028	Starch and sucrose metabolism	Unassigned	H2O[c] + Maltose[c] <=> 2 D-Glucose[c]	-1000	1000	d	-20.810	14.584
R00802	Starch and sucrose metabolism	CAC0425	H2O[c] + Sucrose[c] <=> D-Glucose[c] + D-Fructose[c]	-1000	1000		-19.079	12.853
R00805	Starch and sucrose metabolism	Unassigned	H2O[c] + 0.32 H+[c] + Sucrose 6-phosphate[c] <=> Orthophosphate[c] + Sucrose[c]	-1000	1000		-9.689	24.115
R00837	Starch and sucrose metabolism	CAC0533	H2O[c] + "alpha,alpha-Trehalose 6-phosphate"[c] <=> D-Glucose[c] + D-Glucose 6-phosphate[c]	-1000	1000		-19.545	13.319
R00838	Starch and sucrose metabolism	CAC0533	H2O[c] + Maltose 6-phosphate[c] <=> D-Glucose[c] + D-Glucose 6-phosphate[c]	-1000	1000		-19.545	13.319
R00948	Starch and sucrose metabolism	CAC2237|CAC2238	ATP[c] + 0.49 H+[c] + D-Glucose 1-phosphate[c] <=> Diphosphate[c] + ADP-glucose[c]	-1000	1000		-18.351	20.491
R01555	Starch and sucrose metabolism	CAC2685	Orthophosphate[c] + Maltose[c] <=> D-Glucose[c] + 0.33 H+[c] + beta-D-Glucose 1-phosphate[c]	-1000	1000		-26.816	6.164
R02727	Starch and sucrose metabolism	Unassigned	Orthophosphate[c] + "alpha,alpha-Trehalose"[c] <=> D-Glucose[c] + 0.33 H+[c] + beta-D-Glucose 1-phosphate[c]	-1000	1000		-26.816	6.164
R02728	Starch and sucrose metabolism	CAC2614	0.01 H+[c] + beta-D-Glucose 1-phosphate[c] <=> beta-D-Glucose 6-phosphate[c]	-1000	1000	d	-8.757	8.757
R02778	Starch and sucrose metabolism	Unassigned	H2O[c] + 0.32 H+[c] + "alpha,alpha-Trehalose 6-phosphate"[c] <=> Orthophosphate[c] + "alpha,alpha-Trehalose"[c]	-1000	1000		-10.399	24.825
R03921	Starch and sucrose metabolism	CAC0425	H2O[c] + Sucrose 6-phosphate[c] -> D-Glucose 6-phosphate[c] + D-Fructose[c]	0	1000		-18.983	12.757
R00022	amino sugar and nucleotide sugar metabolism	CAC0182	H2O[c] + Chitobiose[c] <=> 2 N-Acetyl-D-Glucosamine[c]	-1000	1000		NaN	NaN
R00414	amino sugar and nucleotide sugar metabolism	Unassigned	H2O[c] + UDP-N-acetyl-D-glucosamine[c] <=> UDP[c] + 0.28 H+[c] + N-Acetyl-D-mannosamine[c]	-1000	1000		-22.046	12.420
R00420	amino sugar and nucleotide sugar metabolism	Unassigned	UDP-N-acetyl-D-glucosamine[c] <=> UDP-N-acetyl-D-mannosamine[c]	-1000	1000		-13.652	13.652
R05199	amino sugar and nucleotide sugar metabolism	Unassigned	N-Acetyl-D-Glucosamine[c] + Protein N(pi)-phospho-L-histidine[c] <=> N-Acetyl-D-glucosamine 6-phosphate[c] + Protein histidine[c]	-1000	1000		NaN	NaN
R08555	amino sugar and nucleotide sugar metabolism	CAC0175	H2O[c] + N-Acetylmuramic acid 6-phosphate|N-Acetylmuramic acid 6-phosphate|MurNAc 6-phosphate[c] <=> 0.03 H+[c] + (R)-Lactate[c] + N-Acetyl-D-glucosamine 6-phosphate[c]	-1000	1000		-16.862	10.636
R08559	amino sugar and nucleotide sugar metabolism	Unassigned	N-Acetylmuramate[c] + Protein N(pi)-phospho-L-histidine[c] <=> Protein histidine[c] + N-Acetylmuramic acid 6-phosphate|N-Acetylmuramic acid 6-phosphate|MurNAc 6-phosphate[c]	-1000	1000		NaN	NaN
R01433	amino sugar and nucleotide sugar metabolism|starch and sucrose metabolism	CAC3452	D-Xylose[c] <=> H2O[c] + "1,4-beta-D-Xylan"[c]	-1000	1000		NaN	NaN
R01976	butanoate metabolism	CAC2708	NADP+[c] + (S)-3-Hydroxybutanoyl-CoA[c] <- NADPH[c] + H+[c] + Acetoacetyl-CoA[c]	-1000	0		NaN	NaN
R03050	butanoate metabolism	Unassigned	Thiamin diphosphate[c] + 2-Acetolactate[c] <=> Pyruvate[c] + 2-(alpha-Hydroxyethyl)thiamine diphosphate[c]	-1000	1000		NaN	NaN
R00212	butanoate metabolism|pyruvate metabolism	CAC0980	Acetyl-CoA[c] + Formate[c] <=> CoA[c] + Pyruvate[c]	-1000	1000		NaN	NaN
R01105	galactose metabolism	CAC2514	2 H2O[c] + Galactan[c] <=> 2 D-Galactose[c]	-1000	1000		NaN	NaN

R00470	glyoxylate and dicarboxylate metabolism	Unassigned	4-Hydroxy-2-oxoglutarate[c] <=> Pyruvate[c] + Glyoxylate[c]	-1000	1000		-9.242	6.533
R00475	glyoxylate and dicarboxylate metabolism	CAC2542	Oxygen[c] + Glycolate[c] <=> H2O2[c] + Glyoxylate[c]	-1000	1000		-34.587	-13.473
R01334	glyoxylate and dicarboxylate metabolism	CAC0418	H2O[c] + 0.28 H+[c] + 2-Phosphoglycolate[c] <=> Orthophosphate[c] + Glycolate[c]	-1000	1000		-3.309	17.735
R03332	inositol phosphate metabolism	Unassigned	H2O[c] + 1-Phosphatidyl-D-myo-inositol[c] <=> "1,2-Diacyl-sn-glycerol"[c] + Inositol 1-phosphate[c]	-1000	1000		NaN	NaN
R00921	propanoate metabolism	Unassigned	Orthophosphate[c] + Propanoyl-CoA[c] <=> CoA[c] + 0.32 H+[c] + Propanoyl phosphate[c]	-1000	1000		NaN	NaN
R01000	propanoate metabolism	Unassigned	NAD+[c] + 2-Hydroxybutanoic acid[c] <=> NADH[c] + H+[c] + 2-Oxobutanoate[c]	-1000	1000		NaN	NaN
R01353	propanoate metabolism	Unassigned	ATP[c] + 0.16 H+[c] + Propanoate[c] <=> ADP[c] + Propanoyl phosphate[c]	-1000	1000		-24.519	10.719
R06987	propanoate metabolism	CAC0980	CoA[c] + 2-Oxobutanoate[c] <=> Formate[c] + Propanoyl-CoA[c]	-1000	1000		NaN	NaN
R02108	starch and sucrose metabolism	Unassigned	H2O[c] + Starch[c] <=> Dextrin[c]	-1000	1000		NaN	NaN
R02111	starch and sucrose metabolism	Unassigned	Orthophosphate[c] + Starch[c] <=> D-Glucose 1-phosphate[c] + Amylose[c]	-1000	1000		NaN	NaN
R02421	starch and sucrose metabolism	CAC2239	ADP-glucose[c] <=> ADP[c] + Amylose[c]	-1000	1000		NaN	NaN
R02780	starch and sucrose metabolism	Unassigned	"alpha,alpha-Trehalose"[c] + Protein N(pi)-phospho-L-histidine[c] <=> "alpha,alpha-Trehalose 6-phosphate"[c] + Protein histidine[c]	-1000	1000		NaN	NaN
R02886	starch and sucrose metabolism	Unassigned	H2O[c] + 2 Cellulose[c] <=> Cellobiose[c]	-1000	1000		NaN	NaN
R02887	starch and sucrose metabolism	Unassigned	H2O[c] + Cellulose[c] <=> beta-D-Glucose[c]	-1000	1000		NaN	NaN
R03527	starch and sucrose metabolism	Unassigned	H2O[c] + D-Glucoside[c] <=> D-Glucose[c] + ROH[c]	-1000	1000		NaN	NaN
R04111	starch and sucrose metabolism	Unassigned	Maltose[c] + Protein N(pi)-phospho-L-histidine[c] <=> Maltose 6-phosphate[c] + Protein histidine[c]	-1000	1000		NaN	NaN
R05140	starch and sucrose metabolism	CAC1772	D-Glucose[c] + "Levan|Levan|(2,6-beta-D-Fructosyl)n|Levan n|2,6-beta-D-Fructan|(2,6-beta-D-Fructosyl)n+1"[c] <=> 2 Sucrose[c]	-1000	1000		NaN	NaN
R00762	Carbon Fixation	CAC1088|CAC1572	H2O[c] + 0.34 H+[c] + "D-Fructose 1,6-bisphosphate"[c] <0> Orthophosphate[c] + D-Fructose 6-phosphate[c]	0	0		-5.736	20.162
R01067	Carbon Fixation	CAC0944|CAC1348	0.13 H+[c] + D-Fructose 6-phosphate[c] + D-Glyceraldehyde 3-phosphate[c] <0> D-Xylulose 5-phosphate[c] + D-Erythrose 4-phosphate[c]	0	0		-10.320	13.820
R00519	H2 synthesis	Unassigned	NAD+[c] + Formate[c] -> NADH[c] + CO2[c]	0	1000		-40.710	6.341
R01195	H2 synthesis	Unassigned	NADP+[c] + H+[c] + Reduced ferredoxin[c] -> NADPH[c] + Oxidized ferredoxin[c]	0	1000		NaN	NaN
R01196	H2 synthesis	Unassigned	CO2[c] + Acetyl-CoA[c] + H+[c] + Reduced ferredoxin[c] <- CoA[c] + Pyruvate[c] + Oxidized ferredoxin[c]	-1000	0		NaN	NaN
R05875	H2 synthesis	Unassigned	NAD+[c] + H+[c] + Reduced ferredoxin[c] -> NADH[c] + Oxidized ferredoxin[c]	0	1000		NaN	NaN
R07301	H2 synthesis	Unassigned	2 H+[c] + Reduced ferredoxin[c] <=> Oxidized ferredoxin[c] + Hydrogen[c]	-1000	1000		NaN	NaN
R00524	Nitrogen reduction and fixation	Unassigned	H2O[c] + Formamide[c] <=> NH3[c] + Formate[c] + 0.01 H+[c]	-1000	1000		-28.703	-6.943
R00790	Nitrogen reduction and fixation	CAC0094	2 H2O[c] + NH3[c] + 3 Oxidized ferredoxin[c] <- 7.99 H+[c] + Nitrite[c] + 3 Reduced ferredoxin[c]	-1000	0		NaN	NaN
R00791	Nitrogen reduction and fixation	Unassigned	H2O[c] + Nitrite[c] + Oxidized ferredoxin[c] <- 2 H+[c] + Reduced ferredoxin[c] + Nitrate[c]	-1000	0		NaN	NaN
R05185	Nitrogen reduction and fixation	CAC0253|CAC0256|CAC0257	16 H2O[c] + 16 ATP[c] + 1.59 H+[c] + 4 Reduced ferredoxin[c] + Nitrogen[c] -> 16 ADP[c] + 16 Orthophosphate[c] + 2 NH3[c] + 4 Oxidized ferredoxin[c] + Hydrogen[c]	0	1000		NaN	NaN
R00509	Sulfur reduction and fixation	CAC0103|CAC0110	ATP[c] + Adenylyl sulfate[c] <=> ADP[c] + 3-Phosphoadenylyl sulfate[c] + 0.91 H+[c]	-1000	1000		-25.795	16.795
R00529	Sulfur reduction and fixation	CAC0109|CAC0110	ATP[c] + Sulfate[c] + 0.63 H+[c] <=> Diphosphate[c] + Adenylyl sulfate[c]	-1000	1000		NaN	NaN
R00858	Sulfur reduction and fixation	Unassigned	3 H2O[c] + 3 NADP+[c] + Hydrogen sulfide[c] <- 3 NADPH[c] + 3.33 H+[c] + Sulfite[c]	-1000	0	dr	18.673	141.476
R01285	Sulfur reduction and fixation	CAC0391	H2O[c] + H+[c] + Cystathionine[c] <0> NH3[c] + Pyruvate[c] + L-Homocysteine[c]	0	0	df	-29.016	-0.367
R02021	Sulfur reduction and fixation	Unassigned	3-Phosphoadenylyl sulfate[c] + Thioredoxin[c] -> "Adenosine 3,5-bisphosphate"[c] + H+[c] + Sulfite[c] + Thioredoxin disulfide[c]	0	1000		NaN	NaN
R02508	Sulfur reduction and fixation	CAC0390|CAC0930	Succinate[c] + 0.96 H+[c] + Cystathionine[c] <0> L-Cysteine[c] + O-Succinyl-L-homoserine[c]	0	0		-13.757	10.329
R00296	methane metabolism	Unassigned	H2O[c] + CO[c] + Acceptor[c] <=> CO2[c] + Reduced acceptor[c]	-1000	1000		NaN	NaN
R06983	methane metabolism	CAC3375	NAD+[c] + S-(Hydroxymethyl)glutathione[c] <=> NADH[c] + H+[c] + S-Formylglutathione[c]	-1000	1000		-34.962	13.673
R00132	nitrogen metabolism	Unassigned	0.9 H+[c] + HCO3-[c] <=> H2O[c] + CO2[c]	-1000	1000		-21.731	-4.772
R08553	sulfur metabolism	CAC0104	FAD[c] + AMP[c] + 1.33 H+[c] + Sulfite[c] <=> Adenylyl sulfate[c] + FADH2[c]	-1000	1000		-16.567	40.376
R07295	Peptidoglycan biosynthesis	Unassigned	H2O[c] + 3 ATP[c] + NH3[c] + 5 Glycine[c] + UDP-N-acetyl-D-glucosamine[c] + L-Lysine[c] + UDP-N-acetylmuramoyl-L-alanyl-D-glutamate[c] + D-Alanyl-D-alanine[c] <=> Crosslinked peptideglycan[c]	-1000	1000		NaN	NaN
R04573	peptidoglycan biosynthesis	CAC2128	ATP[c] + 0.45 H+[c] + D-Alanyl-D-alanine[c] + UDP-N-acetylmuramoyl-L-alanyl-gamma-D-glutamyl-L-lysine[c] <=> ADP[c] + Orthophosphate[c] + UDPMurAc(oyl-L-Ala-D-gamma-Glu-L-Lys-D-Ala-D-Ala)[c]	-1000	1000		-35.108	24.880
R05032	peptidoglycan biosynthesis	CAC2231	UDP-N-acetyl-D-glucosamine[c] + Undecaprenyl-diphospho-N-acetylmuramoyl-L-alanyl-D-glutamyl-meso-[c] <=> UDP[c] + 0.28 H+[c] + Undecaprenyl-diphospho-N-acetylmuramoyl-(N-acetylglucosamine)-L-[c]	-1000	1000		-33.893	30.493
R05627	peptidoglycan biosynthesis	Unassigned	H2O[c] + "di-trans,poly-cis-Undecaprenyl diphosphate"[c] <=> Orthophosphate[c] + 0.85 H+[c] + "di-trans,poly-cis-Undecaprenyl phosphate"[c]	-1000	1000		-22.099	27.525
R05629	peptidoglycan biosynthesis	CAC2127	UDPMurAc(oyl-L-Ala-D-gamma-Glu-L-Lys-D-Ala-D-Ala)[c] + "di-trans,poly-cis-Undecaprenyl phosphate"[c] <=> 0.24 H+[c] + UMP[c] + MurAc(oyl-L-Ala-D-gamma-Glu-L-Lys-D-Ala-D-Ala)-diphospho-[c]	-1000	1000		-30.696	30.696
R05630	peptidoglycan biosynthesis	CAC2127	UDP-N-acetylmuramoyl-L-alanyl-D-glutamyl-6-carboxy-L-lysyl-D-alanyl-[c] + "di-trans,poly-cis-Undecaprenyl phosphate"[c] <=> 0.24 H+[c] + UMP[c] + Undecaprenyl-diphospho-N-acetylmuramoyl-L-alanyl-D-glutamyl-meso-[c]	-1000	1000		-30.714	30.714
R05662	peptidoglycan biosynthesis	CAC2231	UDP-N-acetyl-D-glucosamine[c] + MurAc(oyl-L-Ala-D-gamma-Glu-L-Lys-D-Ala-D-Ala)-diphospho-[c] <=> UDP[c] + 0.28 H+[c] + Undecaprenyl-diphospho-N-acetylmuramoyl-(N-acetylglucosamine)-L-[c]	-1000	1000		-33.904	30.504
R01123	Biosynthesis of steroids	Unassigned	Isopentenyl diphosphate[c] <=> Dimethylallyl diphosphate[c]	-1000	1000		-5.444	6.764
R01658	Biosynthesis of steroids	CAC2080	Isopentenyl diphosphate[c] + Dimethylallyl diphosphate[c] -> Diphosphate[c] + 0.37 H+[c] + Geranyl diphosphate[c]	0	1000	df	-24.801	-1.199
R02003	Biosynthesis of steroids	CAC2080	Isopentenyl diphosphate[c] + Geranyl diphosphate[c] -> Diphosphate[c] + 0.37 H+[c] + "trans,trans-Farnesyl diphosphate"[c]	0	1000	df	-25.999	-0.001

R02061	Biosynthesis of steroids	Unassigned	Isopentenyl diphosphate[c] + "trans,trans-Farnesyl diphosphate"[c] <=> Diphosphate[c] + 0.37 H+[c] + Geranylgeranyl diphosphate[c]	-1000	1000		-27.314	1.314
R05612	Biosynthesis of steroids	Unassigned	Isopentenyl diphosphate[c] + all-trans-Hexaprenyl diphosphate[c] <=> Diphosphate[c] + 0.37 H+[c] + all-trans-Heptaprenyl diphosphate[c]	-1000	1000		NaN	NaN
R05613	Biosynthesis of steroids	Unassigned	Isopentenyl diphosphate[c] + all-trans-Pentaprenyl diphosphate[c] <=> Diphosphate[c] + 0.37 H+[c] + all-trans-Hexaprenyl diphosphate[c]	-1000	1000		NaN	NaN
R05633	Biosynthesis of steroids	CAC3184	CTP[c] + 0.38 H+[c] + 2-C-Methyl-D-erythritol 4-phosphate[c] <=> Diphosphate[c] + 4-(Cytidine 5-diphospho)-2-C-methyl-D-erythritol[c]	-1000	1000		NaN	NaN
R05634	Biosynthesis of steroids	CAC2902	ATP[c] + 4-(Cytidine 5-diphospho)-2-C-methyl-D-erythritol[c] <=> ADP[c] + 0.86 H+[c] + 2-Phospho-4-(cytidine 5-diphospho)-2-C-methyl-D-erythritol[c]	-1000	1000		NaN	NaN
R05636	Biosynthesis of steroids	CAC2077|CAP0106	Pyruvate[c] + 1.03 H+[c] + D-Glyceraldehyde 3-phosphate[c] <=> CO2[c] + 1-Deoxy-D-xylulose 5-phosphate[c]	-1000	1000		NaN	NaN
R05637	Biosynthesis of steroids	CAC0434	0.02 H+[c] + 2-Phospho-4-(cytidine 5-diphospho)-2-C-methyl-D-erythritol[c] <=> CMP[c] + "2-C-Methyl-D-erythritol 2,4-cyclodiphosphate"[c]	-1000	1000		NaN	NaN
R05688	Biosynthesis of steroids	CAC1795	NADP+[c] + 2-C-Methyl-D-erythritol 4-phosphate[c] <- NADPH[c] + H+[c] + 1-Deoxy-D-xylulose 5-phosphate[c]	-1000	0		NaN	NaN
R05884	Biosynthesis of steroids	Unassigned	NADPH[c] + H+[c] + 1-Hydroxy-2-methyl-2-butenyl 4-diphosphate[c] -> H2O[c] + NADP+[c] + Isopentenyl diphosphate[c]	0	1000		NaN	NaN
R07244	Biosynthesis of steroids	Unassigned	Isopentenyl diphosphate[c] + Geranylgeranyl diphosphate[c] <=> Diphosphate[c] + 0.37 H+[c] + all-trans-Pentaprenyl diphosphate[c]	-1000	1000		NaN	NaN
R07245	Biosynthesis of steroids	Unassigned	Isopentenyl diphosphate[c] + all-trans-Heptaprenyl diphosphate[c] <=> Diphosphate[c] + 0.37 H+[c] + all-trans-Octaprenyl diphosphate[c]	-1000	1000		NaN	NaN
R07256	Biosynthesis of steroids	Unassigned	"2-C-Methyl-D-erythritol 2,4-cyclodiphosphate"[c] <0> H2O[c] + 0.28 H+[c] + 1-Hydroxy-2-methyl-2-butenyl 4-diphosphate[c]	0	0		NaN	NaN
R01624	Fatty acid biosynthesis	CAC0814|CAC2008|CAC3573|CAC3578|CAP0088	Acetyl-CoA[c] + Acyl-carrier protein[c] <=> CoA[c] + Acetyl-[acyl-carrier protein][c]	-1000	1000		NaN	NaN
R01626	Fatty acid biosynthesis	CAC3575	Malonyl-CoA[c] + Acyl-carrier protein[c] -> CoA[c] + Malonyl-[acyl-carrier protein][c]	0	1000		NaN	NaN
R01706	Fatty acid biosynthesis	Unassigned	H2O[c] + Hexadecanoyl-[acp][c] <=> 0.99 H+[c] + Acyl-carrier protein[c] + Hexadecanoic acid[c]	-1000	1000		NaN	NaN
R04385	Fatty acid biosynthesis	CAC3570	ATP[c] + HCO3-[c] + Holo-[carboxylase][c] <=> ADP[c] + Orthophosphate[c] + Carboxybiotin-carboxyl-carrier protein[c]	-1000	1000		NaN	NaN
R04386	Fatty acid biosynthesis	CAC3568|CAC3569|CAC3570	Acetyl-CoA[c] + Carboxybiotin-carboxyl-carrier protein[c] -> Malonyl-CoA[c] + Holo-[carboxylase][c]	0	1000		NaN	NaN
R07131	Fatty acid biosynthesis	Unassigned	7 NADH[c] + 7 NADPH[c] + 14 H+[c] + 7 Malonyl-[acyl-carrier protein][c] + Acetyl-[acyl-carrier protein][c] <=> 7 NAD+[c] + 7 NADP+[c] + 7 CO2[c] + 7 Acyl-carrier protein[c] + Hexadecanoyl-[acp][c]	-1000	1000		NaN	NaN
R01280	Fatty acid metabolism	Unassigned	ATP[c] + CoA[c] + Hexadecanoic acid[c] <=> Diphosphate[c] + AMP[c] + 0.22 H+[c] + Palmitoyl-CoA[c]	-1000	1000		NaN	NaN
R01975	Fatty acid metabolism	Unassigned	NAD+[c] + (S)-3-Hydroxybutanoyl-CoA[c] <- NADH[c] + H+[c] + Acetoacetyl-CoA[c]	-1000	0		NaN	NaN
R07132	Fatty acid metabolism	Unassigned	6 H2O[c] + 6 NAD+[c] + 6 CoA[c] + 7 FAD[c] + Palmitoyl-CoA[c] <0> 6 NADH[c] + 6 Acetyl-CoA[c] + 2.63 H+[c] + Crotonoyl-CoA[c] + 7 FADH2[c]	0	0		NaN	NaN
R07133	Fatty acid metabolism	Unassigned	6 H2O[c] + 6 NADP+[c] + 6 CoA[c] + 7 FAD[c] + Palmitoyl-CoA[c] -> 6 NADPH[c] + 6 Acetyl-CoA[c] + 2.63 H+[c] + Crotonoyl-CoA[c] + 7 FADH2[c]	0	1000		NaN	NaN
R00847	Glycerolipid metabolism	CAC1321	ATP[c] + Glycerol[c] <- ADP[c] + 0.74 H+[c] + sn-Glycerol 3-phosphate[c]	-1000	0		-22.173	13.173
R01036	Glycerolipid metabolism	CAC3375|CAP0035|CAP0162	NAD+[c] + Glycerol[c] <0> NADH[c] + H+[c] + D-Glyceraldehyde[c]	0	0		-22.841	24.152
R01041	Glycerolipid metabolism	CAC3375|CAP0035|CAP0162	NADP+[c] + Glycerol[c] <=> NADPH[c] + H+[c] + D-Glyceraldehyde[c]	-1000	1000		-22.813	24.124
R01514	Glycerolipid metabolism	CAC2834	ATP[c] + D-Glycerate[c] <- ADP[c] + 0.76 H+[c] + 3-Phospho-D-glycerate[c]	-1000	0		-22.138	13.138
R01752	Glycerolipid metabolism	Unassigned	H2O[c] + NAD+[c] + D-Glyceraldehyde[c] <0> NADH[c] + 2 H+[c] + D-Glycerate[c]	0	0		-26.045	25.499
R02240	Glycerolipid metabolism	CAC1294	ATP[c] + "1,2-Diacyl-sn-glycerol"[c] <=> ADP[c] + "1,2-didodecanoyl-sn-glycerol 3-phosphate"[c]	-1000	1000		NaN	NaN
R02241	Glycerolipid metabolism	CAC0965	CoA[c] + "1,2-didodecanoyl-sn-glycerol 3-phosphate"[c] <=> Acyl-CoA[c] + 1-Acyl-sn-glycerol 3-phosphate|1-Acyl-sn-glycerol 3-phosphate|2-Lysophosphatidate|Lysophosphatidate|Lysophosphatidic acid[c]	-1000	1000		NaN	NaN
R02689	Glycerolipid metabolism	Unassigned	UDP-glucose[c] + "1,2-Diacyl-sn-glycerol"[c] <=> UDP[c] + "3-D-Glucosyl-1,2-diacylglycerol"[c]	-1000	1000		NaN	NaN
R04377	Glycerolipid metabolism	Unassigned	UDP-glucose[c] + "3-D-Glucosyl-1,2-diacylglycerol"[c] <=> UDP[c] + Diglucosyl-diacylglycerol[c]	-1000	1000		NaN	NaN
R05081	Glycerolipid metabolism	Unassigned	"Phosphatidylglycerol (didodecanoyl, n-C12:0)"[c] + Diglucosyl-diacylglycerol[c] <=> "1,2-Diacyl-sn-glycerol"[c] + Glycerophosphoglycoglycerolipid[c]	-1000	1000		NaN	NaN
R07287	Glycerolipid metabolism	Unassigned	CoA[c] + Hexadecanoic acid[c] <=> H2O[c] + Acyl-CoA[c]	-1000	1000		NaN	NaN
R00851	Glycerolipid metabolism|glycerophospholipid metabolism	Unassigned	Acyl-CoA[c] + sn-Glycerol 3-phosphate[c] <=> CoA[c] + 1-Acyl-sn-glycerol 3-phosphate|1-Acyl-sn-glycerol 3-phosphate|2-Lysophosphatidate|Lysophosphatidate|Lysophosphatidic acid[c]	-1000	1000		NaN	NaN
R00842	Glycerophospholipid metabolism	CAC1712	NAD+[c] + sn-Glycerol 3-phosphate[c] <0> NADH[c] + 1.11 H+[c] + Glycerone phosphate[c]	0	0		-24.289	22.680
R00844	Glycerophospholipid metabolism	CAC1712	NADP+[c] + sn-Glycerol 3-phosphate[c] <=> NADPH[c] + 1.11 H+[c] + Glycerone phosphate[c]	-1000	1000	d	-24.261	22.652
R00848	Glycerophospholipid metabolism	CAC1322	FAD[c] + 0.37 H+[c] + sn-Glycerol 3-phosphate[c] <=> Glycerone phosphate[c] + FADH2[c]	-1000	1000	d	-24.659	23.079
R00855	Glycerophospholipid metabolism	Unassigned	H2O[c] + CDP-glycerol[c] -> CMP[c] + 1.6 H+[c] + sn-Glycerol 3-[illegible]	0	1000		-24.033	5.407
R00856	Glycerophospholipid metabolism	Unassigned	CTP[c] + 0.38 H+[c] + sn-Glycerol 3-phosphate[c] <=> Diphosphate[c] + CDP-glycerol[c]	-1000	1000	d	-13.671	15.811
R01799	Glycerophospholipid metabolism	CAC1792	CTP[c] + "1,2-didodecanoyl-sn-glycerol 3-phosphate"[c] <=> Diphosphate[c] + CDP-diacylglycerol[c]	-1000	1000		NaN	NaN
R01801	Glycerophospholipid metabolism	CAC1814|CAC3596	sn-Glycerol 3-phosphate[c] + CDP-diacylglycerol[c] <=> CMP[c] + "Phosphatidylglycerophosphate (didodecanoyl, n-C12:0)"[c]	-1000	1000		NaN	NaN
R02027	Glycerophospholipid metabolism	Unassigned	H2O[c] + "Phosphatidylglycerol (didodecanoyl, n-C12:0)"[c] <0> sn-Glycerol 3-phosphate[c] + "1,2-Diacyl-sn-glycerol"[c]	0	0		NaN	NaN
R02029	Glycerophospholipid metabolism	Unassigned	H2O[c] + 0.47 H+[c] + "Phosphatidylglycerophosphate (didodecanoyl, n-C12:0)"[c] <=> Orthophosphate[c] + "Phosphatidylglycerol (didodecanoyl, n-C12:0)"[c]	-1000	1000		NaN	NaN
R02030	Glycerophospholipid metabolism	CAC2875|CAC3316	CDP-diacylglycerol[c] + "Phosphatidylglycerol (didodecanoyl, n-C12:0)"[c] <=> CMP[c] + "cardiolipin (tetradodecanoyl, n-C12:0)"[c]	-1000	1000		NaN	NaN
R07234	Glycerophospholipid metabolism	Unassigned	L-Lysine[c] + "Phosphatidylglycerol (didodecanoyl, n-C12:0)"[c] <=> H2O[c] + 3-Phosphatidyl-1-(3-O-L-lysyl)glycerol[c]	-1000	1000		NaN	NaN

R07034	arachidonic acid metabolism	Unassigned	2 Glutathione[c] + "5(S)-HPETE|5(S)-HPETE|5(S)-Hydroperoxy-6-trans-8,11,14-cis-eicosatetraenoic acid|(6E,8Z,11Z,14Z)-(5S)-5-Hydroperoxyeicosa-6,8,11,14-tetraenoate|(6E,8Z,11Z,14Z)-(5S)-5-Hydroperoxyeicosa-6,8,11,14-tetraenoic acid|(5S,6E,8Z,11Z,14Z)-5-Hydroperoxyicosa-6,8,11,14-tetraenoate"[c] <=> H2O[c] + Glutathione disulfide[c] + "5(S)-HETE|5(S)-HETE|5-Hydroxyeicosatetraenoate|5-HETE|(6E,8Z,11Z,14Z)-(5S)-5-Hydroxyicosa-6,8,11,14-tetraenoic acid"[c]	-1000	1000		NaN	NaN
R07035	arachidonic acid metabolism	Unassigned	2 Glutathione[c] + "15(S)-HPETE|15(S)-HPETE|(5Z,8Z,11Z,13E)-(15S)-15-Hydroperoxyicosa-5,8,11,13-tetraenoic acid|15-Hydroperoxyeicosatetraenoate|15-Hydroperoxyicosatetraenoate|15-Hydroperoxyeicosatetraenoic acid|15-Hydroperoxyicosatetraenoic acid|(5Z,8Z,11Z,13E)-(15S)-15-Hydroperoxyicosa-5,8,11,13-tetraenoate"[c] <=> H2O[c] + Glutathione disulfide[c] + "(15S)-15-Hydroxy-5,8,11-cis-13-trans-eicosatetraenoate|(15S)-15-Hydroxy-5,8,11-cis-13-trans-eicosatetraenoate|(15S)-15-Hydroxy-5,8,11-cis-13-trans-icosatetraenoate|(5Z,8Z,11Z,13E)-(15S)-15-Hydroxyicosa-5,8,11,13-tetraenoic acid|15(S)-HETE"[c]	-1000	1000		NaN	NaN
R04361	ether lipid metabolism	Unassigned	Acyl-CoA[c] + 1-Alkyl-sn-glycero-3-phosphate[c] <=> CoA[c] + 2-Acyl-1-alkyl-sn-glycero-3-phosphate[c]	-1000	1000		NaN	NaN
R07381	ether lipid metabolism	Unassigned	H2O[c] + O-1-Alk-1-enyl-2-acyl-sn-glycero-3-phosphoethanolamine[c] <=> Ethanolamine phosphate[c] + 1-Alkenyl-2-acylglycerol[c]	-1000	1000		NaN	NaN
R00749	glycerophospholipid metabolism	Unassigned	Ethanolamine[c] -> NH3[c] + 0.01 H+[c] + Acetaldehyde[c]	0	1000	df	-29.082	-12.347
R01030	glycerophospholipid metabolism	Unassigned	H2O[c] + sn-glycero-3-Phosphocholine[c] <=> 0.75 H+[c] + sn-Glycerol 3-phosphate[c] + Choline[c]	-1000	1000		-19.643	10.017
R01312	glycerophospholipid metabolism	Unassigned	H2O[c] + "Phosphatidylcholine|Phosphatidylcholine|Lecithin|Phosphatidyl-N-trimethylethanolamine|1,2-Diacyl-sn-glycero-3-phosphocholine|Choline phosphatide|3-sn-Phosphatidylcholine"[c] <=> Choline phosphate[c] + "1,2-Diacyl-sn-glycerol"[c]	-1000	1000		NaN	NaN
R01470	glycerophospholipid metabolism	Unassigned	H2O[c] + 0.25 H+[c] + sn-glycero-3-Phosphoethanolamine[c] <=> sn-Glycerol 3-phosphate[c] + Ethanolamine[c]	-1000	1000		-15.870	6.244
R02052	glycerophospholipid metabolism	Unassigned	H2O[c] + Phosphatidylethanolamine|Phosphatidylethanolamine|(3-Phosphatidyl)ethanolamine|(3-Phosphatidyl)-ethanolamine|Cephalin|O-(1-beta-Acyl-2-acyl-sn-glycero-3-phospho)ethanolamine|1-Acyl-2-acyl-sn-glycero-3-phosphoethanolamine[c] <=> Ethanolamine phosphate[c] + "1,2-Diacyl-sn-glycerol"[c]	-1000	1000		NaN	NaN
R02055	glycerophospholipid metabolism	Unassigned	"Phosphatidylserine|Phosphatidylserine|Phosphatidyl-L-serine|1,2-Diacyl-sn-glycerol 3-phospho-L-serine|3-O-sn-Phosphatidyl-L-serine|O3-Phosphatidyl-L-serine"[c] <=> CO2[c] + Phosphatidylethanolamine|Phosphatidylethanolamine|(3-Phosphatidyl)ethanolamine|(3-Phosphatidyl)-ethanolamine|Cephalin|O-(1-beta-Acyl-2-acyl-sn-glycero-3-phospho)ethanolamine|1-Acyl-2-acyl-sn-glycero-3-phosphoethanolamine[c]	-1000	1000		NaN	NaN
R02746	glycerophospholipid metabolism	CAC2246	H2O[c] + 1-Acyl-sn-glycero-3-phosphocholine|1-Acyl-sn-glycero-3-phosphocholine|1-Acyl-sn-glycerol-3-phosphocholine|alpha-Acylglycerophosphocholine|2-Lysolecithin|2-Lysophosphatidylcholine|1-Acylglycerophosphocholine[c] <=> sn-glycero-3-Phosphocholine[c] + Fatty acids[c]	-1000	1000		NaN	NaN
R02747	glycerophospholipid metabolism	CAC2246	H2O[c] + 2-Acyl-sn-glycero-3-phosphocholine|2-Acyl-sn-glycero-3-phosphocholine|2-Acylglycero-3-phosphocholine|1-Lysophosphatidylcholine|1-Lysolecithin|3-Lysolecithin[c] <=> sn-glycero-3-Phosphocholine[c] + Fatty acids[c]	-1000	1000		NaN	NaN
R03416	glycerophospholipid metabolism	CAC2246	H2O[c] + 1-Acyl-sn-glycero-3-phosphoethanolamine|1-Acyl-sn-glycero-3-phosphoethanolamine|L-2-Lysophosphatidylethanolamine[c] <=> sn-glycero-3-Phosphoethanolamine[c] + Fatty acids[c]	-1000	1000		NaN	NaN
R03417	glycerophospholipid metabolism	CAC2246	H2O[c] + 2-Acyl-sn-glycero-3-phosphoethanolamine|2-Acyl-sn-glycero-3-phosphoethanolamine|L-1-Lysophosphatidylethanolamine|O-(2-Acyl-sn-glycero-3-phospho)-ethanolamine[c] <=> sn-glycero-3-Phosphoethanolamine[c] + Fatty acids[c]	-1000	1000		NaN	NaN
R01800	glycerophospholipid metabolism|glycine, serine and threonine metabolism	Unassigned	L-Serine[c] + CDP-diacylglycerol[c] <=> CMP[c] + "Phosphatidylserine|Phosphatidylserine|Phosphatidyl-L-serine|1,2-Diacyl-sn-glycerol 3-phospho-L-serine|3-O-sn-Phosphatidyl-L-serine|O3-Phosphatidyl-L-serine"[c]	-1000	1000		NaN	NaN
R05645	lipopolysaccharide biosynthesis	Unassigned	Sedoheptulose 7-phosphate[c] <=> D-glycero-D-manno-Heptose 7-phosphate[c]	-1000	1000		NaN	NaN
R05647	lipopolysaccharide biosynthesis	CAC3053	H2O[c] + 0.23 H+[c] + "D-glycero-D-manno-Heptose 1,7-bisphosphate"[c] <=> Orthophosphate[c] + D-glycero-D-manno-Heptose 1-phosphate[c]	-1000	1000		NaN	NaN
R00127	Purine metabolism	CAC3112	ATP[c] + AMP[c] + 0.56 H+[c] -> 2 ADP[c]	0	1000		-23.873	23.873
R00190	Purine metabolism	CAC2275|CAC3203	Diphosphate[c] + AMP[c] + 0.39 H+[c] <=> 5-Phospho-alpha-D-ribose 1-diphosphate[c] + Adenine[c]	-1000	1000		-14.623	20.643
R00332	Purine metabolism	CAC1718	ATP[c] + 0.57 H+[c] + GMP[c] <=> ADP[c] + GDP[c]	-1000	1000	d	-20.575	20.575
R00430	Purine metabolism	CAC0518|CAC1036	Pyruvate[c] + GTP[c] <- GDP[c] + Phosphoenolpyruvate[c] + 0.91 H+[c]	-1000	0		-12.269	21.489
R01127	Purine metabolism	CAC1395	0.14 H+[c] + 1-(5-Phosphoribosyl)-5-formamido-4-imidazolecarboxamide[c] <=> H2O[c] + IMP[c]	-1000	1000		-15.612	11.649
R01130	Purine metabolism	CAC2701	H2O[c] + NAD+[c] + IMP[c] -> NADH[c] + H+[c] + Xanthosine 5-phosphate[c]	0	1000		-26.441	29.595
R01132	Purine metabolism	CAC3203	Diphosphate[c] + 0.37 H+[c] + IMP[c] <=> 5-Phospho-alpha-D-ribose 1-diphosphate[c] + Hypoxanthine[c]	-1000	1000		-13.952	19.972
R01134	Purine metabolism	CAC3471	NADP+[c] + NH3[c] + IMP[c] <- NADPH[c] + 1.98 H+[c] + GMP[c]	-1000	0		-7.971	47.951
R01138	Purine metabolism	CAC0518|CAC1036	Phosphoenolpyruvate[c] + 0.9 H+[c] + dADP[c] -> Pyruvate[c] + dATP[c]	0	1000		-22.160	12.940
R01229	Purine metabolism	CAC2275|CAC3203	Diphosphate[c] + 0.37 H+[c] + GMP[c] <- 5-Phospho-alpha-D-ribose 1-diphosphate[c] + Guanine[c]	-1000	0		-13.944	19.964
R01244	Purine metabolism	CAC0887	H2O[c] + 0.95 H+[c] + Adenine[c] -> NH3[c] + Hypoxanthine[c]	0	1000		-34.569	-1.457
R01547	Purine metabolism	CAC3112	ATP[c] + 0.56 H+[c] + dAMP[c] <=> ADP[c] + dADP[c]	-1000	1000		-21.041	21.041
R01560	Purine metabolism	CAC3005	H2O[c] + 0.96 H+[c] + Adenosine[c] -> NH3[c] + Inosine[c]	0	1000		-35.337	-0.689
R01561	Purine metabolism	CAC2064	0.32 H+[c] + Adenine[c] + alpha-D-Ribose 1-phosphate[c] <=> Orthophosphate[c] + Adenosine[c]	-1000	1000		-9.697	25.589
R01676	Purine metabolism	CAC0282	H2O[c] + 0.89 H+[c] + Guanine[c] -> NH3[c] + Xanthine[c]	0	1000	df	-34.881	-1.945
R01858	Purine metabolism	CAC0518|CAC1036	Pyruvate[c] + dGTP[c] <- Phosphoenolpyruvate[c] + 0.91 H+[c] + dGDP[c]	-1000	0		-12.108	21.328
R01863	Purine metabolism	CAC2064	Orthophosphate[c] + Inosine[c] <=> 0.33 H+[c] + Hypoxanthine[c] + alpha-D-Ribose 1-phosphate[c]	-1000	1000		-24.919	9.027
R01967	Purine metabolism	Unassigned	ATP[c] + Deoxyguanosine[c] <=> ADP[c] + 0.84 H+[c] + dGMP[c]	-1000	1000	d	-24.967	15.967
R01968	Purine metabolism	Unassigned	H2O[c] + 0.32 H+[c] + dGMP[c] -> Orthophosphate[c] + Deoxyguanosine[c]	0	1000		-9.508	23.934
R01969	Purine metabolism	CAC2064	Orthophosphate[c] + Deoxyguanosine[c] <=> 0.26 H+[c] + Guanine[c] + 2-Deoxy-D-ribose 1-phosphate[c]	-1000	1000		-24.736	8.844

R02014	Purine metabolism	CAC0480|CAC1209	ATP[c] + Thioredoxin[c] -> H2O[c] + dATP[c] + Thioredoxin disulfide[c]	0	1000		NaN	NaN
R02017	Purine metabolism	CAC1047|CAC3276|CAC3277	H2O[c] + dADP[c] + Thioredoxin disulfide[c] <- ADP[c] + Thioredoxin[c]	-1000	0		NaN	NaN
R02019	Purine metabolism	CAC1047|CAC3276|CAC3277	H2O[c] + Thioredoxin disulfide[c] + dGDP[c] <- GDP[c] + Thioredoxin[c]	-1000	0		NaN	NaN
R02020	Purine metabolism	CAC0480|CAC1209	H2O[c] + dGTP[c] + Thioredoxin disulfide[c] <- GTP[c] + Thioredoxin[c]	-1000	0		NaN	NaN
R02088	Purine metabolism	Unassigned	H2O[c] + 0.32 H+[c] + dAMP[c] -> Orthophosphate[c] + Deoxyadenosine[c]	0	1000		-10.339	24.765
R02089	Purine metabolism	Unassigned	ATP[c] + Deoxyadenosine[c] -> ADP[c] + 0.85 H+[c] + dAMP[c]	0	1000		-25.543	16.543
R02090	Purine metabolism	CAC1718	ATP[c] + 0.57 H+[c] + dGMP[c] <=> ADP[c] + dGDP[c]	-1000	1000		-20.466	20.466
R02142	Purine metabolism	CAC3203	Diphosphate[c] + 0.28 H+[c] + Xanthosine 5-phosphate[c] <- 5-Phospho-alpha-D-ribose 1-diphosphate[c] + Xanthine[c]	-1000	0		-14.206	20.226
R02556	Purine metabolism	CAC3005	H2O[c] + 0.96 H+[c] + Deoxyadenosine[c] <=> NH3[c] + Deoxyinosine[c]	-1000	1000		NaN	NaN
R02557	Purine metabolism	CAC2064	Orthophosphate[c] + Deoxyadenosine[c] <=> 0.25 H+[c] + Adenine[c] + 2-Deoxy-D-ribose 1-phosphate[c]	-1000	1000		-25.428	9.536
R02748	Purine metabolism	CAC2064	Orthophosphate[c] + Deoxyinosine[c] <=> 0.26 H+[c] + Hypoxanthine[c] + 2-Deoxy-D-ribose 1-phosphate[c]	-1000	1000		NaN	NaN
R04144	Purine metabolism	CAC1396	ATP[c] + Glycine[c] + 0.47 H+[c] + 5-Phosphoribosylamine[c] <=> ADP[c] + Orthophosphate[c] + 5-Phosphoribosylglycinamide[c]	-1000	1000		NaN	NaN
R04208	Purine metabolism	CAC1393	ATP[c] + 2-(Formamido)-N1-(5-phosphoribosyl)acetamidine[c] <=> ADP[c] + Orthophosphate[c] + 0.52 H+[c] + Aminoimidazole ribotide[c]	-1000	1000		2.855	46.188
R04209	Purine metabolism	CAC1390	1.01 H+[c] + 1-(5-Phospho-D-ribosyl)-5-amino-4-imidazolecarboxylate[c] <=> CO2[c] + Aminoimidazole ribotide[c]	-1000	1000		-27.293	-3.536
R04463	Purine metabolism	CAC1655	H2O[c] + ATP[c] + L-Glutamine[c] + 5-Phosphoribosyl-N-formylglycinamide[c] <=> ADP[c] + Orthophosphate[c] + L-Glutamate[c] + 1.54 H+[c] + 2-(Formamido)-N1-(5-phosphoribosyl)acetamidine[c]	-1000	1000		NaN	NaN
R04559	Purine metabolism	CAC1821	1.84 H+[c] + 1-(5-Phosphoribosyl)-4-(N-succinocarboxamide)-5-aminoimidazole[c] + 1-(5-Phosphoribosyl)-5-amino-4-(N-succinocarboxamide)-imidazole[c] <=> Fumarate[c] + 1-(5-Phosphoribosyl)-5-amino-4-imidazolecarboxamide[c]	-1000	1000		NaN	NaN
R04591	Purine metabolism	CAC1391	ATP[c] + L-Aspartate[c] + 1-(5-Phospho-D-ribosyl)-5-amino-4-imidazolecarboxylate[c] <=> ADP[c] + Orthophosphate[c] + 1.35 H+[c] + 1-(5-Phosphoribosyl)-4-(N-succinocarboxamide)-5-aminoimidazole[c] + 1-(5-Phosphoribosyl)-5-amino-4-(N-succinocarboxamide)-imidazole[c]	-1000	1000		NaN	NaN
R00156	Pyrimidine metabolism	Unassigned	ATP[c] + UDP[c] <=> ADP[c] + UTP[c]	-0.1	0.1	d	-19.125	19.125
R00158	Pyrimidine metabolism	CAC1848	ATP[c] + 0.57 H+[c] + UMP[c] <=> ADP[c] + UDP[c]	-1000	1000	d	-19.113	19.113
R00512	Pyrimidine metabolism	CAC1848	ATP[c] + CMP[c] + 0.57 H+[c] <=> ADP[c] + CDP[c]	-1000	1000	d	-19.161	19.161
R00513	Pyrimidine metabolism	CAC0672	ATP[c] + Cytidine[c] <=> ADP[c] + CMP[c] + 0.84 H+[c]	-0.1	0.1	d	-23.669	14.669
R00516	Pyrimidine metabolism	CAC0672	UTP[c] + Cytidine[c] <=> UDP[c] + CMP[c] + 0.85 H+[c]	-0.1	0.1	d	-21.128	12.128
R00517	Pyrimidine metabolism	CAC0672	GTP[c] + Cytidine[c] <=> GDP[c] + CMP[c] + 0.85 H+[c]	-1000	1000	d	-22.981	13.981
R00568	Pyrimidine metabolism	CAC0025	H2O[c] + CTP[c] + 0.99 H+[c] -> NH3[c] + UTP[c]	0	1000		-29.268	-0.078
R00570	Pyrimidine metabolism	Unassigned	ATP[c] + CDP[c] <=> ADP[c] + CTP[c]	-1000	1000		-19.173	19.173
R00573	Pyrimidine metabolism	CAC2892	H2O[c] + ATP[c] + L-Glutamine[c] + UTP[c] -> ADP[c] + Orthophosphate[c] + L-Glutamate[c] + CTP[c] + 1.53 H+[c]	0	1000		-15.758	41.084
R00964	Pyrimidine metabolism	CAC0672	ATP[c] + Uridine[c] -> ADP[c] + 0.84 H+[c] + UMP[c]	0	1000		-23.621	14.621
R00965	Pyrimidine metabolism	CAC2652	0.96 H+[c] + Orotidine 5-phosphate[c] -> CO2[c] + UMP[c]	0	1000	df	-27.603	-3.225
R00966	Pyrimidine metabolism	CAC2113|CAC2879	Uracil[c] + 5-Phospho-alpha-D-ribose 1-diphosphate[c] <=> Diphosphate[c] + 0.37 H+[c] + UMP[c]	-1000	1000		-17.629	11.609
R00967	Pyrimidine metabolism	CAC0672	UTP[c] + Uridine[c] <=> UDP[c] + 0.85 H+[c] + UMP[c]	-1000	1000	d	-21.064	12.064
R00968	Pyrimidine metabolism	CAC0672	GTP[c] + Uridine[c] <=> GDP[c] + 0.85 H+[c] + UMP[c]	-1000	1000	d	-22.929	13.929
R00974	Pyrimidine metabolism	Unassigned	H2O[c] + 0.98 H+[c] + Cytosine[c] -> NH3[c] + Uracil[c]	0	1000	df	-28.039	-1.307
R01548	Pyrimidine metabolism	CAC0672	dATP[c] + Cytidine[c] <=> CMP[c] + 0.84 H+[c] + dADP[c]	-1000	1000	d	-23.545	14.545
R01549	Pyrimidine metabolism	CAC0672	dATP[c] + Uridine[c] <=> 0.84 H+[c] + UMP[c] + dADP[c]	-1000	1000	d	-23.496	14.496
R01567	Pyrimidine metabolism	CAC2887	ADP[c] + 0.84 H+[c] + dTMP[c] <=> ATP[c] + Thymidine[c]	-1000	1000		-14.444	23.444
R01570	Pyrimidine metabolism	Unassigned	Orthophosphate[c] + Thymidine[c] <=> 0.26 H+[c] + Thymine[c] + 2-Deoxy-D-ribose 1-phosphate[c]	-1000	1000		-22.244	6.352
R01663	Pyrimidine metabolism	CAC2876	H2O[c] + 0.98 H+[c] + dCMP[c] -> NH3[c] + dUMP[c]	0	1000		-28.995	-0.351
R01664	Pyrimidine metabolism	Unassigned	H2O[c] + 0.32 H+[c] + dCMP[c] -> Orthophosphate[c] + Deoxycytidine[c]	0	1000		-7.163	21.589
R01869	Pyrimidine metabolism	Unassigned	NAD+[c] + (S)-Dihydroorotate[c] <=> NADH[c] + 0.98 H+[c] + Orotate[c]	-1000	1000		NaN	NaN
R01870	Pyrimidine metabolism	CAC0027	Diphosphate[c] + 0.34 H+[c] + Orotidine 5-phosphate[c] <=> 5-Phospho-alpha-D-ribose 1-diphosphate[c] + Orotate[c]	-1000	1000		-11.651	17.671
R01878	Pyrimidine metabolism	CAC1544|CAC2609	H2O[c] + 0.98 H+[c] + Cytidine[c] -> NH3[c] + Uridine[c]	0	1000	df	-29.264	-0.082
R01880	Pyrimidine metabolism	CAC0672	dGTP[c] + Uridine[c] <=> 0.85 H+[c] + UMP[c] + dGDP[c]	-1000	1000	d	-22.795	13.795
R01993	Pyrimidine metabolism	CAC0519	H2O[c] + (S)-Dihydroorotate[c] <=> 0.97 H+[c] + N-Carbamoyl-L-aspartate[c]	-1000	1000		NaN	NaN
R02016	Pyrimidine metabolism	CAC0869	NADP+[c] + Thioredoxin[c] <- NADPH[c] + H+[c] + Thioredoxin disulfide[c]	-1000	0		NaN	NaN
R02022	Pyrimidine metabolism	CAC0480|CAC1209	H2O[c] + Thioredoxin disulfide[c] + dCTP[c] <- CTP[c] + Thioredoxin[c]	-1000	0		NaN	NaN
R02023	Pyrimidine metabolism	CAC0480|CAC1209	H2O[c] + Thioredoxin disulfide[c] + dUTP[c] <- UTP[c] + Thioredoxin[c]	-1000	0		NaN	NaN
R02091	Pyrimidine metabolism	CAC0672	dGTP[c] + Cytidine[c] <=> CMP[c] + 0.85 H+[c] + dGDP[c]	-1000	1000	d	-22.848	13.848
R02093	Pyrimidine metabolism	Unassigned	ATP[c] + dTDP[c] -> ADP[c] + dTTP[c]	0	1000		-18.955	18.955
R02094	Pyrimidine metabolism	Unassigned	ATP[c] + 0.57 H+[c] + dTMP[c] <=> ADP[c] + dTDP[c]	-1000	1000		-18.943	18.943
R02096	Pyrimidine metabolism	CAC0672	dTTP[c] + Cytidine[c] <=> CMP[c] + 0.85 H+[c] + dTDP[c]	-1000	1000	d	-20.901	11.901
R02097	Pyrimidine metabolism	CAC0672	Uridine[c] + dTTP[c] <=> 0.85 H+[c] + UMP[c] + dTDP[c]	-1000	1000	d	-20.834	11.834
R02099	Pyrimidine metabolism	CAC2887	ATP[c] + Deoxyuridine[c] <=> ADP[c] + 0.84 H+[c] + dUMP[c]	-1000	1000	d	-23.490	14.490
R02100	Pyrimidine metabolism	CAC1210|CAC1425	H2O[c] + dUTP[c] -> Diphosphate[c] + 1.22 H+[c] + dUMP[c]	0	1000		-22.541	6.055
R02296	Pyrimidine metabolism	CAC1546	Orthophosphate[c] + Cytidine[c] <=> 0.32 H+[c] + Cytosine[c] + alpha-D-Ribose 1-phosphate[c]	-1000	1000		-22.465	6.573
R02325	Pyrimidine metabolism	CAC0025	H2O[c] + 0.99 H+[c] + dCTP[c] -> NH3[c] + dUTP[c]	0	1000		-29.040	-0.306
R02326	Pyrimidine metabolism	Unassigned	ATP[c] + dCDP[c] -> ADP[c] + dCTP[c]	0	1000		-19.049	19.049
R02327	Pyrimidine metabolism	CAC0672	Uridine[c] + dCTP[c] <=> 0.85 H+[c] + UMP[c] + dCDP[c]	-1000	1000	d	-20.962	11.962
R02332	Pyrimidine metabolism	CAC0672	Uridine[c] + dUTP[c] -> 0.85 H+[c] + UMP[c] + dUDP[c]	0	1000		NaN	NaN
R02371	Pyrimidine metabolism	CAC0672	dCTP[c] + Cytidine[c] <=> CMP[c] + 0.85 H+[c] + dCDP[c]	-1000	1000	d	-21.028	12.028
R02372	Pyrimidine metabolism	CAC0672	dUTP[c] + Cytidine[c] -> CMP[c] + 0.85 H+[c] + dUDP[c]	0	1000		NaN	NaN
R02483	Pyrimidine metabolism	Unassigned	Orthophosphate[c] + Deoxyuridine[c] <=> 0.26 H+[c] + Uracil[c] + 2-Deoxy-D-ribose 1-phosphate[c]	-1000	1000		-22.330	6.438
R02485	Pyrimidine metabolism	CAC1544|CAC2609	H2O[c] + 0.98 H+[c] + Deoxycytidine[c] -> NH3[c] + Deoxyuridine[c]	0	1000		-29.012	-0.334
R00239	Urea cycle and metabolism of amino groups	CAC3253	ATP[c] + L-Glutamate[c] + 0.2 H+[c] <=> ADP[c] + L-Glutamyl 5-phosphate[c]	-1000	1000		-24.597	10.797
R00259	Urea cycle and metabolism of amino groups	CAC2391|CAC3020	Acetyl-CoA[c] + L-Glutamate[c] <=> CoA[c] + N-Acetyl-L-glutamate[c]	-1000	1000		NaN	NaN
R02282	Urea cycle and metabolism of amino groups	CAC2391|CAC3020	L-Glutamate[c] + 2.19 H+[c] + N-Acetylornithine[c] <=> L-Ornithine[c] + N-Acetyl-L-glutamate[c]	-1000	1000		-11.780	11.780
R02283	Urea cycle and metabolism of amino groups	CAC2388	2-Oxoglutarate[c] + N-Acetylornithine[c] <=> L-Glutamate[c] + 0.69 H+[c] + N-Acetyl-L-glutamate 5-semialdehyde[c]	-1000	1000		-12.469	10.469
R02649	Urea cycle and metabolism of amino groups	CAC2389	ATP[c] + 0.19 H+[c] + N-Acetyl-L-glutamate[c] <=> ADP[c] + N-Acetyl-L-glutamate 5-phosphate[c]	-1000	1000		-24.743	10.943

R03313	Urea cycle and metabolism of amino groups	CAC3254	NADP+[c] + Orthophosphate[c] + L-Glutamate 5-semialdehyde[c] <=> NADPH[c] + 1.28 H+[c] + L-Glutamyl 5-phosphate[c]	-1000	1000		-35.663	15.891
R03443	Urea cycle and metabolism of amino groups	CAC2390	NADP+[c] + Orthophosphate[c] + N-Acetyl-L-glutamate 5-semialdehyde[c] <=> NADPH[c] + 1.29 H+[c] + N-Acetyl-L-glutamate 5-phosphate[c]	-1000	1000		-35.768	15.996
R07352	Urea cycle and metabolism of amino groups	Unassigned	Pyruvate[c] + L-Ornithine[c] <=> L-Alanine[c] + 2.86 H+[c] + L-Glutamate 5-semialdehyde[c]	-1000	1000	d	-11.990	9.990
R00086	purine metabolism	Unassigned	H2O[c] + ATP[c] -> ADP[c] + Orthophosphate[c] + 0.52 H+[c]	0	1000		-14.996	20.422
R00089	purine metabolism	Unassigned	ATP[c] -> Diphosphate[c] + 0.37 H+[c] + "3,5-Cyclic AMP"[c]	0	1000		-20.043	13.014
R00429	purine metabolism	Unassigned	ATP[c] + GTP[c] <=> AMP[c] + 0.84 H+[c] + Guanosine 3-diphosphate 5-triphosphate[c]	-1000	1000		NaN	NaN
R00434	purine metabolism	Unassigned	GTP[c] <- Diphosphate[c] + 0.37 H+[c] + "3,5-Cyclic GMP|3,5-Cyclic GMP|Guanosine 3,5-cyclic monophosphate|Guanosine 3,5-cyclic phosphate|Cyclic GMP|cGMP"[c]	-1000	0		-19.325	12.296
R01054	purine metabolism	Unassigned	H2O[c] + ADP-ribose[c] <=> AMP[c] + 1.69 H+[c] + D-Ribose 5-phosphate[c]	-1000	1000		-28.430	9.804
R01230	purine metabolism	Unassigned	ATP[c] + NH3[c] + Xanthosine 5-phosphate[c] <=> Diphosphate[c] + AMP[c] + 2.19 H+[c] + GMP[c]	-1000	1000		-15.026	35.366
R02147	purine metabolism	Unassigned	Orthophosphate[c] + Guanosine[c] <=> 0.33 H+[c] + Guanine[c] + alpha-D-Ribose 1-phosphate[c]	-1000	1000		-24.911	9.019
R02297	purine metabolism	Unassigned	Orthophosphate[c] + Xanthosine[c] <=> 0.42 H+[c] + Xanthine[c] + alpha-D-Ribose 1-phosphate[c]	-1000	1000		-25.172	9.280
R03409	purine metabolism	Unassigned	H2O[c] + Guanosine 3-diphosphate 5-triphosphate[c] -> Orthophosphate[c] + 0.53 H+[c] + "Guanosine 3,5-bis(diphosphate)"[c]	0	1000		NaN	NaN
R03537	purine metabolism	CAC0353	H2O[c] + "2,3-Cyclic AMP"[c] <=> 0.92 H+[c] + 3-AMP[c]	-1000	1000		NaN	NaN
R04378	purine metabolism	CAC2275	Diphosphate[c] + 0.38 H+[c] + 1-(5-Phosphoribosyl)-5-amino-4-imidazolecarboxamide[c] <=> 5-Phospho-alpha-D-ribose 1-diphosphate[c] + 5-Amino-4-imidazolecarboxyamide[c]	-1000	1000		-11.544	17.564
R05135	purine metabolism	CAC0353	H2O[c] + "2,3-Cyclic GMP"[c] <=> 0.93 H+[c] + Guanosine 3-phosphate[c]	-1000	1000		NaN	NaN
R07405	purine metabolism	CAC1390	5-Carboxyamino-1-(5-phospho-D-ribosyl)imidazole[c] <=> 0.09 H+[c] + 1-(5-Phospho-D-ribosyl)-5-amino-4-imidazolecarboxylate[c]	-1000	1000		-2.115	17.175
R01867	pyrimidine metabolism	CAC2650	Oxygen[c] + 0.02 H+[c] + (S)-Dihydroorotate[c] <=> H2O2[c] + Orotate[c]	-1000	1000		NaN	NaN
R02018	pyrimidine metabolism	Unassigned	H2O[c] + Thioredoxin disulfide[c] + dUDP[c] <=> UDP[c] + Thioredoxin[c]	-1000	1000		NaN	NaN
R02024	pyrimidine metabolism	Unassigned	H2O[c] + Thioredoxin disulfide[c] + dCDP[c] <- CDP[c] + Thioredoxin[c]	-1000	0		NaN	NaN
R02484	pyrimidine metabolism	Unassigned	Orthophosphate[c] + Deoxyuridine[c] <=> 0.26 H+[c] + Uracil[c] + 2-Deoxy-D-ribose 1-phosphate[c]	-1000	1000		-22.330	6.438
R03538	pyrimidine metabolism	CAC0353	H2O[c] + "2,3-Cyclic UMP"[c] <=> 0.92 H+[c] + 3-UMP[c]	-1000	1000		NaN	NaN
R03929	pyrimidine metabolism	CAC0353	H2O[c] + "2,3-Cyclic CMP"[c] <=> 0.92 H+[c] + 3-CMP[c]	-1000	1000		NaN	NaN
R06370	limonene and pinene degradation	CAC3392	Acceptor[c] + 2-Hydroxy-4-isopropenylcyclohexane-1-carboxyl-CoA[c] <=> Reduced acceptor[c] + 4-Isopropenyl-2-oxy-cyclohexanecarboxyl-CoA|4-Isopropenyl-2-oxy-cyclohexanecarboxyl-CoA|4-Isopropenyl-2-ketocyclohexane-1-carboxyl-CoA[c]	-1000	1000		NaN	NaN
R06402	limonene and pinene degradation	CAC3392	Oxygen[c] + Acceptor[c] + Myrtenol[c] <=> 2 H2O[c] + Reduced acceptor[c] + Myrtenal[c]	-1000	1000		NaN	NaN
R06405	limonene and pinene degradation	CAC3392	Pinocarveol[c] <=> Pinocarvone[c]	-1000	1000		NaN	NaN
R06413	limonene and pinene degradation	CAC3392	NAD+[c] + "3-Hydroxy-2,6-dimethyl-5-methylene-heptanoyl-CoA"[c] <=> NADH[c] + H+[c] + "2,6-Dimethyl-5-methylene-3-oxo-heptanoyl-CoA"[c]	-1000	1000		NaN	NaN
R02328	polyketide sugar unit biosynthesis|streptomycin biosynthesis	CAC2333	0.49 H+[c] + D-Glucose 1-phosphate[c] + dTTP[c] <=> Diphosphate[c] + dTDP-glucose[c]	-1000	1000		-15.518	17.658
R02777	polyketide sugar unit biosynthesis|streptomycin biosynthesis	Unassigned	NADP+[c] + dTDP-6-deoxy-L-mannose[c] <=> NADPH[c] + H+[c] + dTDP-4-dehydro-6-deoxy-L-mannose[c]	-1000	1000		-28.181	23.652
R06513	polyketide sugar unit biosynthesis|streptomycin biosynthesis	CAC2332	dTDP-glucose[c] -> H2O[c] + "4,6-Dideoxy-4-oxo-dTDP-D-glucose"[c]	0	1000	df	-33.494	-3.429
R06514	polyketide sugar unit biosynthesis|streptomycin biosynthesis	CAC2331	"4,6-Dideoxy-4-oxo-dTDP-D-glucose"[c] <=> dTDP-4-dehydro-6-deoxy-L-mannose[c]	-1000	1000		-12.596	12.596
R00299	streptomycin biosynthesis	Unassigned	ATP[c] + D-Glucose[c] <0> ADP[c] + 0.84 H+[c] + D-Glucose 6-phosphate[c]	0	0		-23.115	14.115
R05555	terpenoid backbone biosynthesis	Unassigned	Isopentenyl diphosphate[c] + "trans,trans-Farnesyl diphosphate"[c] <=> Diphosphate[c] + 0.37 H+[c] + "trans,trans,cis-Geranylgeranyl diphosphate"[c]	-1000	1000		NaN	NaN
R06447	terpenoid backbone biosynthesis	Unassigned	7 Isopentenyl diphosphate[c] + "trans,trans,cis-Geranylgeranyl diphosphate"[c] <=> 7 Diphosphate[c] + 2.6 H+[c] + "di-trans,poly-cis-Undecaprenyl diphosphate"[c]	-1000	1000		NaN	NaN
R07219	terpenoid backbone biosynthesis	CAC1847	H2O[c] + NADP+[c] + Dimethylallyl diphosphate[c] <- NADPH[c] + H+[c] + 1-Hydroxy-2-methyl-2-butenyl 4-diphosphate[c]	-1000	0		NaN	NaN
R08209	terpenoid backbone biosynthesis	CAC1847	H2O[c] + NAD+[c] + Isopentenyl diphosphate[c] <- NADH[c] + H+[c] + 1-Hydroxy-2-methyl-2-butenyl 4-diphosphate[c]	-1000	0		NaN	NaN
R08210	terpenoid backbone biosynthesis	CAC1847	H2O[c] + NAD+[c] + Dimethylallyl diphosphate[c] <- NADH[c] + H+[c] + 1-Hydroxy-2-methyl-2-butenyl 4-diphosphate[c]	-1000	0		NaN	NaN
R08689	terpenoid backbone biosynthesis	CAC1797	1.72 H+[c] + Reduced ferredoxin[c] + "2-C-Methyl-D-erythritol 2,4-cyclodiphosphate"[c] -> H2O[c] + Oxidized ferredoxin[c] + 1-Hydroxy-2-methyl-2-butenyl 4-diphosphate[c]	0	1000		NaN	NaN
ABC	Transport reactions	CAC0427 / CAC0428 / CAC0429	H2O[c] + ATP[c] + sn-Glycerol 3-phosphate[e] -> ADP[c] + Orthophosphate[c] + 0.52 H+[c] + sn-Glycerol 3-phosphate[c]	0	1000		NaN	NaN
ABC	Transport reactions	CAC0111 / CAC0112 / CAC0377 / CAC0378 / CAC0380 / CAC3618 / CAC3619 / CAC3620	H2O[c] + ATP[c] + L-Glutamine[e] -> ADP[c] + Orthophosphate[c] + L-Glutamine[c] + 0.52 H+[c]	0	1000		NaN	NaN
ABC	Transport reactions	CAC1473 / CAC1474 / CAC1475 / CAC1476	H2O[c] + ATP[c] + Glycine[e] -> ADP[c] + Orthophosphate[c] + Glycine[c] + 0.52 H+[c]	0	1000		NaN	NaN
ABC	Transport reactions	CAC1473 / CAC1474 / CAC1475 / CAC1476	H2O[c] + ATP[c] + L-Proline[e] -> ADP[c] + Orthophosphate[c] + 0.52 H+[c] + L-Proline[c]	0	1000		NaN	NaN
ABC	Transport reactions	CAC0984 / CAC0985 / CAC0986	H2O[c] + ATP[c] + L-Methionine[e] -> ADP[c] + Orthophosphate[c] + L-Methionine[c] + 0.52 H+[c]	0	1000		NaN	NaN
ABC	Transport reactions	CAC0837 / CAC0838 / CAC0839 / CAC0840	H2O[c] + ATP[c] + Putrescine[c] -> ADP[c] + Orthophosphate[c] + 0.52 H+[c] + Putrescine[e]	0	1000		NaN	NaN
ABC	Transport reactions	CAC1453	H2O[c] + ATP[c] + D-Ribose[e] -> ADP[c] + Orthophosphate[c] + 0.52 H+[c] + D-Ribose[c]	0	1000		NaN	NaN
ABC	Transport reactions	CAC0837 / CAC0838 / CAC0839 / CAC0840	H2O[c] + ATP[c] + Spermidine[c] -> ADP[c] + Orthophosphate[c] + 0.52 H+[c] + Spermidine[e]	0	1000		NaN	NaN
Amino Acid-Polyamir	Transport reactions	CAC2719	H+[e] + Ethanolamine[e] -> H+[c] + Ethanolamine[c]	0	1000		NaN	NaN
Amino Acid-Polyamir	Transport reactions	CAC3164 / CAC3347	L-Lysine[e] + H+[e] -> L-Lysine[c] + H+[c]	0	1000		NaN	NaN
Ammonium Transpo	Transport reactions	CAC0682	2 NH3[e] + H+[c] <0> 2 NH3[c] + H+[e]	0	0		NaN	NaN
Auxin Efflux Carrier (	Transport reactions	CAC0366 / CAC2949	H+[e] + (S)-Malate[e] -> H+[c] + (S)-Malate[c]	0	1000		NaN	NaN
Branched Chain Amir	Transport reactions	CAC1610	H+[e] + L-Isoleucine[e] -> H+[c] + L-Isoleucine[c]	0	1000		NaN	NaN
Branched Chain Amir	Transport reactions	CAC1610	H+[e] + L-Leucine[e] -> H+[c] + L-Leucine[c]	0	1000		NaN	NaN
Branched Chain Amir	Transport reactions	CAC1610	H+[e] + L-Valine[e] -> H+[c] + L-Valine[c]	0	1000		NaN	NaN
Dicarboxylate/Amino	Transport reactions	CAC1783	L-Glutamate[e] + H+[e] -> L-Glutamate[c] + H+[c]	0	1000		NaN	NaN

Divalent Anion:Na+ S	Transport reactions	CAC1590	2-Oxoglutarate[c] + Sodium[c] -> 2-Oxoglutarate[e] + Sodium[e]	0	0.1		NaN	NaN
Divalent Anion:Na+ S	Transport reactions	CAC1590	(S)-Malate[c] + Sodium[c] -> (S)-Malate[e] + Sodium[e]	0	0.1		NaN	NaN
Formate-Nitrite Tran	Transport reactions	CAC1512	Formate[e] + H+[c] -> Formate[c] + H+[e]	0	1000		NaN	NaN
Formate-Nitrite Tran	Transport reactions	CAC1512	H+[e] + Nitrate[c] -> H+[c] + Nitrate[e]	0	1000		NaN	NaN
Gluconate:H+ Sympo	Transport reactions	CAC2835 / CAC3605	H+[e] + D-Gluconic acid[e] -> H+[c] + D-Gluconic acid[c]	0	1000		NaN	NaN
Inorganic Phosphate	Transport reactions	CAC3093	Orthophosphate[e] + Sodium[e] -> Orthophosphate[c] + Sodium[c]	0	0.1		NaN	NaN
L-Lysine Exporter (Ly	Transport reactions	CAC2593	L-Lysine[c] + H+[e] -> L-Lysine[e] + H+[c]	0	1000		NaN	NaN
Major Intrinsic Protei	Transport reactions	CAC0770 / CAC1319	Glycerol[e] -> Glycerol[c]	0	1000		NaN	NaN
MerTP Mercuric Ion	Transport reactions	CAC3654	Spermine[e] -> Spermine[c]	0	1000		NaN	NaN
Nucleobase:Cation Sy	Transport reactions	CAC2112 / CAC2772 / CAC2820	H+[e] + Uracil[e] -> H+[c] + Uracil[c]	0	1000		NaN	NaN
Nucleobase:Cation Sy	Transport reactions	CAC0872 / CAC2772 / CAC2820	H+[e] + Xanthine[e] -> H+[c] + Xanthine[c]	0	1000		NaN	NaN
PTS	Transport reactions	CAC0383 / CAC0384 / CAC0386	H2O[c] + ATP[c] + Cellobiose[e] -> ADP[c] + Orthophosphate[c] + 0.52 H+[c] + Cellobiose[c]	0	1000		NaN	NaN
PTS	Transport reactions	CAC1457 / CAC1458 / CAC1459 / CAC1460	Phosphoenolpyruvate[c] + 0.06 H+[c] + D-Fructose[e] -> Pyruvate[c] + D-Fructose 6-phosphate[c]	0	1000		NaN	NaN
PTS	Transport reactions	CAC0233 / CAC0234 / CAC2956 / CAC2957 / CAC2958	Phosphoenolpyruvate[c] + 0.04 H+[c] + D-Fructose[e] -> Pyruvate[c] + D-Fructose 1-phosphate[c]	0	1000		NaN	NaN
PTS	Transport reactions	CAC2956 / CAC2957 / CAC2958	Phosphoenolpyruvate[c] + 0.15 H+[c] + Galactitol[e] -> Pyruvate[c] + Galactitol 1-phosphate[c]	0	1000		NaN	NaN
PTS	Transport reactions	CAC2964 / CAC2965	Phosphoenolpyruvate[c] + 0.06 H+[c] + Lactose[e] -> Pyruvate[c] + Lactose 6-phosphate[c]	0	1000		NaN	NaN
PTS	Transport reactions	CAC0154 / CAC0156	Phosphoenolpyruvate[c] + 0.15 H+[c] + Mannitol[e] -> Pyruvate[c] + D-Mannitol 1-phosphate[c]	0	1000		NaN	NaN
PTS	Transport reactions	CAC1457 / CAC1458 / CAC1459 / CAC1460 /CAP0066 / CAP0067 / CAP0068	Phosphoenolpyruvate[c] + 0.06 H+[c] + D-Mannose[e] -> Pyruvate[c] + D-Mannose 6-phosphate[c]	0	1000		NaN	NaN
PTS	Transport reactions	CAC1353, CAC1354	Phosphoenolpyruvate[c] + 0.06 H+[c] + N-Acetyl-D-Glucosamine[e] -> Pyruvate[c] + N-Acetyl-D-glucosamine 6-phosphate[c]	0	1000		NaN	NaN
PTS	Transport reactions	CAC0423	Phosphoenolpyruvate[c] + 0.06 H+[c] + Sucrose[e] -> Pyruvate[c] + Sucrose 6-phosphate[c]	0	1000		NaN	NaN
R07141_T_S0	Transport reactions	Unassigned	H+[e] + (S)-Lactate[e] <=> H+[c] + (S)-Lactate[c]	-1000	1000		NaN	NaN
R07147_T	Transport reactions	Unassigned	CO2[c] -> CO2[e]	0	1000		NaN	NaN
R07159_T_S0	Transport reactions	Unassigned	Ethanol[e] <- Ethanol[c]	-1000	0		NaN	NaN
R07164_T	Transport reactions	Unassigned	H2O[e] <=> H2O[c]	-1000	1000		NaN	NaN
R07166_T	Transport reactions	Unassigned	H+[e] + Potassium[e] <=> H+[c] + Potassium[c]	-0.1	0.1		NaN	NaN
R07182_T	Transport reactions	CAC0444	H+[c] + Sodium[e] <0> H+[e] + Sodium[c]	0	0		NaN	NaN
R07183_T_S0	Transport reactions	Unassigned	NH3[e] + 0.99 H+[c] <=> NH3[c] + 0.99 H+[e]	-1000	1000		NaN	NaN
R07187_T	Transport reactions	CAC0618|CAC0619|CAC0620|CAC1399|CAC1400|CAC1401	H2O[c] + ATP[c] + Nitrate[e] -> ADP[c] + Orthophosphate[c] + 0.52 H+[c] + Nitrate[c]	0	1000		NaN	NaN
R07189_T	Transport reactions	CAC1706	H2O[c] + ATP[c] + Orthophosphate[e] -> ADP[c] + 2 Orthophosphate[c] + 0.52 H+[c]	0	1000		NaN	NaN
R07190_T	Transport reactions	CAC3093	Orthophosphate[e] + H+[e] -> Orthophosphate[c] + H+[c]	0	1000		NaN	NaN
R07194_T	Transport reactions	Unassigned	D-Glucose[e] + Phosphoenolpyruvate[c] + 0.06 H+[c] -> Pyruvate[c] + D-Glucose 6-phosphate[c]	0	1000		NaN	NaN
R07204_T	Transport reactions	Unassigned	H2O[c] + ATP[c] + Sulfate[e] -> ADP[c] + Orthophosphate[c] + Sulfate[c] + 0.52 H+[c]	0	1000		NaN	NaN
R07208_T_S0	Transport reactions	Unassigned	1-Butanol[e] <- 1-Butanol[c]	-1000	0		NaN	NaN
R07209_T_S0	Transport reactions	Unassigned	Acetone[e] <- Acetone[c]	-1000	0		NaN	NaN
R07232_T	Transport reactions	Unassigned	Hydrogen[e] <=> Hydrogen[c]	-1000	1000		NaN	NaN
R07241_T	Transport reactions	Unassigned	Nitrogen[e] <=> Nitrogen[c]	-1000	1000		NaN	NaN
R07272_T_S0	Transport reactions	Unassigned	0.99 H+[e] + Butanoic acid[e] <=> 0.99 H+[c] + Butanoic acid[c]	-1000	1000		NaN	NaN
R07273_T_S0	Transport reactions	Unassigned	Acetate[e] + H+[e] <=> Acetate[c] + H+[c]	-1000	1000		NaN	NaN
R07277_T	Transport reactions	Unassigned	H+[e] + Biotin[e] -> H+[c] + Biotin[c]	0	1000		NaN	NaN
R07278_T	Transport reactions	Unassigned	H+[e] + 4-Aminobenzoate[e] -> H+[c] + 4-Aminobenzoate[c]	0	1000		NaN	NaN
R07300_T	Transport reactions	Unassigned	Reduced ferredoxin[e] -> Reduced ferredoxin[c]	0	1000		NaN	NaN
R07302_T	Transport reactions	Unassigned	Thioredoxin[e] -> Thioredoxin[c]	0	1000		NaN	NaN
R07305_T	Transport reactions	Unassigned	D-Glucose[e] + H+[e] -> D-Glucose[c] + H+[c]	0	0.1		NaN	NaN
R07306_T	Transport reactions	Unassigned	H2O[c] + ATP[c] + D-Glucose[e] -> ADP[c] + Orthophosphate[c] + D-Glucose[c] + 0.52 H+[c]	0	1000		NaN	NaN
R07311_T	Transport reactions	CAC3680|CAC2681|CAC3682	H2O[c] + ATP[c] + 2 Potassium[e] + 3 Sodium[c] <0> ADP[c] + Orthophosphate[c] + 0.52 H+[c] + 2 Potassium[c] + 3 Sodium[e]	0	0		NaN	NaN
R07354_T	Transport reactions	CAC0744|CAP0140	3 H+[e] + 2 Sodium[c] <=> 3 H+[c] + 2 Sodium[e]	-0.1	0.1		NaN	NaN
R07355_T	Transport reactions	CAC2864|CAC2865|CAC2866|CAC2867|CAC2868|CAC2869|CAC2870|CAC2871	ADP[c] + Orthophosphate[c] + 3 H+[e] <=> H2O[c] + ATP[c] + 2.48 H+[c]	-1000	1000		NaN	NaN
R07356_T	Transport reactions	CAC3550|CAC3551	ADP[c] + Orthophosphate[c] + 0.52 H+[c] + Sodium[e] <=> H2O[c] + ATP[c] + Sodium[c]	-0.1	0.1		NaN	NaN
R07359_T	Transport reactions	Unassigned	H2O[c] + ATP[c] + Acetoin[c] -> ADP[c] + Orthophosphate[c] + 0.52 H+[c] + Acetoin[e]	0	1000		NaN	NaN
R07368_T	Transport reactions	Unassigned	Acetate[e] + Acetoacetyl-CoA[c] -> Acetyl-CoA[c] + Acetoacetate[c]	0	1000		NaN	NaN
R07369	Transport reactions	CAP0163|CAP0164	Butanoic acid[e] + Acetoacetyl-CoA[c] -> 0.01 H+[c] + Butanoyl-CoA[c] + Acetoacetate[c]	0	1000		NaN	NaN
R07380_T	Transport reactions	Unassigned	Succinate[c] + H+[c] -> Succinate[e] + H+[e]	0	1000		NaN	NaN
Threonine/Serine Ex	Transport reactions	CAC2265	H+[e] + L-Threonine[c] -> H+[c] + L-Threonine[e]	0	1000		NaN	NaN
Voltage-gated Ion Ch	Transport reactions	CAC1317	Potassium[e] <0> Potassium[c]	0	0		NaN	NaN
R01074	Biotin metabolism	Unassigned	ATP[c] + 0.63 H+[c] + Biotin[c] <=> Diphosphate[c] + Biotinyl-5-AMP[c]	-1000	1000		NaN	NaN
R07275	Biotin metabolism	Unassigned	Biotinyl-5-AMP[c] <=> AMP[c] + Holo-[carboxylase][c]	-1000	1000		NaN	NaN
R00428	Folate biosynthesis	CAC3626	H2O[c] + GTP[c] <=> Formamidopyrimidine nucleoside triphosphate[c]	-1000	1000		-19.229	8.772
R00937	Folate biosynthesis	CAC3004	NAD+[c] + Tetrahydrofolate[c] <- NADH[c] + H+[c] + Folate[c]	-1000	0		-12.568	35.448
R00939	Folate biosynthesis	CAC3004	NADP+[c] + Tetrahydrofolate[c] <- NADPH[c] + H+[c] + Dihydrofolate[c]	-1000	0		-30.085	22.136
R00940	Folate biosynthesis	CAC3004	NADP+[c] + Tetrahydrofolate[c] <- NADPH[c] + H+[c] + Folate[c]	-1000	0		-12.545	35.425
R02235	Folate biosynthesis	CAC3004	NAD+[c] + Dihydrofolate[c] <0> NADH[c] + H+[c] + Folate[c]	0	0		-33.750	18.741
R02236	Folate biosynthesis	CAC3004	NADP+[c] + Dihydrofolate[c] -> NADPH[c] + H+[c] + Folate[c]	0	1000		-33.727	18.718
R02237	Folate biosynthesis	CAC2398	ATP[c] + L-Glutamate[c] + 0.47 H+[c] + Dihydropteroate[c] <=> ADP[c] + Orthophosphate[c] + Dihydrofolate[c]	-1000	1000		-30.567	20.339
R03067	Folate biosynthesis	CAC2926	4-Aminobenzoate[c] + "2-Amino-7,8-dihydro-4-hydroxy-6-(diphosphooxymethyl)pteridine"[c] -> Diphosphate[c] + 0.37 H+[c] + Dihydropteroate[c]	0	1000	df	-39.860	-5.460
R03503	Folate biosynthesis	CAC2927	ATP[c] + "2-Amino-4-hydroxy-6-hydroxymethyl-7,8-dihydropteridine"[c] <=> AMP[c] + 0.84 H+[c] + "2-Amino-7,8-dihydro-4-hydroxy-6-(diphosphooxymethyl)pteridine"[c]	-1000	1000		-25.216	16.216
R03504	Folate biosynthesis	CAC2927	"2-Amino-4-hydroxy-6-(D-erythro-1,2,3-trihydroxypropyl)-7,8-"[c] <=> Glycolaldehyde[c] + "2-Amino-4-hydroxy-6-hydroxymethyl-7,8-dihydropteridine"[c]	-1000	1000		-4.259	24.630
R04621	Folate biosynthesis	CAC1003|CAC1729|CAC1736|CAC2137|CAC2674|CAC2687|CAC2828|CAC3396|CAC3715	Orthophosphate[c] + "2-Amino-4-hydroxy-6-(D-erythro-1,2,3-trihydroxypropyl)-7,8-"[c] <=> H2O[c] + 0.23 H+[c] + Dihydroneopterin phosphate[c]	-1000	1000		-23.716	9.290

R04638	Folate biosynthesis	CAC1003|CAC1729|CAC1736|CAC2137|CAC2674|CAC2687|CAC2828|CAC3396|CAC3715	H2O[c] + "2-Amino-4-hydroxy-6-(erythro-1,2,3-trihydroxypropyl)dihydropteridine"[c] <=> Diphosphate[c] + 1.13 H+[c] + Dihydroneopterin phosphate[c]	-1000	1000		NaN	NaN
R04639	Folate biosynthesis	CAC3626	H2O[c] + "2-Amino-4-hydroxy-6-(erythro-1,2,3-trihydroxypropyl)dihydropteridine"[c] <=> "2,5-Diamino-6-(5-triphosphoryl-3,4-trihydroxy-2-oxopentyl)-"[c]	-1000	1000		NaN	NaN
R05046	Folate biosynthesis	CAC3626	H2O[c] + Formamidopyrimidine nucleoside triphosphate[c] <=> Formate[c] + H+[c] + "2,5-Diaminopyrimidine nucleoside triphosphate"[c]	-1000	1000		NaN	NaN
R05048	Folate biosynthesis	CAC3626	"2,5-Diaminopyrimidine nucleoside triphosphate"[c] <=> "2,5-Diamino-6-(5-triphosphoryl-3,4-trihydroxy-2-oxopentyl)-"[c]	-1000	1000		NaN	NaN
R00103	Nicotinate and nicotinamide metabolism	Unassigned	H2O[c] + NAD+[c] <0> AMP[c] + 1.69 H+[c] + Nicotinamide D-ribonucleotide[c]	0	0		-29.709	11.083
R00104	Nicotinate and nicotinamide metabolism	CAC2075	ATP[c] + NAD+[c] -> NADP+[c] + ADP[c] + 0.93 H+[c]	0	1000		-28.511	19.511
R00118	Nicotinate and nicotinamide metabolism	Unassigned	H2O[c] + NADP+[c] + 0.41 H+[c] <0> NAD+[c] + Orthophosphate[c]	0	0		-14.174	28.600
R00137	Nicotinate and nicotinamide metabolism	CAC1262	ATP[c] + 0.48 H+[c] + Nicotinamide D-ribonucleotide[c] -> NAD+[c] + Diphosphate[c]	0	1000		-19.336	21.476
R02294	Nicotinate and nicotinamide metabolism	CAC2064	1.33 H+[c] + Nicotinamide[c] + alpha-D-Ribose 1-phosphate[c] <=> Orthophosphate[c] + N-Ribosylnicotinamide[c]	-1000	1000		NaN	NaN
R02322	Nicotinate and nicotinamide metabolism	Unassigned	H2O[c] + Nicotinamide D-ribonucleotide[c] <=> NH3[c] + 0.01 H+[c] + Nicotinate D-ribonucleotide[c]	-1000	1000		-19.498	10.052
R02323	Nicotinate and nicotinamide metabolism	Unassigned	Orthophosphate[c] + N-Ribosylnicotinamide[c] <=> H2O[c] + 0.32 H+[c] + Nicotinamide D-ribonucleotide[c]	-1000	1000		NaN	NaN
R03004	Nicotinate and nicotinamide metabolism	Unassigned	H2O[c] + Deamino-NAD+[c] <0> AMP[c] + 1.69 H+[c] + Nicotinate D-ribonucleotide[c]	0	0		-29.581	10.955
R03005	Nicotinate and nicotinamide metabolism	CAC1262	ATP[c] + 0.48 H+[c] + Nicotinate D-ribonucleotide[c] <=> Diphosphate[c] + Deamino-NAD+[c]	-1000	1000		-19.209	21.349
R03348	Nicotinate and nicotinamide metabolism	CAC1023	CO2[c] + Diphosphate[c] + Nicotinate D-ribonucleotide[c] <- 1.62 H+[c] + 5-Phospho-alpha-D-ribose 1-diphosphate[c] + "Pyridine-2,3-dicarboxylate"[c]	-1000	0		6.561	40.528
R04292	Nicotinate and nicotinamide metabolism	Unassigned	2 H2O[c] + Orthophosphate[c] + "Pyridine-2,3-dicarboxylate"[c] <=> 0.33 H+[c] + Glycerone phosphate[c] + Iminoaspartate[c]	-1000	1000		NaN	NaN
R07293	Nicotinate and nicotinamide metabolism	Unassigned	L-Aspartate[c] + 0.03 H+[c] + Fumarate[c] -> Succinate[c] + Iminoaspartate[c]	0	1000		NaN	NaN
R00936	One carbon pool by folate	CAC3004	NAD+[c] + Tetrahydrofolate[c] <0> NADH[c] + H+[c] + Dihydrofolate[c]	0	0		-30.108	22.159
R01217	One carbon pool by folate	Unassigned	2 H+[c] + Reduced ferredoxin[c] + "5,10-Methylenetetrahydrofolate"[c] <=> Oxidized ferredoxin[c] + 5-Methyltetrahydrofolate[c]	-1000	1000		NaN	NaN
R01655	One carbon pool by folate	CAC2083|CAC3201	H2O[c] + "5,10-Methenyltetrahydrofolate"[c] <=> H+[c] + 10-Formyltetrahydrofolate[c]	-1000	1000		-4.176	31.550
R02101	One carbon pool by folate	CAC3003	"5,10-Methylenetetrahydrofolate"[c] + dUMP[c] <=> dTMP[c] + Dihydrofolate[c]	-1000	1000		-34.867	3.107
R02300	One carbon pool by folate	Unassigned	H+[c] + 5-Formyltetrahydrofolate[c] <=> H2O[c] + "5,10-Methenyltetrahydrofolate"[c]	-1000	1000		-30.902	-0.101
R02301	One carbon pool by folate	CAC1090	ATP[c] + 0.48 H+[c] + 5-Formyltetrahydrofolate[c] -> ADP[c] + Orthophosphate[c] + "5,10-Methenyltetrahydrofolate"[c]	0	1000		-36.232	10.655
R04325	One carbon pool by folate	CAC1394	10-Formyltetrahydrofolate[c] + 5-Phosphoribosylglycinamide[c] -> Tetrahydrofolate[c] + 5-Phosphoribosyl-N-formylglycinamide[c]	0	1000		NaN	NaN
R04326	One carbon pool by folate	CAC1394	H2O[c] + "5,10-Methenyltetrahydrofolate"[c] + 5-Phosphoribosylglycinamide[c] -> H+[c] + Tetrahydrofolate[c] + 5-Phosphoribosyl-N-formylglycinamide[c]	0	1000		NaN	NaN
R04560	One carbon pool by folate	CAC1395	10-Formyltetrahydrofolate[c] + 1-(5-Phosphoribosyl)-5-amino-4-imidazolecarboxamide[c] <=> 0.16 H+[c] + Tetrahydrofolate[c] + 1-(5-Phosphoribosyl)-5-formamido-4-imidazolecarboxamide[c]	-1000	1000		-39.058	-0.422
R07243	One carbon pool by folate	Unassigned	5-Formyltetrahydrofolate[c] <=> 10-Formyltetrahydrofolate[c]	-1000	1000		-0.803	25.363
R00006	Pantothenate and CoA biosynthesis	CAC3169|CAC3176|CAC3652	CO2[c] + 2-Acetolactate[c] <- 2 Pyruvate[c] + H+[c]	-1000	0		9.266	30.854
R00130	Pantothenate and CoA biosynthesis	CAC1099	ATP[c] + Dephospho-CoA[c] -> ADP[c] + CoA[c] + 0.91 H+[c]	0	1000		-26.514	17.514
R01209	Pantothenate and CoA biosynthesis	CAC3170|CAC3604	"2,3-Dihydroxy-3-methylbutanoate"[c] -> H2O[c] + 3-Methyl-2-oxobutanoic acid[c]	0	1000	df	-19.652	-2.970
R01214	Pantothenate and CoA biosynthesis	CAC1479	2-Oxoglutarate[c] + L-Valine[c] <=> L-Glutamate[c] + 0.04 H+[c] + 3-Methyl-2-oxobutanoic acid[c]	-1000	1000		-10.753	10.753
R01226	Pantothenate and CoA biosynthesis	CAC2914	H2O[c] + 3-Methyl-2-oxobutanoic acid[c] + "5,10-Methylenetetrahydrofolate"[c] <=> Tetrahydrofolate[c] + 2-Dehydropantoate[c]	-1000	1000		-16.946	23.129
R01623	Pantothenate and CoA biosynthesis	CAC0604|CAC3421	H2O[c] + Acyl-carrier protein[c] <=> Pantetheine 4-phosphate[c] + Apo-[acyl-carrier-protein][c]	-1000	1000		NaN	NaN
R01625	Pantothenate and CoA biosynthesis	CAC0489	CoA[c] + Apo-[acyl-carrier-protein][c] <=> "Adenosine 3,5-bisphosphate"[c] + Acyl-carrier protein[c]	-1000	1000		NaN	NaN
R02472	Pantothenate and CoA biosynthesis	CAC2937	NADP+[c] + (R)-Pantoate[c] <- NADPH[c] + H+[c] + 2-Dehydropantoate[c]	-1000	0		-5.496	36.996
R03018	Pantothenate and CoA biosynthesis	Unassigned	ATP[c] + Pantothenate[c] -> ADP[c] + 0.6 H+[c] + D-4-Phosphopantothenate[c]	0	1000		NaN	NaN
R03035	Pantothenate and CoA biosynthesis	CAC1738	ATP[c] + 0.23 H+[c] + Pantetheine 4-phosphate[c] <=> Diphosphate[c] + Dephospho-CoA[c]	-1000	1000		-17.716	19.856
R03051	Pantothenate and CoA biosynthesis	CAC0091	NADPH[c] + H+[c] + 2-Acetolactate[c] <=> NADP+[c] + "2,3-Dihydroxy-3-methylbutanoate"[c]	-1000	1000		-22.682	24.291
R03269	Pantothenate and CoA biosynthesis	CAC1720	H+[c] + (R)-4-Phosphopantothenoyl-L-cysteine[c] -> CO2[c] + Pantetheine 4-phosphate[c]	0	1000	df	-28.497	-5.872
R04233	Pantothenate and CoA biosynthesis	CAC1720	CTP[c] + 0.46 H+[c] + L-Cysteine[c] + D-4-Phosphopantothenate[c] -> Orthophosphate[c] + CDP[c] + (R)-4-Phosphopantothenoyl-L-cysteine[c]	0	1000		NaN	NaN
R00066	Riboflavin metabolism	CAC0591|CAC0593	0.52 H+[c] + 2 "6,7-Dimethyl-8-(1-D-ribityl)lumazine"[c] -> Riboflavin[c] + 5-Amino-6-(1-D-ribitylamino)uracil[c]	0	1000	df	-58.382	-15.118
R00161	Riboflavin metabolism	CAC1806	ATP[c] + FMN[c] + 0.39 H+[c] -> Diphosphate[c] + FAD[c]	0	1000		-21.614	23.754
R00425	Riboflavin metabolism	CAC0592	3 H2O[c] + GTP[c] <=> Diphosphate[c] + Formate[c] + 2.22 H+[c] + "2,5-Diamino-6-(5-phosphoribosylamino)-4-pyrimidineone"[c]	-1000	1000		-27.866	18.977
R00549	Riboflavin metabolism	CAC1806	ATP[c] + Riboflavin[c] -> ADP[c] + FMN[c] + 0.75 H+[c]	0	1000		-25.374	16.374
R03458	Riboflavin metabolism	CAC0590	NADP+[c] + 5-Amino-6-(5-phosphoribitylamino)uracil[c] <=> NADPH[c] + 0.85 H+[c] + 5-Amino-6-(5-phosphoribosylamino)uracil[c]	-1000	1000		NaN	NaN
R03459	Riboflavin metabolism	CAC0590	H2O[c] + 0.98 H+[c] + "2,5-Diamino-6-(5-phosphoribosylamino)-4-pyrimidineone"[c] -> NH3[c] + 5-Amino-6-(5-phosphoribosylamino)uracil[c]	0	1000	df	-33.569	-3.257
R04457	Riboflavin metabolism	Unassigned	Orthophosphate[c] + "6,7-Dimethyl-8-(1-D-ribityl)lumazine"[c] <=> 1.8 H+[c] + D-Ribose 5-phosphate[c] + 5-Amino-6-(5-phosphoribitylamino)uracil[c]	-1000	1000		NaN	NaN
R07252	Riboflavin metabolism	Unassigned	ATP[c] + 5-Amino-6-(1-D-ribitylamino)uracil[c] -> H2O[c] + ADP[c] + 0.85 H+[c] + 5-Amino-6-(5-phosphoribosylamino)uracil[c]	0	1000	df	-79.933	-36.770
R00617	Thiamine metabolism	Unassigned	ATP[c] + 0.39 H+[c] + Thiamin monophosphate[c] <=> ADP[c] + Thiamin diphosphate[c]	-1000	1000		-20.252	20.252
R00619	Thiamine metabolism	Unassigned	ATP[c] + Thiamine[c] <=> AMP[c] + Thiamin diphosphate[c] + 0.87 H+[c]	-1000	1000		-24.748	15.748

R03223	Thiamine metabolism	CAC0495|CAC2920	0.62 H+[c] + 4-Methyl-5-(2-phosphoethyl)-thiazole[c] + 2-Methyl-4-amino-5-hydroxymethylpyrimidine diphosphate[c] <=> Diphosphate[c] + Thiamin monophosphate[c]	-1000	1000		-25.325	6.125
R03471	Thiamine metabolism	CAC3095	ATP[c] + 4-Amino-5-hydroxymethyl-2-methylpyrimidine[c] <=> ADP[c] + 0.7 H+[c] + 4-Amino-2-methyl-5-phosphomethylpyrimidine[c]	-1000	1000		NaN	NaN
R03472	Thiamine metabolism	Unassigned	4-Amino-5-hydroxymethyl-2-methylpyrimidine[c] -> 1.98 H+[c] + Aminoimidazole ribotide[c]	0	1000	df	-315.455	-296.745
R04509	Thiamine metabolism	CAC3095	ATP[c] + 0.31 H+[c] + 4-Amino-2-methyl-5-phosphomethylpyrimidine[c] <=> ADP[c] + 2-Methyl-4-amino-5-hydroxymethylpyrimidine diphosphate[c]	-1000	1000		NaN	NaN
R07250	Thiamine metabolism	Unassigned	Pyruvate[c] + 1.03 H+[c] + D-Glyceraldehyde 3-phosphate[c] -> CO2[c] + 1-Deoxy-D-xylulose 5-phosphate[c]	0	1000		NaN	NaN
R07251	Thiamine metabolism	Unassigned	Glycine[c] + 1.09 H+[c] + L-Cysteine[c] + 1-Deoxy-D-xylulose 5-phosphate[c] <=> 3 H2O[c] + CO2[c] + L-Alanine[c] + 4-Methyl-5-(2-phosphoethyl)-thiazole[c]	-1000	1000		NaN	NaN
R01717	Ubiquinone biosynthesis	Unassigned	Chorismate[c] <=> Isochorismate[c]	-1000	1000		-8.479	8.479
R04030	Ubiquinone biosynthesis	Unassigned	ATP[c] + CoA[c] + 2-Succinylbenzoate[c] <=> Diphosphate[c] + AMP[c] + 0.21 H+[c] + 2-Succinylbenzoyl-CoA[c]	-1000	1000		-39.005	14.973
R04031	Ubiquinone biosynthesis	CAC3571	H2O[c] + 2-Succinylbenzoate[c] <- "(1R,6R)-6-Hydroxy-2-succinylcyclohexa-2,4-diene-1-carboxylate"[c]	-1000	0	dr	19.552	39.691
R04150	Ubiquinone biosynthesis	Unassigned	2-Succinylbenzoyl-CoA[c] -> CoA[c] + 0.01 H+[c] + "1,4-Dihydroxy-2-naphthoate"[c]	0	1000	df	-36.668	-1.007
R04993	Ubiquinone biosynthesis	CAC0523|CAC0700|CAC1284|CAC1435|CAC2132|CAC2784|CAC2885|CAC2986|CAC3154	S-Adenosyl-L-methionine[c] + 2-Demethylmenaquinone[c] <=> S-Adenosyl-L-homocysteine[c] + Menaquinone[c]	-1000	1000		-30.371	10.591
R05617	Ubiquinone biosynthesis	Unassigned	0.63 H+[c] + "1,4-Dihydroxy-2-naphthoate"[c] + all-trans-Octaprenyl diphosphate[c] -> CO2[c] + Diphosphate[c] + 2-Demethylmenaquinone[c]	0	1000	df	-196.556	-153.595
R06860	Ubiquinone biosynthesis	Unassigned	2-Oxoglutarate[c] + H+[c] + Isochorismate[c] -> CO2[c] + Pyruvate[c] + "(1R,6R)-6-Hydroxy-2-succinylcyclohexa-2,4-diene-1-carboxylate"[c]	0	1000	df	-58.800	-28.389
R01078	biotin metabolism	Unassigned	2 S-Adenosyl-L-methionine[c] + 2 H+[c] + Sulfur[c] + Dethiobiotin[c] + 2 e-[c] <=> 2 L-Methionine[c] + Biotin[c] + 2 5-Deoxyadenosine[c]	-1000	1000		NaN	NaN
R03182	biotin metabolism	CAC1361	ATP[c] + CO2[c] + "7,8-Diaminononanoate"[c] <=> ADP[c] + Orthophosphate[c] + 3.04 H+[c] + Dethiobiotin[c]	-1000	1000		-35.454	10.226
R03231	biotin metabolism	CAC1362	S-Adenosyl-L-methionine[c] + 1.44 H+[c] + 8-Amino-7-oxononanoate[c] <=> "7,8-Diaminononanoate"[c] + S-Adenosyl-4-methylthio-2-oxobutanoate[c]	-1000	1000		NaN	NaN
R00942	folate biosynthesis	CAC2398	ATP[c] + L-Glutamate[c] + 0.47 H+[c] + Tetrahydrofolate[c] <=> ADP[c] + Orthophosphate[c] + Tetrahydrofolyl-[Glu](2)[c]	-1000	1000		NaN	NaN
R03066	folate biosynthesis	CAC2926	4-Aminobenzoate[c] + "2-Amino-4-hydroxy-6-hydroxymethyl-7,8-dihydropteridine"[c] -> H2O[c] + Dihydropteroate[c]	0	1000	df	-36.119	-1.715
R04286	folate biosynthesis	Unassigned	"2-Amino-4-hydroxy-6-(erythro-1,2,3-trihydroxypropyl)dihydropteridine"[c] <=> 0.28 H+[c] + Triphosphate[c] + "6-Pyruvoyltetrahydropterin|6-Pyruvoyltetrahydropterin|6-(1,2-Dioxopropyl)-5,6,7,8-tetrahydropterin|6-Pyruvoyl-5,6,7,8-tetrahydropterin"[c]	-1000	1000		NaN	NaN
R00481	nicotinate and nicotinamide metabolism	CAC1024	Oxygen[c] + L-Aspartate[c] -> H2O2[c] + 0.01 H+[c] + Iminoaspartate[c]	0	1000		NaN	NaN
R01724	nicotinate and nicotinamide metabolism	Unassigned	Diphosphate[c] + Nicotinate D-ribonucleotide[c] <=> 0.63 H+[c] + 5-Phospho-alpha-D-ribose 1-diphosphate[c] + Nicotinate[c]	-1000	1000		-4.987	24.187
R02295	nicotinate and nicotinamide metabolism	Unassigned	Orthophosphate[c] + Nicotinate D-ribonucleoside[c] <=> 1.33 H+[c] + Nicotinate[c] + alpha-D-Ribose 1-phosphate[c]	-1000	1000		NaN	NaN
R02971	pantothenate and CoA biosynthesis	Unassigned	ATP[c] + Pantetheine[c] <=> ADP[c] + 0.6 H+[c] + Pantetheine 4-phosphate[c]	-1000	1000		-23.181	14.181
R04230	pantothenate and CoA biosynthesis	CAC1720	ATP[c] + L-Cysteine[c] + D-4-Phosphopantothenate[c] -> Diphosphate[c] + AMP[c] + 0.22 H+[c] + (R)-4-Phosphopantothenoyl-L-cysteine[c]	0	1000		NaN	NaN
R04231	pantothenate and CoA biosynthesis	CAC1720	CTP[c] + L-Cysteine[c] + D-4-Phosphopantothenate[c] -> Diphosphate[c] + CMP[c] + 0.23 H+[c] + (R)-4-Phosphopantothenoyl-L-cysteine[c]	0	1000		NaN	NaN
R04391	pantothenate and CoA biosynthesis	CAC3200	ATP[c] + N-((R)-Pantothenoyl)-L-cysteine[c] <=> ADP[c] + 0.6 H+[c] + (R)-4-Phosphopantothenoyl-L-cysteine[c]	-1000	1000		-23.186	14.186
R07302	porphyrin and chlorophyll metabolism	CAC0582	ATP[c] + (R)-1-Aminopropan-2-ol[c] + Adenosyl cobyrinate hexaamide[c] <=> ADP[c] + Orthophosphate[c] + 0.45 H+[c] + Adenosyl cobinamide[c]	-1000	1000		NaN	NaN
R04148	riboflavin metabolism	CAC1372	Nicotinate D-ribonucleotide[c] + Dimethylbenzimidazole[c] <=> 1.14 H+[c] + Nicotinate[c] + "N1-(5-Phospho-alpha-D-ribosyl)-5,6-dimethylbenzimidazole"[c]	-1000	1000		-26.011	11.002
R07281	riboflavin metabolism	CAC0592	D-Ribulose 5-phosphate[c] -> Formate[c] + 1.03 H+[c] + "3,4-Dihydroxy-2-butanone 4-phosphate"[c]	0	1000	df	-24.225	-7.404
R04987	ubiquinone synthesis	Unassigned	NADPH[c] + Oxygen[c] + H+[c] + 2-Octaprenylphenol[c] <=> H2O[c] + NADP+[c] + 2-Octaprenyl-6-hydroxyphenol[c]	-1000	1000		NaN	NaN
R05000	ubiquinone synthesis	Unassigned	4-Hydroxybenzoate[c] + all-trans-Polyprenyl diphosphate[c] <=> Diphosphate[c] + 4-Hydroxy-3-polyprenylbenzoate[c]	-1000	1000		NaN	NaN
R05615	ubiquinone synthesis	CAC0800	4-Hydroxybenzoate[c] + all-trans-Octaprenyl diphosphate[c] <=> Diphosphate[c] + 0.37 H+[c] + 3-Octaprenyl-4-hydroxybenzoate[c]	-1000	1000		NaN	NaN
R08768	ubiquinone synthesis	Unassigned	NADPH[c] + Oxygen[c] + 2-Polyprenylphenol[c] <=> H2O[c] + NADP+[c] + 2-Polyprenyl-6-hydroxyphenol[c]	-1000	1000		NaN	NaN
R00174	vitamin B6 metabolism	CAC1622	ATP[c] + Pyridoxal[c] <=> ADP[c] + Pyridoxal phosphate[c] + 0.65 H+[c]	-1000	1000		-23.303	14.303
R01909	vitamin B6 metabolism	CAC1622	ATP[c] + Pyridoxine[c] <=> ADP[c] + 0.64 H+[c] + Pyridoxine phosphate[c]	-1000	1000		-23.304	14.304
R02493	vitamin B6 metabolism	CAC1622	ATP[c] + Pyridoxamine[c] <=> ADP[c] + 1.74 H+[c] + Pyridoxamine phosphate[c]	-1000	1000		-23.322	14.322
R05086	vitamin B6 metabolism	Unassigned	H2O[c] + 0.16 H+[c] + O-Phospho-4-hydroxy-L-threonine[c] <=> Orthophosphate[c] + 4-Hydroxy-L-threonine[c]	-1000	1000		NaN	NaN
R07456	vitamin B6 metabolism	Unassigned	L-Glutamine[c] + 0.79 H+[c] + D-Glyceraldehyde 3-phosphate[c] + D-Ribulose 5-phosphate[c] <- Pyridoxal phosphate[c] + L-Glutamate[c]	-1000	0	dr	387.546	418.103
EX_cid0000001	Exchange reactions	Unassigned	H2O[e] <=>	-1000	1000		NaN	NaN
EX_cid0000009	Exchange reactions	Unassigned	Orthophosphate[e] <=>	-1000	1000		NaN	NaN
EX_cid0000011	Exchange reactions	Unassigned	CO2[e] <=>	-1000	1000		NaN	NaN
EX_cid0000013	Exchange reactions	Unassigned	NH3[e] <=>	-1000	1000		NaN	NaN
EX_cid0000024	Exchange reactions	Unassigned	L-Glutamate[e] ->	0	1000		NaN	NaN
EX_cid0000025	Exchange reactions	Unassigned	2-Oxoglutarate[e] ->	0	1000		NaN	NaN
EX_cid0000028	Exchange reactions	Unassigned	D-Glucose[e] <=>	-1000	1000		NaN	NaN
EX_cid0000030	Exchange reactions	Unassigned	Acetate[e] <=>	-1000	1000		NaN	NaN
EX_cid0000034	Exchange reactions	Unassigned	Glycine[e] ->	0	1000		NaN	NaN
EX_cid0000039	Exchange reactions	Unassigned	Succinate[e] ->	0	1000		NaN	NaN
EX_cid0000042	Exchange reactions	Unassigned	L-Lysine[e] ->	0	1000		NaN	NaN
EX_cid0000050	Exchange reactions	Unassigned	Formate[e] ->	0	1000		NaN	NaN
EX_cid0000051	Exchange reactions	Unassigned	Sulfate[e] <=>	-1000	1000		NaN	NaN
EX_cid0000055	Exchange reactions	Unassigned	L-Glutamine[e] ->	0	1000		NaN	NaN
EX_cid0000061	Exchange reactions	Unassigned	L-Methionine[e] ->	0	1000		NaN	NaN
EX_cid0000068	Exchange reactions	Unassigned	H+[e] <=>	-1000	1000		NaN	NaN
EX_cid0000077	Exchange reactions	Unassigned	Sucrose[e] ->	0	1000		NaN	NaN
EX_cid0000081	Exchange reactions	Unassigned	sn-Glycerol 3-phosphate[e] ->	0	1000		NaN	NaN

EX_cid0000083	Exchange reactions	Unassigned	D-Fructose[e] ->	0	1000	NaN	NaN
EX_cid0000092	Exchange reactions	Unassigned	Uracil[e] ->	0	1000	NaN	NaN
EX_cid0000099	Exchange reactions	Unassigned	Glycerol[e] ->	0	1000	NaN	NaN
EX_cid0000103	Exchange reactions	Unassigned	Biotin[e] ->	0	1000	NaN	NaN
EX_cid0000104	Exchange reactions	Unassigned	D-Ribose[e] ->	0	1000	NaN	NaN
EX_cid0000106	Exchange reactions	Unassigned	L-Leucine[e] ->	0	1000	NaN	NaN
EX_cid0000117	Exchange reactions	Unassigned	Putrescine[e] ->	0	1000	NaN	NaN
EX_cid0000121	Exchange reactions	Unassigned	Reduced ferredoxin[e] ->	0	1000	NaN	NaN
EX_cid0000123	Exchange reactions	Unassigned	N-Acetyl-D-Glucosamine[e] ->	0	1000	NaN	NaN
EX_cid0000128	Exchange reactions	Unassigned	L-Proline[e] ->	0	1000	NaN	NaN
EX_cid0000129	Exchange reactions	Unassigned	(S)-Malate[e] ->	0	1000	NaN	NaN
EX_cid0000136	Exchange reactions	Unassigned	D-Mannose[e] ->	0	1000	NaN	NaN
EX_cid0000151	Exchange reactions	Unassigned	L-Valine[e] ->	0	1000	NaN	NaN
EX_cid0000153	Exchange reactions	Unassigned	Cellobiose[e] ->	0	1000	NaN	NaN
EX_cid0000154	Exchange reactions	Unassigned	(S)-Lactate[e] ->	0	1000	NaN	NaN
EX_cid0000155	Exchange reactions	Unassigned	L-Threonine[e] ->	0	1000	NaN	NaN
EX_cid0000156	Exchange reactions	Unassigned	Ethanolamine[e] ->	0	1000	NaN	NaN
EX_cid0000166	Exchange reactions	Unassigned	Acetone[e] ->	0	1000	NaN	NaN
EX_cid0000186	Exchange reactions	Unassigned	Potassium[e] <0>	0	0	NaN	NaN
EX_cid0000189	Exchange reactions	Unassigned	Lactose[e] ->	0	1000	NaN	NaN
EX_cid0000190	Exchange reactions	Unassigned	Nitrate[e] ->	0	1000	NaN	NaN
EX_cid0000192	Exchange reactions	Unassigned	Butanoic acid[e] <=>	-1000	1000	NaN	NaN
EX_cid0000203	Exchange reactions	Unassigned	D-Gluconic acid[e] ->	0	1000	NaN	NaN
EX_cid0000222	Exchange reactions	Unassigned	Hydrogen[e] ->	0	1000	NaN	NaN
EX_cid0000237	Exchange reactions	Unassigned	Spermidine[e] ->	0	1000	NaN	NaN
EX_cid0000249	Exchange reactions	Unassigned	Thioredoxin[e] ->	0	1000	NaN	NaN
EX_cid0000284	Exchange reactions	Unassigned	Xanthine[e] ->	0	1000	NaN	NaN
EX_cid0000288	Exchange reactions	Unassigned	Mannitol[e] ->	0	1000	NaN	NaN
EX_cid0000293	Exchange reactions	Unassigned	L-Isoleucine[e] ->	0	1000	NaN	NaN
EX_cid0000324	Exchange reactions	Unassigned	Acetoin[e] ->	0	1000	NaN	NaN
EX_cid0000325	Exchange reactions	Unassigned	Ethanol[e] ->	0	1000	NaN	NaN
EX_cid0000362	Exchange reactions	Unassigned	4-Aminobenzoate[e] ->	0	1000	NaN	NaN
EX_cid0000418	Exchange reactions	Unassigned	Nitrogen[e] <=>	-1000	1000	NaN	NaN
EX_cid0000429	Exchange reactions	Unassigned	Spermine[e] ->	0	1000	NaN	NaN
EX_cid0000559	Exchange reactions	Unassigned	Sodium[e] <0>	0	0	NaN	NaN
EX_cid0000607	Exchange reactions	Unassigned	Galactitol[e] ->	0	1000	NaN	NaN
EX_cid0001027	Exchange reactions	Unassigned	1-Butanol[e] ->	0	1000	NaN	NaN
EX_cid0001354	Exchange reactions	Unassigned	Biomass[c] ->	0	1000	NaN	NaN

Appendix B. Compounds in *iMM864*

Compound ID	Name	Molecular formula	Formal charge (with specified molecular formula)	Average charge (pH 7, 47°C, 1 atm)	Basic pKa's (at 47°C, 1 atm)	Acidic pKa's (at 47°C, 1 atm)	ΔG of formation (kcal/mol)	Uncertainty of ΔG (kcal/mol)
cid0000001[c]	H2O	H2O	0	-4.10E-10	-1.8	15.7	-56.687	1
cid0000001[e]	H2O	H2O	0	-4.10E-10	-1.8	15.7	-56.687	1
cid0000002[c]	ATP	C10H16N5O13P3	0	-3.28468635	5.13|3.38|-3.85|-7.03	0.87|2.31|2.83|7.4|12.6	-673.85	6.08627
cid0000003[c]	NAD+	C21H28N7O14P2	1	-0.999994914	5.13|3.36|-3.85|-4.22|-7.03	1.79|2.67|11.38|11.94|12.7	-529.59	8.71385
cid0000004[c]	NADH	C21H29N7O14P2	0	-1.999999082	5.13|3.36|2.67|-3.67|-3.78|-3.85	-7.03|1.79|12.28|12.9|14	-524.32	8.53589
cid0000005[c]	NADPH	C21H30N7O17P3	0	-3.938021438	5.03|3.36|-3.78|-7.03	0.65|1.81|2.67|5.82|12.75	-736.82	8.51575
cid0000006[c]	NADP+	C21H29N7O17P3	1	-2.938041459	5.03|3.36|-7.03	0.65|1.81|2.67|5.82|11.66	-742.09	8.69413
cid0000007[c]	Oxygen	O2	0	0			3.9197	1
cid0000008[c]	ADP	C10H15N5O10P2	0	-2.280041501	5.13|3.32|-3.67|-3.85|-7.03	1.71|2.65|7.41|12.46|13.98	-465.85	6.07158
cid0000009[c]	Orthophosphate	H3PO4	0	-1.528746998		1.8|6.95|12.9	-261.974	1
cid0000009[e]	Orthophosphate	H3PO4	0	-1.528746998		1.8|6.95|12.9	-261.974	1
cid0000010[c]	CoA	C21H36N7O16P3S	0	-3.917258247	5.06|3.37|-7.03|9.6	0.81|1.83|2.68|5.96|10.07	-751.994	6.90415
cid0000011[c]	CO2	CO2	0	0			-92.26	1
cid0000011[e]	CO2	CO2	0	0			-92.26	1
cid0000012[c]	Diphosphate	P2H4O7	0	-2.656292086		1.68|3.04|6.88|7.94	-480.93	1
cid0000013[c]	NH3	NH3	0	0.986384109	8.86		-18.97	1
cid0000013[e]	NH3	NH3	0	0.986384109	8.86		-18.97	1
cid0000014[c]	UDP	C9H14N2O12P2	0	-2.285578876	-3.66|-3.79|-4.29|-5.4	1.75|3.19|7.4|9.7|12.62|14.07	-605.77	3.77447
cid0000015[c]	FAD	C27H33N9O15P2	0	-2.511478996	5.12|3.36|-3.67|-3.85|-7.03	1.79|2.67|6.98|12.46|13.98	-529.37	10.7647
cid0000016[c]	Protein	C2H4NO2R(C2H2NOR)n	NaN	NaN			NaN	NaN
cid0000017[c]	Pyridoxal phosphate	C8H10NO6P	0	-1.75481939	4.11|-5.84	1.68|6.69|8	-272	3.3286
cid0000018[c]	S-Adenosyl-L-methionine	C15H22N6O5S	0	1.009137626	9.41|5.12|2.77|1.67|-3.68|-3.85|-7.03	12.44|13.95	-58.34	7.43407
cid0000019[c]	AMP	C10H14N5O7P	0	-1.839953587	5.09|2.75|-3.67|-3.85|-6.38|-7.03	1.21|6.28|12.46|13.98|18.54	-257.85	6.06668
cid0000020[c]	S-Adenosyl-L-homocysteine	C14H20N6O5S	0	-0.99629313	9.5|5.12|2.78|-3.65|-3.85|-7.03	1.76|12.47|14.01	-67.82	6.37167
cid0000021[c]	Pyruvate	C3H4O3	0	-0.999914893	-9.58	2.93	-112.69	0.600303
cid0000023[c]	Acetyl-CoA	C23H38N7O17P3S	0	-3.916416148	5.06|3.37|-3.87|-7.03	0.81|1.83|2.68|5.96|12.61	NaN	NaN
cid0000024[c]	L-Glutamate	C5H9NO4	0	-1.998126689	9.54	1.88|4.27	-155.84	0.923232
cid0000024[e]	L-Glutamate	C5H9NO4	0	-1.998126689	9.54	1.88|4.27	-155.84	0.923232

cid0000025[c]	2-Oxoglutarate	C5H6O5	0	-1.999259171	-9.67	2.66|3.87	-188.9	0.764221
cid0000025[e]	2-Oxoglutarate	C5H6O5	0	-1.999259171	-9.67	2.66|3.87	-188.9	0.764221
cid0000026[c]	H2O2	H2O2	0	-3.02E-05	-4.19|-4.19	11.52|14.4	-32.05	1
cid0000027[c]	UDP-glucose	C15H24N2O17P2	0	-2.001846799	-3.65|-3.66|-3.68|-3.79|-3.96	1.71|3.16|9.7|12.07|12.66|13.26|14.05|14.82	-762.55	6.2395
cid0000028[c]	D-Glucose	C6H12O6	0	-5.01E-05	-2.98|-3.65|-3.68|-3.94|-4.39|-4.39	11.3|12.69|13.58|14.51|15.12	-218.28	3.08844
cid0000028[e]	D-Glucose	C6H12O6	0	-5.01E-05	-2.98|-3.65|-3.68|-3.94|-4.39|-4.39	11.3|12.69|13.58|14.51|15.12	-218.28	3.08844
cid0000030[c]	Acetate	C2H4O2	0	-0.996544613		4.54	-88.29	1
cid0000030[e]	Acetate	C2H4O2	0	-0.996544613		4.54	-88.29	1
cid0000032[c]	GDP	C10H15N5O11P2	0	-2.28493945	1.34|-1.08|-3.67|-3.85	1.96|3.2|7.4|10.16|12.46|13.98	-516.3	5.48627
cid0000033[c]	Oxaloacetate	C4H4O5	0	-1.999619939	-9.87	2.41|3.58|15.52	-190.52	0.70109
cid0000034[c]	Glycine	C2H5NO2	0	-0.992908621	9.24	2.31	-79.44	0.719975
cid0000034[e]	Glycine	C2H5NO2	0	-0.992908621	9.24	2.31	-79.44	0.719975
cid0000036[c]	DNA	C10H17O8PR2(C5H8O5PR)n	NaN	NaN			NaN	NaN
cid0000037[c]	Acyl-CoA	C22H35N7O17P3SR	NaN	NaN			NaN	NaN
cid0000038[c]	L-Alanine	C3H7NO2	0	-0.98230371	9.48	2.47	-79.63	0.792898
cid0000039[c]	Succinate	C4H6O4	0	-1.953276588		3.55|5.69	-162.96	0.566107
cid0000039[e]	Succinate	C4H6O4	0	-1.953276588		3.55|5.69	-162.96	0.566107
cid0000040[c]	UDP-N-acetyl-D-glucosamine	C17H27N3O17P2	0	-2.001846802	-3.52|-3.63|-3.66|-3.79	1.72|3.16|9.7|12.03|12.59|13.11|13.94|14.55	-756.9	6.47247
cid0000041[c]	GTP	C10H16N5O14P3	0	-3.284905911	1.57|-3.67|-3.85	0.79|2.55|3.29|7.4|10.16|12.46|13.98	-724.3	5.50253
cid0000042[c]	L-Lysine	C6H14N2O2	0	1.898519498	10.29|9.44	2.74	-67.46	1.54572
cid0000042[e]	L-Lysine	C6H14N2O2	0	1.898519498	10.29|9.44	2.74	-67.46	1.54572
cid0000043[c]	Glyoxylate	C2H2O3	0	-0.999959264	-9.24	2.61	-111.04	0.539281
cid0000044[c]	L-Aspartate	C4H7NO4	0	-1.987203654	9.61	1.7|5.11	-157.46	0.871695
cid0000045[c]	Glutathione	C10H17N3O6S	0	-2.000338832	9.22|-1.18|-9.63	1.94|3.74|10.05|12.78|15.04	-212.664	3.13384
cid0000046[c]	UDP-D-galactose	C15H24N2O17P2	0	-2.001846799	-3.65|-3.66|-3.68|-3.79|-3.96	1.71|3.16|9.7|12.07|12.66|13.26|14.05|14.82	-762.55	6.2395
cid0000047[c]	3-Phosphoadenylyl sulfate	C10H15N5O13P2S	0	-3.916419972	5.06|2.98|-3.87|-7.03	-2.08|0.85|2.38|5.96|12.61	-580.35	6.21469
cid0000048[c]	"Adenosine 3,5-bisphosphate"	C10H15N5O10P2	0	-3.763778362	5.03|2.75|-3.87|-7.03	0.7|1.37|5.81|6.43|12.61	-470.35	6.07597
cid0000049[c]	CMP	C9H14N3O8P	0	-1.849022523	0.6|-3.66|-3.79|-5.52	1.34|6.25|12.56|14.03	-345.38	3.83089
cid0000050[c]	Formate	CH2O2	0	-0.998141374		4.27	-83.9	1
cid0000050[e]	Formate	CH2O2	0	-0.998141374		4.27	-83.9	1
cid0000051[c]	Sulfate	H2SO4	0	-1.999992057		-3.03|1.9	NaN	NaN
cid0000051[e]	Sulfate	H2SO4	0	-1.999992057		-3.03|1.9	NaN	NaN

cid0000052[c]	FMN	C17H21N4O9P	0	-2.269074299	-2.61|-3.36|-3.54|-3.62|-7.53	1.49|6.39|7.1|12.86|14.02|15.11	-337.52	5.7801
cid0000053[c]	L-Arginine	C6H14N4O2	0	1.989065237	12.41|9.12|-0.54	2.41	NaN	NaN
cid0000054[c]	CTP	C9H16N3O14P3	0	-3.284573511	0.55|-3.66|-3.79	1.14|2.52|3.28|7.4|12.56|14.03	-761.38	3.86184
cid0000055[c]	L-Glutamine	C5H10N2O3	0	-0.994234521	9.31|-1	2.15|16.24	-113.4	1.62273
cid0000055[e]	L-Glutamine	C5H10N2O3	0	-0.994234521	9.31|-1	2.15|16.24	-113.4	1.62273
cid0000056[c]	L-Serine	C3H7NO3	0	-0.998166961	8.93|-2.85	2.03|15.17	-115.86	0.82189
cid0000057[c]	Formaldehyde	CH2O	0	2.88E-14	-6.54		-31.2	1
cid0000058[c]	Thiamin diphosphate	C12H19N4O7P2S	1	-1.279934953	5.53|-2.15|-6.03|-8.85	1.76|3.2|7.41|17.93	-368.32	5.13987
cid0000061[c]	L-Methionine	C5H11NO2S	0	-0.978763997	9.5	2.53	-67.62	1.71535
cid0000061[e]	L-Methionine	C5H11NO2S	0	-0.978763997	9.5	2.53	-67.62	1.71535
cid0000062[c]	Phosphoenolpyruvate	C3H5O6P	0	-2.90514853		0.76|3.55|6.02	-316.08	1.17946
cid0000063[c]	UTP	C9H15N2O15P3	0	-3.285546096	-3.66|-3.79|-4.33	0.88|2.51|3.28|7.4|9.7|12.62|14.07	-813.77	3.79806
cid0000065[c]	L-Ornithine	C5H12N2O2	0	1.882057177	10.29|9.44	2.67	-69.08	1.47425
cid0000066[c]	L-Tryptophan	C11H12N2O2	0	-0.982697355	9.4	2.54|16.16	-16.71	3.20266
cid0000067[c]	L-Phenylalanine	C9H11NO2	0	-0.983473164	9.45	2.47	-42.76	1.73789
cid0000068[c]	H+	H	1	1			-9.53	0
cid0000068[e]	H+	H	1	1			-9.53	0
cid0000069[c]	ITP	C10H15N4O14P3	0	-3.294822766	-0.81|-3.67|-3.85	0.88|2.51|3.28|7.39|8.95|12.46|13.98	-729.58	5.50868
cid0000070[c]	L-Tyrosine	C9H11NO3	0	-0.998518888	9.19|-5.96	2|9.79	-82.24	1.87976
cid0000071[c]	Malonyl-CoA	C24H38N7O19P3S	0	-4.914513894	5.08|3.25|-7.03	0.81|1.83|2.65|3.89|5.97	NaN	NaN
cid0000072[c]	Acetaldehyde	C2H4O	0	-3.16E-08	-6.87	14.5	-33.4	1
cid0000073[c]	D-Fructose 6-phosphate	C6H13O9P	0	-1.849532598	-3.45|-3.69|-4.03|-4.42|-4.86	1.22|6.25|10.28|12.73|13.99|14.68	-431.67	2.62301
cid0000074[c]	Urea	CH4N2O	0	-1.44E-09	-2.37	15.73	-48.7	1
cid0000075[c]	Sulfur	S	0	0			NaN	NaN
cid0000076[c]	Nitrite	HNO2	0	-0.999791114	-3.47	3.32	-8.9	1
cid0000077[c]	Sucrose	C12H22O11	0	-1.45E-05	-2.98|-2.98|-3.46|-3.65|-3.68|-3.69|-3.95|-3.95	11.84|12.39|13.04|13.51|13.94|14.39|14.77|15.23	-377.65	5.53849
cid0000077[e]	Sucrose	C12H22O11	0	-1.45E-05	-2.98|-2.98|-3.46|-3.65|-3.68|-3.69|-3.95|-3.95	11.84|12.39|13.04|13.51|13.94|14.39|14.77|15.23	-377.65	5.53849
cid0000079[c]	Succinyl-CoA	C25H40N7O19P3S	0	-4.914488236	5.09|3.28|-7.03	0.81|1.83|2.66|3.97|5.97	NaN	NaN

cid0000080[c]	D-Glucose 6-phosphate	C6H13O9P	0	-1.849068954	-3.65|-3.68|-3.94|-4.39|-4.39	1.22|6.25|11.3|12.69|13.62|14.9	-430.78	3.01132
cid0000081[c]	sn-Glycerol 3-phosphate	C3H9O6P	0	-1.746911696	-2.97|-3.39	1.51|6.53|13.66|15.57	-328.68	0.756384
cid0000081[e]	sn-Glycerol 3-phosphate	C3H9O6P	0	-1.746911696	-2.97|-3.39	1.51|6.53|13.66|15.57	-328.68	0.756384
cid0000082[c]	Sulfite	H2SO3	0	-1.011879818		-3.67|8.92	-126.15	1
cid0000083[c]	D-Fructose	C6H12O6	0	-0.000524534	-2.98|-3.45|-3.69|-4.03|-4.42|-4.86	10.28|12.73|13.91|14.47|15	-219.17	2.71119
cid0000083[e]	D-Fructose	C6H12O6	0	-0.000524534	-2.98|-3.45|-3.69|-4.03|-4.42|-4.86	10.28|12.73|13.91|14.47|15	-219.17	2.71119
cid0000084[c]	GDP-mannose	C16H25N5O16P2	0	-2.00069914	3.17|-3.67|-3.68|-3.85|-3.96	1.3|1.92|10.15|12.06|12.66|13.66|14.24	-673.08	7.40161
cid0000085[c]	L-Cysteine	C3H7NO2S	0	-0.995643908	9.05|-9.63	2.35|10.17	-75.104	1.49331
cid0000086[c]	beta-Alanine	C3H7NO2	0	0.420933537	10.31	4.08	-77.82	0.781581
cid0000087[c]	Propanoyl-CoA	C24H40N7O17P3S	0	-3.916416148	5.06|3.37|-3.87|-7.03	0.81|1.83|2.68|5.96|12.61	NaN	NaN
cid0000088[c]	Tetrahydrofolate	C19H23N7O6	0	-1.999368181	4.62|2.59|-2.12|-6.07	3.2|3.85|11.12	-113.97	6.04918
cid0000089[c]	D-Glucose 1-phosphate	C6H13O9P	0	-1.85766884	-2.98|-3.65|-3.68|-3.96|-4.4	1.16|6.22|12.22|13.2|14.42|15.03	-430.78	3.01132
cid0000090[c]	IDP	C10H14N4O11P2	0	-2.294855477	0.57|-2.28|-3.67|-3.85	1.78|3.19|7.39|8.95|12.46|13.98	-521.58	5.49244
cid0000091[c]	UMP	C9H13N2O9P	0	-1.850966461	-3.66|-3.79|-4.29|-5.4	1.23|6.25|9.7|12.63|14.07	-397.77	3.76658
cid0000092[c]	Uracil	C4H4N2O2	0	-0.001695365	-5.51	9.77|13.79	-61.07	3.07152
cid0000092[e]	Uracil	C4H4N2O2	0	-0.001695365	-5.51	9.77|13.79	-61.07	3.07152
cid0000093[c]	Anthranilate	C7H7NO2	0	-0.992297184	1.95	4.89|19.44	-48.99	1.89101
cid0000094[c]	2-Oxobutanoate	C4H6O3	0	-0.999845142	-9.65	3.19	-111.07	0.625459
cid0000095[c]	Glycerone phosphate	C3H7O6P	0	-1.857663072	-3.32|-8.44	1.19|6.22|13.78|15.79	-320.66	0.646196
cid0000096[c]	CDP	C9H15N3O11P2	0	-2.284606285	0.77|-3.66|-3.79|-5.52	1.8|3.19|7.4|12.56|14.03	-553.38	3.83865
cid0000097[c]	Choline	C5H14NO	1	0.999999893	-3.25	13.97	12.19	3.9388
cid0000099[c]	Glycerol	C3H8O3	0	-2.45E-07	-2.97|-2.97|-3.37	13.61|15.17|16.06	-116.18	0.887983
cid0000099[e]	Glycerol	C3H8O3	0	-2.45E-07	-2.97|-2.97|-3.37	13.61|15.17|16.06	-116.18	0.887983
cid0000100[c]	D-Ribose 5-phosphate	C5H11O8P	0	-1.849067839	-3.68|-3.94|-4.39|-4.39	1.22|6.25|11.31|12.91|14.31	-394.12	2.63513
cid0000101[c]	D-Glyceraldehyde 3-phosphate	C3H7O6P	0	-1.791749348	-3.76|-7.63	1.4|6.42|12.82|18.84	-319.2	0.629828

cid0000102[c]	5-Phospho-alpha-D-ribose 1-diphosphate	C5H13O14P3	0	-4.133683523	-3.68|-3.96|-4.4	1.08|1.78|3.08|6.22|7.43|12.28|13.91	-814.62	2.64373
cid0000103[c]	Biotin	C10H16N2O3S	0	-0.997494689	-1.86	4.4|13.55	-109.02	4.41402
cid0000103[e]	Biotin	C10H16N2O3S	0	-0.997494689	-1.86	4.4|13.55	-109.02	4.41402
cid0000104[c]	D-Ribose	C5H10O5	0	-4.90E-05	-2.98|-3.68|-3.94|-4.39|-4.39	11.31|12.9|14.15|14.86	-181.62	2.6995
cid0000104[e]	D-Ribose	C5H10O5	0	-4.90E-05	-2.98|-3.68|-3.94|-4.39|-4.39	11.31|12.9|14.15|14.86	-181.62	2.6995
cid0000105[c]	Fumarate	C4H4O4	0	-1.997434377		3.55|4.41	-143.7	1.43379
cid0000106[c]	L-Leucine	C6H13NO2	0	-0.959924294	9.52	2.79	-76.58	1.04067
cid0000106[e]	L-Leucine	C6H13NO2	0	-0.959924294	9.52	2.79	-76.58	1.04067
cid0000107[c]	D-Galactose	C6H12O6	0	-5.01E-05	-2.98|-3.65|-3.68|-3.94|-4.39|-4.39	11.3|12.69|13.58|14.51|15.12	-218.28	3.08844
cid0000108[c]	Ferricytochrome c	C42H44FeN8O8S2R4	NaN	NaN			NaN	NaN
cid0000109[c]	Ferrocytochrome c	C42H44FeN8O8S2R4	NaN	NaN			NaN	NaN
cid0000110[c]	Glutathione disulfide	C20H32N6O12S2	0	-3.999242057	9.61|9.01	1.44|2.03|3.29|3.88|13.45|13.99	-418.15	6.21062
cid0000112[c]	Isopentenyl diphosphate	C5H12O7P2	0	-2.284601625		1.76|3.2|7.4	-439.84	1.15838
cid0000113[c]	IMP	C10H13N4O8P	0	-1.8603877	0.51|-2.28|-3.67|-3.85|-4.96	1.32|6.25|8.93|12.46|13.98	-313.58	5.48702
cid0000114[c]	dATP	C10H16N5O12P3	0	-3.284683727	5.14|3.39|-3.24|-7	0.87|2.32|2.84|7.4|13.98	-634.01	5.98247
cid0000116[c]	D-Alanine	C3H7NO2	0	-0.98230371	9.48	2.47	-79.63	0.792898
cid0000117[c]	Putrescine	C4H12N2	0	1.998741881	10.51|9.9		10.56	1.49878
cid0000117[e]	Putrescine	C4H12N2	0	1.998741881	10.51|9.9		10.56	1.49878
cid0000118[c]	L-Histidine	C6H9N3O2	0	-0.996958905	9.25|6.14	1.85|13.1	-37.34	2.326
cid0000119[c]	Butanoyl-CoA	C25H42N7O17P3S	0	-3.916416148	5.06|3.37|-3.87|-7.03	0.81|1.83|2.68|5.96|12.61	NaN	NaN
cid0000121[c]	Reduced ferredoxin		4	4			NaN	NaN
cid0000121[e]	Reduced ferredoxin		4	4			NaN	NaN
cid0000122[c]	Oxidized ferredoxin		6	6			NaN	NaN
cid0000123[c]	N-Acetyl-D-Glucosamine	C8H15NO6	0	-2.51E-05	-0.78|-2.98|-3.52|-3.63|-4.23|-4.61	11.6|12.81|13.45|14.29|14.92	-212.63	3.26946
cid0000123[e]	N-Acetyl-D-Glucosamine	C8H15NO6	0	-2.51E-05	-0.78|-2.98|-3.52|-3.63|-4.23|-4.61	11.6|12.81|13.45|14.29|14.92	-212.63	3.26946
cid0000124[c]	3-Methyl-2-oxobutanoic acid	C5H8O3	0	-0.999765632	-9.72	3.37	-111.26	0.772381

cid0000125[c]	"5,10-Methylenetetrahydrofolate"	C20H23N7O6	0	-1.999528286	4.6|-0.34|-1.14|-6.43	2.93|3.74|11.11	-93.65	6.17665
cid0000126[c]	GMP	C10H14N5O8P	0	-1.849695798	1.73|-1.08|-3.67|-3.85|-8.29	1.05|6.25|10.16|12.46|13.98	-308.3	5.48084
cid0000127[c]	Adenine	C5H5N5	0	0.02498925	5.43|3.15|-6.3|-6.5	9.91|19.9	78.85	5.4578
cid0000128[c]	L-Proline	C5H9NO2	0	-0.686038892	11.33	1.94	-62.54	1.88794
cid0000128[e]	L-Proline	C5H9NO2	0	-0.686038892	11.33	1.94	-62.54	1.88794
cid0000129[c]	(S)-Malate	C4H6O5	0	-1.986685778	-3.91	3.2|5.13|14.3	-201	0.620573
cid0000129[e]	(S)-Malate	C4H6O5	0	-1.986685778	-3.91	3.2|5.13|14.3	-201	0.620573
cid0000130[c]	L-Asparagine	C4H8N2O3	0	-0.999451847	8.43|-2.63	2|16.09	-115.02	1.59397
cid0000131[c]	Nicotinamide	C6H6N2O	0	0.00042599	3.63|-2.91	13.39	5.55	3.01158
cid0000132[c]	Palmitoyl-CoA	C37H66N7O17P3S	0	-3.916416148	5.06|3.37|-3.87|-7.03	0.81|1.83|2.68|5.96|12.61	NaN	NaN
cid0000133[c]	L-Homocysteine	C4H9NO2S	0	-0.985783025	9.41|-9.56	2.46|10.28	-73.484	1.52397
cid0000134[c]	4-Hydroxybenzoate	C7H6O3	0	-0.999740307	-6.06	4.38|9.67	-92.53	1.78919
cid0000135[c]	Citrate	C6H8O7	0	-2.975819697	-4.19	3.05|4.67|5.39|13.92	-280.44	0.992783
cid0000136[c]	D-Mannose	C6H12O6	0	-5.01E-05	-2.98|-3.65|-3.68|-3.94|-4.39|-4.39	11.3|12.69|13.58|14.51|15.12	-218.28	3.08844
cid0000136[e]	D-Mannose	C6H12O6	0	-5.01E-05	-2.98|-3.65|-3.68|-3.94|-4.39|-4.39	11.3|12.69|13.58|14.51|15.12	-218.28	3.08844
cid0000137[c]	Glycolate	C2H4O3	0	-0.999661287	-3.61	3.53|14.78	-122.98	0.378977
cid0000138[c]	Propanoate	C3H6O2	0	-0.994408033		4.75	-85.13	0.357272
cid0000139[c]	Acetoacetate	C4H6O3	0	-0.998953973	-7.47	4.02|15.22	-113.53	0.507192
cid0000140[c]	Phenylpyruvate	C9H8O3	0	-0.99978625	-9.76	3.33|16.1	-75.82	1.6589
cid0000142[c]	Hydroxypyruvate	C3H4O4	0	-0.999962946	-3.39	2.57|14.01	-148.92	0.638106
cid0000143[c]	Carbamoyl phosphate	CH4NO5P	0	-1.881137509		1.1|6.13|15.18	-310.26	1.07291
cid0000144[c]	5-Methylthioadenosine	C11H15N5O3S	0	0.013009049	5.12|2.73|-3.65|-3.85|-5.04|-6.38|-7.52	12.47|14.01|18.54	1.27	6.2403
cid0000146[c]	Thymine	C5H6N2O2	0	-0.000954082	-5	10.02|14.04	-61.48	2.99596
cid0000149[c]	D-Xylose	C5H10O5	0	-4.90E-05	-3.53|-3.67|-3.94|-4.35|-4.39	11.31|12.79|13.76|14.97	-180.06	2.7387
cid0000151[c]	L-Valine	C5H11NO2	0	-0.959019942	9.6	2.72	-78.2	1.02575
cid0000151[e]	L-Valine	C5H11NO2	0	-0.959019942	9.6	2.72	-78.2	1.02575
cid0000153[c]	Cellobiose	C12H22O11	0	-5.62E-05	-2.98|-2.98|-3.65|-3.68|-3.69|-3.94|-3.95|-4.39	11.25|12.17|12.8|13.32|14|14.41|14.78|15.22	-376.76	6.0443
cid0000153[e]	Cellobiose	C12H22O11	0	-5.62E-05	-2.98|-2.98|-3.65|-3.68|-3.69|-3.94|-3.95|-4.39	11.25|12.17|12.8|13.32|14|14.41|14.78|15.22	-376.76	6.0443

cid0000154[c]	(S)-Lactate	C3H6O3	0	-0.999397829	-3.67	3.78|14.59	-123.17	0.503933
cid0000154[e]	(S)-Lactate	C3H6O3	0	-0.999397829	-3.67	3.78|14.59	-123.17	0.503933
cid0000155[c]	L-Threonine	C4H9NO3	0	-0.996745504	9|-2.94	2.21|14.95	-116.05	0.986458
cid0000155[e]	L-Threonine	C4H9NO3	0	-0.996745504	9|-2.94	2.21|14.95	-116.05	0.986458
cid0000156[c]	Ethanolamine	C2H7NO	0	0.997189538	9.55|-2.53	15.61	-36.22	0.790626
cid0000156[e]	Ethanolamine	C2H7NO	0	0.997189538	9.55|-2.53	15.61	-36.22	0.790626
cid0000157[c]	D-Glucuronate	C6H10O7	0	-0.999886821	-3.69|-3.73|-3.94|-4.4|-4.45	3.21|11.31|12.73|13.66|14.92|19.98	-261.5	2.99756
cid0000160[c]	3-Phospho-D-glycerate	C3H7O7P	0	-2.767925559	-4.15	1.3|3.49|6.48|13.53	-371.9	0.581707
cid0000162[c]	D-Ribulose 5-phosphate	C5H11O8P	0	-1.759776851	-3.33|-3.58|-3.98|-8.53	1.48|6.5|11.48|13.95|14.54|18.5	-393.5	1.14024
cid0000164[c]	2-Dehydro-3-deoxy-D-gluconate	C6H10O6	0	-0.999919299	-2.97|-3.27|-3.49|-9.71	2.91|13.24|14.22|14.77|15.92	-220.14	1.1757
cid0000165[c]	dADP	C10H15N5O9P2	0	-2.280038922	5.14|3.32|-3.24|-6.37|-7	1.71|2.66|7.41|13.98|18.54	-426.01	5.96752
cid0000166[c]	Acetone	C3H6O	0	-3.03E-13	-7.19	19.51	-38.52	1
cid0000166[e]	Acetone	C3H6O	0	-3.03E-13	-7.19	19.51	-38.52	1
cid0000167[c]	Maltose	C12H22O11	0	-5.62E-05	-2.98|-2.98|-3.65|-3.68|-3.69|-3.94|-3.95|-3.95	11.25|12.17|12.8|13.32|14|14.41|14.78|15.22	-376.76	6.0443
cid0000169[c]	Adenosine	C10H13N5O4	0	0.013008889	5.12|2.73|-2.98|-3.67|-3.85|-5.05|-6.38|-6.38	12.45|13.89|14.78|18.54	-45.35	6.08449
cid0000171[c]	Thymidine	C10H14N2O5	0	-0.001095277	-2.98|-3.24|-4.2|-4.96	9.96|13.91|14.79	-145.84	3.54474
cid0000173[c]	D-Glutamate	C5H9NO4	0	-1.998126689	9.54	1.88|4.27	-155.84	0.923232
cid0000174[c]	beta-D-Glucose	C6H12O6	0	-5.01E-05	-2.98|-3.65|-3.68|-3.94|-4.39|-4.39	11.3|12.69|13.58|14.51|15.12	-218.28	3.08844
cid0000175[c]	3-Oxopropanoate	C3H4O3	0	-0.999424911	-7.17	3.76|14.7	-111.88	0.433247
cid0000176[c]	Adenylyl sulfate	C10H14N5O10PS	0	-1.999980026	5.13|2.98|-3.67|-3.85|-6.38|-7.03	-2.05|2.37|12.46|13.98|18.54	-367.85	6.22188
cid0000177[c]	Acetyl phosphate	C2H5O5P	0	-1.839950183	-7.39	1.24|6.28	-301.65	0.525365
cid0000178[c]	Acyl-carrier protein	HSR	-1	-1			NaN	NaN
cid0000179[c]	D-Xylulose 5-phosphate	C5H11O8P	0	-1.759776851	-3.33|-3.58|-3.98|-8.53	1.48|6.5|11.48|13.95|14.54|18.5	-393.5	1.14024

cid0000180[c]	Succinate semialdehyde	C4H6O3	0	-0.998652859	-6.96	4.13|15.31	-110.26	0.529348
cid0000181[c]	4-Methyl-2-oxopentanoate	C6H10O3	0	-0.999661271	-9.66	3.53	-109.64	0.79209
cid0000182[c]	10-Formyltetrahydrofolate	C20H23N7O7	0	-2.000886478	5.42|3.65|3.58	-1.57|2.83|10.02|15.04	-130.47	6.22221
cid0000183[c]	Dimethylallyl diphosphate	C5H12O7P2	0	-2.284608179		1.75|3.18|7.4	-439.18	1.11211
cid0000184[c]	3-Phospho-D-glyceroyl phosphate	C3H8O10P2	0	-3.641447685	-4.19|-7.8	1.01|1.61|6.04|6.64|11.96	-586.8	0.719433
cid0000185[c]	CO	CO	0	0.999952139	11.32		-28.6568	1
cid0000186[c]	Potassium	K	1	1			NaN	NaN
cid0000186[e]	Potassium	K	1	1			NaN	NaN
cid0000187[c]	dCMP	C9H14N3O7P	0	-1.846044941	1.56|-3.24|-5.51	0.96|6.26|13.99	-305.54	3.66372
cid0000188[c]	Guanine	C5H5N5O	0	-0.004137479	2.19|-0.76|-8.41	9.38|10.72	28.4	5.0286
cid0000189[c]	Lactose	C12H22O11	0	-5.62E-05	-2.98|-2.98|-3.65|-3.68|-3.69|-3.94|-3.95|-4.39	11.25|12.17|12.8|13.32|14|14.41|14.78|15.22	-376.76	6.0443
cid0000189[e]	Lactose	C12H22O11	0	-5.62E-05	-2.98|-2.98|-3.65|-3.68|-3.69|-3.94|-3.95|-4.39	11.25|12.17|12.8|13.32|14|14.41|14.78|15.22	-376.76	6.0443
cid0000190[c]	Nitrate	HNO3	0	-0.999999996	-6.05|-9.97	-1.4	-26.61	1
cid0000190[e]	Nitrate	HNO3	0	-0.999999996	-6.05|-9.97	-1.4	-26.61	1
cid0000192[c]	Butanoic acid	C4H8O2	0	-0.991937231		4.91	-83.51	0.469201
cid0000192[e]	Butanoic acid	C4H8O2	0	-0.991937231		4.91	-83.51	0.469201
cid0000195[c]	Hexadecanoic acid	C16H32O2	0	-0.991166222		4.95	-64.07	2.47801
cid0000196[c]	Pyridoxal	C8H9NO3	0	-0.0955069	4.11|-3.05|-5.84	7.97|14.66	-59.5	3.342
cid0000197[c]	Chorismate	C10H10O6	0	-1.998380204	-3.36|-5.07	3.39|4.21|13.74	-169.49	2.81459
cid0000199[c]	Nicotinate	C6H5NO2	0	-0.999938153	4.19	2.79	-36.89	2.84018
cid0000200[c]	Prephenate	C10H10O6	0	-1.99924188	-2.12|-9.69	2.89|3.88|16.54	-186.17	2.63469
cid0000201[c]	Riboflavin	C17H20N4O6	0	-0.517263608	-2.61|-2.97|-3.36|-3.52|-3.62|-7.53	6.97|12.85|13.96|14.94|15.84	-125.02	5.80973
cid0000202[c]	(R)-Lactate	C3H6O3	0	-0.999397829	-3.67	3.78|14.59	-123.17	0.503933
cid0000203[c]	D-Gluconic acid	C6H12O7	0	-0.99975716	-2.97|-3.52|-3.65|-3.72|-4.25	3.39|12.59|13.36|14.22|15.09|15.87	-268.66	1.7793
cid0000203[e]	D-Gluconic acid	C6H12O7	0	-0.99975716	-2.97|-3.52|-3.65|-3.72|-4.25	3.39|12.59|13.36|14.22|15.09|15.87	-268.66	1.7793
cid0000204[c]	D-Glycerate	C3H6O4	0	-0.999737359	-3.04|-4.13	3.42|13.5|15.65	-159.4	0.654042
cid0000205[c]	L-Arabinose	C5H10O5	0	-4.90E-05	-3.53|-3.67|-3.94|-4.35|-4.39	11.31|12.79|13.76|14.97	-180.06	2.7387

cid0000206[c]	Hypoxanthine	C5H4N4O	0	-0.01273115	1.03|-1.89	8.89|10.27	23.12	5.03533
cid0000207[c]	L-Homoserine	C4H9NO3	0	-0.99519734	9.16|-2.4	2.22|15.93	-114.24	0.876361
cid0000208[c]	Glycolaldehyde	C2H4O2	0	-5.88E-08	-3.12|-7.52	14.23|19.94	-70.28	0.449359
cid0000217[c]	CDP-diacylglycerol	C14H19N3O15P2R2	NaN	NaN			NaN	NaN
cid0000220[c]	D-Mannose 6-phosphate	C6H13O9P	0	-1.849068954	-3.65|-3.68|-3.94|-4.39|-4.39	1.22|6.25|11.3|12.69|13.62|14.9	-430.78	3.01132
cid0000221[c]	D-Erythrose 4-phosphate	C4H9O7P	0	-1.755523657	-3.57|-3.88|-7.63	1.48|6.51|12.19|12.27|13.71	-355.62	0.931721
cid0000222[c]	Hydrogen	H2	0	0			4.2065	1
cid0000222[e]	Hydrogen	H2	0	0			4.2065	1
cid0000223[c]	Hydrogen sulfide	H2S	0	-0.686300401	-8.97	6.66|13.8	-6.66	1
cid0000224[c]	dGTP	C10H16N5O13P3	0	-3.284905909	1.6|-1.07|-3.24	0.8|2.55|3.29|7.4|10.16|13.98	-684.46	5.38748
cid0000225[c]	HCO3-	HCO3	-1	-0.89934408	6.05	10.64	-140.26	1
cid0000227[c]	Inosine	C10H12N4O5	0	-0.011612215	0.61|-2.12|-2.98|-3.67|-3.85|-4.97	8.93|12.45|13.89|14.78	-101.08	5.50671
cid0000228[c]	Orotate	C5H4N2O4	0	-1.001834234	-6.03	2.83|9.72|13.63	-142.48	3.10946
cid0000229[c]	Uridine	C9H12N2O6	0	-0.001991299	-2.98|-3.66|-3.79|-4.29|-5.4	9.7|12.62|13.97|14.8	-185.27	3.79519
cid0000230[c]	ADP-ribose	C15H23N5O14P2	0	-2.000004512	5.13|3.36|-3.85|-3.94|-4.39|-7.03	1.79|2.67|11.29|12.54|13.36	-585.97	7.59458
cid0000233[c]	D-Xylulose	C5H10O5	0	-0.0005126	-3.45|-3.56|-4.03|-4.38|-4.86	10.29|12.84|14.12|14.75	-180.95	2.44897
cid0000234[c]	Isocitrate	C6H8O7	0	-2.97470337	-4.02	3.07|4.68|5.41|14.06	-279.02	0.955217
cid0000236[c]	Pyridoxine	C8H11NO3	0	0.0326659	5.58|-2.98|-3.04|-5.11	9.4|14.53|15.2	-67.43	3.35277
cid0000237[c]	Spermidine	C7H19N3	0	2.964122785	10.9|10.11|8.43		25.92	2.07962
cid0000237[e]	Spermidine	C7H19N3	0	2.964122785	10.9|10.11|8.43		25.92	2.07962
cid0000239[c]	Thiosulfate	HS2O3	-1	-1.999999999		-2.28	-122.7	1
cid0000240[c]	GDP-L-fucose	C16H25N5O15P2	0	-2.000559566	1.3|-3.67|-3.68|-3.85|-3.96	1.92|3.17|10.15|12.06|12.66|13.67|14.25	-636.85	7.35121
cid0000241[c]	L-Citrulline	C6H13N3O3	0	-0.993676942	9.23|-1.73	2.27|15.33	-115.58	2.30252
cid0000243[c]	Deoxyguanosine	C10H13N5O4	0	-0.000684592	1.83|-1.08|-2.98|-3.24|-4.96|-8.38	10.16|13.89|14.79	-55.96	5.37366
cid0000244[c]	Acetoacetyl-CoA	C25H40N7O18P3S	0	-3.916857094	5.06|3.37|-7.03	0.81|1.83|2.68|5.96|10.35	NaN	NaN
cid0000245[c]	D-Galacturonate	C6H10O7	0	-0.999886821	-3.69|-3.73|-3.94|-4.4|-4.45	3.21|11.31|12.73|13.66|14.92|19.98	-261.5	2.99756
cid0000246[c]	4-Aminobutanoate	C4H9NO2	0	0.697683961	10.22	4.53	-76.2	0.874669
cid0000247[c]	(S)-Dihydroorotate	C5H6N2O4	0	-1.017281639	-8.19	3.28|8.75|17	NaN	NaN

cid0000248[c]	Geranyl diphosphate	C10H20O7P2	0	-2.284608179		1.75|3.18|7.4	-411.09	2.07043
cid0000249[c]	Thioredoxin	C10H14N4O4S2R4	NaN	NaN			NaN	NaN
cid0000249[e]	Thioredoxin	C10H14N4O4S2R4	NaN	NaN			NaN	NaN
cid0000250[c]	Thioredoxin disulfide	C10H12N4O4S2R4	NaN	NaN			NaN	NaN
cid0000251[c]	"Phosphatidylglycerol (didodecanoyl, n-C12:0)"	C30H58O10P1	-1	-1			NaN	NaN
cid0000259[c]	6-Phospho-D-gluconate	C6H13O10P	0	-2.710405953	-3.54|-3.65|-3.72|-4.25	1.49|3.44|6.61|12.6|13.37|14.29|15.27	-481.16	1.64179
cid0000260[c]	Ethanolamine phosphate	C2H8NO4P	0	-1.742518556	7.8	1.54|6.54	-248.72	0.81407
cid0000270[c]	D-Glucosamine 6-phosphate	C6H14NO8P	0	-1.851954203	8.23|-3.51|-3.63|-4.22|-6.13	1.22|6.24|11.73|12.98|14.46	-387.24	3.01027
cid0000271[c]	Geranylgeranyl diphosphate	C20H36O7P2	0	-2.284608179		1.75|3.18|7.4	-354.91	4.0673
cid0000272[c]	"D-Fructose 1,6-bisphosphate"	C6H14O12P2	0	-3.716225015	-3.69|-4.03|-4.42|-4.88	0.89|1.49|5.92|6.52|10.29|12.75|14.17	-644.17	2.59596
cid0000274[c]	N-Acetyl-D-glucosamine 6-phosphate	C8H16NO9P	0	-1.84904341	-0.79|-3.52|-3.64|-4.23|-4.61	1.23|6.25|11.62|12.83|13.5|14.48	-425.13	3.21651
cid0000275[c]	dAMP	C10H14N5O6P	0	-1.836830561	5.11|2.77|-3.24|-5.03|-6.37|-7.5	1.22|6.29|13.98|18.54	-218.01	5.96253
cid0000276[c]	dGDP	C10H15N5O10P2	0	-2.284939448	1.35|-1.06|-3.24|-8.29	1.96|3.2|7.4|10.16|13.98	-476.46	5.37088
cid0000277[c]	dGMP	C10H14N5O7P	0	-1.846719812	1.74|-1.06|-3.24|-4.95|-8.33	1.06|6.26|10.16|13.98	-268.46	5.36533
cid0000278[c]	dTDP	C10H16N2O11P2	0	-2.285140292	-3.24|-4.2|-4.96	1.75|3.19|7.4|9.96|14.01	-566.34	3.54052
cid0000279[c]	dTMP	C10H15N2O8P	0	-1.847114115	-3.24|-4.2|-4.96	1.23|6.26|9.96|14.01	-358.34	3.53211
cid0000280[c]	dUMP	C9H13N2O8P	0	-1.847945112	-3.24|-4.27|-5.4	1.23|6.26|9.71|14.01	-357.93	3.59642
cid0000282[c]	Thiamine	C12H17N4OS	1	1.033511707	5.54|-2.15|-2.58|-6.03|-8.33	15.5|19.26	52.18	5.13041
cid0000283[c]	Cytosine	C4H5N3O	0	0.005669434	4.83	9.98	-8.68	2.76743
cid0000284[c]	Xanthine	C5H4N4O2	0	-0.100915144	-0.7	7.95|10.77|16.63	-27.73	5.34182
cid0000284[e]	Xanthine	C5H4N4O2	0	-0.100915144	-0.7	7.95|10.77|16.63	-27.73	5.34182
cid0000285[c]	Guanosine	C10H13N5O5	0	-0.000685192	1.79|-1.1|-2.98|-3.67|-3.85|-4.98|-8.37	10.16|12.46|13.89|14.78	-95.8	5.50055
cid0000288[c]	Mannitol	C6H14O6	0	-2.57E-06	-2.97|-2.97|-3.52|-3.52|-3.64|-3.64	12.59|13.38|14.19|14.94|15.57|16.11	-225.44	1.97678

cid0000288[e]	Mannitol	C6H14O6	0	-2.57E-06	-2.97|-2.97|-3.52|-3.52|-3.64|-3.64	12.59|13.38|14.19|14.94|15.57|16.11	-225.44	1.97678
cid0000292[c]	D-Aspartate	C4H7NO4	0	-1.987203654	9.61	1.7|5.11	-157.46	0.871695
cid0000293[c]	L-Isoleucine	C6H13NO2	0	-0.95308987	9.59	2.79	-76.58	1.04067
cid0000293[e]	L-Isoleucine	C6H13NO2	0	-0.95308987	9.59	2.79	-76.58	1.04067
cid0000295[c]	Dihydrofolate	C19H21N7O6	0	-1.998258312	3.68|1.98|-1.05|-6.32	3.16|4.27|10.93|17.93	-109.12	6.02032
cid0000296[c]	"1,2-didodecanoyl-sn-glycerol 3-phosphate"	C27H51O8P1	-2	-2			NaN	NaN
cid0000304[c]	cis-Aconitate	C6H6O6	0	-2.966452899		2.11|3.73|5.54	-222.28	1.5004
cid0000305[c]	trans-Cinnamate	C9H8O2	0	-0.996774501		4.51	-32.27	2.0802
cid0000309[c]	N-Acetylornithine	C7H14N2O3	0	-0.311506034	9.9|-1.17	3.82|15.84	-106.97	1.60659
cid0000310[c]	N-Carbamoyl-L-aspartate	C5H8N2O5	0	-1.982520521	-2.59	3.33|5.25|14.73	-203.96	1.97181
cid0000311[c]	N-Formimino-L-glutamate	C6H10N2O4	0	-1.997243041	10.88|-9.73	2.49|4.21	-156.28	3.30921
cid0000312[c]	5-Methyltetrahydrofolate	C20H25N7O6	0	-1.99933661	4.64|2.62|-0.65|-6.46	3.22|3.87|11.11|20	-101.7	5.70109
cid0000313[c]	L-Aspartate 4-semialdehyde	C4H7NO3	0	-0.998290331	8.98|-7.48	1.95|14.31	-104.76	0.848283
cid0000314[c]	"5,10-Methenyltetrahydrofolate"	C20H22N7O6	1	-0.999180771	1.31|-0.84|-6.04	3.22|4.05|10.52|15.56	-97	6.23585
cid0000315[c]	alpha-D-Galactose 1-phosphate	C6H13O9P	0	-1.85766884	-2.98|-3.65|-3.68|-3.96|-4.4	1.16|6.22|12.22|13.2|14.42|15.03	-430.78	3.01132
cid0000317[c]	"trans,trans-Farnesyl diphosphate"	C15H28O7P2	0	-2.284608179		1.75|3.18|7.4	-383	3.0641
cid0000319[c]	Nicotinamide D-ribonucleotide	C11H15N2O8P	0	-0.851987746	1.21|-2.24|-3.73|-4.22	6.24|11.39|11.99|13.73|18.93	-337.74	4.02412
cid0000320[c]	dCTP	C9H16N3O13P3	0	-3.284568138	1.47|-3.24|-5.52	0.76|2.54|3.29|7.4|13.99	-721.54	3.69608
cid0000321[c]	dTTP	C10H17N2O14P3	0	-3.285107516	-3.24|-4.2|-4.96	0.88|2.51|3.28|7.4|9.96|14.01	-774.34	3.56566
cid0000322[c]	dUTP	C9H15N2O14P3	0	-3.285523936	-3.24|-4.27|-5.4	0.88|2.51|3.28|7.4|9.71|14.01	-773.93	3.62938
cid0000323[c]	Indole	C8H7N	0	-3.63E-10		16.44	54.41	3.18607

cid0000324[c]	Acetoin	C4H8O2	0	-1.91E-07	-3.36|-7.87	13.72|17.82	-72.12	0.690533
cid0000324[e]	Acetoin	C4H8O2	0	-1.91E-07	-3.36|-7.87	13.72|17.82	-72.12	0.690533
cid0000325[c]	Ethanol	C2H6O	0	3.53E-10	-2.16	16.47	-43.44	1
cid0000325[e]	Ethanol	C2H6O	0	3.53E-10	-2.16	16.47	-43.44	1
cid0000326[c]	Cytidine	C9H13N3O5	0	-2.22E-06	0.78|-2.98|-3.66|-3.79|-5.53	12.55|13.93|14.79	-132.88	3.85903
cid0000330[c]	Formamide	CH3NO	0	9.12E-09	-1.03	16.67	-28.36	0.738802
cid0000331[c]	L-Cystine	C6H12N2O4S2	0	-1.999978084	9.34|8.74	1.56|2.27	-143.03	2.86496
cid0000332[c]	Raffinose	C18H32O16	0	-2.00E-05	-3.65|-3.65|-3.68|-3.68|-3.69|-3.95|-3.95|-3.95	11.7|12.15|12.54|12.99|13.41|13.92|14.53|15.07	-536.13	8.50738
cid0000333[c]	Shikimate	C7H10O5	0	-0.998743612	-3.22|-3.38|-3.6	4.1|13.02|14.39|15.33	-171.29	1.90852
cid0000335[c]	ADP-glucose	C16H25N5O15P2	0	-1.999965106	5.13|3.29|-3.68|-3.85|-3.96|-7.03	1.67|2.63|12.11|12.75|13.93	-622.63	7.84531
cid0000338[c]	Folate	C19H19N7O6	0	-1.999544615	2.12|0.84|-1.83	3.38|4.17|9.99|15.89|18.09	-107.8	6.32065
cid0000339[c]	L-Cysteate	C3H7NO5S	0	-1.999998262	8.79	-1.72|1.24	-198.112	1.66935
cid0000341[c]	L-Ribulose	C5H10O5	0	-0.0005126	-3.45|-3.56|-4.03|-4.38|-4.86	10.29|12.84|14.12|14.75	-180.95	2.44897
cid0000343[c]	CDP-glycerol	C12H21N3O13P2	0	-1.999825221	0.78|-2.97|-3.39|-3.66|-3.79	1.88|3.25|12.52|13.53|14.17|15.58	-608.06	4.06249
cid0000344[c]	D-Mannonate	C6H12O7	0	-0.99975716	-2.97|-3.52|-3.65|-3.72|-4.25	3.39|12.59|13.36|14.22|15.09|15.87	-268.66	1.7793
cid0000345[c]	(R)-Pantoate	C6H12O4	0	-0.999088994	-2.79|-4.01	3.96|13.76|15.17	-159.58	0.98645
cid0000346[c]	Deoxyuridine	C9H12N2O5	0	-0.00194605	-2.98|-3.24|-4.27|-5.4	9.71|13.91|14.79	-145.43	3.60883
cid0000347[c]	p-Benzenediol	C6H6O2	0	-0.002085057	-5.89|-5.89	9.68|11.55	-49.38	1.76409
cid0000350[c]	Pyridoxamine	C8H12N2O2	0	0.998620326	9.82|3.77|-2.97|-6.39	7.82|14.85	-23.89	3.37072
cid0000351[c]	Triphosphate	P3H5O10	0	-3.566296943		0.87|2.43|3.22|7.1|7.71	NaN	NaN
cid0000353[c]	Cystathionine	C7H14N2O4S	0	-1.999932531	9.66|8.98	1.79|2.51	-138.33	2.18919
cid0000355[c]	Methylglyoxal	C3H4O2	0	-4.17E-10	-8.02	16.38	-59.99	0.647043
cid0000359[c]	D-Tagaturonate	C6H10O7	0	-1.000350446	-3.45|-3.77|-4.04|-4.48|-4.86	3.21|10.29|12.78|14.03|14.7	-262.39	2.59534
cid0000360[c]	Deoxyadenosine	C10H13N5O3	0	0.013617319	5.14|2.76|-2.98|-3.24|-5.03|-6.37|-7.5	13.89|14.79|18.54	-5.51	5.97002
cid0000362[c]	4-Aminobenzoate	C7H7NO2	0	-0.994145462	2.69	4.77	-48.99	1.89101
cid0000362[e]	4-Aminobenzoate	C7H7NO2	0	-0.994145462	2.69	4.77	-48.99	1.89101
cid0000363[c]	"3,5-Cyclic AMP"	C10H12N5O6P	0	-0.999996386	5.12|2.79|-3.87|-5.05|-6.38|-7.52	1.78|12.59|18.54	-191.87	7.59097
cid0000365[c]	D-Glyceraldehyde	C3H6O3	0	-1.58E-06	-3|-3.74|-7.62	12.8|15.11|18.72	-106.7	0.697188
cid0000369[c]	Choline phosphate	C5H15NO4P	1	-0.868540653		1.15|6.18	-200.31	3.94357
cid0000373[c]	3-Sulfino-L-alanine	C3H7NO4S	0	-1.999997308	9.09	-0.78|1.43	NaN	NaN

cid0000376[c]	alpha-D-Ribose 1-phosphate	C5H11O8P	0	-1.857667961	-2.98|-3.68|-3.96|-4.4	1.16|6.22|12.29|13.83|14.77	-394.12	2.63513
cid0000377[c]	N-Acetyl-L-glutamate	C7H11NO5	0	-1.998052907	-1.17	3.43|4.29|15.41	-193.73	1.4617
cid0000378[c]	Pyridoxine phosphate	C8H12NO6P	0	-1.616510204	5.55|-3.04|-5.11	1.74|6.8|9.4|14.84	-279.93	3.32034
cid0000381[c]	2-Phospho-D-glycerate	C3H7O7P	0	-2.909038517	-3.06	0.81|3.48|6|14.73|19.27	-371.9	0.581707
cid0000382[c]	D-Mannose 1-phosphate	C6H13O9P	0	-1.85766884	-2.98|-3.65|-3.68|-3.96|-4.4	1.16|6.22|12.22|13.2|14.42|15.03	-430.78	3.01132
cid0000390[c]	"1,2-Diacyl-sn-glycerol"	C5H6O5R2	NaN	NaN			NaN	NaN
cid0000392[c]	D-Mannitol 1-phosphate	C6H15O9P	0	-1.751241859	-2.97|-3.52|-3.54|-3.64|-3.64	1.49|6.52|12.59|13.4|14.25|15.08|15.87	-437.94	1.81941
cid0000393[c]	N-Acetyl-D-mannosamine	C8H15NO6	0	-2.51E-05	-0.78|-2.98|-3.52|-3.63|-4.23|-4.61	11.6|12.81|13.45|14.29|14.92	-212.63	3.26946
cid0000394[c]	Pyridoxamine phosphate	C8H13N2O5P	0	-1.749810674	10.11|3.77|-6.39	1.74|6.74|7.86	-236.39	3.35743
cid0000395[c]	Xanthosine 5-phosphate	C10H13N4O9P	0	-1.858068112	0.07|-3.67|-3.85|-4.76	1.26|6.25|9.03|12.45|13.8|14.44	-364.43	5.56989
cid0000397[c]	beta-D-Glucose 1-phosphate	C6H13O9P	0	-1.85766884	-2.98|-3.65|-3.68|-3.96|-4.4	1.16|6.22|12.22|13.2|14.42|15.03	-430.78	3.01132
cid0000398[c]	"LL-2,6-Diaminoheptanedioate"	C7H14N2O4	0	-1.999834057	9.83|9.23	1.85|2.59	-147.1	1.61313
cid0000399[c]	gamma-L-Glutamyl-L-cysteine	C8H14N2O5S	0	-2.000153246	9.24|-1.22|-9.63	1.91|3.78|10.12|15.6	-182.084	2.14017
cid0000400[c]	sn-glycero-3-Phosphocholine	C8H21NO6P	1	7.02E-06	-2.97|-3.39	1.86|13.64|15.57	-254.99	4.1153
cid0000401[c]	(S)-3-Methyl-2-oxopentanoic acid	C6H10O3	0	-0.999668978	-9.72	3.52	-109.64	0.79209
cid0000402[c]	2-Deoxy-D-ribose 1-phosphate	C5H11O7P	0	-1.787926008	-2.98|-3.26|-4.38	1.37|6.43|13.87|14.78	-354.28	2.35882
cid0000403[c]	2-Deoxy-D-ribose 5-phosphate	C5H11O7P	0	-1.846048879	-3.26|-3.95|-4.37	1.23|6.26|12.36|14.08	-354.28	2.35882
cid0000404[c]	5-Dehydro-4-deoxy-D-glucarate	C6H8O7	0	-1.99978186	-3.35|-4.22|-9.71	2.5|3.34|13.22|14.79|15.51	-263.36	1.05834

cid0000405[c]	"meso-2,6-Diaminoheptanedioate"	C7H14N2O4	0	-1.999834057	9.83|9.23	1.85|2.59	-147.1	1.61313
cid0000413[c]	dTDP-4-dehydro-6-deoxy-L-mannose	C16H24N2O15P2	0	-2.001172454	-3.24|-4.01|-4.02	1.71|3.16|9.88|10.76|13.21|14.08|18.02	-680.33	5.72588
cid0000414[c]	"alpha,alpha-Trehalose 6-phosphate"	C12H23O14P	0	-1.849032002	-3.65|-3.65|-3.68|-3.68|-3.95|-3.95	1.22|6.25|11.91|12.43|12.99|13.49|14.46|15.04	-589.26	5.97345
cid0000416[c]	UDP-N-acetylmuramoyl-L-alanyl-D-glutamate	C28H43N5O23P2	0	-4.000443879		1.71|2.96|3.53|4.19|9.7|11.85|12.41|13.58	-958.02	7.81357
cid0000418[c]	Nitrogen	N2	0	0			4.4694	1
cid0000418[e]	Nitrogen	N2	0	0			4.4694	1
cid0000422[c]	dCDP	C9H15N3O10P2	0	-2.284601675	1.23|-3.24|-5.52	1.9|3.2|7.4|13.99	-513.54	3.67184
cid0000423[c]	Amylose	(C6H10O5)n	NaN	NaN			NaN	NaN
cid0000425[c]	Dextrin	(C12H20O10)n	NaN	NaN			NaN	NaN
cid0000429[c]	Spermine	C10H26N4	0	3.930076366	11.1|10.5|8.74|8.14		41.28	3.01332
cid0000429[e]	Spermine	C10H26N4	0	3.930076366	11.1|10.5|8.74|8.14		41.28	3.01332
cid0000431[c]	Urocanate	C6H6N2O2	0	-0.999101906	6.13	3.85|13.89	-26.85	2.59176
cid0000433[c]	CDP-ribitol	C14H25N3O15P2	0	-1.999826668	0.78|-3.52|-3.54|-3.63|-3.66|-3.79	1.88|3.25|12.35|12.93|13.65|14.19|15.03	-680.9	4.30384
cid0000438[c]	D-Altronate	C6H12O7	0	-0.99975716	-2.97|-3.52|-3.65|-3.72|-4.25	3.39|12.59|13.36|14.22|15.09|15.87	-268.66	1.7793
cid0000439[c]	D-Glucarate	C6H10O8	0	-1.999655848	-3.73|-3.73|-4.25|-4.25	2.83|3.54|12.6|13.34|14.25|15.28	-311.88	1.64663
cid0000440[c]	L-Arogenate	C10H13NO5	0	-1.998816311	9.5|-2.12	1.96|4.07|16.54	-153.11	2.68513
cid0000441[c]	Menaquinone	C16H16O2(C5H8)n	NaN	NaN			37.52	4.33494
cid0000442[c]	dTDP-glucose	C16H26N2O16P2	0	-2.000950767	-2.98|-3.24|-3.65|-3.68|-3.96	1.71|3.16|9.96|12.2|13.14|13.93|14.52|15.07	-723.12	5.90303
cid0000445[c]	Deamino-NAD+	C21H27N6O15P2	1	-1.999991113	5.13|3.46|2.92|-3.85|-4.22	-7.03|1.74|2.46|11.7|12.66	-572.03	8.60533
cid0000446[c]	L-Histidinol	C6H11N3O	0	1.151130626	9.22|6.27|-2.75	14.32|15.19	5.88	2.34883
cid0000448[c]	Pantothenate	C9H17NO5	0	-0.997768321	-2.79|-3.81|-5.78	4.35|12.69|15.05|15.92	-188.54	1.70138
cid0000450[c]	Crotonoyl-CoA	C25H40N7O17P3S	0	-3.916416148	5.06|3.37|-3.87|-7.03	0.81|1.83|2.68|5.96|12.61	NaN	NaN
cid0000453[c]	Deoxycytidine	C9H13N3O4	0	2.27E-06	1.38|-2.98|-3.24|-5.53	13.89|14.79	-93.04	3.6759
cid0000454[c]	Dephospho-CoA	C21H35N7O13P2S	0	-2.00080365	5.13|3.37|-3.81|-3.85|-7.03|-9.6	1.79|2.67|10.07|12.34|12.95	-539.494	6.91981
cid0000455[c]	Isochorismate	C10H10O6	0	-1.998453083	-3.57|-5.07	3.39|4.19|13.58	-169.49	2.81459
cid0000459[c]	2-Acetolactate	C5H8O4	0	-0.999722043	-4.59|-8.14	3.45|12.42|17.4	-153.18	0.887525

cid0000460[c]	D-Fructuronate	C6H10O7	0	-1.000350446	-3.45|-3.77|-4.04|-4.48|-4.86	3.21|10.29|12.78|14.03|14.7	-262.39	2.59534
cid0000463[c]	Dihydropteroate	C14H14N6O3	0	-0.994524374	3.54|1.6|-1.13|-6.33|-6.56	4.75|10.92|14.14|17.23	-2.14	5.56691
cid0000466[c]	3-Dehydroquinate	C7H10O6	0	-0.999804879	-3.27|-3.92|-4.07|-8.06	3.3|12.36|13.58|14.85|15.81	-214.49	1.84123
cid0000469[c]	Mercaptopyruvate	C3H4O3S	0	-1.002367422	-9.85|-9.88	2.91|9.61	-108.164	1.40059
cid0000470[c]	2-Dehydropantoate	C6H10O4	0	-0.999822214	-2.82|-9.84	3.25|14.98	-149.1	0.975957
cid0000471[c]	O-Acetyl-L-serine	C5H9NO4	0	-0.999416122	8.6|-7.35	1.86	-153.31	1.17126
cid0000472[c]	2-Phosphoglycolate	C2H5O6P	0	-2.809958321		1.14|3.6|6.37	-335.48	0.425727
cid0000473[c]	D-Alanyl-D-alanine	C6H12N2O3	0	-0.973462078	8.39|-4.48	3.73|13.82	-110.4	1.65139
cid0000474[c]	O-Phospho-L-serine	C3H8NO6P	0	-2.795515587	7.24	1.2|2.07|6.41	-328.36	0.844466
cid0000480[c]	S-Formylglutathione	C11H17N3O7S	0	-1.999697559	9.31|-1.18	1.76|3.49|12.12|14.32	-244.85	3.36804
cid0000483[c]	"7,8-Diaminononanoate"	C9H20N2O2	0	1.520535258	9.97|7.33	4.73	-64.41	1.73067
cid0000487[c]	UDP-N-acetylmuramate	C20H31N3O19P2	0	-3.001360628	-3.64|-3.66|-3.79	1.71|3.04|3.8|9.7|12.06|12.64|13.22|14.12	-820.27	6.50175
cid0000491[c]	D-Ribitol 5-phosphate	C5H13O8P	0	-1.75124104	-2.97|-3.52|-3.54|-3.63	1.49|6.52|12.77|13.78|14.83|15.82	-401.52	1.44335
cid0000493[c]	Thiamin monophosphate	C12H18N4O4PS	1	-0.660996384	5.51|-2.15|-6.03|-8.85	1.66|6.71|17.93	-160.32	5.13408
cid0000494[c]	"alpha,alpha-Trehalose"	C12H22O11	0	-1.23E-05	-2.98|-2.98|-3.65|-3.65|-3.68|-3.68|-3.95|-3.95	11.91|12.43|12.98|13.45|14.16|14.55|14.9|15.33	-376.76	6.0443
cid0000496[c]	8-Amino-7-oxononanoate	C9H17NO3	0	-0.931911813	8.08|-7.95	4.45|17.5	-99.93	1.2366
cid0000497[c]	D-Fructose 1-phosphate	C6H13O9P	0	-1.866392636	-2.98|-3.69|-4.03|-4.42|-4.88	1.16|6.19|10.29|12.74|14.05|14.82	-431.67	2.62301
cid0000498[c]	Sorbitol 6-phosphate	C6H15O9P	0	-1.751241859	-2.97|-3.52|-3.54|-3.64|-3.64	1.49|6.52|12.59|13.4|14.25|15.08|15.87	-437.94	1.81941
cid0000499[c]	D-Tagatose 6-phosphate	C6H13O9P	0	-1.849532598	-3.45|-3.69|-4.03|-4.42|-4.86	1.22|6.25|10.28|12.73|13.99|14.68	-431.67	2.62301
cid0000501[c]	L-Histidinol phosphate	C6H12N3O4P	0	-1.686286448	7.53|5.95	1.59|6.66|13.1	-206.62	2.35682
cid0000502[c]	L-Ribulose 5-phosphate	C5H11O8P	0	-1.759776851	-3.33|-3.58|-3.98|-8.53	1.48|6.5|11.48|13.95|14.54|18.5	-393.5	1.14024

cid0000503[c]	O-Phospho-L-homoserine	C4H10NO6P	0	-2.562971685	9.46	1.52|2.28|6.89	-326.74	0.897569
cid0000504[c]	Orotidine 5-phosphate	C10H13N2O11P	0	-2.815599883	-3.66|-3.79|-4.33	1.21|2.88|6.36|9.68|12.63|14.07	-479.18	3.79757
cid0000507[c]	D-Galactose 6-phosphate	C6H13O9P	0	-1.849068954	-3.65|-3.68|-3.94|-4.39|-4.39	1.22|6.25|11.3|12.69|13.62|14.9	-430.78	3.01132
cid0000508[c]	O-Succinyl-L-homoserine	C8H13NO6	0	-1.998707946	9.46|-7.08	1.69|4.11	-227.9	1.39094
cid0000509[c]	4-Hydroxy-2-oxoglutarate	C5H6O6	0	-1.999786315	-3.89|-9.72	2.45|3.33|14.11|17.59	-226.94	0.805399
cid0000511[c]	N-Acetyl-D-galactosamine	C8H15NO6	0	-2.51E-05	-0.78|-2.98|-3.52|-3.63|-4.23|-4.61	11.6|12.81|13.45|14.29|14.92	-212.63	3.26946
cid0000512[c]	Pantetheine 4-phosphate	C11H23N2O7PS	0	-1.60287022	-1.46|-3.81|-9.6	1.79|6.82|10.07|12.69|15.71|16.22	-347.644	3.14517
cid0000514[c]	S-Adenosylmethioninamine	C14H23N6O3S	1	2.012200389	10.09|5.12|2.73|-3.68|-3.85|-5.06|-6.38|-6.38	12.45|13.95|18.54	21.3	7.43897
cid0000516[c]	(S)-3-Hydroxybutanoyl-CoA	C25H42N7O18P3S	0	-3.916416148	5.06|3.37|-3.87|-7.03	0.81|1.83|2.68|5.96|12.61	NaN	NaN
cid0000517[c]	2-Hydroxy-3-oxopropanoate	C3H4O4	0	-0.999892502	-4.5|-7.78	3.04|12.67	-149.92	0.560364
cid0000520[c]	L-Glutamate 5-semialdehyde	C5H9NO3	0	-0.996596222	9.11|-7	2.12|14.18	-103.14	0.90116
cid0000522[c]	UDP-N-acetyl-D-mannosamine	C17H27N3O17P2	0	-2.001846802	-3.52|-3.63|-3.66|-3.79	1.72|3.16|9.7|12.03|12.59|13.11|13.94|14.55	-756.9	6.47247
cid0000523[c]	beta-D-Glucose 6-phosphate	C6H13O9P	0	-1.849068954	-3.65|-3.68|-3.94|-4.39|-4.39	1.22|6.25|11.3|12.69|13.62|14.9	-430.78	3.01132
cid0000524[c]	Inositol 1-phosphate	C6H13O9P	0	-1.86589341	-3.65|-3.65|-3.65|-3.67|-3.67	1.16|6.19|12.37|13.01|13.73|14.56|15.37	-432.46	2.89952
cid0000525[c]	3-(4-Hydroxyphenyl)pyruvate	C9H8O4	0	-1.003071034	-5.96|-9.76	2.91|9.5|16.85	-115.3	1.80698
cid0000528[c]	Nicotinate D-ribonucleotide	C11H15NO9P	1	-1.851950838	-3.73|-4.22|-4.54	1.2|2.77|6.24|11.72|13.73|19.16	-380.18	3.89751
cid0000532[c]	Malonyl-[acyl-carrier protein]	C3H3O3SR	NaN	NaN			NaN	NaN

cid0000533[c]	UDP-N-acetylmuramoyl-L-alanine	C23H36N4O20P2	0	-3.00154475	-3.66|-3.79	1.71|3|3.65|9.7|12.08|12.63|13.17|14.12	-851.04	7.05363
cid0000537[c]	GDP-4-dehydro-6-deoxy-D-mannose	C16H23N5O15P2	0	-2.000699148	3.17|-3.67|-3.85|-4.01|-4.02	1.3|1.92|10.15|11.83|12.52|13.32|14.07	NaN	NaN
cid0000539[c]	"Guanosine 3,5-bis(diphosphate)"	C10H17N5O17P4	0	-4.56897253	1.61	1.09|2.09|2.92|3.48|7.1|7.7|10.16	NaN	NaN
cid0000540[c]	all-trans-Hexaprenyl diphosphate	C30H52O7P2	0	-2.284608179		1.75|3.18|7.4	NaN	NaN
cid0000541[c]	sn-glycero-3-Phosphoethanolamine	C5H14NO6P	0	-0.999909447	7.75|-2.97|-3.39	1.87|13.64|15.57	-303.4	1.43061
cid0000543[c]	"D-Glucono-1,5-lactone 6-phosphate"	C6H11O9P	0	-1.823884131	-3.66|-3.72|-4.26|-7.45	1.3|6.33|11.62|13.07|14.64	-428.52	2.48334
cid0000544[c]	N-Acetyl-L-glutamate 5-semialdehyde	C7H11NO4	0	-0.999475561	-1.17|-6.95	3.72|14.03|15.17	-141.03	1.44786
cid0000547[c]	3-(Imidazol-4-yl)-2-oxopropyl phosphate	C6H9N2O5P	0	-1.90322067	6.65|-8.41	1.23|6.03|12.55|16.53	NaN	NaN
cid0000548[c]	5-Amino-6-(5-phosphoribosylamino)uracil	C9H15N4O9P	0	-1.852897234	3.27|-3.66|-3.78|-5.02	1.21|6.25|9.4|12.46|13.19|14.14	-394.67	4.27585
cid0000549[c]	5-O-(1-Carboxyvinyl)-3-phosphoshikimate	C10H13O10P	0	-3.759092775	-3.64|-5.06	1.31|3.38|4.19|6.5|13.15	-427.57	2.39808
cid0000551[c]	4-Amino-5-hydroxymethyl-2-methylpyrimidine	C6H9N3O	0	0.128852164	6.17|-1.6|-3.06	14.41	8.46	3.36686
cid0000555[c]	"2-Amino-4-hydroxy-6-hydroxymethyl-7,8-dihydropteridine"	C7H9N5O2	0	-0.000262019	2.42|-0.2|-3.02|-5.41|-6.4|-7.29	10.54|12.87|14.56|18.25	9.08	5.63535

cid0000556[c]	1-(2-Carboxyphenylamino)-1-deoxy-D-ribulose 5-phosphate	C12H16NO9P	0	-2.753826462	0.27|-3.58|-3.97	1.48|4.6|6.51|11.81|13.46|14.61|17.85	-392.53	2.27623
cid0000557[c]	"2,5-Diamino-6-(5-phosphoribosylamino)-4-pyrimidineone"	C9H16N5O8P	0	-1.846120408	4.29|-3.66|-3.78|-4.26|-9.26	1.22|6.26|11.11|12.59|14.04	-338.54	4.20173
cid0000559[c]	Sodium	Na	1	1			NaN	NaN
cid0000559[e]	Sodium	Na	1	1			NaN	NaN
cid0000563[c]	dUDP	C9H14N2O11P2	0	-2.285556715	-3.24|-4.27|-5.4	1.75|3.19|7.4|9.71|14.01	NaN	NaN
cid0000564[c]	FADH2	C27H35N9O15P2	0	-2.031298673	5.13|3.36|-3.85|-7.03	1.79|2.67|8.49|12.26|12.87	-538.18	10.2139
cid0000565[c]	3-AMP	C10H14N5O7P	0	-1.916423753	5.06|2.74|-2.98|-3.87|-6.38|-7.03	0.86|5.96|12.6|14.6|18.54	NaN	NaN
cid0000566[c]	3-UMP	C9H13N2O9P	0	-1.926807453	-2.98|-3.81|-4.29|-5.4	0.87|5.91|9.7|12.84|14.6	NaN	NaN
cid0000567[c]	Butanal	C4H8O	0	-1.82E-09	-6.94	15.74	-30.81	0.527683
cid0000572[c]	Salicin	C13H18O7	0	-6.31E-06	-2.94|-2.98|-3.65|-3.68|-3.95|-4.3|-5.37	12.2|13.18|14.24|14.71|15.19	NaN	NaN
cid0000576[c]	Selenide	H2Se	0	0			NaN	NaN
cid0000584[c]	Stachyose	C24H42O21	0	-2.34E-05	-3.68|-3.68|-3.68|-3.69|-3.95|-3.95|-3.95|-3.95	11.63|12.05|12.39|12.77|13.37|13.74|14.08|14.5	NaN	NaN
cid0000594[c]	tRNA(Ile)	C15H21N5O10PR(C5H8O6PR)n	0	0			NaN	NaN
cid0000595[c]	tRNA(Leu)	C15H21N5O10PR(C5H8O6PR)n	0	0			NaN	NaN
cid0000597[c]	tRNA(Met)	C15H21N5O10PR(C5H8O6PR)n	0	0			NaN	NaN
cid0000602[c]	tRNA(Trp)	C15H21N5O10PR(C5H8O6PR)n	0	0			NaN	NaN
cid0000603[c]	tRNA(Val)	C15H21N5O10PR(C5H8O6PR)n	0	0			NaN	NaN
cid0000605[c]	Cadaverine	C5H14N2	0	1.998741881	10.51|9.9		12.18	1.58867
cid0000606[c]	Chitobiose	C16H28N2O11	0	-3.16E-05	-2.98|-2.98|-3.52|-3.52|-3.63|-4.23	11.5|12.22|12.77|13.19|13.62|14.16|14.59|15.08	NaN	NaN
cid0000607[c]	Galactitol	C6H14O6	0	-2.57E-06	-2.97|-2.97|-3.52|-3.52|-3.64|-3.64	12.59|13.38|14.19|14.94|15.57|16.11	NaN	NaN
cid0000607[e]	Galactitol	C6H14O6	0	-2.57E-06	-2.97|-2.97|-3.52|-3.52|-3.64|-3.64	12.59|13.38|14.19|14.94|15.57|16.11	NaN	NaN

cid0000613[c]	Xanthosine	C10H12N4O6	0	-0.009246191	0.1|-2.98|-3.67|-3.85|-4.76	9.03|12.45|13.74|14.3|14.9	-151.93	5.58929
cid0000614[c]	D-Glucoside	C6H11O6R	NaN	NaN			NaN	NaN
cid0000623[c]	Dethiobiotin	C10H18N2O3	0	-0.995752472	-1.77	4.63|13.83	-115.31	2.90195
cid0000625[c]	L-Histidinal	C6H9N3O	0	0.863598452	7.51|6.06|-7.67	13.09|16.39	15.36	2.3385
cid0000629[c]	L-Leucyl-tRNA	C21H32N6O11PR(C5H8O6PR)n	1	1			NaN	NaN
cid0000641[c]	Salicyl alcohol	C7H8O2	0	-0.001200821	-2.92|-5.25	9.92|15.11	-47.76	1.77281
cid0000645[c]	"2,3-Cyclic AMP"	C10H12N5O6P	0	-0.999994762	5.12|2.78|-2.98|-5.05|-6.38|-7.52	1.71|14.58|18.54	-193.43	7.57691
cid0000646[c]	"2,3-Cyclic CMP"	C9H12N3O7P	0	-0.999993717	0.64|-2.98|-5.51	1.8|14.58	-280.96	5.93975
cid0000647[c]	"2,3-Cyclic UMP"	C9H11N2O8P	0	-1.001985535	-2.98|-4.29|-5.4	1.76|9.7|14.59	-333.35	5.89848
cid0000653[c]	(2S)-2-Isopropylmalate	C7H12O5	0	-1.964147584	-4.14	3.63|5.57|13.73	-201.18	0.964585
cid0000656[c]	Butanoylphosphate	C4H9O5P	0	-1.843021473	-7.42	1.23|6.27	-298.41	0.631941
cid0000660[c]	L-Valyl-tRNA(Val)	C20H30N6O11PR(C5H8O6PR)n	1	1			NaN	NaN
cid0000662[c]	Sucrose 6-phosphate	C12H23O14P	0	-1.849034104	-3.46|-3.65|-3.68|-3.69|-3.95|-4.04	1.22|6.25|11.84|12.4|13.06|13.56|14.06|14.82	-590.15	5.46108
cid0000664[c]	2-Isopropylmaleate	C7H10O4	0	-1.89699748		2.79|6.06	-143.02	1.50255
cid0000665[c]	3-Dehydroshikimate	C7H8O5	0	-0.999841647	-3.27|-3.93|-8	3.21|12.42|14.72|15.28	-166.28	1.85042
cid0000671[c]	N-Acetylmuramate	C11H19NO8	0	-0.999644502	-0.78|-2.98|-3.64|-4.23|-4.48	3.58|11.61|12.9|13.52|14.72	-276	3.34607
cid0000673[c]	2-Succinylbenzoate	C11H10O5	0	-1.996032633	-7.57	3.42|4.6|16.84	-160.84	2.05662
cid0000681[c]	1-(5-Phospho-D-ribosyl)-ATP	C15H25N5O20P4	0	-5.13366507	1.71|-3.85	0.65|1.19|2.56|3.29|6.22|7.43|12.6	-1015.22	9.0676
cid0000682[c]	Phosphoribosyl-AMP	C15H23N5O14P2	0	-3.738110843	5.95|-3.67|-3.79|-3.85	0.81|1.31|1.83|6.55|12.28|12.9|14	-599.22	9.05446
cid0000688[c]	Propanoyl phosphate	C3H7O5P	0	-1.843021473	-7.42	1.23|6.27	-300.03	0.553934
cid0000702[c]	Maltose 6-phosphate	C12H23O14P	0	-1.84907493	-3.65|-3.68|-3.69|-3.94|-3.95|-4.39	1.22|6.25|11.25|12.18|12.81|13.35|14.2|14.87	-589.26	5.97345
cid0000710[c]	4-Phospho-L-aspartate	C4H8NO7P	0	-2.806524809	8.6|-7.68	1.08|1.89|6.38	-372.36	0.916779

cid0000711[c]	5-Methylthio-D-ribose	C6H12O4S	0	-4.90E-05	-3.66|-3.94|-4.38|-4.39	11.31|12.94|14.33	NaN	NaN
cid0000712[c]	5-Phosphoribosylamine	C5H12NO7P	0	-1.851943224	8|-3.66|-3.77|-6	1.23|6.24|12.59|14.05	-350.58	2.65794
cid0000715[c]	Dimethylbenzimidazole	C9H10N2	0	0.212071454	6.43	12.73	46.86	3.34953
cid0000717[c]	L-Isoleucyl-tRNA(Ile)	C21H32N6O11PR(C5H8O6PR)n	1	1			NaN	NaN
cid0000719[c]	N-Ribosylnicotinamide	C11H15N2O5	1	0.999959263	-2.23|-2.98|-3.73|-4.22|-4.57	11.39|11.99|13.68|14.74|18.93	NaN	NaN
cid0000720[c]	2-Succinylbenzoyl-CoA	C32H44N7O20P3S	0	-4.914415169	5.1|3.31|-7.03	0.81|1.83|2.67|4.14|5.97	-859.92	7.43841
cid0000722[c]	Shikimate 3-phosphate	C7H11O8P	0	-2.77963772	-3.23|-3.62	1.32|4.1|6.45|13.12|14.95	-383.79	1.85096
cid0000726[c]	3-Phosphonooxypyruvate	C3H5O7P	0	-2.863178102		1.02|2.77|6.2|17.44	-361.42	0.666933
cid0000731[c]	L-Glutamyl 5-phosphate	C5H10NO7P	0	-2.806524182	9.51|-7.45	1.12|1.98|6.38	-370.74	0.965914
cid0000735[c]	dTDP-6-deoxy-L-mannose	C16H26N2O15P2	0	-2.000950766	-3.24|-3.61|-3.68|-3.96|-4.31	1.71|3.16|9.96|12.22|13.21|14.01|14.83	-686.89	5.85869
cid0000736[c]	"L-2,3-Dihydrodipicolinate"	C7H7NO4	0	-1.999168682	-1.05	3.17|3.92	NaN	NaN
cid0000740[c]	Aminoimidazole ribotide	C8H14N3O7P	0	-1.851945454	7.92|-3.31|-3.67|-3.85|-5.59	1.22|6.24|12.46|13.98	-297.64	3.50051
cid0000743[c]	N-(L-Arginino)succinate	C10H18N4O6	0	-2.982328964	12.39|9.13|-0.64	2.14|3.23|5.11	NaN	NaN
cid0000750[c]	5-Formyltetrahydrofolate	C20H23N7O7	0	-1.999505993	4.33|2.6|-1.83|-6.12	3.18|3.76|11.09|19.95	-142.75	5.91477
cid0000751[c]	D-4-Phosphopantothenate	C9H18NO8P	0	-2.600280882	-3.81|-5.78	1.79|4.47|6.82|12.69|15.79	NaN	NaN
cid0000752[c]	Indoleglycerol phosphate	C11H14NO6P	0	-1.755518303	-3.45|-3.56	1.49|6.51|13.1|14.53|16.24	-267.57	3.22576
cid0000755[c]	L-Tryptophanyl-tRNA(Trp)	C26H31N7O11PR(C5H8O6PR)n	1	1			NaN	NaN
cid0000756[c]	S-Ribosyl-L-homocysteine	C9H17NO6S	0	-0.996059106	9.5|-3.66|-3.94|-4.38|-4.39	1.8|11.32|12.94|14.33	NaN	NaN
cid0000759[c]	(R)-3-Hydroxybutanoyl-CoA	C25H42N7O18P3S	0	-3.916416148	5.06|3.37|-3.87|-7.03	0.81|1.83|2.68|5.96|12.61	NaN	NaN

cid0000764[c]	"1,4-Dihydroxy-2-naphthoate"	C11H8O4	0	-1.00225809	-6.05|-6.33	2.44|9.64|14.64	-122.199	4.45267
cid0000765[c]	4-Imidazolone-5-propanoate	C6H8N2O3	0	-1.798853025	0.14	4.03|6.4	-86.31	1.86669
cid0000766[c]	Apo-[acyl-carrier-protein]		NaN	NaN			NaN	NaN
cid0000767[c]	"Pyridine-2,3-dicarboxylate"	C7H5NO4	0	-1.999224355	5.26	0.29|3.89	-119.77	2.95603
cid0000772[c]	"D-Tagatose 1,6-bisphosphate"	C6H14O12P2	0	-3.716225015	-3.69|-4.03|-4.42|-4.88	0.89|1.49|5.92|6.52|10.29|12.75|14.17	-644.17	2.59596
cid0000773[c]	"N6-(1,2-Dicarboxyethyl)-AMP"	C14H18N5O11P	0	-3.831639446	4.65|3.27|-3.85|-7.24	1.2|2.52|5.24|6.29|12.6	-408.89	6.14903
cid0000774[c]	5-Phosphoribosylglycinamide	C7H15N2O8P	0	-1.849038068	8.14|-3.66|-3.78|-4.21|-5.01	1.23|6.25|11.54|12.62|14.05	NaN	NaN
cid0000776[c]	"Phosphatidylglycerophosphate (didodecanoyl, n-C12:0)"	C30H57O13P2	-3	-3			NaN	NaN
cid0000783[c]	(S)-1-Pyrroline-5-carboxylate	C5H7NO2	0	-0.999991841	6.07	1.82|19.87	-59.27	1.69239
cid0000784[c]	2-Dehydro-3-deoxy-D-glucarate	C6H8O7	0	-1.99978186	-3.35|-4.22|-9.71	2.5|3.34|13.22|14.79|15.51	NaN	NaN
cid0000785[c]	Acetyl-[acyl-carrier protein]	C2H3OSR	NaN	NaN			NaN	NaN
cid0000786[c]	"2,3,4,5-Tetrahydrodipicolinate"	C7H9NO4	0	-1.99892922	-1.99	3.28|4.03	NaN	NaN
cid0000796[c]	"2,3-Dihydroxy-3-methylbutanoate"	C5H10O4	0	-0.999370165	-3.21|-4.27	3.8|13.14|15.19	-161.2	0.970695
cid0000799[c]	"3-D-Glucosyl-1,2-diacylglycerol"	C11H16O10R2	NaN	NaN			NaN	NaN
cid0000805[c]	"2,3-Dihydroxy-3-methylpentanoate"	C6H12O4	0	-0.999150362	-3.32|-4.28	3.93|13.11|14.94	-159.58	0.98645

cid0000807[c]	N-Acetyl-L-glutamate 5-phosphate	C7H12NO8P	0	-2.813489489	-1.17|-7.43	1.23|3.56|6.36|15.37	-408.63	1.48902
cid0000808[c]	all-trans-Octaprenyl diphosphate	C40H68O7P2	0	-2.284608179		1.75|3.18|7.4	-242.55	8.10437
cid0000810[c]	3-Hydroxy-3-methyl-2-oxobutanoic acid	C5H8O4	0	-0.9998979	-3.55	3.01|13.66	-150.72	0.960029
cid0000812[c]	all-trans-Heptaprenyl diphosphate	C35H60O7P2	0	-2.284608179		1.75|3.18|7.4	NaN	NaN
cid0000813[c]	all-trans-Pentaprenyl diphosphate	C25H44O7P2	0	-2.284608179		1.75|3.18|7.4	NaN	NaN
cid0000815[c]	(2S)-2-Isopropyl-3-oxosuccinate	C7H10O5	0	-1.998929446	-9.95	2.93|4.03|17.3	-189.28	1.01259
cid0000817[c]	N-Acetyl-D-glucosamine 1-phosphate	C8H16NO9P	0	-1.851953183	-0.79|-2.98|-3.52|-3.63|-4.62	1.18|6.24|12.27|13.01|14.2|14.87	-425.13	3.21651
cid0000820[c]	"(R)-2,3-Dihydroxy-3-methylbutanoate"	C5H10O4	0	-0.999370165	-3.21|-4.27	3.8|13.14|15.19	-161.2	0.970695
cid0000821[c]	L-1-Pyrroline-3-hydroxy-5-carboxylate	C5H7NO3	0	-0.999475483	2.59|-3.14	3.72|14.25	-99.11	1.65996
cid0000823[c]	5-(2-Hydroxyethyl)-4-methylthiazole	C6H9NOS	0	0.000131806	3.12|-2.53	15.62	-7.11	2.53705
cid0000824[c]	N-(5-Phospho-D-ribosyl)anthranilate	C12H16NO9P	0	-2.845195709	-2.12|-3.66|-3.78|-4.32	1.23|4.48|6.26|12.06|12.93|14.22	-393.15	3.29013
cid0000825[c]	4-Methyl-5-(2-phosphoethyl)-thiazole	C6H10NO4PS	0	-1.671238342	2.58	1.61|6.69	-219.61	2.54446
cid0000826[c]	"6,7-Dimethyl-8-(1-D-ribityl)lumazine"	C13H18N4O6	0	-0.517263465	0.29|-2.97|-3.36|-3.52|-3.62	6.97|12.85|13.96|14.94|15.84	-138.92	5.29758
cid0000827[c]	"(4S)-4,6-Dihydroxy-2,5-dioxohexanoate"	C6H8O6	0	-0.999946049	-3.33|-3.61|-8.46|-9.76	2.74|13|13.75|14.3	-212.12	1.08288

cid0000828[c]	(R)-4-Phosphopantothenoyl-L-cysteine	C12H23N2O9PS	0	-2.602710937	-3.81|-9.63	1.78|3.49|6.82|10.05|12.69|15.42|15.97	-427.284	3.15353
cid0000829[c]	5-Phosphoribosyl-N-formylglycinamide	C8H15N2O9P	0	-1.849057985	-1.35|-3.66|-3.78|-4.32	1.23|6.25|11.41|12.61|14.04|15.56	NaN	NaN
cid0000830[c]	"N6-Acetyl-LL-2,6-diaminoheptanedioate"	C9H16N2O5	0	-1.999197842	9.53|-1.17	2.02|3.9|15.61	NaN	NaN
cid0000832[c]	"(2R,3S)-3-Isopropylmalate"	C7H12O5	0	-1.967918123	-4.02	3.68|5.52|14.04	-199.76	1.1373
cid0000833[c]	Carboxybiotin-carboxyl-carrier protein	C18H26N5O6SR2	NaN	NaN			NaN	NaN
cid0000834[c]	"N-Succinyl-LL-2,6-diaminoheptanedioate"	C11H18N2O7	0	-2.997764685	9.53|-1.48	1.89|3.57|4.35|14.14	NaN	NaN
cid0000836[c]	S-Adenosyl-4-methylthio-2-oxobutanoate	C15H20N5O6S	1	2.47E-05	5.13|3.04|-3.68|-3.85|-6.38|-7.03	2.44|12.44|13.95|18.31|18.92	NaN	NaN
cid0000844[c]	2-Dehydro-3-deoxy-6-phospho-D-gluconate	C6H11O9P	0	-2.70573388	-3.27|-3.51|-9.71	1.48|2.98|6.62|13.31|14.68|15.25	-432.64	1.07975
cid0000845[c]	5-Amino-6-(5-phosphoribitylamino)uracil	C9H17N4O9P	0	-2.001641664	6.52|-3.35|-3.54|-3.62	1.49|4.35|9.41|12.67|13.27|14.12|15.16	NaN	NaN
cid0000847[c]	N-Succinyl-2-L-amino-6-oxoheptanedioate	C11H15NO8	0	-2.997713011	-1.48	2.78|3.51|4.36|13.92	NaN	NaN
cid0000850[c]	3-Phosphatidyl-1-(3-O-L-lysyl)glycerol	C14H25N2O11PR2	NaN	NaN			NaN	NaN
cid0000852[c]	Guanosine 3-diphosphate 5-triphosphate	C10H18N5O20P5	0	-5.568942917		0.82|1.72|2.48|3.02|3.53|7.1|7.7|10.16	NaN	NaN

cid0000855[c]	4-Amino-2-methyl-5-phosphomethylpyrimidine	C6H10N3O4P	0	-1.574275813	6.07|-1.61	1.74|6.87	NaN	NaN
cid0000857[c]	"di-trans,poly-cis-Undecaprenyl diphosphate"	C55H92O7P2	0	-2.284608179		1.75|3.18|7.4	-158.28	11.1392
cid0000863[c]	UDP-N-acetyl-3-(1-carboxyvinyl)-D-glucosamine	C20H29N3O19P2	0	-3.001441974	-3.65|-3.66|-3.79	1.71|3.02|3.74|9.7|12.03|12.63|13.21|14.12	-800.68	6.61347
cid0000865[c]	2-(Formamido)-N1-(5-phosphoribosyl)acetamidine	C8H16N3O8P	0	-1.857663849	7.38|-1.83|-3.66|-3.78|-5.6	1.23|6.22|12.57|14.02|15.6	-380.7	4.62785
cid0000867[c]	D-erythro-1-(Imidazol-4-yl)glycerol 3-phosphate	C6H11N2O6P	0	-1.715255332	5.79|-3.61|-3.78	1.48|6.6|12.34|13.11|14.32	NaN	NaN
cid0000868[c]	1-(5-Phosphoribosyl)-5-amino-4-imidazolecarboxamide	C9H15N4O8P	0	-1.84302494	4.8|-3.67|-3.85|-4.14|-8.25	1.22|6.27|12.45|13.84|14.54	-336.61	3.86718
cid0000870[c]	2-Dehydro-3-deoxy-D-arabino-heptonate 7-phosphate	C7H13O10P	0	-2.686257448	-3.27|-3.54|-3.61|-9.71	1.47|2.92|6.66|12.88|13.98|14.44|15.63	NaN	NaN
cid0000871[c]	5-Amino-6-(1-D-ribitylamino)uracil	C9H16N4O6	0	-0.001589774	4.36|-2.97|-3.35|-3.52|-3.62|-7.15	9.41|12.66|13.25|14.06|14.99|15.85	-189.57	3.69305
cid0000872[c]	1-(5-Phosphoribosyl)-5-formamido-4-imidazolecarboxamide	C10H15N4O9P	0	-1.999958028	6.25|-3.67|-3.85|-4.53	1.21|2.68|12.23|12.82|13.61|14.2	-372.85	4.03262
cid0000874[c]	1-(5-Phospho-D-ribosyl)-5-amino-4-imidazolecarboxylate	C9H14N3O9P	0	-2.865889533	7.11|-3.67|-3.85|-4.78|-7.96	1.17|2.14|6.19|12.46|13.98	-379.05	3.61602

cid0000875[c]	2-Methyl-4-amino-5-hydroxymethylpyrimidine diphosphate	C6H11N3O7P2	0	-2.270749802	6.15|-1.61	1.74|3.18|7.43	-412.04	3.38125
cid0000876[c]	"N1-(5-Phospho-alpha-D-ribosyl)-5,6-dimethylbenzimidazole"	C14H19N2O7P	0	-1.784056286	5.81|-3.67|-3.85|-4.76	1.22|6.44|12.46|13.98	-289.84	4.2704
cid0000877[c]	"2-Amino-7,8-dihydro-4-hydroxy-6-(diphosphooxymethyl)pteridine"	C7H11N5O8P2	0	-2.284724696	1.67|-0.13|-5.41|-6.4	2.44|3.25|7.4|10.54|12.88	-411.42	5.6327
cid0000878[c]	1-(5-Phosphoribosyl)-4-(N-succinocarboxamide)-5-aminoimidazole	C12H20N5O9P	0	-1.846068592	4.45|-3.67|-3.85|-4.19	1.22|6.26|11.61|12.52|13.97|15.55	NaN	NaN
cid0000879[c]	1-(5-Phosphoribosyl)-5-amino-4-(N-succinocarboxamide)-imidazole	C13H19N4O12P	0	-3.83598956	4.54|-3.67|-3.85	1.22|3|5.13|6.28|12.46|13.98	-487.65	3.88388
cid0000881[c]	"2-Amino-4-hydroxy-6-(D-erythro-1,2,3-trihydroxypropyl)-7,8-"	C9H13N5O4	0	0.000134613	3.58|-0.6|-2.98|-3.53|-3.7|-6.36	10.61|11.37|13.3|14.56|15.86	-75.95	5.22276
cid0000882[c]	"UDP-N-acetylmuramoyl-L-alanyl-D-gamma-glutamyl-meso-2,6-"	C35H55N7O26P2	0	-5.000177973	9.3	1.49|2.07|2.95|3.47|4.01|9.92|13.19	-1056.26	8.82691
cid0000884[c]	UDP-N-acetylmuramoyl-L-alanyl-D-glutamyl-6-carboxy-L-lysyl-D-alanyl-	C41H65N9O28P2	0	-5.000129758	9.3	1.51|2.1|2.98|3.51|4.03|9.92|13.18	-1117.8	10.8764

cid0000885[c]	"2-Amino-4-hydroxy-6-(erythro-1,2,3-trihydroxypropyl)dihydropteridine"	C9H16N5O13P3	0	-3.284690285	3.68|-3.55|-3.7	0.87|2.47|3.1|7.4|10.92|12.81|14.31	NaN	NaN
cid0000886[c]	5-(5-Phospho-D-ribosylaminoformimino)-1-(5-phosphoribosyl)-	C15H25N5O15P2	0	-3.829081359	6.75|0.73|-3.78|-3.85	1.21|1.69|5.78|6.26|12.37|12.99	-651.87	8.64621
cid0000887[c]	N-(5-Phospho-D-1-ribulosylformimino)-5-amino-1-(5-phospho-D-	C15H25N5O15P2	0	-3.660224699	7.35|0.81|-3.85|-3.97	1.3|1.79|6.02|6.61|12.14|12.79	NaN	NaN
cid0000890[c]	2-(alpha-Hydroxyethyl)thiamine diphosphate	C14H23N4O8P2S	1	-1.27993622	5.53|-2.15|-3.86|-6.05|-9.32	1.76|3.2|7.41|12.58|19.8	NaN	NaN
cid0000894[c]	5-Deoxyadenosine	C10H13N5O3	0	0.013009126	5.12|2.73|-3.63|-3.85|-5.03|-6.38|-7.52	12.48|14.04|18.54	-9.12	6.05972
cid0000896[c]	Hydroxyacetone	C3H6O2	0	-1.32E-07	-3.29|-7.81	13.88|17.94	NaN	NaN
cid0000919[c]	Sedoheptulose 7-phosphate	C7H15O10P	0	-1.754199012	-3.33|-3.54|-3.65|-3.69|-3.99	1.49|6.52|9.5|13.29|14.09|14.63|15.59|18.32	-466.34	1.85468
cid0000922[c]	Lactose 6-phosphate	C12H23O14P	0	-1.84907493	-3.65|-3.68|-3.69|-3.94|-3.95|-4.39	1.22|6.25|11.25|12.18|12.81|13.35|14.2|14.87	NaN	NaN
cid0000923[c]	Melibiose	C12H22O11	0	-5.62E-05	-2.98|-3.65|-3.65|-3.68|-3.68|-3.94|-3.95|-3.95	11.25|12.13|12.69|13.18|13.69|14.35|14.79|15.27	NaN	NaN
cid0000924[c]	D-Gal alpha 1->6D-Gal alpha 1->6D-Glucose	C18H32O16	0	-6.03E-05	-3.65|-3.68|-3.68|-3.68|-3.94|-3.95|-3.95|-3.95	11.22|11.96|12.42|12.87|13.31|13.84|14.34|14.92	NaN	NaN
cid0000930[c]	Deoxyinosine	C10H12N4O4	0	-0.011612117	0.63|-2.1|-2.98|-3.24|-4.95	8.93|13.89|14.79	NaN	NaN
cid0000931[c]	L-Allothreonine	C4H9NO3	0	-0.996745504	9|-2.94	2.21|14.95	-116.05	0.986458
cid0000932[c]	N-Acetyl-L-2-amino-6-oxopimelate	C9H13NO6	0	-1.999450676	-1.16|-9.66	2.91|3.74|15.33	NaN	NaN
cid0000935[c]	Phenylpropanoate	C9H10O2	0	-0.994658368		4.73	-48.26	1.60652
cid0000960[c]	Hexadecanoyl-[acp]	C16H31OSR	-1	-1			NaN	NaN

cid0000965[c]	3-Octaprenyl-4-hydroxybenzoate	C47H70O3	0	-1.00106667	-6.11	4.35|9.48	NaN	NaN
cid0000966[c]	2-Octaprenylphenol	C46H70O	0	-0.004655576	-6.01	9.33	NaN	NaN
cid0000967[c]	2-Octaprenyl-6-hydroxyphenol	C46H70O2	0	-0.006128191	-6.3|-6.34	9.21|12.66	NaN	NaN
cid0000970[c]	"(1R,6R)-6-Hydroxy-2-succinylcyclohexa-2,4-diene-1-carboxylate"	C11H12O6	0	-1.997815185	-3.14|-5.86	3.63|4.34|14.51|18.32	-192.47	2.40987
cid0000971[c]	2-Demethylmenaquinone	C15H14O2(C5H8)n	0	0			37.93	4.15089
cid0000974[c]	3-CMP	C9H14N3O8P	0	-1.924828848	0.49|-2.98|-3.81|-5.52	1.1|5.91|12.74|14.6	NaN	NaN
cid0000975[c]	Iminoaspartate	C4H5NO4	0	-1.999045555	2.48	3.28|3.98	NaN	NaN
cid0000976[c]	Nicotinate D-ribonucleoside	C11H14NO6	1	3.85E-05	-2.98|-3.73|-4.22|-4.54	2.76|11.72|13.67|14.74|19.16	NaN	NaN
cid0000980[c]	Undecaprenyl-diphospho-N-acetylmuramoyl-(N-acetylglucosamine)-L-	C94H156N8O26P2	0	-3.999414164	10.19	1.69|2.81|3.29|3.78|11.78|12.35|13.61	-743.5	16.3424
cid0000982[c]	Crosslinked peptideglycan		NaN	NaN			NaN	NaN
cid0000983[c]	Undecaprenyl-diphospho-N-acetylmuramoyl-L-alanyl-D-glutamyl-meso-	C87H143N7O23P2	0	-4.998937848	9.53	1.5|2.1|2.98|3.51|4.03|12.05|13.63	-670.31	14.6672
cid0000984[c]	Undecaprenyl-diphospho-N-acetylmuramoyl-(N-acetylglucosamine)-L-	C95H156N8O28P2	0	-4.998940155	9.52	1.5|2.1|2.98|3.51|4.03|11.95|13.59	-823.14	16.3334
cid0000986[c]	Biotinyl-5-AMP	C20H28N7O9PS	0	-1.000003212	5.12|2.74|-3.67|-3.85|-7.03	0.82|12.41|13.36|14.09	NaN	NaN

cid0000987[c]	Formamidopyrimidine nucleoside triphosphate	C10H18N5O15P3	0	-3.284643187	3.99|-3.78	0.87|2.49|3.2|7.4|11.07|12.72|13.7	-790.78	4.61752
cid0000988[c]	"2,5-Diaminopyrimidine nucleoside triphosphate"	C9H18N5O14P3	0	-3.284625481	4.34|-3.66|-3.78	0.87|2.5|3.24|7.4|11.11|12.59|14.04	NaN	NaN
cid0000989[c]	Dihydroneopterin phosphate	C9H14N5O7P	0	-1.755630616	3.46|-0.68|-3.55|-3.7|-6.27	1.48|6.51|10.92|12.81|14.32	-288.45	5.202
cid0001003[c]	"cardiolipin (tetradodecanoyl, n-C12:0)"	C57H108O17P2	-2	-2			NaN	NaN
cid0001012[c]	(S)-2-Aceto-2-hydroxybutanoate	C6H10O4	0	-0.99960794	-4.67|-8.15	3.6|12.23|17.38	-151.56	0.904729
cid0001014[c]	D-arabino-Hex-3-ulose 6-phosphate	C6H13O9P	0	-1.760095641	-3.01|-3.58|-3.87|-3.99	1.48|6.5|10.43|13.1|14.31|15.7|18.31	-429.92	1.48757
cid0001019[c]	Diglucosyl-diacylglycerol	C17H26O15R2	NaN	NaN			NaN	NaN
cid0001020[c]	Glycerophosphoglycoglycerolipid	C20H33O20PR2	NaN	NaN			NaN	NaN
cid0001021[c]	Lipoteichoic acid	C92H201O140P25R2	NaN	NaN			NaN	NaN
cid0001023[c]	O-Phospho-4-hydroxy-L-threonine	C4H10NO7P	0	-2.691230137	8.93|-3.44	1.31|2.07|6.65|13.87	NaN	NaN
cid0001024[c]	4-Hydroxy-L-threonine	C4H9NO4	0	-0.999298616	8.62|-2.97|-3.42	1.92|13.8|15.62	NaN	NaN
cid0001027[c]	1-Butanol	C4H10O	0	1.04E-09	-1.94	16.95	-40.29	0.623335
cid0001027[e]	1-Butanol	C4H10O	0	1.04E-09	-1.94	16.95	-40.29	0.623335
cid0001028[c]	"2,5-Diamino-6-(5-triphosphoryl-3,4-trihydroxy-2-oxopentyl)-"	C9H18N5O14P3	0	-3.284622645	4.45|-3.58|-3.97	0.88|2.51|3.25|7.4|11.1|12.31|14.14	NaN	NaN
cid0001029[c]	alpha-D-Glucosamine 1-phosphate	C6H14NO8P	0	-1.905213388	6.66|-2.98|-3.51|-3.63|-6.14	1.18|6.02|12.9|14.2|14.88	NaN	NaN

cid0001030[c]	Arbutin	C12H16O7	0	-0.001511293	-2.98|-3.65|-3.68|-3.95|-4.3|-5.35|-5.9	9.82|12.2|13.2|14.42|15.03	-207.86	3.61418
cid0001031[c]	Arbutin 6-phosphate	C12H17O10P	0	-1.850497159	-3.65|-3.68|-3.95|-4.3|-5.35|-5.9	1.22|6.25|9.82|12.2|13.21|14.74	-420.36	3.54851
cid0001032[c]	Salicin 6-phosphate	C13H19O10P	0	-1.849026145	-2.94|-3.65|-3.68|-3.95|-4.3|-5.37	1.22|6.25|12.2|13.2|14.42|15.01	NaN	NaN
cid0001033[c]	Guanosine 3-phosphate	C10H14N5O8P	0	-1.927100006	1.67|-1.08|-2.98|-3.87|-8.29	0.78|5.9|10.16|12.61|14.6	NaN	NaN
cid0001034[c]	"2,3-Cyclic GMP"	C10H12N5O7P	0	-1.000680638	1.41|-1.08|-2.98|-4.97|-8.34	2.03|10.16|14.58	-243.88	7.1165
cid0001045[c]	Holo-[carboxylase]	C17H27N5O4SR2	NaN	NaN			NaN	NaN
cid0001048[c]	Galactitol 1-phosphate	C6H15O9P	0	-1.751241859	-2.97|-3.52|-3.54|-3.64|-3.64	1.49|6.52|12.59|13.4|14.25|15.08|15.87	NaN	NaN
cid0001059[c]	Adenosyl cobinamide	C58H84CoN16O11	1	1.07145469	5.87|5.26|4.76|4.08|2.69|-3.65|-3.85|-3.85	12.47|14	NaN	NaN
cid0001075[c]	D-glycero-D-manno-Heptose 7-phosphate	C7H15O10P	0	-1.751287558	-3.55|-3.65|-3.68|-3.94|-4.39|-4.39	1.49|6.52|11.29|12.61|13.27|13.85|14.93	NaN	NaN
cid0001076[c]	D-glycero-D-manno-Heptose 1-phosphate	C7H15O10P	0	-1.857669262	-2.97|-3.52|-3.65|-3.68|-3.96|-4.4	1.16|6.22|12.19|13|13.62|14.71|15.6	-467.2	3.11981
cid0001082[c]	Tetrahydrofolyl-[Glu](2)	C24H30N8O9	0	-2.999052928	4.66|3.01|-5.83	2.41|3.52|4.01|11.12|13.93	NaN	NaN
cid0001088[c]	"trans,trans,cis-Geranylgeranyl diphosphate"	C20H36O7P2	0	-2.284608179		1.75|3.18|7.4	NaN	NaN
cid0001089[c]	2-C-Methyl-D-erythritol 4-phosphate	C5H13O7P	0	-1.755518739	-3.1|-3.57|-3.61	1.49|6.51|12.9|14.16|15.42	NaN	NaN
cid0001090[c]	4-(Cytidine 5-diphospho)-2-C-methyl-D-erythritol	C14H25N3O14P2	0	-1.999826275	0.78|-3.1|-3.57|-3.61|-3.66|-3.79	1.88|3.25|12.39|13.01|13.83|14.38|15.44	NaN	NaN

cid0001091[c]	2-Phospho-4-(cytidine 5-diphospho)-2-C-methyl-D-erythritol	C14H26N3O17P3	0	-3.868499632	0.62|-3.63|-3.66|-3.79	1.22|1.95|3.26|6.18|12.47|13.22|14.09	NaN	NaN
cid0001092[c]	1-Deoxy-D-xylulose 5-phosphate	C5H11O7P	0	-1.75975016	-3.58|-3.95|-7.93	1.48|6.5|12.32|14.17|17.21	NaN	NaN
cid0001093[c]	"2-C-Methyl-D-erythritol 2,4-cyclodiphosphate"	C5H12O9P2	0	-1.999834808	-3.13|-3.63	1.81|3.22|13.13|14.42	NaN	NaN
cid0001096[c]	"D-glycero-D-manno-Heptose 1,7-bisphosphate"	C7H16O13P2	0	-3.613097616	-3.55|-3.65|-3.68|-3.96	0.99|1.66|6.04|6.69|12.19|13.01|13.64|14.78	NaN	NaN
cid0001102[c]	1-Hydroxy-2-methyl-2-butenyl 4-diphosphate	C5H12O8P2	0	-2.284608182	-2.73	1.75|3.18|7.4|15.16	NaN	NaN
cid0001106[c]	"4,6-Dideoxy-4-oxo-dTDP-D-glucose"	C16H24N2O15P2	0	-2.001172454	-3.24|-4.01|-4.02	1.71|3.16|9.88|10.76|13.21|14.08|18.02	-680.33	5.72588
cid0001117[c]	(R)-3-Hydroxy-3-methyl-2-oxopentanoate	C6H10O4	0	-0.999855875	-3.66	3.16|13.4	-149.1	0.975957
cid0001127[c]	"3,4-Dihydroxy-2-butanone 4-phosphate"	C4H9O6P	0	-1.791750014	-3.85|-7.92	1.39|6.42|12.66|17.56	-320.85	0.682806
cid0001354[c]	Biomass		0	0			NaN	NaN
cid0001364[c]	Cell Wall		NaN	NaN			NaN	NaN
cid0001454[c]	Fatty acids		NaN	NaN			NaN	NaN
cid0001472[c]	Generic lipid content	C20H28O	0	0			NaN	NaN
cid0001493[c]	Granulose		NaN	NaN			NaN	NaN
cid0001620[c]	Pool Solutes		NaN	NaN			NaN	NaN
cid0001685[c]	Wall Teichoic acid		NaN	NaN			NaN	NaN
cid0001687[c]	Acceptor		NaN	NaN			NaN	NaN
cid0001688[c]	Reduced acceptor		NaN	NaN			NaN	NaN
cid0001689[c]	Amino acid	C2H4NO2R	NaN	NaN			NaN	NaN

cid0001690[c]	RNA	C10H18O13P2R2(C5H8O6PR)n	NaN	NaN			NaN	NaN
cid0001696[c]	2-Oxo acid	C2HO3R	NaN	NaN			NaN	NaN
cid0001709[c]	Starch	(C12H20O10)n	NaN	NaN			NaN	NaN
cid0001739[c]	Cellulose	(C6H10O5)n	NaN	NaN			NaN	NaN
cid0001745[c]	Pantetheine	C11H22N2O4S	0	-0.000850414	-1.46|-2.79|-3.81|-6.23|-9.6	10.07|12.69|15.02|15.86|16.34	-135.144	3.15935
cid0001747[c]	DNA cytosine	C9H14N3O7P(C5H8O5PR)n(C5H8O5PR)n	NaN	NaN			NaN	NaN
cid0001755[c]	O-Acetyl-L-homoserine	C6H11NO4	0	-0.993967905	9.46|-7.03	2.02	-151.69	1.21011
cid0001756[c]	N(pi)-Methyl-L-histidine	C7H11N3O2	0	-0.992979891	9.43|6.46	1.96	-25.07	2.41836
cid0001758[c]	trans-4-Hydroxy-L-proline	C5H9NO3	0	-0.964252289	10.62|-2.88	1.64|14.86	-102.38	1.72265
cid0001762[c]	1-Phosphatidyl-D-myo-inositol	C11H17O13PR2	NaN	NaN			NaN	NaN
cid0001765[c]	ROH	HOR	NaN	NaN			NaN	NaN
cid0001793[c]	2-Methylmaleate	C5H6O4	0	-1.941918019		2.5|5.79	-144.45	1.42178
cid0001796[c]	"1,4-beta-D-Xylan"	(C5H8O4)n	NaN	NaN			NaN	NaN
cid0001802[c]	N-Methyltyramine	C9H13NO	0	0.998487855	9.82|-5.45	10.54	2.21	2.03796
cid0001809[c]	(R)-2-Methylmalate	C5H8O5	0	-1.980429095	-3.97	3.35|5.3|14.14	-202.61	0.833196
cid0001821[c]	Sorbose 1-phosphate	C6H13O9P	0	-1.86084099	-2.97|-3.52|-3.68|-3.99	1.18|6.21|10.4|13.67|14.85|15.62|15.97	NaN	NaN
cid0001823[c]	DNA 5-methylcytosine	C10H16N3O7P(C5H8O5PR)n(C5H8O5PR)n	NaN	NaN			NaN	NaN
cid0001824[c]	Thiamin triphosphate	C12H20N4O10P3S	1	-2.27990132	5.53|-2.15|-6.03	0.88|2.52|3.29|7.41|17.93	-576.32	5.15722
cid0001830[c]	(R)-1-Aminopropan-2-ol	C3H9NO	0	0.997494408	9.6|-2.67	15.3	-36.41	0.820819
cid0001857[c]	1-Alkyl-sn-glycero-3-phosphate	C3H8O6PR	NaN	NaN			NaN	NaN
cid0001863[c]	N-((R)-Pantothenoyl)-L-cysteine	C12H22N2O6S	0	-1.000588557	-1.99|-2.79|-3.81|-9.63	3.48|10.05|12.69|14.94|15.52|16	-214.784	3.16768
cid0001888[c]	UDPMurAc(oyl-L-Ala-D-gamma-Glu-L-Lys-D-Ala-D-Ala)	C40H65N9O26P2	0	-4.002020987	10.32	1.7|2.82|3.29|3.78|9.58|12.05|13.63	-1038.16	10.8303

cid0001893[c]	O-1-Alk-1-enyl-2-acyl-sn-glycero-3-phosphoethanolamine	C8H14NO7PR2	NaN	NaN			NaN	NaN
cid0001896[c]	MurAc(oyl-L-Ala-D-gamma-Glu-L-Lys-D-Ala-D-Ala)-diphospho-	C86H143N7O21P2	0	-3.999406689	10.2	1.69|2.81|3.29|3.78|12.04|13.34|13.93	-590.67	14.6751
cid0001912[c]	L-Selenomethionine	C5H11NO2Se	0	-0.997702708	9.5	1.56	NaN	NaN
cid0001913[c]	Selenomethionyl-tRNA(Met)	C20H30N6O11PSeR(C5H8O6PR)n	NaN	NaN			NaN	NaN
cid0001915[c]	e-		NaN	NaN			NaN	NaN
cid0001930[c]	3-Sulfinylpyruvate	C3H4O5S	0	-1.999983782	-9.87	-1|2.21|19.48	NaN	NaN
cid0001934[c]	"3,4-Dihydroxyphenylethylene glycol"	C8H10O4	0	-0.006128193	-2.98|-3.38|-6.29|-6.3	9.21|12.63|13.92|15.68	NaN	NaN
cid0001935[c]	"3,4-Dihydroxymandelaldehyde"	C8H8O4	0	-0.006270054	-3.75|-6.29|-6.3|-7.67	9.2|12.48|13.28	NaN	NaN
cid0001945[c]	4-Hydroxy-2-oxo-heptanedioate	C7H10O6	0	-1.99897762	-2.78|-9.71	2.84|4.01|15.1|18.68	NaN	NaN
cid0001959[c]	L-Selenocysteine	C3H7NO2Se	0	-0.999900187	8.42	1.27	NaN	NaN
cid0001960[c]	Se-Adenosylselenomethionine	C15H23N6O5Se	1	0.001945943	9.41|5.12|2.77|-3.68|-3.85|-7.03	1.57|12.44|13.95	NaN	NaN
cid0001961[c]	Se-Adenosyl-L-selenohomocysteine	C14H20N6O5Se	0	-0.998715352	9.5|5.12|2.75|-3.65|-3.85|-7.03	1.3|12.47|14.01	NaN	NaN
cid0001962[c]	R		NaN	NaN			NaN	NaN
cid0001963[c]	CH3-R		NaN	NaN			NaN	NaN
cid0001964[c]	Selenohomocysteine	C4H9NO2Se	0	-0.998373095	9.5	1.41	NaN	NaN
cid0001965[c]	Cyanohydrin	C2HNOR2	NaN	NaN			NaN	NaN
cid0001966[c]	Cyanoglycoside	C8H11NO6R2	NaN	NaN			NaN	NaN
cid0001971[c]	Galactan	(C12H20O11)n	NaN	NaN			NaN	NaN
cid0001976[c]	2-Polyprenylphenol	C11H14O(C5H8)n	NaN	NaN			NaN	NaN
cid0001979[c]	3-Mercaptolactate	C3H6O3S	0	-1.000584018	-3.92|-9.67	3.73|9.95|14.57	-118.644	1.36207

cid0001986[c]	all-trans-Polyprenyl diphosphate	C5H12O7P2(C5H8)n	NaN	NaN			-411.09	2.07043
cid0001987[c]	4-Hydroxy-3-polyprenylbenzoate	C12H14O3(C5H8)n	NaN	NaN			NaN	NaN
cid0001988[c]	UDP-N-acetylmuramoyl-L-alanyl-gamma-D-glutamyl-L-lysine	C34H55N7O24P2	0	-4.001962904	10.32	1.7|2.8|3.29|3.82|9.58|12.05|13.65	-976.62	8.79135
cid0001991[c]	2-Acyl-1-alkyl-sn-glycero-3-phosphate	C4H7O7PR2	NaN	NaN			NaN	NaN
cid0001993[c]	2-Hydroxybutanoic acid	C4H8O3	0	-0.999023768	-3.79	3.99|14.29	NaN	NaN
cid0002017[c]	Hordenine	C10H15NO	0	0.993578613	9.19|-5.45	10.31	12.46	2.90402
cid0002036[c]	Adenosyl cobyrinate hexaamide	C55H77CoN15O11	1	0.000630426	5.87|5.27|4.8|4.27|2.66|-3.85|-7.05	3.74|12.6	NaN	NaN
cid0002138[c]	2-Hydroxy-4-isopropenylcyclohexane-1-carboxyl-CoA	C31H50N7O18P3S	0	-3.916416148	5.06|3.37|-3.87|·7.03	0.81|1.83|2.68|5.96|12.61	NaN	NaN
cid0002143[c]	"2,6-Dimethyl-5-methylene-3-oxo-heptanoyl-CoA"	C31H50N7O18P3S	0	-3.916416148	5.06|3.37|-3.87|·7.03	0.81|1.83|2.68|5.96|12.61	NaN	NaN
cid0002197[c]	5-Carboxyamino-1-(5-phospho-D-ribosyl)imidazole	C9H14N3O9P	0	-2.776150634	5.83|-1.16|-3.67|-3.85|-4.76	1.18|2.26|6.46|12.46|13.98|18.96	-386.58	3.66195
cid0002199[c]	[Enzyme]-cysteine	C4H6N2O2SR2	NaN	NaN			NaN	NaN
cid0002200[c]	[Enzyme]-S-sulfanylcysteine	C4H6N2O2S2R2	NaN	NaN			NaN	NaN
cid0002356[c]	2-Polyprenyl-6-hydroxyphenol	C11H14O2(C5H8)n	NaN	NaN			3.55	2.93817

cid0002358[c]	"di-trans,poly-cis-Undecaprenyl phosphate"	C55H91O4P	0	-1.607657175	1.79|6.81	49.72	11.1365
cid0002414[c]	Protein histidine	C7H8N4O2R2	NaN	NaN		NaN	NaN
cid0002415[c]	D-Galactosamine	C6H13NO5	0	0		-174.74	3.06678
cid0002416[c]	Protein N(pi)-phospho-L-histidine	C7H9N4O5PR2	NaN	NaN		NaN	NaN
cid0002417[c]	N-Acetyl-D-galactosamine 6-phosphate	C8H16NO9P	0	0		-425.13	3.21651
cid0002418[c]	D-Galactosamine 6-phosphate	C6H14NO8P	0	0		-387.24	3.01027
cid0002419[c]	"Phosphatidylcholine|Phosphatidylcholine|Lecithin|Phosphatidyl-N-trimethylethanolamine|1,2-Diacyl-sn-glycero-3-phosphocholine|Choline phosphatide|3-sn-Phosphatidylcholine"	C10H18NO8PR2	NaN	NaN		NaN	NaN
cid0002424[c]	Phosphatidylethanolamine|Phosphatidylethanolamine|(3-Phosphatidyl)ethanolamine|(3-Phosphatidyl)-ethanolamine|Cephalin|O-(1-beta-Acyl-2-acyl-sn-glycero-3-phospho)ethanolamine|1-Acyl-2-acyl-sn-glycero-3-phosphoethanolamine	C7H12NO8PR2	NaN	NaN		NaN	NaN

cid0002429[c]	1-Acyl-sn-glycerol 3-phosphate|1-Acyl-sn-glycerol 3-phosphate|2-Lysophosphatidate|Lysophosphatidate|Lysophosphatidic acid	C4H8O7PR	NaN	NaN			NaN	NaN
cid0002432[c]	"3,5-Cyclic GMP|3,5-Cyclic GMP|Guanosine 3,5-cyclic monophosphate|Guanosine 3,5-cyclic phosphate|Cyclic GMP|cGMP"	C10H12N5O7P	0	-1.000680136	1.41|-1.08|-3.87|-4.97|-8.34	2.05|10.16|12.59	-242.32	7.13147
cid0002433[c]	5-Amino-2-oxopentanoic acid|5-Amino-2-oxopentanoic acid|5-Amino-2-oxopentanoate|2-Oxo-5-amino-pentanoate|2-Oxo-5-aminopentanoate|alpha-Keto-delta-aminopentanoate|2-Oxo-5-aminovalerate	C5H9NO3	0	-0.852723119	9.79|-9.68	3.11|19.75	-102.14	1.0142

cid0002434[c]	"(R)-2-Hydroxybutane-1,2,4-tricarboxylate|(R)-2-Hydroxybutane-1,2,4-tricarboxylate|Homocitrate|Homocitric acid|3-Hydroxy-3-carboxyadipic acid|(R)-2-Hydroxy-1,2,4-butanetricarboxylic acid"	C7H10O7	0	-2.982498541	-4.08	3.09|3.93|5.25|13.92	NaN	NaN
cid0002436[c]	Thiocysteine	C3H7NO2S2	0	-1.000756427	8.9	2.04|9.6	NaN	NaN
cid0002437[c]	2-Aminoacrylate|2-Aminoacrylate|Dehydroalanine	C3H5NO2	0	-0.996648497	8.64	2.58	-60.04	1.31463
cid0002440[c]	"Phosphatidylserine|Phosphatidylserine|Phosphatidyl-L-serine|1,2-Diacyl-sn-glycerol 3-phospho-L-serine|3-O-sn-Phosphatidyl-L-serine|O3-Phosphatidyl-L-serine"	C8H12NO10PR2	NaN	NaN			NaN	NaN
cid0002441[c]	1-Alkenyl-2-acylglycerol	C6H8O4R2	NaN	NaN			NaN	NaN

cid0002442[c]	"6-Pyruvoyltetrahydropterin|6-Pyruvoyltetrahydropterin|6-(1,2-Dioxopropyl)-5,6,7,8-tetrahydropterin|6-Pyruvoyl-5,6,7,8-tetrahydropterin"	C9H11N5O3	0	0.004171825	4.63|-2.76|-6.47	11.12|15.34	NaN	NaN
cid0002443[c]	5-Guanidino-2-oxopentanoate|5-Guanidino-2-oxopentanoate|5-Guanidino-2-oxo-pentanoate|2-Oxo-5-guanidinopentanoate|2-Oxo-5-guanidino-pentanoate|2-Oxoarginine	C6H11N3O3	0	0.921709519	12.38|-0.81|-9.69	3.01|19.43	NaN	NaN
cid0002444[c]	5-Amino-4-imidazolecarboxyamide	C4H6N4O	0	0.017941855	5.27|-4.35|-7.42	10.47|15.91	0.09	2.81745
cid0002445[c]	1-Acyl-sn-glycero-3-phosphocholine|1-Acyl-sn-glycero-3-phosphocholine|1-Acyl-sn-glycerol-3-phosphocholine|alpha-Acylglycerophosphocholine|2-Lysolecithin|2-Lysophosphatidylcholine|1-Acylglycerophosphocholine	C9H20NO7PR	NaN	NaN			NaN	NaN

cid0002446[c]	2-Acyl-sn-glycero-3-phosphocholine|2-Acyl-sn-glycero-3-phosphocholine|2-Acylglycero-3-phosphocholine|1-Lysophosphatidylcholine|1-Lysolecithin|3-Lysolecithin	C9H20NO7PR	NaN	NaN			NaN	NaN
cid0002447[c]	1-Acyl-sn-glycero-3-phosphoethanolamine|1-Acyl-sn-glycero-3-phosphoethanolamine|L-2-Lysophosphatidylethanolamine	C6H13NO7PR	NaN	NaN			NaN	NaN
cid0002448[c]	"(15S)-15-Hydroxy-5,8,11-cis-13-trans-eicosatetraenoate|(15S)-15-Hydroxy-5,8,11-cis-13-trans-eicosatetraenoate|(15S)-15-Hydroxy-5,8,11-cis-13-trans-icosatetraenoate|(5Z,8Z,11Z,13E)-(15S)-15-Hydroxyicosa-5,8,11,13-tetraenoic acid|15(S)-HETE"	C20H32O3	0	-0.993436431	-1.58	4.82|17.8	-11.01	4.29491
cid0002449[c]	"5(S)-HETE|5(S)-HETE|5-Hydroxyeicosatetraenoate|5-HETE|(6E,8Z,11Z,14Z)-(5S)-5-Hydroxyicosa-6,8,11,14-tetraenoic acid"	C20H32O3	0	-0.996212506	-1.55	4.58|17.87	NaN	NaN

cid0002451[c]	"5(S)-HPETE|5(S)-HPETE|5(S)-Hydroperoxy-6-trans-8,11,14-cis-eicosatetraenoic acid|(6E,8Z,11Z,14Z)-(5S)-5-Hydroperoxyeicosa-6,8,11,14-tetraenoate|(6E,8Z,11Z,14Z)-(5S)-5-Hydroperoxyeicosa-6,8,11,14-tetraenoic acid|(5S,6E,8Z,11Z,14Z)-5-Hydroperoxyicosa-6,8,11,14-tetraenoate"	C20H32O4	0	-0.9975708	-4.24|-5.09	4.39|11.71	-34.21	4.37174
cid0002453[c]	3-Sulfopyruvate|3-Sulfopyruvate|3-Sulfopyruvic acid	C3H4O6S	0	-1.999988519		-1.76|2.06|18.41	NaN	NaN
cid0002454[c]	Selenite	SeO3	-2	-1.17E-05	16.86|11.93		NaN	NaN
cid0002455[c]	Adenylylselenate|Adenylylselenate|Adenosine-5-phosphoselenate	C10H14N5O10PSe	0	-1.000298093	5.12|2.77|-3.67|-3.85|-6.38|-7.03	1.57|10.52|12.46|13.98|18.54	NaN	NaN
cid0002456[c]	3-Phosphoadenylylselenate|3-Phosphoadenylylselenate|3-Phosphoadenosine-5-phosphoselanate	C10H15N5O13P2Se	0	-2.916713643	5.06|2.77|-3.87|-7.03	0.78|1.65|5.96|10.53|12.61	NaN	NaN
cid0002457[c]	Selenate|Selenate|Selenic acid	H2SeO4	0	-0.000524532		10.28|14.55	NaN	NaN
cid0002458[c]	L-Selenocystathionine	C7H14N2O4Se	0	-1.999991644	9.54|8.36	1.2|1.9	NaN	NaN
cid0002459[c]	O-Phosphorylhomoserine	C4H10NO6P	0	-2.562971685	9.46	1.52|2.28|6.89	-326.74	0.897569
cid0002461[c]	L-erythro-4-Hydroxyglutamate	C5H9NO5	0	-1.999591994	9.16|-3.83	1.68|3.61|14.24	NaN	NaN

cid0002462[c]	"15(S)-HPETE|15(S)-HPETE|(5Z,8Z,11Z,13E)-(15S)-15-Hydroperoxyicosa-5,8,11,13-tetraenoic acid|15-Hydroperoxyeicosatetraenoate|15-Hydroperoxyicosatetraenoate|15-Hydroperoxyeicosatetraenoic acid|15-Hydroperoxyicosatetraenoic acid|(5Z,8Z,11Z,13E)-(15S)-15-Hydroperoxyicosa-5,8,11,13-tetraenoate"	C20H32O4	0	-0.993455928	-4.24|-5.09	4.82|11.71	NaN	NaN
cid0002463[c]	2-Acyl-sn-glycero-3-phosphoethanolamine|2-Acyl-sn-glycero-3-phosphoethanolamine|L-1-Lysophosphatidylethanolamine|O-(2-Acyl-sn-glycero-3-phospho)-ethanolamine	C6H13NO7PR	NaN	NaN			NaN	NaN
cid0002465[c]	"Levan|Levan|(2,6-beta-D-Fructosyl)n|Levan n|2,6-beta-D-Fructan|(2,6-beta-D-Fructosyl)n+1"	C12H22O11(C6H10O5)n	NaN	NaN			NaN	NaN
cid0002466[c]	Pinocarvone	C10H14O	0	1.02E-12	-4.99		NaN	NaN

cid0002467[c]	4-Isopropenyl-2-oxy-cyclohexanecarboxyl-CoA|4-Isopropenyl-2-oxy-cyclohexanecarboxyl-CoA|4-Isopropenyl-2-ketocyclohexane-1-carboxyl-CoA	C31H48N7O18P3S	0	-3.916527712	5.06|3.37|-7.03	0.81|1.83|2.68|5.96|10.94	NaN	NaN
cid0002468[c]	Myrtenol	C10H16O	0	1.24E-09	-1.88	17.1	NaN	NaN
cid0002469[c]	Myrtenal	C10H14O	0	3.39E-12	-4.47		NaN	NaN
cid0002470[c]	Pinocarveol	C10H16O	0	3.08E-09	-1.51	17.94	NaN	NaN
cid0002471[c]	"3-Hydroxy-2,6-dimethyl-5-methylene-heptanoyl-CoA"	C31H52N7O18P3S	0	-3.916416148	5.06|3.37|-3.87|-7.03	0.81|1.83|2.68|5.96|12.61	NaN	NaN
cid0002472[c]	S-(Hydroxymethyl)glutathione	C11H19N3O7S	0	-1.999536083	9.31|-1.18|-2.95	1.79|3.67|12.27|14.25|14.87	-243.03	3.27634
cid0002473[c]	Iminoglycine|Iminoglycine|Iminoacetic acid	C2H3NO2	0	-0.999149269	3.27	3.93	-95.02	3.29849
cid0002474[c]	C15810|C15810|Thiamine biosynthesis intermediate 1		NaN	NaN			NaN	NaN
cid0002475[c]	C15813|C15813|Thiamine biosynthesis intermediate 4		NaN	NaN			NaN	NaN
cid0002476[c]	C15814|C15814|Thiamine biosynthesis intermediate 5		NaN	NaN			NaN	NaN
cid0002477[c]	C15815|C15815|Thiamine biosynthesis intermediate 6		NaN	NaN			NaN	NaN
cid0002478[c]	Aminopropylcadaverine	C8H21N3	0	2.964122785	10.9|10.11|8.43		27.54	2.188

cid0002479[c]	N-Acetylmuramic acid 6-phosphate|N-Acetylmuramic acid 6-phosphate|MurNAc 6-phosphate	C11H20NO11P	0	-2.813517637	-0.79|-3.64|-4.23	1.22|3.54|6.36|11.63|12.93|13.57	-488.5	3.31358